# GRAVITATION THEORY AND GRAVITATIONAL COLLAPSE

B. Kent Harrison, Kip S. Thorne, Masami Wakano, John Archibald Wheeler



A neutron star more massive than a critical limit, about equal to the mass of the Sun, will inevitably undergo gravitational collapse. The reasoning which has forced physicists to this conclusion is given its first systematic presentation in this volume by Professor Wheeler, an international expert on nuclear fission and geometrodynamics, and three of his colleagues in nuclear physics.

At the Symposium on Relativistic Astrophysics held in Dallas, Texas, in December, 1963, Wheeler proposed that a portion of the collapsing matter disappears from existence. His proposal aroused such intense interest that half a day was set aside during the conference to discuss his findings. Too long for inclusion in the collected proceedings published by The University of Chicago Press in 1964 under the title Ouasi-stellar Sources and Gravitational Collapse, the work of Wheeler and his collaborators here receives more detailed treatment as a separate monograph.

The four authors develop the subject from basic principles to theo-

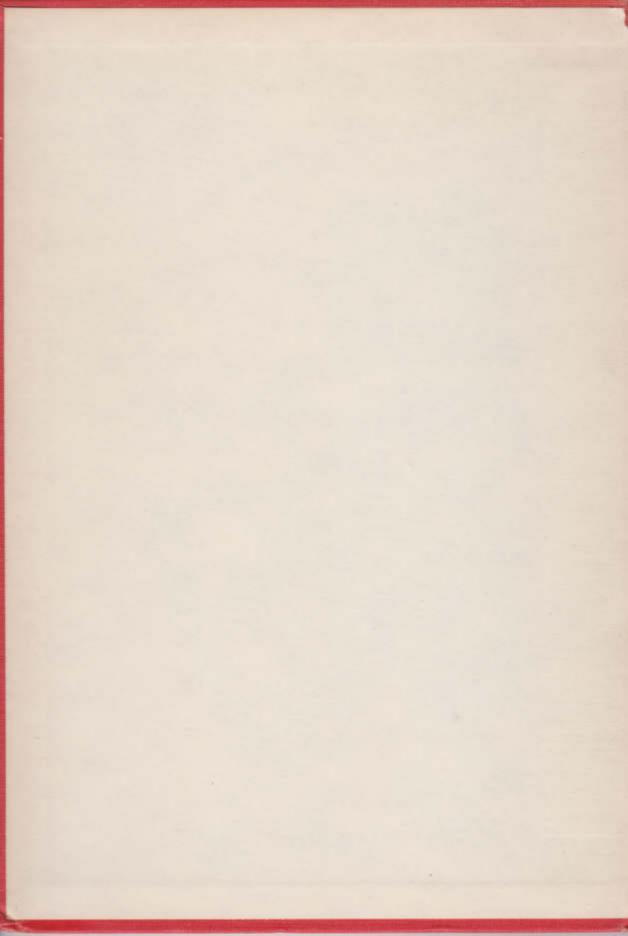
(Continued on back flap)

GRAVITATION THEORY

and GRAVITATIONAL COLLAPSE

HARRISON . THORNE WAKANO . WHEELER

CHICAGO







# GRAVITATION THEORY

and

GRAVITATIONAL COLLAPSE

# GRAVITATION THEORY

and

# GRAVITATIONAL COLLAPSE

B. KENT HARRISON

Physics Department, Brigham Young University

KIP S. THORNE

Palmer Physical Laboratory, Princeton University

MASAMI WAKANO

Department of Nuclear Science, Kyoto University

JOHN ARCHIBALD WHEELER

Palmer Physical Laboratory, Princeton University

THE UNIVERSITY OF CHICAGO PRESS

Chicago and London



Library of Congress Catalog Card Number: 65-17293

THE UNIVERSITY OF CHICAGO PRESS, CHICAGO & LONDON The University of Toronto Press, Toronto 5, Canada

© 1965 by The University of Chicago. All rights reserved Published 1965. Composed and printed by The University OF Chicago Press, Chicago, Illinois, U.S.A. Dedicated to OSKAR KLEIN on his seventieth birthday, September 15, 1964



#### FOREWORD

For the December, 1963, Dallas International Symposium on Gravitational Collapse and Relativistic Astrophysics one of us (J. A. Wheeler) was asked to report on the present status of the relativistic theory of gravitational collapse. Gravitational collapse occurs when the inward pull of the gravity produced by a collection of matter exceeds the elastic forces developed by the compression of that matter. Collections of matter of planetary mass and less are well known to be stable against such collapse. However, when an amount of cold matter is assembled with the mass exceeding a critical figure not very far from the mass of the Sun, then the system becomes unstable against collapse, as has been known ever since the pioneering work of Landau in 1932. In the intervening years special aspects of the transition with increasing mass from stable to unstable configurations have been studied; and a beginning has been made in analyzing the first stages of the dynamics of collapse by many workers, including Chandrasekhar, Oppenheimer, Serber, Volkoff, Schatzman, ourselves, Klein, Zel'dovich, Fowler, Hoyle, Cameron, Chiu, Salpeter, Colgate, White, Misner, Sharp, Bondi, Gratton, Bardeen, and others. In the report presented at the conference an attempt was made to present a survey of principal conclusions out of this work and to point up significant issues still outstanding. Among these issues two forced themselves to the attention more insistently than any others: Is there any consideration of principle which prevents gravitational collapse of the inner portions of a system from proceeding to completion? And when matter collapses how can the baryons which compose it escape destruction? The conference report concluded that no escape is now known-under appropriate conditions of assemblyfrom a new physical process. In this process baryons disappear. Today one is far from being able to give any definitive account of the final stages of this process. It presents deep and fascinating problems which lie in the no man's land between elementary particle physics and quantized geometrodynamics, some of which are discussed in another volume by one of us (J. A. W., Geometrodynamics and the Issue of the Final State [New York: Gordon & Breach, 1965]). However, an analysis of the physics of a supercritical mass makes the process of disappearance of baryons seem inescapable. To present such an analysis was the purpose of the original report.

To translate this one-hour report into a systematic account of the theory, conclusions, and problems has required much more space than was originally envisaged. Happily the original speaker was able to secure the collaboration of his past Princeton associates in the study of gravitational collapse. In addition the University of Chicago Press suggested that this particular conference report should be presented as a separate volume rather than as one of the parts of the conference proceedings. Even in this expanded account we have had to forego any discussion of the collapse of hot systems. We have limited attention to the idealized case where the system to begin with is composed of cold matter catalyzed to the end point of thermonuclear evolution. In the discussion of such systems, we have discovered a few new features, including the existence of an infinite number of critical points, a variational derivation of the theory of hydrostatic equilibrium, and proof that no physically acceptable relation between pressure and density that one can postulate is adequate to prevent gravitational collapse. Perhaps more interesting than

any of these new points is the conclusion that gravitational collapse must occur for a subcritical mass as well as for a supercritical mass. The mechanism involves a quantum mechanical tunneling process in which not the entire assemblage of baryons but a limited number of particles coalesces and disappears. It is not possible to make a proper calculation of the rate. Therefore one must rely for the present on observation rather than theory to tell whether this new process of spontaneous collapse proceeds at a detectable rate,

\* \* \*

The results described in this joint report were obtained in some cases in collaboration; in other cases, individually, as follows. B. Kent Harrison: theory of equation of state at nuclear and subnuclear densities (jointly with Wheeler); Table 13, which gives pressure, mass density, and number density and analytical fits to these values (eqs. [258]-[261]); new integrations of the general relativity equation of hydrostatic equilibrium; Figures 5, 6, and 7, and Appendix Tables A1, A2, and A3 for the results of these integrations; and first reasoning that there are infinitely many maxima in the curve of equilibrium mass as a function of central density. Kip S. Thorne: derivation of general-relativity equation of hydrostatic equilibrium from variational principle (jointly with D. Meltzer; also independently by W. J. Cocke; also independently by Wheeler); relation of stability of equilibrium configurations to second variation of mass-energy (Appendix B); Figure 13 for mass-energy of configurations of uniform density, as a function of density, for selected values of the baryon number; and Table 14 for the contributions to the pressure from electrons and neutrons at selected values of the density. Masami Wakano; Figure 18 and the related analysis in the text of the approach to pure Fe<sup>ss</sup> for the partition of lowest energy as A is raised from 1 up to 105 (jointly with Wheeler); first integrations of the general relativity equation of hydrostatic equilibrium using the H-W equation of state; 1957 versions of Figures 5, 6, 7, and 8 (extended by Harrison in 1964 from 10<sup>18</sup> g/cm<sup>2</sup> up to 10<sup>22</sup> g/cm<sup>3</sup>); Figures 23–26, giving methods of integration and further details of the results; and Appendix C on variational methods (jointly with Wheeler). John A. Wheeler: present proof that there are infinitely many maxima in the curve of equilibrium mass as a function of central density; the "slide rule" for separating out contributions of long-range and short-range forces to mass-energy at any compaction; present proof-using this "slide rule"-that mass collapses to zero for sufficiently great compaction regardless of all details of the equation of state; discussion of the mechanism of collapse and the issue of the final state; and conclusion that there exists in nature a new kind of elementary particle transformation, spontaneous gravitational collapse; and that all matter must manifest, however weakly, a new form of radioactivity, in which baryon

One of us (K. S. T.) thanks the Danforth Foundation and the National Science Foundation for fellowships during the course of this work; another (B. K. H.) expresses appreciation to the U.S. Atomic Energy Commission and the Los Alamos Scientific Laboratory, under whose auspices some of the work in this report was done; finally, a third (J. A. W.) thanks the National Science Foundation for a fellowship during the period of this research, and also expresses appreciation to Dr. Richard Eden; Clare College; the Department of Applied Mathematics and Theoretical Physics of Cambridge University; and to the Oak Ridge National Laboratory for hospitality. We are indebted to the Office of Scientific Research of the United States Air Force and to the National Science Foundation for financial assistance with research expenses connected with this

work.

Appreciation is expressed to H. Bondi, Dieter Brill, Keith Brueckner, A. G. W. Cameron, H. Y. Chiu, Sterling Colgate, Bryce DeWitt, Robert Dicke, P. A. M. Dirac, Freeman Dyson, William A. Fowler, L. Gratton, Fred Hoyle, Richard Lindquist, Robert

Marshak, Michael May, M. A. Melvin, Charles Misner, R. E. Peierls, E. Salpeter, E. Schatzman, E. Schücking, M. Schwarzschild, Dennis Sciama, L. Shepley, David Sharp, B. Strømgren, Samuel Treiman, L. van Hove, Joseph Weinberg, and other colleagues for stimulating and valuable discussions.



## CONTENTS

List of Figures	XV
LIST OF TABLES	xvii
<ol> <li>Introduction</li></ol>	1
2. Mass-Energy on a Spacelike Hypersurface of Time Symmetry	11
3. Hydrostatic Equilibrium and Extremal Mass-Energy The theorem • Relation of the variational treatment to Tolman's field-theoretical derivation of the equation of equilibrium: introduction to an extended discussion • The relativistic generalization of the gravitational potential and its observational significance • Case of compensating redshift and blueshift • The constancy of the injection energy • Correspondence between neutron star and statistical atom model • Natural and unique definition of the potential exp (ν/2) only for equilibrium configurations • The sense in which the gravitational potential exp (ν/2) does and does not appear in the variational analysis • The space in which each point represents one configuration • The Zel'dovich sequence	16
<ol> <li>Central Density and the Regeneration of Pressure</li></ol>	26
5. Denumerable Infinity of Critical Masses	30

6.	Mass and Radius of Equilibrium Configurations: 1932-1964	42
	Landau's pioneering analysis • The Chandrasekhar limit • The cold neutron star of Oppenheimer and Volkoff • Inverse beta-decay; a universal equation of state; the final revelation of the first point of instability; the 1964 Harrison-Wakano-Wheeler curves	
7.	THEORY OF THE STABILITY OF EQUILIBRIUM CONFIGURATIONS	50
	The frequency of the acoustical modes of spherical symmetry $\cdot$ Zel'dovich on solutions with energy excess $\cdot$ Einstein on solutions with energy excess $\cdot$ A geon as a third example of a solution with energy excess $\cdot$ Three kinds of system with energy excess: a comparison and contrast $\cdot$ Baryons added and baryons taken away in repeated cycles to "pump up" the central density and the excess energy to maximum values $\cdot$ Stabilization required to reach unstable configurations $\cdot$ The coupled rates of change of $M^*(\rho_0)$ and $A(\rho_0)$ $\cdot$ Infinite dimensional configuration space and neutral stability $\cdot$ The contrasting stability of the two branches of $M^*(A)$ $\cdot$ Changes in stability diagnosed by changes in radius $\cdot$ Final survey of the changes in stability $\cdot$ Quantitative analysis of rate of change of stability at critical point $\cdot$ Present stability analysis compared and contrasted with one that makes detailed calculations of frequencies $\cdot$ Why more modes become unstable as the central density rises	
8.	No Escape from Collapse	69
	Four reasons for considering configurations of uniform density $\cdot$ Separation of longand short-range forces; the "slide rule" $\cdot$ Volume-density relation for uniform configurations of specified total mass-energy $\cdot$ The slide rule, its use, and the interpretation of the results $\cdot$ Continuous sequence of configurations with fixed $A$ but mass-energy going to zero $\cdot$ No barrier to collapse of a suprasolar mass $\cdot$ Collapse barrier for substellar systems $\cdot$ Not technologically feasible to put in enough energy to push a substellar mass over the barrier $\cdot$ The barrier falls at big $A$ and low $A$ and has a maximum at intermediate $A$	
9.	EQUATION OF STATE OF COLD, CATALYZED MATTER	83
	The end point of thermonuclear evolution • Symmetry against $A \to -A$ • Electrical neutrality • Definition of neutrino neutrality • The final state when $A$ is small • An aside on $A=5$ , $A=8$ , and fluctuations in geometry • The regime of scallops in the over-all packing fraction • New type of periodicity for $A$ of order of $10^4$ and more • The long-range forces begin to affect local conditions when $A \sim 10^{20}$ ("compression") • Frame in which flow of baryons and flow of energy both vanish • The universal character of the equation of state • Pressure but no shearing stress • Three ways to give operational meaning to the energy density • Limitation on curvature or density at which the concept of equation of state makes sense • An aside: universe sharply curved as viewed from fast particle • The function $\rho(n)$ as a thermodynamic potential • Alternative choices for the thermodynamic potential • Baryon number as deduced from pressure and density measurements • $\gamma$ -law in the relativistic and non-relativistic domains: comparison and contrast • $\gamma$ one or greater for stability against the collapse of matter • $\gamma$ two or less for consistency with causality • The soft "hard core"	

10. THE HARRISON-WHEELER EQUATION OF STATE	108
Equation in form of table of values and analytical fits to them • Derivation: region up to $10^4$ atmospheres • Feynman, Metropolis, and Teller from 15 g/cm² to $10^4$ g/cm² • Chandrasekhar from $10^4$ g/cm² to $10^7$ g/cm² • Separated nuclei in beta-equilibrium with a relativistic electron gas: $\sim 10^7$ g/cm² to $\sim 4 \times 10^{12}$ g/cm² • Regime of stabilized neutron drip • Mixture of ideal electron, proton, and neutron Fermi gases from $p=4.54 \times 10^{12}$ g/cm² to $10^{18}$ g/cm³, and from $10^{18}$ g/cm² to the highest densities; alternatives	
11. Gravitational Collapse—to What?	124
Curvature nearly to closure the theme of the analysis $\cdot$ Time symmetry and collapse from infinity reconciled $\cdot$ Geometric description of collapse of cloud of dust: the Friedmann region $\cdot$ Geometric description of collapse of cloud of dust: the Schwarzschild region $\cdot$ A two-dimensional model for the Schwarzschild geometry at a moment of time symmetry $\cdot$ The nature of time in general relativity $\cdot$ The evolution of the Schwarzschild geometry with time $\cdot$ The two connected quasi-Euclidean spaces deformed to a "cylinder" $\cdot$ Join between Schwarzschild and Friedmann geometries $\cdot$ Connection between the dynamics of collapse and the analysis of momentarily static configurations $\cdot$ A spacelike slice characterized by an arbitrarily specified value of the mass-energy $\cdot$ Segment of opening $\chi_1 > \chi_0$ slicing through the Friedmann 4-geometry $\cdot$ How reconcile a changing mass-energy with a constant mass-energy? $\cdot$ Potential and kinetic energy related to intrinsic and extrinsic curvature $\cdot$ Gravitational collapse as a model for the study of the dynamics of the universe $\cdot$ Communication to outside cut off $\cdot$ For whom the bell tolls $\cdot$ New quantum aspects of collapse $\cdot$ Obstacles to defining and applying the law of conservation of baryons $\cdot$ Barrier penetration for $A \sim A_{\text{sea}}$ $\cdot$ Barrier penetration for $A < < A_{\text{sea}}$ $\cdot$ Barrier penetration $\cdot$ Baryon appearance and the one-sidedness of matter $\cdot$ Observable at normal density?	
Appendices	
A. Numerical Integration of the General-Relativity Equation of Hydrostatic Equilibrium: Methods and Results	149
B. Theory of the Stability of Equilibrium Configurations: Derivation from Energy Considerations	156
C. Variational Technique Tested in Non-relativistic Domain on Polytropes	163
AUTHOR INDEX	167
Subject Index	170

# LIST OF FIGURES

1.	Schwarzschild Correction Factor Exp $(\nu/2)$ Interpreted as a Gravitational Potential	22
	Comparison of Equilibrium Configurations of Finite and Infinite Central Density	32
	Oscillatory Difference between Configurations of Finite and Infinite Central Density: $\xi$ versus $\eta$	36
	Oscillatory Difference between Configurations of Finite and Infinite Central Density: $\Delta m(r)$ versus $\Delta \rho(r)$ at Fixed $r$	38
	HWW Catalogue of Equilibrium Configurations of Cold, Catalyzed Matter: Mass $M$ versus Central Density $\rho_0$	46
	HWW Catalogue: Radius R versus Central Density ρ <sub>0</sub>	47
7.	HWW Catalogue: Mass $M$ versus Radius $R$	48
	HWW Catalogue: Mass M versus Baryon Number A	53
9.	Mass $M$ versus Baryon Number and Compaction in the Neighborhood of a Critical Point	63
	Lowest Radial Modes of Oscillation: Square of the Frequency versus Central Density	65
11.	Momentarily Static and Homogeneous Configurations of Fixed Mass: Density-Volume Relationship	71
12.	Momentarily Static and Homogeneous Configurations: Contours of Constant Mass in Density-Volume Diagram	74
13.	Mass-Energy versus Density for Momentarily Static and Homogeneous Configurations (HW Equation of State)	76
14.	Potential Barrier against Gravitational Collapse for Configurations of Uniform Density and $A\ll A_{\rm crit}\approx 10^{17}$	78
15.	Geometry of Momentarily Static and Homogeneous Configurations as a Function of the Degree of Compaction	79
16.	Gravitational Collapse at the Terrestrial Level	81
17.	Hysterisis in the Pressure-Density Relation	86
18.	Lowest Energy State of an A-Baryon System for $A < 350$	90
	Equation of State in a Zone of Phase Transition: Passage from "Analytical Form" to "Physical Form"	103
20.	Collapse: Time-Symmetric and Non-Time-Symmetric	125
	Join between Friedmann and Schwarzschild Geometries	127

#### LIST OF FIGURES

22.	Quantum Mechanical Split of History into Multifoliate Histories	143
	Lifetime of an A-Baryon System against Tunneling the Barrier against Collapse	145
24.	Flow Diagram for Numerical Integration of General-Relativity Equation of Hydrostatic Equilibrium	150
25.	Flow Diagram: Detail on Pressure versus Density Relation	
	HWW Equilibrium Configurations: Pressure and Density versus Schwarzschild Radial Coordinate	
27.	HWW Configurations: Baryon Number Related to $p$ and $\rho_0$	154

## LIST OF TABLES

	Potential Barrier against Gravitational Collapse Compared with the Potential Barrier against Nuclear Fission in the Continuum Limit (Liquid Drop)	4
2.	Relation between Certain Physical Quantities as Measured in the Conventional Units and the Same Physical Quantities as Expressed in Purely Geometrical Terms of Length, as Appropriate in General Relativity	12
	Zones Considered in Analyzing Difference between Actual Configuration ( $\rho_0$ Large) and Limiting Configuration ( $\rho_0$ Infinite)	33
4.	Configuration in Region Where Asymptotic $\gamma$ -Law Applies, for the Case $\gamma = \frac{4}{3}$	33
5.	Tentative Determination of the Amplitude  Q  and the Phase $\delta$ , for $\gamma = 4/3$	37
6.	Mass-Energy, $M^*$ , for a Fixed Number of Particles, $A$ , of Rest Mass, $\mu_4$ , Moving in Circular Orbits at $r = r_0$ .	56
	Change in Radius near a Critical Point as Criterion for the Relative Stability of the High- $\rho_0$ and Low- $\rho_0$ Branches of the Function $M^*(A)$ near That Point	64
8.	The Relation between Density and Volume for Momentarily Static, Spherically Symmetric Configurations of Uniform Density	73
9.	Density of a Dust Cloud at Collapse as Function of Mass before Assembly	77
10.	Barrier against Collapse for Ideal Fermi Gas in High-Density Limit	80
11.	Lowest Energy State of A-Baryon System for $A \le 1008$	89
12.	Optimum Partition of A Baryons into Individual Nuclei for $A \sim 56000$ (Schematic)	92
13.	Pressure for 47 Values of the Density (B. K. H.)	109
14.	Dominant Nucleus for Selected Pressures	117
	Simple Expressions for Equation of State of Cold, Catalyzed Matter	120
16.	Features of Equilibrium Configurations for Selected A-Values	122
۸1.	Equilibrium Configurations of Cold, Catalyzed Matter up to $10^9~\rm g/cm^3$ (B, K, H, and M, W,)	152
12.	Equilibrium Configurations of Cold, Catalyzed Matter from 10° to 10 <sup>14</sup> g/cm <sup>2</sup> (B. K. W. and M. W.)	152
	Equilibrium Configurations of Cold, Catalyzed Matter from $10^{14}$ to $10^{22}$ g/cm <sup>2</sup> (M. W. as Extended by B. K. H.)	153
	Contributions to the Energy of Equilibrium Configurations as Calculated from the Trial Functions of Equation (C9)	164
72.	Equilibrium Configurations: Variational Treatment Compared with Emden's Exact Analysis	165



### chapter 1 INTRODUCTION

#### NEW MOTIVATION FOR LOOKING AT AN OLD PROBLEM

Evidence has recently been uncovered for the production of an energy as great as 10<sup>66</sup> or 10<sup>61</sup> erg in a limited time, in a limited space, and therefore out of a limited amount of matter. The astrophysical observations do not prove, but have led some investigators to suggest, that a new process is going on in which the output of massenergy per unit of mass exceeds (Burbidge 1962; Hoyle and Fowler 1963a, b; Hoyle, Fowler, Burbidge, and Burbidge 1964) the 1 part in 112 obtainable by thermonuclear combustion. Therefore, attention has turned to gravitational collapse as a mechanism by which in principle a fraction of the latent energy of matter much larger than 1 per cent can be set free.

The concept of gravitational collapse has a long history. Already in the nineteenth century the balance between the outward push of pressure and the inward pull of gravitation had been studied in some detail. The spherical configuration of equilibrium for any given mass of matter under one and another postulate about the equation connecting pressure with density ("equation of state") had been determined (see, e.g., Emden [1907]). Even then the central question had been posed: How can any system possibly

<sup>&</sup>lt;sup>4</sup> Fractional conversion of normal matter to energy as attainable by presently known mechanisms. Example:  ${}_{54}$ Pu<sup>229</sup> (spontaneous fission followed by capture of all emitted neutrons into the fission fragments, followed by beta decay)  $\rightarrow {}_{54}$ Ru<sup>59</sup> +  ${}_{16}$ Ce<sup>140</sup>; fractional loss of energy per gram, 0.001007/1.000218 = 0.001007, equivalent to 0.001007 $c^2 = 9.05 \times 10^{17}$  erg/gm (masses on C<sup>12</sup> scale).

Fractional Co of Matter to		Final Product	Hes	Feit	Equimolar Mixture of Ru <sup>60</sup> and Ce <sup>160</sup>
Fuel and process	Mass per mass No.	Its mass per mass No.	1.000631	0.998838	0.999211
H, fusion Pu <sup>228</sup> , fission	1.007825 1.000218		0.007118 No	0.008917 No	0.008547 0.001007

<sup>&</sup>lt;sup>1</sup> Evidence originally presented at the Dallas Conference on Gravitational Collapse (Robinson, Schild, and Schucking 1964; hereinafter cited as "CGC"). See also Burbidge, Burbidge, and Sandage (1963), Lynds and Sandage (1963), Greenstein (1963), and Greenstein and Schmidt (1964); and see Ambartsunyan (1958), esp. pp. 265–267, for earlier considerations arguing for the occurrence of violent energy evolution in the nuclei of certain galaxies.

<sup>&</sup>lt;sup>2</sup> Time within an order of magnitude of ~10°-10° years as deduced from (1) the spatial extension of the products of explosion and (2) the rate of loss of energy from those products by synchrotron radiation; see CGC for further details.

<sup>&</sup>lt;sup>2</sup> In contrast to a diameter of ~10° light-years for a typical galaxy, for the quasi-stellar source 3C 273 a linear extension less than 10 light-years is deduced (1) from rises and falls in light output by as much as a factor 2 in a time of the order of 10 years, as chronicled by Smith and Hoffleit (1963) and in CGC; and (2) from the ratio of total luminosity to light output per unit area as derived from electron density and temperature—themselves in turn inferred from the relative intensities of selected spectral lines (see Greenstein and Schmidt [1964]).

sustain itself against collapse when the mass—and resulting gravitational forces—are increased more and more?

This is not the place to review the fascinating history of this issue of a critical mass for gravitational collapse, 5 nor of how it has sharpened and deepened with the development of atomic physics and relativity, nor what decisive contributions came from Chandrasekhar, 6 Landau (1932), 7 Tolman (1939), Oppenheimer and Volkoff (1939), Zel'dovich (1962), and others. However much has been done, still more remains to be done before the investigator will be in any position to treat gravitational collapse with all completeness. A realistic analysis of collapse in the context of astrophysics would evidently have to take into account angular momentum, magnetic fields, turbulence, shock waves, the curvature of spacetime, and other complications. 8

#### GRAVITATIONAL COLLAPSE AND THE ISSUE OF THE FINAL STATE

More pressing than these questions of detail is an issue of principle: Does gravitational collapse, under conditions however idealized, provide a means to convert a large fraction (much more than 1 per cent!) of the mass of ordinary matter into energy? And if so, what is the final state of the matter after the reaction? These two problems of principle are the center of attention in the present report.

The nature of the questions is not new. From physical chemistry we long ago learned to assess a reaction by examining the initial and final states and the difference in energy between them. One can postpone as a detail—an important detail, but still a detail—looking at the mechanism and rate of the reaction which leads from the one state to the other.

State of what? The state of a system of A baryons. In other words, we ask this question: Given an electrically neutral system of A baryons; given in principle the means to catalyze all nuclear reactions to the end point of thermonuclear evolution; given the means to cool the system as close as desired to absolute zero; given that the pressures of neutrinos and antineutrinos in equilibrium with the matter are zero, as befits a free system of A baryons; what is the ground state energy of this A-baryon system? Or are there two ground states, one for normal matter and the other for matter that has undergone gravitational collapse?

At the level of everyday nuclear physics one never thinks of the possibility of two ground states, one normal, the other collapsed; attention focuses exclusively on the study of the normal state! For A=1 the familiar ground-state configuration is one free hydrogen atom. For A=4 it is a helium atom; for A=56, an iron atom. Likewise, when a system of  $A=56\times 10^6$  baryons is catalyzed to the end point of the familiar

- <sup>5</sup> Some aspects of this history are, however, briefly recapitulated in chap, vi below in connection with the present treatment of stable and unstable equilibrium. See also Harrison, Wakano, and Wheeler (1958); Wheeler (1964σ, b).
- \*See Chandrasekhar (1935); see also the precursors of this work (Stoner 1929, 1930; Chandrasekhar 1931a, b, 1932, 1934). In his 1932 work Chandrasekhar concluded: "Great progress in the analysis of stellar structure is not possible before we can answer the following question: Given an enclosure containing electrons and atomic nuclei (total charge zero), what happens if we go on compressing the material indefinitely?" See also Chandrasekhar (1939).
  - <sup>7</sup> See also Oppenheimer and Serber (1938) and Landau and Lifshitz (1958), chap. xi.
- <sup>8</sup> For the general concept of gravitational collapse as a mechanism actually at work in astrophysical evolution see Burbidge (1962); Hoyle and Fowler (1963a, b); Hoyle at al. (1964). Specific models include, first, contraction of a single superstar of mass as great as 10<sup>8</sup> M☉ (Hoyle and Fowler 1963a, b); Iben 1963; Michel 1963). A second model envisages a great number of stars of more familiar mass, in an unusually dense cluster, which evolve dynamically to a compactified configuration (see Gold in CGC; also Ulam and Walden [1964]). A third proposal pictures a mass of gas ~10<sup>8</sup> M☉ which (a) originally rotates slowly, (b) evolves dynamically into a disk like configuration, and (e) breaks up by gravitational instability into separate masses, which then (d) individually undergo gravitational collapse (see Hoyle and Fowler in CGC). A fourth concept treats a galaxy—or a region of a galaxy—so dense that many supernovae are formed in it at about the same time (Field 1964).

type of thermonuclear evolution, it takes the form of 10<sup>6</sup> atoms of Fe<sup>56</sup> placed in a body-centered cubic lattice. In this system the priority of the forces is very clear, each being marked off from the next in its degree of influence by many powers of 10: (1) nuclear forces; (2) solid-state forces and the energy of the atomic electrons; (3) gravitational energy.

When the number of baryons is increased to  $A \sim 10^{56}$  and  $A \sim 10^{57}$ , gravitational forces build up so much pressure that electrons are promoted to relativistic energies. They transmute bound protons to neutrons. The nuclear composition changes from Fe<sup>56</sup> in the direction of heavier and more neutron-rich nuclei. Nuclear energy, electron en-

ergy, and gravitational energy no longer differ greatly in order of magnitude.

With still further increase in the baryon number one comes, according to every analysis, to a point,  $A = A_{\rm crit}$ , where gravitational forces dominate. Even when A is a little short of  $A_{\rm crit}$ , the input of a little energy of compression from outside will compact the system enough for gravitational forces to win out and for collapse to start. In other words, for  $A < A_{\rm crit}$  there exists a potential barrier which must be overcome—or pene-

trated—before the system can shrink to the new configuration (Table 1).

Thus a system of baryons numbering a little less than  $A_{\rm crit}$  possesses not only an equilibrium configuration of "normal" character, but also another configuration of still lower energy. Moreover, a system with  $A > A_{\rm crit}$  has not even a potential barrier to restrain it from passage to this collapsed state. What, then, is the nature of this state? And if there is a collapsed configuration for A a little more than  $A_{\rm crit} \sim 10^{57}$  and for A a little less than  $A_{\rm crit}$ , does such a state also exist for A much less than  $A_{\rm crit}$ ? For  $A = 10^{56}$ ? For A = 56? And for a single hydrogen atom? And if so, with what new kind of elementary process is one confronted here? Moreover, if the process of collapse of a baryon, or a group of baryons, is possible in principle, it must take place in actuality. Quantum-mechanical leakage through the barrier against collapse will inevitably occur, however low its rate. What, then, is the half-life of ordinary matter against spontaneous transformation to a collapsed state? All these questions, extending from astrophysics to elementary-particle physics, make the issue of the final state one of the most important problems in the history of physics.

How many bridges must one cross before he can treat all these aspects of gravitational collapse? The road evidently extends some distance into the future! The long-term character of the investigation imposes on any reviewer of today a special obligation. He must distinguish as sharply as he can between (1) what are truly puzzles and (2) what are clear and definite conclusions. What follows attempts this distinction. The definite points are set off from the issues, as an experiment, by the old-fashioned style in which they are treated—a style listing definitions, hypotheses, and theorems. However, the subject matter is physics, not Euclidean geometry. Therefore, there is no pretense either to the

almost unshatterable rigor or to the meticulous detail of Euclidean reasoning.

#### A SURVEY OF THIS REPORT

The problems split themselves into two groups: (1) What can be said about the massenergy of any given configuration containing A baryons? (2) What can be said about

the rate of passage from one configuration to another?

The analysis of the energy divides itself naturally into a part having to do with the long-range force of gravitation and a part having to do with the local energy density of compressed matter. Chapter ii briefly reviews the immediately relevant parts of Einstein's theory of gravitation. To determine the mass-energy of configurations of matter, it proves useful to analyze the geometry on a spacelike hypersurface. This three-dimensional geometry, according to general relativity, satisfies a certain simple condition, the Fourès condition (Theorem 1), the analog of div  $E = 4\pi\rho$  in electrostatics. This condition becomes particularly simple when applied on a spacelike hypersurface of time symmetry, such as is appropriate for describing a momentarily static configuration. The mass-energy

of any static spherically symmetric system—thus automatically including the equivalent negative mass-energy associated with the long-range gravitational interactions themselves—expresses itself (Theorem 2) as the simple integral,  $\int \rho^* 4\pi r^2 dr$ , of the local density of

mass-energy, regardless of any pressures that do or do not exist in the system.

Chapter iii gives a general procedure to compare the energies of static configurations of spherical symmetry, both those which are in equilibrium and those which are not. This mass-energy is defined, for example, by its effect on planetary orbits or by the bending of light which it produces. A variational treatment is given on this basis, following the Lagrangian formulation of hydrodynamics (particle labels taken as coordinates). By extremizing the mass as sensed externally, one is led directly (Theorem 3) to the general relativity equation of hydrostatic equilibrium. A treatment which starts with no mention of "pressure" ends up with an equation for the determination of pressure; and starting with no mention of "gravitational potential"—an undefined quantity for an

TABLE 1

POTENTIAL BARRIER AGAINST GRAVITATIONAL COLLAPSE COMPARED WITH THE POTENTIAL BARRIER AGAINST NUCLEAR FISSION IN THE CONTINUUM LIMIT (LIQUID DROP)

	Nuclear Fission	Gravitational Collapse
System	One nucleus consisting of $Z$ protons and $N=A-Z$ neutrons	One giant system consisting of A baryons, cold, and catalyzed to the end point of thermonuclear evolution
Parameter specifying criticality of system	Fissility parameter $x = \frac{c_1(Z^2/A)}{1 + c_2[(N-A)/A]^2}$	Baryon number A
Condition for existence of a stable minimum	x<1	$A < A_{crit}$
Nature of deformation for passage over bar- rier	Dumbbell-shaped depar- ture from sphericity	Compaction
Number of parameters needed to specify the most general deformation of this type (number of coordinates in configuration space!)	â	ω
Principal large-scale features of contour plot of energy as a function of deformation (one coordinate for energy, an infinite number of coordinates for deformation)	a) Minimum (normal nucleus before fission)     b) Saddle (fission barrier)     c) Separated configuration of much lower energy	a) Minimum ("normal configuration")     b) Saddle (summit of barrier against gravitational collapse)     c) Collapsed configuration of much lower energy
Energy which must be supplied to carry sys- tem from minimum to top of barrier, in case when criticality parameter is close to the critical value	Small energy ("triggering energy")	Small energy ("triggering energy")
Energy which is set free by subsequent pas- sage downhill on other side of barrier	Large energy	Large energy
Final configuration	Fission fragments	Final state of gravitational collapse

arbitrary configuration—it also ends up with a formula for this quantity. This formula (Theorem 4) expresses the constancy—throughout the interior of an equilibrium configuration—of the "injection energy," the energy required to bring in a baryon from infinity and inject it at that point. Theorem 5 states that any solution of the variational problem automatically satisfies all of Einstein's field equations, not merely the Fourès condition. The variational approach to the problem of mass-energy opens the way to analyzing the energy of all configurations, not only equilibrium configurations. As an example of this type of reasoning the properties of a sequence of configurations considered by Zel'dovich are reviewed. This sequence provides one route for passing continuously from normal

dimensions, over an energy barrier, to a collapsed condition.

Chapter iv analyzes the properties of equilibrium configurations of cold matter catalyzed to the end point of thermonuclear evolution, and thus endowed with a unique equation of state. The principal theorems here have to do with (Theorem 6) the monotonic fall of the pressure from the center to the surface; (Theorem 7) the existence of one and only one equilibrium configuration—and it with well-defined mass M, baryon number A, and radius R—for each value of the central density  $\rho_0$ ; the subtle sense in which the pressure in a highly compressed configuration is, and is not, a regeneralizely self-multiplying quantity (the idealized case of an incompressible fluid being taken up as one example); and (Theorem 8) the finiteness of M, A, and R as the central density goes to infinity. In connection with this last point it is assumed that the equation of state follows asymptotically at high pressures a " $\gamma$ -law" with the ratio (pressure)/(density of mass-energy) approaching a constant, ( $\gamma = 1$ ), with  $\gamma$  in the physically admissible range from just over 1

("soft") to 2 ("hard").

Chapter v formulates a new feature (first recognized by B. K. Harrison) of the solutions of the general-relativity equation of hydrostatic equilibrium on the hypothesis of an asymptotic  $\gamma$ -law (Theorem 9): the mass M, the baryon number A, and the radius R execute damped oscillations periodic in the logarithm of the central density as this central density approaches infinity. Of course, expressed as a function of time, the density is completely static for these equilibrium configurations! The characteristic period of the oscillations,  $\Delta \ln \rho_0$ , is evaluated in terms of  $\gamma$ . In the proof of the theorem the range of r-values is divided into three zones. In Zone I, near the origin, for  $\gamma = \frac{4}{3}$  numerical results of Bondi are available. In Zone II an analytic formula is derived for the oscillations for all values of  $\gamma$ . The adjustable amplitude and phase factors in this formula are determined for the case  $\gamma = \frac{4}{3}$  by joining onto the Bondi values. In Zone III—reaching to the surface—where no  $\gamma$ -law applies, and the equation of state is complicated, an exact "law of conservation of normalized area in phase space" is derived for the propagation of the (static) oscillation through the interior to the surface. In this way it is shown that the mass M and radius R execute out-of-phase oscillations as  $\ln \rho_0$  is increased.

As background for the physical interpretation of the infinite number of oscillations in the critical mass as a function of the central density, we recall in chapter vi the history of our knowledge of the curve  $M=M(\rho_0)$ . Attention focuses here particularly on the points of principle that came to light in the earlier work. Landau's 1932 order-of-magnitude reasoning is reviewed, according to which a sufficiently large collection of cold matter cannot sustain itself against gravitational collapse. The same elementary analysis also shows that there ought to be two configurations just at the point of instability against collapse—one with a density of the order of  $10^{10}$  g/cm³, but both, remarkably enough, with masses of the order of the mass of the Sun. In 1935 Chandrasekhar determined equilibrium configurations of the model of a degenerate electron gas, a model valid for densities from  $10^4$  to  $10^7$  g/cm³. In 1939 Oppenheimer and Volkoff adopted the model of a degenerate neutron gas and found for the first time one of the two points of instability predicted by Landau, the one at the higher central density ( $\sim 10^{10}$  g/cm³). In 1956 Schatzman, going back to the model of a degenerate electron gas, obtained a first indication of the location of

the first Landau point of instability. In 1958 Harrison, Wakano, and Wheeler formulated the concept of "cold matter, catalyzed to the end-point of thermonuclear evolution." They put together all available theoretical information to construct an approximation, as close as they knew how to construct, to the equation of state of cold, catalyzed matter. For the first time from a single equation of state, as employed in the general-relativity equation of hydrostatic equilibrium, they were able to determine the masses and central densities of both of the critical points predicted by Landau, as well as the properties of the third critical configuration ( $\rho_0 \sim 3 \times 10^{13} \text{ g/cm}^3$ ) marking the return to stability on the way from one Landau configuration to the other. The important features of the entire family of equilibrium configurations are summarized in Figures 5, 6, and 7, as obtained in the 1957-1958 calculations of Wakano and in Harrison's 1964 extension of these results to higher densities. Methods of integration and tables of results appear in Appendix A. Among all equilibrium configurations, the following are calculated to show the extremes of binding; (1) the smallest increase in mass-energy per unit of mass brought in from infinity, 0.845, for a central density of 3 × 10<sup>16</sup> g/cm<sup>3</sup>; (2) the smallest ratio of total mass-energy to mass before assembly, 0.974, for  $\rho_0 = 7 \times 10^{15} \,\mathrm{g/cm^3}$ ; and (3) the greatest ratio of total mass-energy to mass before assembly, 1.095, for p<sub>0</sub> = 8 × 1017 g/cm3,

Chapter vii takes up the stability analysis of equilibrium configurations. Stability is discussed in terms of the frequency (stability!) or growth constant (instability!) of the characteristic acoustical modes  $(n=1,2,3,\ldots)$  of purely radial, spherically symmetrical, oscillation of the system. Chandrasekhar's procedure, by which in principle one can determine these frequencies, is outlined. An independent derivation of this procedure from the second variation of mass-energy for fixed baryon number (given independently by W. J. Cocke and by Thorne) is presented in Appendix B. What indications one has had in limited density regions as to the stability of the lowest mode (n=1) of acoustical vibration are reviewed. Also reviewed are 1962 considerations of Zel'dovich showing that, for a certain range of central densities beyond the higher Landau critical point, an equilibrium configuration, while stable against any one-at-a-time removal of Fe<sup>56</sup>, is unstable in principle—that is, unstable insofar as its energy content is concerned—against

a collective transformation in which it disperses into free Fe<sup>56</sup> atoms.

We describe a dynamical system considered by Einstein in 1939 which shows this same phenomenon of energy excess in the large with stability of the orbit of each particle individually; a collection of particles moving in circular orbits, without collision, at speeds close to the speed of light, and held in orbit by the gravitational field of the assembly as a whole. The simplest configurations of this kind form a one-parameter family (Table 6). For the most tightly bound of these configurations the ratio of total mass-energy to mass, at rest and before assembly, is 0.961; whereas the same ratio is 1.027 for the configuration with the highest energy excess.

A third example of a system with energy excess is also discussed—a geon, or collection of electromagnetic energy held together by its own gravitational attraction. In all three examples—the cold, catalyzed stars, Einstein's cloud of particles, and the geon—the energy excess traces back to the same source: to particles or radiation traveling close to or at the speed of light.

The concept of energy excess is used to explain the infinite number of maxima and minima in the curve of equilibrium mass  $M^*$  as a function of central density  $\rho_0$ . With increasing central density a larger and larger portion of the deep interior— $r \sim (\rho_0^*)^{-1/2}$ —is raised to relativistic Fermi energies. Conditions there become "geon-like" and the matter acquires excess energy. This portion of the medium is teetering between explosion and gravitational collapse. An acoustical mode is or is not coupled to this decisive degree of freedom according to whether it has only one zone of density decrease in the critical region of high density or many alternating zones of density increase or decrease in this region. In this way one finds it possible to understand why the number of modes which

are unstable increases at high central density as  $\ln \rho_0$ , and why the equilibrium radius

rises and falls periodically with  $\ln \rho_0$ .

The principal theorems deal with the following: Theorem 14, the configuration of tightest binding; Theorem 15, the value of dM\*/dA as related to mass and radius; Theorem 16, the coincidence of maxima and minima of  $M^*$  ( $\rho_0$ ) and A ( $\rho_0$ ); Theorem 17,  $dM^*/d\rho_0 = 0$  as the necessary and sufficient condition for an acoustical mode to change stability; Theorem 18, the correlation between stability and chemical potential; and Theorem 19, the law of variation of mass-energy near a critical point. Equation (155) gives the law of change of the frequency of the critical acoustical mode at a critical point (maximum or minimum in  $dM^*/d\rho_0$ ). The stability of all the radial acoustical modes

is diagnosed in an unambiguous way and indicated on Figures 5, 6, and 7.

Why a sufficiently compacted system is unstable against gravitational collapse is further clarified by considering (chap, viii) configurations of uniform density. This type of configuration has a unique feature. A clean separation can be made, in the calculation of the mass-energy, between those features which have to do with (1) short-range forces associated with compression and (2) long-range forces associated with gravitation. In consequence of this separation it is possible to construct a "slide rule" to calculate, for a given baryon number A, the mass-energy M\* as a function of the degree of compaction ("potential energy-curve for gravitational collapse"). One portion of the slide rule is constructed once and for all from the general-relativity theory of gravitation. It contains no reference to the equation of state. That appears on the other portion of the slide rule, a curve of log ρ (gm/cm<sup>3</sup>) as a function of log (baryons/cm<sup>3</sup>). This separation of factors allows one to see and prove that no equation of state which is compatible with causality and with freedom of matter from microscopic collapse can save a system from having a configuration which is unstable against collective gravitational collapse.

Also given in chapter viii are curves for the gravitational-collapse potential as computed via the "slide rule" or otherwise from the Harrison-Wheeler equation of state for selected values of the baryon number A. There is no barrier against gravitational collapse for a system containing more baryons than a certain critical number,  $A_{\rm crit} \sim 10^{57}$ . For smaller A there is a barrier. Its height increases with decreasing A. The height reaches a maximum for  $A \sim A_{crit}/4$ . It decreases for still smaller A. To bring an amount of matter of the order of 1600 tons ( $A \sim 10^{33}$ ) to the summit of the collapse barrier is calculated, on one assumption about the equation of state (Fermi gas), to require a compaction to ~10<sup>-11</sup> cm and 10<sup>49</sup> g/cm<sup>3</sup> and an input of mass-energy of compression of the order of  $10^{17}$  g. This barrier is enormously smaller than the barrier for  $A \sim A_{exis}/4$  but also enormously higher than any energy which it is technologically feasible to supply. The 10-11 cm extension, the 1049 g/cm3 density, and the 1017 g of mass-energy after compression mark the smallest system ( $A = A_{quantum}$ ) to which one can apply considerations of classical general relativity without having to confront the new features called for by a proper quantum analysis.

An alteration in the equation of state leaves these three numbers unchanged and affects only the estimates of 1600 tons and  $A_{\rm quantum} \sim 10^{33}$  for the smallest system whose collapse

is subject to treatment by classical general relativity.

Chapter ix treats the assumptions contained in the idea of equation of state of cold, catalyzed matter: a subsystem which (1) has reached the "end point of thermonuclear evolution," (2) is electrically neutral, (3) is "neutrino-neutral," (4) contains at no point any relative streaming velocities out of which energy can be extracted, (5) is subject to gravitational fields small compared to 1028 cm/sec2, (6) is under the influence of inhomogeneities in the gravitational field or "tide-producing forces" or a Riemannian curvature of space smaller in order of magnitude than the inverse square of the Compton wavelength. The transition is traced out in detail between small A systems, where one speaks of packing fraction and where the concept of an equation of state is not appropriate, to systems containing so many baryons that this statistical concept makes sense. The alternative thermodynamical potentials suitable for describing a relativistic equation of state are reviewed. The difference between a " $\gamma$ -law equation of state" in relativistic and non-relativistic theory is brought out. An asymptotic quantity

$$\gamma_{\text{asym}} = \lim_{\rho \to \infty} d \ln \rho / d \ln n$$

is defined. The limitations imposed on  $\gamma_{asym}$  by the condition that matter be stable against microscopic collapse ( $\gamma_{asym} > 1$ ) and by the principle of causality (velocity of sound less than velocity of light;  $\gamma_{asym} < 2$ ) are spelled out. Zel'dovich's "soft-hard-core" model of nucleon-nucleon repulsions is described as an argument that the limit  $\gamma_{asym} \rightarrow 2$  is in

principle conceivable.

Chapter x turns from the general principles underlying the concept of the equation of state to the detailed tracing-out of the unique and universal equation of state of cold, catalyzed matter as best it can be evaluated from present-day knowledge. Chapter x presents an extensive table of values of pressure, density of mass-energy, and number density of baryons. Analytic fits to the tabulated numbers are given such as are suitable for use in electronic-computer integrations of the equation of hydrostatic equilibrium. Past work on the problem of the equation of state is recapitulated. The basis for the derivation of the present Harrison-Wheeler equation of state is described, regime by regime, from densities a few per cent more than that of iron up to nuclear densities and beyond.

Chapter xi, the final portion of the report, turns from statics to dynamics. The question is raised why one should be concerned about collapse to impossible densities from a configuration of time symmetry when the very words "time symmetry" imply a start from impossible conditions. However, a closer analysis of the dynamics near the summit of the collapse barrier ( $A < A_{crit}$ !) leads to Theorem 24, according to which the timesymmetric motion, after the moment of time symmetry, gives an arbitrarily good representation of collapse from infinity. A detailed review is given of the collapse of a cloud of dust from a momentarily static configuration of uniform density to indefinitely high density. The smooth join between the Friedmann 4-geometry inside the collapsing cloud and the Schwarzschild 4-geometry outside is depicted graphically. The selection of one spacelike hypersurface through this 4-geometry, or some such hypersurface, or any such hypersurface, is recalled to be the generalization of what one does in Newtonian mechanics when he selects a time, some time, any time at which to observe a system. Throughout this dynamics the mass-energy, M, of the system as observed from outside (4-geometry, deflection of light, motion of planets) remains constant. Yet appropriate spacelike slices through the 4-geometry are shown to manifest smaller mass-energies M<sub>1</sub> (smaller coefficient of 1/r in the asymptotic representation of the 3-geometry at large distances). One finds in this way for the first time the relation (Theorem 36) between the analysis of spherically symmetric configurations which are momentarily static, and which have mass-energy  $M_1$  less than M, and the dynamics of a system of mass-energy M which contains the same number of baryons. The quantity  $M_1$  reveals itself as the sum of rest-mass energy, compressional energy, and gravitational energy, and therefore in effect the potential energy of the given configuration. From this potential the kinetic energy is found by taking the difference  $M-M_1$ . Thus one finds a solid foundation for the concept of potential-energy-curve in treating gravitational collapse. One sees in what a subtle sense the geometry of the collapsing cloud of matter does and does not approach pinch-off from the geometry of the surrounding space.

It has often been noted that in collapse each region in the interior loses the ability to emit energy by way of its retarded radiation field well before the density of energy in that region, as calculated classically, has risen to infinity. It is shown that advanced potentials do not help to bring energy out of the collapsing matter and do not save the

geometry, as calculated classically, from developing infinite curvature.

It is recalled how many points of connection there are between the dynamics of the

collapse and the theory of the expansion and recontraction of a model universe, the stellar system serving as a sealed down but otherwise realistic model for a major segment of the closed space of Einstein's standard cosmology. In both cases the classical analysis shows itself to be faulty beyond a certain stage because it predicts conditions patently

impossible: infinite density and infinite curvature.

Therefore, it is concluded that one cannot believe the classical prediction that infinite curvature prevents radiation from escaping from the region of collapse. Instead, one must necessarily go over in the final stages of contraction to a proper quantum-mechanical description, in which one speaks not deterministically, but of the probability amplitude \$\psi\$ for this, that, or the other geometry. Associated with such a description are probability amplitudes for the system to emerge from the reaction in one or another specific

outgoing channel ("S-matrix mode of description").

If the number of baryons in the universe has not had for all time some inexplicable value, then it would seem reasonable to think of baryon number as a dynamical variable with its own laws of change. Such a change is most naturally conceived of as taking place in a region of density 1049 g/cm3 or higher, whether in a collapsing collection of matter or in the expansion or recontraction of the universe. One is therefore led to postulate (Proposition 40) that in gravitational collapse the number of baryons which remain in identifiable form must be subject to change. The changes of topology-and the quantum mechanical indeterminacies-that are associated with the final stages of collapse put difficulties in the way of applying or even stating a principle of conservation of baryons with any well-defined significance. On the other hand, it does make sense to speak of the number of baryons that have disappeared in the sense that they have lost the possibility of sending signals to a faraway observer.

A cold, catalyzed system containing  $A > A_{\text{crit}}$  baryons, started from rest in a spherically symmetrical configuration, will straightaway start to collapse. When  $A < A_{erit}$ , the potential-energy barrier against collapse must be surmounted or tunneled. The standard quantum-mechanical theory of barrier penetration is used to estimate the probability for this tunneling process. Calculations based on the model of a collective collapse of the system as a whole are shown to lead to a gross overestimate of the time for barrier tunneling. In bringing about collapse it is far easier for a small number of baryons to go through the potential barrier together (as in alpha-particle decay of Sm147;  $T_{1/2} = 1.5 \times 10^{11} \text{ yr}$ ) than for the whole system collectively to implode (cf. the collective phenomenon of fission of Sm<sup>147</sup>;  $T_{1/2} > 10^{25} \text{ yr!}$ ) Regardless of the precise value of the rate constant it is concluded that there exists in nature a new kind of elementary particle transformation, spontaneous gravitational collapse; and that, associated with this process all matter must manifest, however weakly, a new form of radioactivity, in which the baryon number changes.

The association of particles in this process of disappearance of baryons implies a similar association of particles in the time-reversed process where baryons first come into evidence. This associative character of the new mechanism ("associative transmigration") gives an opportunity for the baryon or antibaryon character of the matter already present in the early days of the universe to influence the particle or antiparticle quality of particles then in process of appearance. It is noted that this autocatalytic nature of the process of batchwise appearance conceivably offers an explanation for the one-sided

character of the matter in the universe as presently known.

#### REFERENCES

Ambartsumyan, V. A. 1958, "On the Evolution of Galaxies," in Onzieme Conseil de Physique Solvay, La Structure et l'évolution de l'univers (Brussels: Stoops), esp. pp. 265-267.
Burbidge, G. R. 1962, Ann. Rev. Nuclear Sci., 12, 507.
Burbidge, G. R., Burbidge, E. M., and Sandage, A. R. 1963, Ap. J., 137, 1005.

Chandrasekhar, S. 1934, Observatory, 57, 373.

. 1935, M.N., 95, 207.

- 1939, Introduction to the Study of Stellar Structure (Chicago: University of Chicago Press).

Emden, R. 1907, Gaskugeln (Leipzig: Teubner).

Field, G. 1964, Ap. J., 140, 1434.
Greenstein, J. L., 1963, Sci. Amer., 209, No. 6, 54.
Greenstein, J. L., and Schmidt, M. 1964, Ap. J., 140, 1.
Harrison, B. K., Wakano, M., and Wheeler, J. A. 1958, in Onzième Conseil de Physique Solvay, La Structure et l'évolution de l'univers (Brussels: Stoops).

Hoyle, F., and Fowler, W. A. 1963a, M.N., 125, 169. . 1963b, Nature, 197, 533.

Hoyle, F., Fowler, W. A., Burbidge, G. R., and Burbidge, E. M. 1964, Ap. J., 139, 909.

Iben, I. 1963, Ap. J., 138, 1090.

Landau, L. D. 1932, Phys. Zs. Sowjetenian, 1, 285.

Landau, L. D., and Lifshitz, E. M. 1951, The Classical Theory of Fields (1st ed.; Reading, Mass.: Addison-Wesley Publishing Co.; 2d ed., 1959).
. 1958, Statistical Physics, trans. E. Peierls and R. F. Peierls (Reading, Mass.: Addison-Wesley

Publishing Co.; London: Pergamon Press).

Lynds, C. R., and Sandage, A. R. 1963, Ap. J., 137, 1005.

Michel, F. C. 1963, Ap. J., 138, 1097.

Oppenheimer, J. R., and Serber, R. 1938, Phys. Rev., 54, 530.

Oppenheimer, J. R., and Volkoff, G. 1939, Phys. Rev., 55, 374.

Robinson, I., Schild, A., and Schucking, E. L. (eds.). 1964, Quasi-stellar Sources and Gravitational Collapse (Chicago: University of Chicago Press).

Smith H. and Hoffleit D. 1963, Nature 198, 650.

. 1964b, "Geometrodynamics and the Issue of the Final State," in Relativity, Groups and Topology, ed. C. and B. DeWitt (New York: Gordon and Breach).

Zel'dovich, Ya. B. 1962, Zhur. eksp. Teor. Fiz. (USSR), 42, 641 (English translation in Soviet Phys.— J.E.T.P., 15, 446).

## MASS-ENERGY ON A SPACELIKE HYPERchapter 2 SURFACE OF TIME SYMMETRY

#### HYPOTHESES ACCEPTED IN GENERAL RELATIVITY

Gravitation is vital in the energy balance of the configurations of interest. In the most compact configurations the gravitational energy is a large fraction of the total energy. Einstein's standard general relativity will be accepted as a guide into this state of affairs. Between the predictions of Einstein's theory and such limited observations as exist, no purported discrepancy has ever been substantiated, as one hardly needs to recall. Neither has any argument of principle against Einstein's theory ever been sustained. Nor is there any rival set of ideas available which is at all comparable to general relativity in comprehensiveness, scope, and simplicity. Thus it is natural that work on the problem of the critical mass and gravitational collapse over the last 30 years has taken Einstein's theory as its foundation. Today there is less reason than ever to depart from this philosophy. Therefore the following standard ideas are accepted here as working hypotheses:

#### Hypothesis 1, Riemannian Geometry

Short of the level at which quantum fluctuations in the geometry become relevant, the geometry of the physical world is that of a classical Riemannian four-dimensional manifold. The spacetime interval CD between any two nearby events C and D has a well-defined meaning, relative to the standard interval AB between two nearby fiducial events A and B ("geometrodynamical standard meter"), independent of any coordinates that are or are not used to label the points of spacetime, independent of the large or small distance from AB to CD, independent of the curvature of the intervening spacetime, and independent of the route through spacetime by which the intercomparison is carried out.

# Hypothesis 2. Equivalence Principle; Locally Lorentz Character of Spacetime

The geometry of spacetime—again at the classical level of analysis—is everywhere locally regular in this sense: At any arbitrary event E the local geometry is tangent to a suitably chosen flat reference geometry ("tangent space") of the standard Lorentz (-+++) character.

Commentary.—The geometrical content of this hypothesis stands independent of the choice or even the use of any coordinate system. However, if one chooses to employ a coordinate system, then there will be some coordinate systems in which light rays and material particles appear to undergo acceleration. That this acceleration is the same for all kinds of matter is shown with great accuracy by the Dicke-Eötvös experiment.<sup>2</sup> Einstein's principle of the equivalence of gravitation and inertial (accelerational) forces

<sup>&</sup>lt;sup>1</sup> For more on the implications of this hypothesis, and the evidence for it, see Marzke and Wheeler (1964).

<sup>&</sup>lt;sup>2</sup> For a recent account see Dicke (1964),

can be regarded for the present purpose as stating that there always exist choices of the coordinate system which make the apparent accelerations of neutral test particles reduce to zero in the given locality.

#### Hypothesis 3. Geodesic Hypothesis

Light rays and neutral particles follow geodesics through spacetime insofar as the wavelength of the light or particle is sufficiently short compared to the scale of the curvature of the geometry and the other relevant physical dimensions to permit so detailed a description of the motion through space and time.<sup>3</sup>

#### Hypothesis 4. Einstein's Field Equations

The curvature of spacetime is connected with the tensor T<sub>µ</sub>, of stress, energy flow, and energy density by the equation (for background see, e.g., Landau and Lifshitz [1962])

$$R_{\mu\nu} - \frac{1}{2} g_{\mu\nu}R = 8\pi (G/c^4)T_{\mu\nu}$$
. (1)

Commentary.—General relativity, or "geometrodynamics," is so geometrical in character that it is often the custom—and here also in some places a convenience—to measure familiar physical quantities in purely geometrical units, as indicated by a few examples collected in Table 2.

We now wish to apply Einstein's theory to determine the energy of a collection of

#### TABLE 2

RELATION BETWEEN CERTAIN PHYSICAL QUANTITIES AS MEASURED IN THE CONVENTIONAL UNITS (cm, g, sec) AND THE SAME PHYSICAL QUANTITIES (DENOTED BY ASTERISES) AS EXPRESSED IN PURELY GEOMETRICAL TERMS OF LENGTHS, AS APPROPRIATE IN GENERAL RELATIVITY\*

Quantity	Conventional Units	Geometrized Units
Time. Mass. Mass of sun. Mass of H atom. (1/56) mass of Fe <sup>86</sup> Energy Density. Typical order of magnitude for nuclear density.	t (sec) M(g) $M \odot = 1.987 \times 10^{10} g$ $M_B = 1.6734 \times 10^{-24} g$ $\mu_s = 1.659 \times 10^{-24} g$ E(erg) $\rho(g/cm^3)$ $\rho = 2 \times 10^{14} g/cm^3$	$t^*$ (cm) = $ct$ = 2.997925×10 <sup>10</sup> $t$ $M^*$ (cm) = $GM/c^3$ = 0.742×10 <sup>-28</sup> $M$ $M_{\odot}^*$ = 1.474×10 <sup>9</sup> cm $M_{H}^*$ = 1.242×10 <sup>-32</sup> cm $\mu_*^*$ = 1.231×10 <sup>-32</sup> cm $M^*$ (cm) = $GE/c^4$ = 0.8258×10 <sup>-49</sup> $E$ $\rho^*$ (cm <sup>-2</sup> ) = $G\rho/c^2$ = 0.742×10 <sup>-28</sup> $\rho$ $\rho^*$ = 1.48×10 <sup>-14</sup> cm <sup>-2</sup>
The characteristic or Planck length	$L^* = (hG/c^3)^{1/2} = 1.616 \times 10^{-23} \text{ cm}$	L*=1.616×10 <sup>-33</sup> cm
The characteristic or Planck mass	$m^* = (\hbar c/G)^{1/2} = 2.177 \times 10^{-6}$ g	$m^{**}=L^*=1.616\times 10^{-10}$ cm
Characteristic density of en- ergy or mass associated with quantum fluctuations	$\hbar c/L^{*a} = 4.64 \times 10^{114} \text{ erg/cm}^3$ $\hbar/cL^{*a} = 5.16 \times 10^{93} \text{g/cm}^3$	L*-2=3.83×10 <sup>th</sup> cm <sup>-2</sup>

<sup>\*</sup> Sometimes asterisks are omitted from the text to cut down on notational baggage. Conversion factors are based on "New Values for the Physical Constants as Recommended by the National Academy of Sciences-National Research Council," Physics Today (February, 1964), p. 48.

h The following three characteristic quantities are also denoted, in spite of possible confusion, by asterisks.

<sup>&</sup>lt;sup>3</sup> Commentary.—(1) These geodesics provide a means actually to calibrate (see n. 1) an unknown interval at one place in spacetime in terms of a standard interval somewhere else, without any appeal to measuring rods or clocks of atomic constitution. (2) The transformation of the geodesic principle from an independent hypothesis (as listed here for the sake of brevity) to the status of a deduction from the field equations of general relativity, through the work of Einstein, Grommer, Infeld, Hoffmann, and others, is a development of great importance to which, however, only passing reference is appropriate here.

matter interacting by way of the long-range forces of gravitation. For this purpose we shall limit attention in the earlier sections of this report to configurations which are momentarily static—whatever they may be doing in the future or were doing in the past. The gravitational field—and therefore the geometry—associated with this matter will also be momentarily static. This circumstance will greatly simplify the analysis. The 4-geometry will be symmetric in time between past and future with respect to the moment when the configuration is static. In other words, this static phase of the system will describe what may be termed a spacelike hypersurface, or 3-geometry, of time symmetry. From an analysis confined to this hypersurface, happily, the theory of gravitation will allow the calculation of the mass-energy of the configuration. Therefore, one configuration can be compared with another as regards total content of energy—where energy manifests itself to the outside world as mass, governing the motion of planets and determining the deflection of light, Among all configurations it will be possible to single out that one, or those particular ones, which—for a given baryon number—extremize the mass. Configurations which are extremal in this sense will be shown to be characterized by a characteristic pressure gradient. This pressure law is identical with the generalrelativity version of the law of hydrostatic equilibrium. But now, in preparation for this treatment of mass and of mass extremization, let that part of general relativity be sorted out which is relevant for analyzing conditions on a spacelike hypersurface.

### GEOMETRODYNAMICS IN BRIEF

Theorem 1. (Geometrodynamics in brief!) On any smooth spacelike hypersurface which slices through a 4-geometry that satisfies Einstein's field equations, the scalar curvature (\*) R of the geometry (\*) G intrinsic to this hypersurface, \* plus the second invariant K<sub>2</sub> of the extrinsic curvature of this hypersurface relative to the enveloping (\*) G, are given by the density of mass-energy as measured in the synchronous (see Landau and Lifshitz [1962]) local Lorentz reference system.

$$^{(3)}R + K_2 = 16\pi\rho^*$$
 (2)

Commentary.—For proof of the theorem see Fourès (1952, 1956). Equation (2) is analogous to two of the Maxwell equations, div  $E = 4\pi\rho_x$ , div B = 0. If one demands that these equations be fulfilled not only on one spacelike hypersurface through a given point P, but on every spacelike hypersurface through every point, one recovers all of Maxwell's equations. Similarly, from equation (2) one recovers all of Einstein's field equations—hence the designation, "geometrodynamics in brief!"

### TIME SYMMETRY

Definition of time symmetry.—A spacelike hypersurface is said to be a hypersurface of time symmetry when the dynamical history and the 4-geometry on the future side of this hypersurface is the time-reversed image of the dynamical history and the 4-geometry in

\*Terminology: (1) Scalar curvature of the geometry intrinsic to the hypersurface. From the chosen point P on the hypersurface <sup>(1)</sup>G construct geodesics of proper length ε radiating out in all directions. Take the proper surface of the resulting 2-sphere, evaluate (18/ε\*)[1 — (surface)/4πε²], and go to the limit ε → 0 to get <sup>(2)</sup>R. (2) Extrinsic curvature. Let the foregoing 2-sphere be composed of dust particles too minute to exert any attraction on one another. Let each particle be at rest in the isochronous Lorentz frame which is tangent to the hypersurface at the point where that dust particle sits. Follow these dust particles for a common proper time τ. The new configuration is in general no longer a 2-sphere but an ellipsoid. The strain tensor, divided by ¬τ, in the limit τ → 0, defines the extrinsic curvature of the hypersurface, a tensor K<sub>4</sub>I. The second invariant of the extrinsic curvature is

$$K_2 = (K_i^i)^2 - K_i^j K_j^i = (TrK)^2 - TrK^2$$
.

\* See also a chapter by her in Witten (1962): (this book is referred to hereinafter as "GICR"). For a formulation and proof of the converse point—that all of the content of general relativity is summarized in, and can be derived from, the Fourès condition, see Wheeler (1962).

the past. Examples: (1) universe at state of maximum expansion; (2) collection of matter which is momentarily stationary—and the associated geometry—before re-explosion or gravitational contraction has got under way; (3) (special case of example [2]) collection of matter in static equilibrium under its own gravitational attraction. Feature: The symmetry with respect to time reversal implies that the hypersurface of time symmetry has zero extrinsic curvature with respect to the enveloping 4-geometry;  $K_i = 0$ ;  $K_2 = 0$ . Therefore equation (2) reduces to the form

$$^{(3)}R = 16\pi\rho^*$$
 (3)

Moreover any configuration of time symmetry—i.e., any static configuration—compatible with this "initial-value equation" is a legitimate starting point for a dynamical analysis. The remaining field equations of Einstein impose no further condition on the choice of this initial configuration itself; they tell only how this configuration will evolve in time.

Definition of Schwarzschild r-coordinate.—Let (\*)g be a 3-geometry of spherical symmetry. This symmetry implies that the proper distance between any two nearby points in (\*)g can be expressed in the form

$$ds^2 = e^{\lambda(r)}dr^2 + r^2(d\theta^2 + \sin^2\theta d\phi^2), \qquad (4)$$

The coordinate r defined by this equation will be called the Schwarzschild r-coordinate, and  $e^{\lambda(r)}$  will be called the Schwarzschild correction factor. The requirement that the 3-geometry be everywhere locally Euclidean makes it necessary that  $\lambda(r)$  vanish at r=0; otherwise the geometry there would be "conical,"

### GEOMETROSTATICS: MASS-ENERGY ON A SPACELIKE HYPERSURFACE OF TIME SYMMETRY; AND A LOOK BEHIND THE SCENE

Theorem 2. The total mass-energy of any spherically symmetric configuration "at a moment" (i.e., "on a hypersurface") of time symmetry is given by the equation

$$M^* = \int^{\text{outer boundary}} \rho^*(r) 4\pi r^2 dr. \qquad (5)$$

Proof.-Write the correction factor of Schwarzschild in the form

$$e^{\lambda(r)} = [1 - 2m^*(r)/r]^{-1},$$
 (6)

At this point this equation amounts to no more than a definition of  $m^*(r)$ . The advantage of the definition is the simple form taken by the intrinsic curvature of the 3-geometry of equation (4):

$$(3)R = 4r^{-2}dm^*(r)/dr.$$
 (7)

From the initial value equation it follows by integration that the "effective mass" m\*(r) inside a sphere of Schwarzschild radius r is

$$m^*(r) = \int_0^r \rho^*(r) 4\pi r^2 dr$$
. (8)

The quantity  $M^*$  (=  $m^*$  evaluated for r at the outer boundary of the configuration) has to be identified with the total mass-energy of the system because it governs the geometry exterior to the matter (Schwarzschild geometry, Schwarzschild mass!). It directly fixes such observables as the period of a planetary orbit, the precession of the perihelion, and the gravitational bending of a ray of light.

Commentary.—The volume element in the integrals (5) and (8) is not the proper

<sup>\*</sup> For the definition and the first fruitful employment of the concept of time symmetry see Brill (1959).

volume. Therefore  $m^*(r)$  is not the "proper mass" inside r. Moreover, while no one can be prevented from defining and computing a "proper mass" integral-different of course from expression (5)—that concept has no utility in the theory of gravitational equilibrium, nor has it any immediate observational significance whatsoever. The "gravitationally effective mass" differs from such a "proper mass" on two accounts: (1) The quantity  $\rho^*(r)$  in equation (8) is not simply the number density of baryons n(r) multiplied by the mass per baryon in cold, catalyzed matter at zero pressure ( $\frac{1}{66}$  of the mass of one Febb atom). The density exceeds that product by an amount equivalent to the massenergy of compression. (2) What is being integrated in equation (5) is not density  $\rho^*(r)$ itself, but density multiplied by a factor which is less than 1. This factor in effect corrects for the negative gravitational potential energy of the interaction of the mass with itself, Thus, the proper volume (eq. [4]) is  $4\pi r^2[1-2m^*(r)/r]^{-1/2}dr$ . Hence the factor which multiplies the proper volume—and which in this sense constitutes the integrand—is  $\rho^*(r)[1-2m^*(r)/r]^{1/2}$ , a quantity evidently lower than  $\rho^*(r)$ . Equation (5), superficially identical with the non-relativistic integral for the mass, is evidently quite subtle. It allows both for the work of compression (positive) and the potential energy of gravitation (negative).

In conclusion, the integral (5) provides a means to determine the total energy of any

momentarily static configuration of spherical symmetry.

### REFERENCES

Brill, D. 1959, Ann. Phys., 7, 466.

Dicke, R. H. 1964, in Relativity, Groups and Topology, ed. B. and C. DeWitt (New York: Gordon and Breach).

Fourès, Yvonne. 1952, Acta Math., 88, 141. -. 1956, J. Rational Mech. Anal., 5, 951.

Landau, L. D., and Lifshitz, E. M. 1951, The Classical Theory of Fields (1st ed.; Reading, Mass.: Addison-Wesley Publishing Co.; 2d ed., 1962).
Martke, R. F., and Wheeler, J. A. 1964, Gravitation and Relativity, ed. H. Y. Chiu and W. F. Hoffmann

(New York: W. A. Benjamin), chap. iii. Wheeler, J. A. 1962, Geometrodynamics (New York: Academic Press).

Witten, L. (ed.), 1962, Gravitation: An Introduction to Current Research (New York: John Wiley & Sons).

# HYDROSTATIC EQUILIBRIUM AND chapter 3 EXTREMAL MASS-ENERGY

A specified number of baryons, A, can be disposed in a configuration of spherical symmetry in any number of ways. For example, the number density of baryons, n(r), may be chosen to be everywhere constant and small inside a sphere of some large radius R, and zero outside. Or a configuration may be selected for attention in which the number density falls off as a Gaussian function of the coordinate r. For each and every momentarily static configuration of spherical symmetry, equation (5) tells the energy of the system. Is there any configuration for which this energy is an extremum? And, if so, how does the density vary with position from place to place in such an extremal configuration? The answer to this question is given by the following theorem.

### THE THEOREM

Theorem 3. Among all momentarily static and spherically symmetric configurations of cold, catalyzed matter which contain a specified number of baryons,

$$A = \int (\text{baryon density}) d(\text{proper volume})$$
  
=  $\int n(r) 4\pi r^2 [1 - 2r^{-1}m^*(r)]^{-1/2} dr$ , (9)

that configuration (or configurations—if any!) which extremizes the mass as sensed from outside,

 $M^* = \int \rho^*(r) 4\pi r^2 dr$ , (10)

satisfies the Tolman-Oppenheimer-Volkoff (TOV) general-relativity equation of hydrostatic equilibrium,1

$$-dp^*/dr = \frac{(\rho^* + p^*)[m^*(r) + 4\pi r^*p^*(r)]}{r[r - 2m^*(r)]}.$$
 (11)

Proof of the extremum principle.—Employ what in hydrodynamics would be known as the Lagrangian approach. Define a particle label, or baryon number parameter a, in the following way: (1) all baryons which lie on a sphere of the same r value have a common a value; (2) this value is equal to the total number of baryons which lie inside this sphere. Then the trial configuration is specified by giving the Schwarzschild coordinate r as a function of a. Any small change which preserves the spherical symmetry is specified by giving the displacement

$$\delta r = \delta r(a)$$
. (12)

<sup>&</sup>lt;sup>1</sup> See Tolman (1934, pp. 242–243; 1939) and Oppenheimer and Volkoff (1939). We have been told that in unpublished work at Cambridge in 1935 John von Neumann integrated the general relativity equation of hydrostatic equilibrium for the special case  $p^* = \rho^*/3$ . A variational treatment based on the Eulerian formulation of hydrodynamics (coordinates attached to points in space rather than particles) has been developed independently by Cocke (1964).

The problem is (1) to find how much this redistribution of the A baryons alters the mass-energy of the system and (2) what is the feature of a configuration which has extremal mass-energy  $M^*$ , in the sense that every arbitrary small first-order variation  $\delta r(a)$  produces zero first-order variation in  $M^*$ . It is assumed that one knows the equation of state of the material; that is (see chap. ix), (1) the functional relation between density of mass-energy and number density of baryons,  $\rho^* = \rho^*(n)$ , and consequently (2) (from the first law of thermodynamics) the pressure,

$$p^* = \text{pressure} = -\frac{d\left(\text{energy per baryon}\right)}{d\left(\text{volume per baryon}\right)} = -\frac{d\left(\rho^*/n\right)}{d\left(1/n\right)} = \frac{nd\rho^*}{dn} - \rho^*. \tag{13}$$

The derivative  $d\rho^*(n)/dn$  occurs sufficiently frequently to deserve a name of its own:

$$\mu^* = (\text{chemical potential}) = d\rho^*/dn = (p^* + \rho^*)/n$$
. (14)

The procedure is to find the effect,  $\delta n$ , of the displacement  $\delta r$  on the density; the effect,  $\delta m^*$ , of this density change on the effective mass  $m^*(r[a])$  at each point in the interior; and from this the change  $\delta M^*$  in the total mass-energy of the configuration. The number density of baryons is

$$n(a) = \frac{d \text{ (number of baryons)}}{d \text{ (proper volume)}} = \frac{1}{4\pi r^2 [1 - 2m^*/r]^{-1/2} (dr/da)}.$$
 (15)

This quantity changes in a deformation partly by reason of changes in r (and in dr/da) and partly by reason of changes in the Schwarzschild correction factor, in which  $m^*$  appears. Thus

$$\begin{split} \delta n(a) &= -\frac{(1-2m^*/r)^{1/2}}{[4\pi r^2 (dr/da)]^2} \Big( 8\pi r \delta r \frac{dr}{da} + 4\pi r^2 \frac{d\delta r}{da} \Big) \\ &+ \frac{(m^*/r^2) \delta r - (\delta m^*)/r}{[1-2m^*/r]^{1/2} [4\pi r^2 (dr/da)]} \,. \end{split} \tag{16}$$

The effect of this density change on the mass shows less directly in  $m^*$  itself than in its derivative:

$$\frac{dm^*}{da} = \frac{d}{da} \int_0^{r(a)} \rho^* 4\pi r^2 dr = \rho^* 4\pi r^2 \frac{dr}{da}.$$
 (17)

The change in this derivative is

$$d(\delta m^*)/da = \delta(dm^*/da) = \mu^* \delta n(4\pi r^2 dr/da) + \rho^* [8\pi r \delta r(dr/da) + 4\pi r^2 (d\delta r/da)].$$
(18)

Insert into the right-hand side of equation (18) the expression for  $\delta n$  given by equation (16). In this way arrive at an equation for the "change,  $\delta m^*(a)$ , in the effective mass out to the a-baryon shell," of the form,

$$d(\delta m^*)/da + r^{-1}(1 - 2m^*/r)^{-1/2}\mu^*\delta m^* = T(a).$$
 (19)

Here the term on the right is fully specified by (1) one's original choice of trial configuration, r = r(a) plus (2) the small change,  $\delta r(a)$ , which one makes in this configuration; thus,

$$\begin{split} T(a) &= [\,r^{-2}m^*(\,1-2m^*/\,r\,)^{-1/2}\mu^* - 8\pi \,r\,(\,d\,r/\,d\,a\,)\,p^*\,]\,\delta\,r \\ &- 4\pi \,r^2p^*d\,(\,\delta\,r\,)\,/\,d\,a\;. \end{split} \label{eq:Taylor}$$

The differential equation (19) for the mass change has a standard form, with a standard type of solution. The one adjustable constant in the solution is fixed by the boundary condition  $\delta m^*(0) = 0$  (arising from the requirement that  $m^*(0)$  itself is zero). Thus one finds

$$\delta M^* (\equiv \delta m^* \text{ evaluated at the outer boundary, } a = A)$$

$$= \exp \left[ -\int_0^A r^{-1} (1 - 2m^*/r)^{-1/2} \mu^* da \right]$$

$$\times \int_0^A T(a) \exp \left[ \int_0^a r^{-1} (1 - 2m^*/r)^{-1/2} \mu^* da' \right] da.$$
(21)

Most of the terms in T(a) are expressed directly in terms of  $\delta r(a)$ , but the last term contains  $d(\delta r)/da$ . Integrate it by parts in equation (21), thus at last arriving at the expression for the change in total mass-energy as desired:

$$\begin{split} \delta M^* &= - \left( 4\pi r^2 p^* \delta \, r \, , \text{ evaluated at outer boundary} \right) \\ &+ \exp \Big[ - \int_0^A r^{-1} (1 - 2m^*/r)^{-1/2} \mu^* da \Big] \int_0^A \Big[ \left( dp^*/dr \right) \\ &+ \frac{(p^* + \rho^*)(m^* + 4\pi r^2 p^*)}{r \left( r - 2m^* \right)} \Big] \delta \, r(a) \exp \Big[ \int_0^a r^{-1} (1 - 2m^*/r)^{-1/2} \mu^* da' \Big] \\ &\times 4\pi r^2 (dr/da) \, da \; . \end{split}$$

Now narrow consideration from more general configurations to equilibrium configurations. Then, by definition, the  $\delta M^*$  of equation (22) must vanish to first order for all first-order displacements  $\delta r(a)$ . It follows (1) that the pressure  $p^*$  at the outer surface of the configuration must vanish and (2) that the pressure in the interior must satisfy the TOV equation (11), as was to be shown.

RELATION OF THE VARIATIONAL TREATMENT TO TOLMAN'S FIELD-THEORETICAL DERIVATION OF THE EQUATION OF EQUILIBRIUM; INTRODUCTION TO AN EXTENDED DISCUSSION

Commentary.—It has often been recognized that the integral of  $\rho^*4\pi r^2 dr$  gives the total mass-energy and that the integral of  $n4\pi r^2(1-2m^*/r)^{-1/2}dr$  gives the total number of particles (see, e.g., Landau [1932]; Tolman [1934, 1939]; Oppenheimer and Volkoff [1939]; Harrison, Wakano, and Wheeler [1958] [hereinafter referred to as "SEU"]; Laudau and Lifshitz [1951, 1958]; Zel'dovich [1962]). However, it does not seem to have been remarked before that these elementary principles, together with the machinery of the calculus of variations, lead directly to the general-relativity equation of hydrostatic equilibrium.<sup>2</sup> Nor is it at first clear how they can lead to this result. Tolman's derivation was founded on the entire system of Einstein's equations, not merely on the analysis of initial value data. He had to concern himself not with the geometry of space alone, but with the geometry of spacetime. This geometry is nevertheless simplified by the circumstance that it is both static and spherically symmetric:

$$d s^{2} = -\exp[\nu(r)] dt^{2} + \exp[\lambda(r)] dr^{2} + r^{2} (d\theta^{2} + \sin^{2}\theta d\phi^{2}).$$
 (23)

\* See, however, the valuable work of Cocke (1964). The present application of the calculus of variations is to be distinguished from the use of an action principle to derive the field equations of Einstein's general relativity—either in the absence of matter, as in many standard texts, or in the more difficult case where hydrodynamics and geometry interact (Taub 1954, 1963). It is also to be distinguished from applications of the calculus of variations to study small vibrations about a configuration of equilibrium (Chandrasekhar [1964]; see also Misner and Zapolsky [1964]). Vibrations have to do with variations in the configuration in space and in time, and therefore do not lend themselves to the present simple analysis of conditions on a single spacelike hypersurface. They require the more complicated treatment of Appendix B.

The new quantity in this expression is the second Schwarzschild correction factor,  $\exp \nu$  (for the correction of  $dt^2$ ) or  $\exp (\nu/2)$  (to be multiplied into dt to give the interval of proper time when dr=0,  $d\theta=0$ ,  $d\phi=0$ ). This quantity is less than unity. Outside of the static configuration it has the value

 $\exp(\nu/2) = (1 - 2M^*/r)^{1/2} = 1 - (M^*/r) + (general relativity corrections).$  (24)

THE RELATIVISTIC GENERALIZATION OF THE GRAVITATIONAL POTENTIAL AND ITS OBSERVATIONAL SIGNIFICANCE

The quantity  $\exp(r/2)$  is the relativistic generalization of the Newtonian concept of gravitational potential. To illustrate the meaning of this quantity, consider the following idealized experiment. Pass a pipe through the static configuration along a diameter. Take an electron of rest energy  $mc^2$  at infinite distance. Lower it slowly—e.g., by an idealized string—to a position of rest at the point r, then cut the electron loose from the string. View the electron in a local Lorentz frame. This frame is at rest relative to the electron at the moment the electron is cut free. Moreover, it falls with the same acceleration as does the electron; and it sees the electron free of all gravitational force (equivalence principle). Therefore the electron remains at rest in the local Lorentz frame; and its energy in that frame remains always at the value  $mc^2$ . At the moment when the electron is cut loose it is also at rest relative to the r,  $\theta$ ,  $\phi$  frame of reference. However, in that frame the energy of the electron is not  $mc^2$  but this amount corrected by the Schwarzschild coefficient; i.e.,

$$E = m c^2 \exp(\nu/2)$$
. (25)

The deficit between this quantity and the energy at infinity represents the work extracted from the electron by the end of the string as this particle is drawn in by the gravitational field:

Work done = Decrease in gravitational potential energy =  $m c^{z} [1 - \exp(\nu/2)]$ . (26)

Let the same point be stated in slightly different terms. Let two electrons, one positive, one negative, be lowered into the pipe at the point r. Let them be cut free and allowed to annihilate before thay have gathered any significant velocity of fall. The energy set free in the annihilation comes off in the local Lorentz frame as two photons, each of energy  $mc^2$ . However, as seen by far-away observers at rest relative to the center of attraction in the asymptotically flat Lorentz frame, the two photons, when they come off in the proper direction to escape out of the opposite ends of the pipe, are redshifted, each to energy  $mc^2 \exp(\nu/2)$ . Thus the difference between  $\exp(\nu/2)$  evaluated at the point r and evaluated at infinity (unity) measures the gravitational potential hill which the photons have to climb to escape.

### CASE OF COMPENSATING REDSHIFT AND BLUESHIFT

No violation of the law of conservation of energy is involved in these considerations. For example, let the  $e^+$  and  $e^-$  start at rest at great distances. Let them fall into the pipe from opposite ends and annihilate at the point r without having had the gravitational energy of fall extracted from them by way of "strings." Then the energy set free in the process of annihilation as observed in the local Lorentz frame will be more than  $2 \text{ mc}^2$ ; it will be  $2 \text{ mc}^2 \exp{(-\nu/2)}$ . However, the resulting bluer-than-normal annihilation photons will be redshifted on their way out to infinity to the normal energy of  $mc^2$  each, as expected.

The "pipe" is an idealized device introduced to separate the effects of gravitational forces from those of pressure. If gravitational forces alone acted, all of the matter would,

<sup>3</sup> Zel'dovich (1962) has objected to an earlier briefer discussion by three of us (B. K. H., M. W., J. A. W.) in SEU of the same point about the meaning of exp (v/2) because it did not seem to him to be

of course, collect at the origin. In actuality the existence of an equilibrium configuration of finite extent implies that a small element of matter, containing dA baryons, is indifferent to being moved from one point in the configuration to another. In other words, the energy required to produce these baryons at infinity and bring them in and inject them into the configuration at the point r is independent of where r lies inside the configuration.

### THE CONSTANCY OF THE INJECTION ENERGY

The injection energy, as observed in a local Lorentz reference frame momentarily at rest with respect to the matter at r, is given by the product

$$\mu^* dA$$
, (27)

where  $\mu^*$  is by definition the chemical potential.

Definition.—The chemical potential  $\mu^*$  is the mass energy which is added to a portion of a system which is in local thermal and pressure and reaction equilibrium—and in which gravitational forces have a negligible influence—when one more baryon (example 1: neutron; example 2: proton plus electron) is brought in from infinity. The chemical potential is calculable (eq. [14]; also chap. ix) from the equation of state  $\rho^* = \rho^*(n)$ , where  $\rho^*$  and n are the density of mass-energy and the number density of baryons, again as observed in the local Lorentz frame.

To identify the injection energy at different points in the medium, where there are different local Lorentz reference systems, reduce all energies to a common standard of reference; energies as measured in the asymptotically flat space far from the configuration, in that Lorentz reference system & which is at rest with respect to that center of attraction. Thus one arrives at Theorem 4.

Theorem 4. Throughout an equilibrium configuration the injection energy, referred to a "common market standard of energy" at infinity, has a common value

Injection energy at point r as referred to "common market standard of energy" at infinity in  $\ell$ 

$$= \mu^*(r) dA \exp[\nu(r)/2]$$
= Constant (independent of r) dA (28)
$$= \mu^*(\text{zero pressure}) dA \exp[\nu(\text{surface})/2]$$

$$= \mu_s^* dA [1 - 2M^*/r_{\text{surface}}]^{1/2}.$$

Here and hereinafter we write  $\mu_s^* = (\frac{1}{5.9}) \ m^*(\text{Fe}^{56})$  (s = "standard") for the mass-energy per baryon in cold matter catalyzed to the end point of thermonuclear evolution and under zero pressure.

### CORRESPONDENCE BETWEEN NEUTRON STAR AND STATISTICAL ATOM MODEL

The constancy of the quantity  $\mu^*(r)$  exp  $(\nu/2)$  expresses in the most direct possible way the balance between pressure and gravitational pull. By way of illustration it is appropriate to consider the case of an idealized neutron gas. There  $\mu^*$  directly translates itself (chap. ix) into an even more familiar concept: the Fermi energy (including rest energy) of this Fermi-Dirac gas—still measured in a local Lorentz frame. This freely

emphasized sufficiently strongly that such a pipe is envisaged as a background to the analysis. It should be noted that the pipe contemplated both here and in that earlier discussion is in some ways the natural generalization to the world of gravitational physics of the idealized slots cut into material media which one uses in electromagnetism to clarify the distinction between B and H, and D and E.

falling reference system is again understood to have been selected so as to make the mean motion in the neutron gas at the point in question vanish at the instant of observation. The analogy and difference compared to the Fermi-Thomas statistical atom model (see, e.g., Gombas [1949]) are interesting. In the atom the quantity that is constant from place to place in the interior is the injection energy,  $\mu_0$ , given by the sum of the local Fermi energy,  $\mu_F(r) = (\text{Fermi momentum})^2/2 \, m$ , and the potential energy,

$$\mu_0 = \text{Injection energy} = \mu_F(r) - eV(r)$$
;

or-in dimensionless units-

$$\mu_0/m c^2 = (\text{Constant}) = (\mu_F/m c^2) - (eV/m c^2).$$
 (29)

In contrast, in the massive cloud of ideal neutron gas what is constant is the *product* (28). Despite the difference in principle between a sum being constant and a product being constant, in effect the atomic and the gravitational analyses agree closely when kinetic and gravitational potential energies are small compared to  $mc^2$ . This agreement shows when one takes the logarithm of equation (28):

$$\ln \left[ \left( \frac{\text{Injection energy as referred to common}}{\text{market standard at infinity}} \right) / m c^2 \right] = \text{Constant}$$

$$= \ln \left[ \left( \frac{\text{Fermi energy-rest } plus}{\text{kinetic-of neutron gas}} \right) / m c^2 \right] + \nu (r) / 2$$

$$= \left( \frac{\text{Fermi } kinetic}{\text{energy}} \right) / m c^2 + \left( \frac{\text{Newtonian gravitational}}{\text{potentional}} \right) / c^2 ,$$

$$(30)$$

a result fully corresponding in form with equation (29) for statistical equilibrium in an atom.

> NATURAL AND UNIQUE DEFINITION OF THE POTENTIAL EXP  $(\nu/2)$ ONLY FOR EQUILIBRIUM CONFIGURATIONS

The quantity exp  $[\nu(r)/2]$  thus possesses a simple interpretation as a gravitational potential. It is well suited for analyzing the balance between the forces that act at a distance to pull matter together and the forces that act locally to push matter apart when one is dealing with an equilibrium configuration. But of how general application is this concept? This potential has a well-defined and simple value for a sphere of incompressible fluid of uniform density  $\rho^*$ , for instance (Fig. 1). Does this mean that for a collapsing cloud of dust of the same density  $\rho^*$  the potential exp  $(\nu/2)$  has the same value as that shown in Figure 1? No! Far from having the same value in the case of the cloud of dust, the quantity  $\exp(\nu/2)$  does not in this case even possess any definition which is at the same time both natural and unique! The reason is clear. The potential  $\exp(\nu/2)$  is defined in the last analysis as the ratio between the interval of proper time ds (eq. [23]) and the lapse dt of coordinate time t. Here t in turn is defined by what in essence is a group-theoretical consideration or conservation law: it is that coordinate in which the geometry is independent of time (and for which the ratio ds/dt approaches asymptotically for large r the value unity). But this definition can only be applied when the physics is static and remains static; that is, when the configuration is one of equilibrium. Otherwise  $\exp (\nu/2)$  is not even defined!

THE SENSE IN WHICH THE GRAVITATIONAL POTENTIAL EXP  $(\nu/2)$  DOES AND DOES NOT APPEAR IN THE VARIATIONAL ANALYSIS

If the potential exp  $(\nu/2)$  has no meaning for non-equilibrium configurations, then how can one possibly expect anything like the law,  $\mu^* \exp(\nu/2) = \text{constant}$ , to emerge out of

any comparison of non-equilibrium configurations; i.e., out of the variational principle of equations (9) and (10)? Answer: The extremization of the mass-energy  $M^*$  for fixed baryon number A selects out an equilibrium configuration for which exp  $(\nu/2)$  is defined. Thus, the condition for an extremum,

$$-dp^*/dr = \frac{(p^* + \rho^*)(m^* + 4\pi r^3 p^*)}{r(r - 2m^*)},$$
(31)

allows itself to be rewritten as a pair of equations. Of these equations the first,

$$\nu = -2\int (p^* + p^*)^{-1}dp^*, \qquad (31)$$

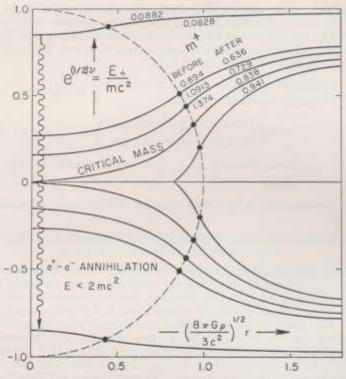


Fig. 1.—Interpretation of the Schwarzschild correction factor  $\exp(\nu/2)$  as effective gravitational potential. This quantity measures the "worth" of energy at r, as measured in a local Lorentz frame momentarily at rest with respect to the matter at r, relative to the "common market standard of energy" at infinity. Its asymptotic value is unity. It falls below unity at large distances as  $1-M^*/r$  (decrease in mass-energy because of work which must be done against Newtonian gravitational field to get that mass-energy to infinity). Multiplied by  $2 mc^*$ , it gives the energy set free by the annihilation of a positive and negative electron at rest at the point in question (under pressure free conditions inside a pipe if the point in question lies within the configuration). The curves are calculated for an interesting idealized case which, however, cannot occur in nature: a sphere of incompressible fluid, of standard density  $\rho^*(cm^-) = (G/c^*)\rho(g/cm^3)$ . For small spheres (weak field) the quantity  $\exp(\nu/2)$  has inside the character of a harmonic oscillator potential. However, for a certain critical mass this quantity—the separation of positive and negative energy states—goes to zero at the center. Details: Outside  $(\nu > R)$ ,  $\exp(\nu/2) = [1 - (8\pi\rho^*/3)(R^2/r)]^{1/2}$ ; inside  $(\nu < R)$ ,  $\frac{\pi}{2}[1 - (8\pi\rho^*/3)R^2]^{1/2} - \frac{\pi}{2}[1 - (8\pi\rho^*/3)r^2]^{1/2}$ ; mass as sensed externally,  $M^* = (4\pi\rho^*/3)R^*$ . The labels  $m^*$  on the curves give the mass before assembly as well as the mass  $M^*$  after assembly in units of  $(4\pi\rho^*/3)(8\pi\rho^*/3)^{-2/2}$ . The critical value of  $M^*$  in these units is  $m^*$  = 0.8382 =  $(8)^{1/2}$ .

now serves formally as a "definition" of v. The second,

$$e^{-\lambda}(r^{-1}d\nu/dr+r^{-2})-r^{-2}=8\pi p^*$$
, (32)

then takes the form of the (rr) component (Tolman 1934, 1939; Oppenheimer and Volkoff 1939) of Einstein's field equation,

$$R_{\alpha\beta} - (R/2) g_{\alpha\beta} = 8\pi T_{\alpha\beta}. \tag{33}$$

This equation, so simply satisfied by the *output* of the variational principle of equations (9) and (10), was not used, however, in the *derivation* of that principle. One can go further and state the following:

Theorem 5. All of the consequences for hydrostatics and for space geometry which can be extracted from Einstein's field equations (or from the significant components of these equations, which are only three in number [Tolman 1934, 1939; Oppenheimer and Volkoff 1939]—[tt], [rr], [θθ]—for the present case of a fluid in a spherically symmetrical configuration of equilibrium) emerge automatically as consequences of the variational principle of equations (9) and (10).

Proof .- The (tt) component of the field equation,

$$e^{-\lambda}(r^{-1}d\lambda/dr - r^{-2}) + r^{-2} = 8\pi\rho^*$$
, (34)

is already automatically satisfied in the formulation of the variational principle (eqs. [6], [8]). The (rr) component (eq. [32]) is satisfied by expression (31) for  $\nu$  by reason of the fact that, for the extremum, pressure varies with distance as given by equation (11). The third and last component of the field equation—the  $(\theta\theta)$  component—

$$e^{-\lambda}(\nu''/2 - \lambda'\nu'/4 + \nu'^2/4 + \nu'/2r - \lambda'/2r) = 8\pi p^*$$
, (35)

is now fulfilled as a consequence (see, e.g., Tolman [1934], p. 244) of equations (31), (32), and (34), Q.E.D.

The quantity  $\exp(\nu/2)$  as it materializes for equilibrium configurations out of the variational analysis differs in an important point of principle from the gravitational potential  $\exp(\nu/2)$  dealt with by Tolman despite all identity in values between the two quantities and all equivalence of the equations they satisfy. The Tolman quantity from the start is defined as the factor that converts coordinate time to proper time, or local Lorentz energy to common market energy. In contrast, the  $\exp(\nu/2)$  of the variational analysis never appears as the coefficient of dt in the metric. The purely spacelike metric under consideration there altogether lacks any dt to be multiplied by a correction coefficient.

If it seems surprising that so much can be derived from the initial-value equation (2) without any reference to the more extended apparatus of Einstein's equations, one has only to recall (see commentary after Theorem 1) that this one equation not only summarizes, but also provides a starting point from which to derive, all of Einstein's equations.

### THE SPACE IN WHICH EACH POINT REPRESENTS ONE CONFIGURATION

The theory of equilibrium configurations,  $C_e$ , is thus a special case of the more general theory of the mass  $M^*$  of any temporarily static and spherically symmetric configuration,  $C_e$ , containing some fixed number A of baryons. There is good reason to have checked this point in such detail. The extremum property of equilibrium configurations means that one can apply the point of view of Morse (1934, 1939, 1951) to the study of gravitational collapse. It also means that one now has for the first time a foundation

from the calculus of variations for the interesting considerations of Zel'dovich (1962). One can introduce, for fixed A, the space  $\mathfrak{C}_A$  (infinite dimensional) in which each point symbolizes one configuration C. Provided only that one introduces a suitable definition of the concept of "nearby" in this space, so that continuity can be defined, and so that the mass-energy M\* becomes a continuous function of position in this space, one does not otherwise care about what parameters or "coordinates" one uses to distinguish one point from another nor does one even care whether any coordinates at all are used ("abstract functional analysis"). Some region R (or regions  $R_1, R_2, \ldots$ ) of this space will describe collapsed configurations. At some quite other point P there will be a point representing the normal configuration of equilibrium, provided that A is not too large. Starting from this point there will exist any number of conceivable routes—each route being a continuous sequence of configurations—leading to the region of collapse. On any one route from P to R the mass-energy M\* will turn out to have a maximum value. This peak value will differ from route to route. Particularly simple to consider will be that route—that sequence of configurations—which is characterized by having uniform density, or by being homogeneous. It will turn out in this case that one can make-again for the first time—a clean separation between those considerations which have to do with general relativity (long-range forces) and those which have to do with the equation of state (short-range forces). In this way it will be possible to prove that whatever the equation of state, provided that it is consistent with fundamental physical principles (chap. viii), there is only a finite energy barrier separating the normal equilibrium configuration from a collapsed configuration.

### THE ZEL'DOVICH SEQUENCE

Zel'dovich (1962) chooses to consider a different sequence of configurations. In each configuration the density of mass-energy is taken to vary inversely as the square of the Schwarzschild coordinate r from r=0 to r=R, and to vanish outside. For such a configuration it is possible to carry through the analysis in closed form only by adopting a specific form for the equation of state. Zel'dovich adopts the equation of state of an ideal neutron gas at ultra-relativistic energy

$$\rho^* = (3^{4/2}\pi^{2/2}/4)L^{*2}n^{4/2}, \qquad (36)$$

where  $L^*$  is the Planck length (see Table 2).

To take  $p^* \sim 1/r^2$  has the advantage that  $m^*(r)$  varies linearly with r. Thus the factor  $1-2m^*(r)/r$  has a value independent of r. Call the constant quantity  $2m^*(r)/r$  the Zel'dovich packing parameter and denote it by the symbol Z. Thus small Z denotes a small departure of space from flatness and large Z (Z close to unity) marks a large departure from flatness. In terms of the parameter Z (adjustable) and the baryon number A (fixed), the typical configuration in the Zel'dovich sequence has the following properties:

$$\rho^* = Z/8\pi r^2 \quad \text{for} \quad r < R$$

$$= 0 \quad \text{for} \quad r > R;$$

$$n = \frac{Z^{3/4}}{2^{3/4}3\pi^{5/4}L^{*3/2}r^{3/2}} \quad \text{for} \quad r < R$$

$$= 0 \quad \text{for} \quad r > R;$$
(38)

$$d \text{ (proper volume)} = 4\pi r^2 (1-Z)^{-1/2} dr$$
; (39)

$$R(\text{boundary}) = \frac{3^{4/2}\pi^{1/6}}{2^{3/2}} \frac{A^{2/2}L^*(1-Z)^{1/2}}{Z^{1/2}};$$
(40)

<sup>&</sup>lt;sup>4</sup> Zel'dovich actually uses for the coefficient in this formula the value (3/x²)<sup>1/3</sup>. The value used here follows directly from Chandrasekhar's standard relativistic equation of state (chap. viii). That Zel'dovich used a value about one-third of that in eq. (36) does not in any way affect his qualitative conclusion. All values in the present text are based on eq. (36).

$$M^*$$
 (total mass energy) =  $\frac{3^{4/3}\pi^{1/6}}{2^{5/2}} A^{2/3}L^* (1-Z)^{1/3}Z^{1/3}$ . (41)

For low compaction the factor  $Z^{1/2}$  in the mass-energy dominates. Thus the energy increases with increasing compaction. The elastic forces supplied by the Fermi gas count the most. With higher compaction the gravitational forces win out, as evidenced by the factor  $(1-Z)^{1/2}$  in  $M^*$ . In other words, the energy is low, not only for a configuration of normal density, but also for one of very high density ("gravitationally collapsed configuration"). The energy barrier which separates the one configuration from the other along the Zel'dovich route is located at  $Z = \frac{3}{5}$  and has the height

$$M^*$$
 (peak) =  $(3^{11/6}\pi^{1/6}/2^{13/6}5^{5/6}) A^{2/3}L^* = 0.528 A^{2/3}L^*$   
=  $0.85 \times 10^{-23} \text{ cm } A^{2/3} = 1.15 \times 10^{-6} \text{ gm } A^{2/3} = 1.03 \times 10^{16} \text{ erg } A^{2/3}$   
=  $0.65 \times 10^{28} \text{ eV } A^{2/3}$ . (42)

Zel'dovich notes that the assumed extreme relativistic equation of state will surely fail at low compaction; the rest-plus-kinetic-energy per baryon will not continue to fall off for low baryon density as n1/3, but will instead level off at or near the nucleon mass. Also at high compaction the equation of state becomes questionable. To be sure, if one assumes that the density of mass-energy increases as the square of the number density of baryons (the most rapid law of rise permitted [cf. chap. ix] by causality) then, Zel'dovich remarks, the qualitative situation is not changed. One still finds a collapsed configuration separated from a normal configuration by a potential barrier. But what about other, more complicated equations of state?

Happily it turns out to be possible for configurations of uniform density to prove the existence of collapsed configurations independent of all details of the equation of state. Moreover, the study of such configurations will shed some light on the characteristics of equilibrium configurations. But before examining such homogeneous configurations it is desirable to look at the general situation as regards equilibrium configurations, to distinguish what is well established from what is problematical.

### REFERENCES

Chandrasekhar, S. 1964, Phys. Rev. Letters, 12, 114, 437.

Cocke, W. J. 1964, personal communication.

Gombas, P. 1949, Die statistische Theorie des Atoms (Vienna: Springer-Verlag).

Harrison, B. K., Wakano, M., and Wheeler, J. A. 1958, in Onzième Conseil de Physique Solvay, La Structure et l'évolution de l'univers (Brussels: Stoops).

Landau, L. D. 1932, Phys. Zs. Sowjetunion, 1, 285.
Landau, L. D., and Lifshitz, E. M. 1951, The Classical Theory of Fields (1st ed.; Reading, Mass.: Addison-Wesley Publishing Co.; 2d ed., 1962).

1958, Statistical Physics, trans. E. Peierls and R. F. Peierls (Reading, Mass.: Addison-Wesley Publishing Co.; London: Pergamon Press).

Misner, C. W., and Zapolsky, H. S. 1964, Phys. Rev. Letters, 12, 635.

Morse, M. 1934, The Calculus of Variations in the Large (Providence, R.I.: American Mathematical Society)

. 1939, Functional Topology and Abstract Variational Theory (Paris: Gauthier-Villars).

1951, "Introduction to Analysis in the Large" (mimeographed notes, Institute for Advanced Study, Princeton, N.J., 2d ed.).
Oppenheimer, J. R., and Volkoff, G. 1939, Phys. Rev., 55, 374.

Taub, A. H. 1954, Phys. Rev., 94, 1468.

. 1963, Proceedings of the 1962 Santa Barbara Conference on Relativity and Topology (Providence, R.I.; American Mathematical Society).

Tolman, R. C. 1934, Relativity, Thermodynamics and Cosmology (Oxford: Clarendon Press).

- 1939, Phys. Rev., 56, 364.

Zel'dovich, Ya. B. 1962, Zhur. eksp. Teor. Fiz. (USSR), 42, 641 (English translation in Soviet Phys.-J.E.T.P., 15, 446).

### CENTRAL DENSITY AND THE chapter 4 REGENERATION OF PRESSURE

What are the principal features of an equilibrium configuration? In such a system does pressure always fall off with distance from the center? Can an unlimited central pressure ever be in equilibrium with a perfectly finite amount of surrounding matter? These and related questions form the subject matter of this chapter and its principal theorems.

### MONOTONIC FALL OF PRESSURE AND DENSITY IN AN EQUILIBRIUM CONFIGURATION

Theorem 6. In a configuration of equilibrium of cold, catalyzed matter the pressure has its maximum value at the center and falls monotonically to zero at the surface. The density falls monotonically from a peak value ρ<sub>0</sub> at the center to the standard value of 7.8 g/cm<sup>3</sup> at the surface (Fe<sup>16</sup>).

The monotonic fall of the pressure follows from the positive definite character of the right-hand side of the TOV equation (11) for -dp/dr; of the density, from the everywhere finite and positive character of  $dp/d\rho$  (chap. ix). The zero value of the pressure at the surface is a consequence of equation (22). At zero pressure and temperature the absolute end point of thermonuclear evolution is well known to be Fe<sup>28</sup>.

THEOREM 7. For each value of the central density ρ<sub>0</sub>\* between zero and "infinity" there is one and only one equilibrium configuration.

Proof.—Equation (8) for dm/dr and equation (11) for dp ( $\rho$ )/dr constitute two first-order and regular equations; therefore, the solution is uniquely specified by the two initial data m(0) = 0 and  $\rho(0) = \rho_0$ . Thus the value of the central density (or central pressure) serves as an index label to catalogue all equilibrium configurations. The total baryon number A differs from configuration to configuration in this catalogue. It does not vary monotonically with central density. Thus, for one number of baryons  $A_1$  there may be four distinct configurations of equilibrium—two stable and two unstable, each with its own  $\rho_0$  value—and for another number of baryons  $A_2$  there may be no equilibrium at all.

### THE SENSE IN WHICH PRESSURE IS AND IS NOT SELF-REGENERATIVE

Further commentary on the TOV general-relativity equation of hydrostatic equilibrium: In conventional as contrasted with geometrized units this equation takes the form

$$-dp/dr = \frac{(\rho + p/c^2)G[m(r) + 4\pi r^3 c^{-2}p(r)]}{r[r - 2(G/c^2)m(r)]}.$$
 (43)

One obtains the equation of hydrostatic equilibrium in the form ordinarily applied in the study of stars and planets by striking out from equation (43) all terms ("relativity terms") which contain a factor of  $c^{-2}$ . Of the three relativistic terms, the one which one thinks of as characteristically geometrical in character, the term  $2(G/c^2)m(r)$  in the denominator, is much less important in its effects (except at densities considerably in

excess of nuclear density, ~10<sup>14</sup> g/cm<sup>3</sup>) than the two pressure terms in the numerator. They give rise to what one can loosely call a regenerative multiplication of pressure, in the following sense: The greater the pressure in the interior, the greater the right-hand term in equation (43), and therefore the greater the pressure gradient between inside and outside (where the pressure vanishes). Therefore, the pressure in the interior is amplified over what one would have expected from the equation of hydrostatic equilibrium in its Newtonian form.

There is one idealized example where one can study this amplification in all detail up to the point where the amplification factor goes to infinity ("divergent chain reaction"). The example is unrealistic in that it assumes an incompressible fluid (speed of sound in excess of speed of light) but is instructive because of its simplicity. The principal prop-

erties of the configuration are

$$\rho^* = \begin{array}{ccc} \text{Constant} & \text{for} & r < R \\ 0 & \text{for} & r > R \end{array}; \tag{44}$$

$$n = \frac{\rho^*/\mu_s}{0} \quad \text{for} \quad r < R$$

$$\text{for} \quad r > R ;$$
(45)

$$d \text{ (proper volume)} = 4\pi r^2 [1 - (8\pi \rho^*/3) r^2]^{-1/2} dr \text{ (inside)};$$
 (46)

$$\frac{d \text{ (proper time)}}{d \text{ (coordinate time)}} = \exp(\nu/2)$$
 (see Fig. 1) 
$$= \frac{\pi}{2} (1 - 8\pi \rho^* R^2/3)^{1/2} - \frac{\pi}{2} (1 - 8\pi \rho^* r^2/3)^{1/2} \text{ inside}$$
 (47) 
$$= (1 - 8\pi \rho^* R^2/3 r)^{1/2} \text{ outside };$$

and, with the abbreviations

$$x = (8\pi \rho^*/3)^{1/2}r$$
,  $X = (8\pi \rho^*/3)^{1/2}R$  (48)

for dimensionless measures of position and of the radius of the configuration, further,

$$M^* = \text{Mass after assembly} = (4\pi \rho^*/3)R^3 = (4\pi \rho^*/3)(3/8\pi \rho^*)^{2/2}X^3;$$
 (49)

 $A \mu_s = \text{Mass before assembly} = (4\pi \rho^*/3)(3/8\pi \rho^*)^{3/2}$ 

$$\times \frac{3}{2} [\arcsin X - X(1 - X^2)^{1/2}]$$
 (50)

= 
$$(4\pi \rho^*/3)(3/8\pi \rho^*)^{3/2}(X^3 + \frac{3}{10}X^5 + \dots);$$

$$p^* = \rho^* \frac{(1-x^2)^{1/2} - (1-X^2)^{1/2}}{3(1-X^2)^{1/2} - (1-x^2)^{1/2}}$$

$$\doteq \frac{\rho^*}{4}(X^2-x^2) \text{ for Newtonian limit of small } X; \tag{51}$$

$$=\frac{(4\rho^*/3)}{16\epsilon+x^2}$$
 (near center) for radius close to critical value

$$R = (3/8\pi\rho^*)^{1/2}(\frac{s}{6})^{1/2}$$
; i.e., for  $X = (\frac{s}{6})^{1/2}(1-\epsilon)$ .

<sup>&</sup>lt;sup>1</sup> Original calculations by K. Schwarzschild; details of derivation accessible in Tolman (1934), pp. 246-247.

The central pressure goes to infinity as the mass approaches a certain perfectly finite critical value ("divergent chain reaction"). This critical value is the same as that for which the separation of positive and negative energy states at the center goes to zero (see Fig. 1, p. 22). The criticality shows itself in the deep interior, not at the surface. There is no evidence of any tendency of the configuration to "cut itself off from the rest of the universe." Not only are the calculated values of the mass before and after assembly finite at the critical point

$$M^* = \text{Mass after assembly} = \left(\frac{8}{9}\right)^{3/2} (\text{ or } 0.838) (4\pi\rho^*/3) (3/8\pi\rho^*)^{3/2};$$
 (52)

$$A\,\mu_s\,^* = \text{Mass before assembly} = \left\{ \begin{array}{l} \frac{3}{2} \left[ \, \arcsin \left( \frac{8}{9} \right)^{1/2} - \, 8^{1/2} / \, 9 \, \right] \\ \text{or} \quad 1.374 \end{array} \right\} \tag{53}$$

$$\times (4\pi\rho^*/3)(3/8\pi\rho^*)^{3/2}$$
;

but also the rate of change at that point is finite:

$$\begin{split} dM^*/d\left(A\mu_*^*\right) &= \frac{\text{Increase(in g) of mass of equilibrium configuration}}{\text{Number of g of unassembled matter dropped in from far away}} \\ &= \frac{3X^2dX}{3X^2(1-X^2)^{-1/2}dX} = \frac{1}{4} (\text{ = value of exp $\nu$/ 2 at surface)} \,. \end{split}$$

Thus, near the limit, each added atom, according to the model, radiates away  $\frac{2}{3}$  of its mass and augments the mass of the system by  $\frac{1}{3}$  as much as would have been expected on Newtonian theory. A characteristic spectral line emitted from an atom at rest on the surface drops in frequency by a factor 3 on its way to a distant receptor, also at rest with respect to the system.

That gravitational forces overwhelm all other forces, even the resistive power of an idealized incompressible fluid, shows that the so-called hard-core nucleon-nucleon interaction (see also chap. ix) does not offer any escape from the issue of gravitational collapse.

How does the regenerative multiplication of pressure come about? There is not the slightest reference to pressure in the expression  $\hat{\rho}^* 4\pi r^2 dr$  for the mass-energy of any given number of baryons in a spherically symmetric and momentarily static configuration. It is irrelevant whether the baryons are present in the form of dust or porous matter or a highly compressed fluid. The pressure makes no appearance. Only the density counts. In this sense there is not, and cannot be, any phenomenon of "regenerative multiplication of pressure."

Why, then, does the pressure come into the TOV equation in such a central way? Because there one is dealing, not with arbitrary static configurations, but with equilibrium configurations. One is concerned not only with the effect of matter upon geometry—or on gravitation—but also with the effect of gravitation upon matter. Will the long-range forces set the matter into motion? What must be the distribution of short-range forces—of pressure—to prevent such acceleration? Are there cases where no finite pressure pattern can stop gravitational collapse? To the discussion of these questions the qualitative concept of "regenerative multiplication of pressure" is relevant. To see this effect at work, moreover, one does not have to appeal to the extreme model of an incompressible fluid (see Fig. 1). Instead, one can look, for example, at the more reasonable model of an ideal neutron gas under extreme relativistic conditions. There  $\rho^*$  goes as  $n^{4/2}$  (eq. [36]), and  $p^* = ndp^*/dn - p^* = p^*/3$ . Oppenheimer and Volkoff (1939) have examined this case in detail. They show that when the central pressure and density go to infinity the mass  $M^*$  and the baryon number A both go to finite values.

<sup>&</sup>lt;sup>3</sup> For a general argument setting an upper limit for this redshift for any static configuration, see Bondi (1964). Appreciation is expressed to Professor Bondi for the opportunity to see and discuss this paper in advance of publication.

### "CENTRAL CRUSH"

Denote by "central crush" the unlimited central pressure achieved for a finite value of the baryon number,  $A = A_{\rm crit}$ . The inescapability of central crush appears from no consideration so clearly as from this, that there exists (Theorem 7) one and only one equilibrium configuration for each value of the central pressure, up to infinite values of this catalogue index of solutions of the TOV equation.

That the equilibrium configuration for  $\rho_0 \to \infty$  has in addition a finite  $M^*$  and A has not yet been established firmly for the most general allowable equation of state. However, this finiteness, quite in general, would seem plausible by reason of the following:

Theorem 8. The baryon number and the mass-energy and the radius of equilibrium configurations all go to finite limits as the central density goes to infinity for every "γ-law equation of state,"

$$\rho^*(n) = \text{Const } n^{\gamma}, \quad \rho^* = (\gamma - 1) \rho^*,$$
 (55)

with y in the physically permissible range (chap. ix) from 1 to 2.

This result of Misner and Zapolsky (1964) was obtained by a generalization of the argument given by Oppenheimer and Volkoff (1939) as follows: The solution of the TOV equation (11) of hydrostatic equilibrium for the  $\gamma$ -law equation of state has a simple analytic form in the special case where the central density goes to infinity:

$$\begin{split} p^* &= (\gamma - 1) \, \rho^* = 2 \, (\gamma - 1)^2 (\gamma^2 + 4\gamma - 4)^{-1} / \, 4\pi \, r^2 \text{ for general } \gamma \\ &= (56\pi r^2)^{-1} \quad \text{for} \quad \gamma = \frac{4}{3} \, ; \end{split}$$

$$m^* = 2(\gamma - 1)(\gamma^2 + 4\gamma - 4)^{-1}r$$
 for general  $\gamma = \frac{3}{14}r$  for  $\gamma = \frac{4}{3}$ . (57)

Provided that the equation of state is representable at high densities by a  $\gamma$ -law, then these analytic formulas apply from (1) the center of the configuration, where  $\rho = \rho_{\rm rentral} = "\infty,"$  out to (2) that radius where  $\rho$  has fallen to a "transition value," defined as the point below which the equation of state departs significantly from the asymptotic  $\gamma$ -law. On the further assumption that this "transition density" has a value of the order of nuclear densities ( $\sim 10^{14}$  to  $10^{15}$  gm/cm\*), Misner and Zapolsky show that no reasonable changes in the equation of state at lower densities (i.e., at points between the transition region and the surface) can alter much the Oppenheimer-Volkoff value for the critical mass, a value of the order of half the mass of the Sun. So much for the limiting configuration with infinite central density!

### REFERENCES

Bondi, H. 1964, Roy. Soc. London Proc., A, 281, 39.
Misner, C. W., and Zapolsky, H. S. 1964, Phys. Rev. Letters, 12, 635.
Oppenheimer, J. R., and Volkoff, G. 1939, Phys. Rev., 55, 374.
Tolman, R. C. 1934, Relativity, Thermodynamics and Cosmology (Oxford: Clarendon Press), pp. 242–243.

### DENUMERABLE INFINITY OF chapter 5 CRITICAL MASSES

### THEOREM ON DAMPED OSCILLATIONS

New insight comes from asking how the mass  $M^*$  varies with central density  $\rho_0$  as  $\rho_0$  approaches infinity. To investigate this question, assume that the equation of state follows a  $\gamma$ -law asymptotically at high densities. Furthermore, understand by the term "fractional departure" such a quantity as

$$(R-R_{\infty})/R_{\infty}$$
 or  $(M-M_{\infty})/M_{\infty}$  or  $(A-A_{\infty})/A_{\infty}$  (58)

measuring the difference between (1) a property of the equilibrium configuration for  $o_0$  finite and (2) the same property of the limiting equilibrium configuration ( $\rho_0$  infinite). Then we find:

Theorem 9. The fractional departure from the limiting configuration varies with In ρ<sub>0</sub> asymptotically for large central density as the amplitude of a damped periodic oscillation varies with time:

(Fractional departure) = Constant 
$$e^{-(\pi/2) \ln \rho_0} \cos[(\beta/2) \ln \rho_0 + \delta]$$
, (39)

with

$$\alpha = \frac{3}{2} - (1/\gamma)$$
 for general  $\gamma$ 

$$= \frac{3}{4}$$
 for  $\gamma = \frac{4}{3}$  (60)

and

$$\beta = [-(9/\gamma^2) + (11/\gamma) - \frac{1}{4}]^{1/2} \text{ for general } \gamma$$

$$= (47)^{1/2}/4 = 1.714 \text{ for } \gamma = \frac{4}{3}.$$
(61)

In other words the amplitude of a peak in  $M^*$  or R or A exceeds the amplitude of the next ensuing trough by a factor

Amplitude fall-off factor = exp 
$$(\pi \alpha/\beta)$$
 for general  $\gamma$   
= exp  $3\pi/(47)^{1/2} = 3.95$  for  $\gamma = \frac{4}{3}$ .

Moreover, the peak-to-trough separation has the standard value (for large  $\rho_0$ ) of

$$\Delta \log_{10} \rho_0 = (\log_{10} e) \Delta \ln \rho_0 = 2 \times 0.4343 \pi / \beta$$
 for general  $\gamma$   
= 1.59 for  $\gamma = \frac{4}{3}$ . (63)

<sup>&</sup>lt;sup>1</sup> Tooper (1964) has calculated the equilibrium configurations for matter which everywhere obeys a γ-law equation of state.

These features of the curve of equilibrium mass as a function of central density were first recognized by Harrison as a consequence of his having extended the numerical integrations of the equation of hydrostatic equilibrium from central density  $\rho_0 = 10^{18}$  g/cm³ up to  $\rho_0 = 10^{22}$  g/cm³. He has subsequently given an analytical treatment of these oscillations (Harrison 1965). The present, independent, analytical treatment is designed to give further physical insight into the origin of the oscillations.

### DETAILS OF PROOF: THREE ZONES; AND THE SCALING LAW WHICH APPLIES IN THE FIRST TWO ZONES

Proof.—Divide the range of r-values from the center to the surface into three zones, as is indicated in Figure 2 and Table 3. In Zones I and II the solution  $\rho(r)$  of the TOV equation of hydrostatic equilibrium satisfies a simple scaling law. The solution for one value of the central density,  $k^2\rho_0$ , where k is a constant, is obtained from the solution for another value of the central density,  $\rho_0$ , by this prescription: Take the values of p and p at the point r. Multiply them by  $k^2$ , and multiply r by 1/k. The existence of this scaling law was noted by Bondi (1964). He pointed out that this law makes it natural to take  $(4\pi\rho_0^*/3)^{1/2}r$  as independent variable—because it is unchanged by this scaling—and similarly to take as dependent variables two scale-invariant quantities u(r) and v(r), defined by

$$p^*(r) = (\gamma - 1) \rho^*(r) = v(r) / 4\pi r^2,$$
 (64)

$$m * (r) = ru(r).$$
 (65)

The existence of the scaling group implies here as always<sup>2</sup> that the order of the differential equation can be reduced; here, from two first-order equations for dm(r)/dr and dp(r)/dr to one. Thus, the equation

$$dm/dr = 4\pi r^2 \rho \tag{66}$$

becomes

$$r du / dr + u = v / (\gamma - 1)$$
 (67)

and allows one to solve for the scale-independent quantity dr/r:

$$dr/r = \frac{du}{(\gamma - 1)^{-1}v - u}$$
 (68)

Similarly TOV equation (11) of hydrostatic equilibrium for dp/dr reduces to a form in which one can sort out the change dr/r from u, v, and the change in v:

$$dr/r = \frac{dv/v}{2 - \gamma(\gamma - 1)^{-1}(u + v)(1 - 2u)^{-1}}.$$
(69)

Comparing equations (68) and (69), one arrives at Bondi's first-order equation

$$\begin{split} \frac{d\,v}{d\,u} &= \frac{v\,[\,\,2\,(\,\gamma\,-\,1\,)\,-\,(\,5\,\gamma\,-\,4\,)\,u\,-\,\gamma\,v\,\,]}{(\,1\,-\,2\,u\,)[\,v\,-\,(\,\gamma\,-\,1\,)\,u\,\,]} \qquad \text{for general } \gamma \\ &= \frac{v\,(\,1\,-\,4\,u\,-\,2\,v\,\,)}{(\,0\,.\,5\,-\,u\,)\,(\,3\,v\,-\,u\,\,)} \qquad \qquad \text{for } \gamma = \frac{4}{3}\,. \end{split}$$

This he has integrated numerically in the special case  $\gamma = \frac{4}{3}$  (or  $p^* = \rho^*/3$ ) from the origin out to a point where the density has fallen to  $\frac{1}{8}$  of the central value (Table 4).

<sup>&</sup>lt;sup>2</sup> See, e.g., Sommerfeld's (1960) section on solution of the Fermi-Thomas equation; see also Sedov (1959) and Chandrasekhar (1939).

Not given in Bondi's paper, but useful in exhibiting the behavior of the solution near the origin, are the first terms in the following series:

$$v(u) = 3(\gamma - 1)u - 3\gamma(3\gamma - 2)u^2/5 + \dots$$
 for general  $\gamma$   
=  $u - \frac{8}{5}u^2 + \dots$  for  $\gamma = \frac{4}{3}$ . (71)

When one goes back to expressing pressure and mass directly as functions of r, or of the dimensionless and scale-invariant quantity

$$s = (4\pi \rho_0^*/3)^{1/2}r, \qquad (72)$$

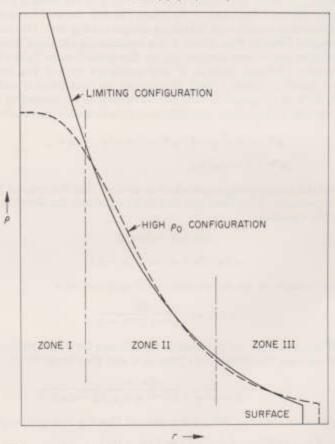


Fig. 2.—Equilibrium configuration of large but finite central density compared with the limiting configuration for which the central density is infinite (schematic only). The asymptotic  $\gamma$ -law equation of state applies in Zone I and II. In Zone I the fractional departure from the limiting configuration is large; in Zone II, small. In Zone III the equation of state is more complicated. The density falls monotonically throughout and reaches the standard value of 7.8 gm/cm² for Fe<sup>16</sup> at the surface. Why the oscillatory departure between the high- $\rho_0$  configuration and the limiting configuration? Looking apart from details (chap. v), one can put the main point as follows:  $[d\Delta m(r)/dr] \simeq [\Delta p(r)]$  (oscillations in mass perturbation out of phase with oscillations in density perturbation because mass is given by integral of density); and  $[-d\Delta p(r)/dr] \simeq [\Delta m(r)]$  (density gradient governed by pressure gradient; pressure gradient governed by acceleration of gravity and therefore by mass). Thus the pair-wise coupling of the two perturbations is responsible for the "oscillation." When the central density is increased beyond the high- $\rho_0$  value in the diagram—say, fourfold—the nodes move inward to half the present r-value. The new curve (in Zones I and II only) is obtained from the present curve by the simple scaling operation of multiplying  $\rho$  values by 4 and dividing r values by 2.

one has two series:

$$u = \frac{m^*(r)}{r} = s^2 - \frac{3\gamma(3\gamma - 2)}{10(\gamma - 1)} s^4 + \dots \qquad \text{for general } \gamma$$

$$= s^2 - \frac{12}{5}s^4 + \dots \qquad \text{for } \gamma = \frac{4}{3},$$

and

$$v = 4\pi r^2 p^* (r) = 3(\gamma - 1) s^2 - \frac{3\gamma(3\gamma - 2)}{2} s^4 + \dots \qquad \text{for general } \gamma$$

$$= s^2 - 4s^4 + \dots \qquad \text{for } \gamma = \frac{4}{3}.$$

## PROOF OF THEOREM 9 CONTINUED: THEORY OF SMALL PERTURBATIONS APPLICABLE IN ZONES II AND III

Zone I has required a special treatment. It includes the origin, and at the origin there is an infinite difference between the density of the limiting configuration (infinite) and the density of the configuration under study (large but finite). The analysis is much

Zones Considered in Analyzing Difference between Actual Configuration ( $\rho_0$  Large) and Limiting

TABLE 3

CONFIGURATION (PR INFINITE)

Zone	Density and Equation of State	Fractional Change in $\rho(r),  \rho(r),  m(r)$	Differential Equation for Δm, Δp
I	$\rho(r)$ high enough so that asymptotic $\gamma$ -law applies $\rho(r)$ from $10^{18}$ (or more) to	Large Small	Non-linear Linear
11	7.8 g/cm³; equation of state complicated	Small	Linear

TABLE 4 Configuration in Region Where Asymptotic  $\gamma\text{-Law}$  Applies, for the Case  $\gamma=\frac{\pi}{4}$ 

([4xpq*/3]1/5r)	μ/μα (p/pa)	± (4πτ²β*)	(m*[r]/r)	$([14v - 1]s^{4/4})$	(Eq. [86])
0.000	1	0.0000	0.000	0.000	1.6048
.181	0.87 0.75	.0285	.030	167 091	-0.394 $-0.455$
.343	0.64	.0755	.090	+ .025	-0.458
.420	0.50	.0932	.120	+ .158 + .288	-0.425 $-0.356$
.505	0.42	.1060	.150	+ .396	-0.330 $-0.249$
.747	0.20	. 1123	.210	+ .460	-0.096
).909	0.126	0.1045	0.231	+0.431	$\pm 0.060$

<sup>\*</sup> As calculated numerically by Bondi (1964) (Zone I of Fig. 2 and Table 3). The last two columns have been added to Bondi's table to exhibit the beginning of oscillations away from the limiting configuration, oscillations which are shown below (eqs. [78] ± 3) to be characteristic of Zone II. The firth column gives the "pressure perturbation factor" it; and the sixth column, the "adjusted mass perturbation factor" it.

simpler in Zones II and III. There the perturbation is small (see Fig. 2). For this reason we return to the basic equations  $(dm/dr = 4\pi r^2 \rho_0$ , and the TOV eq. [11] for dp/dr) and analyze the difference between the high- $\rho_0$  configuration and the limiting configuration to the first order of small quantities. Writing

$$p(r) = p_{\infty}(r) + \Delta p(r) \tag{75}$$

and adopting similar expressions for  $\rho(r)$  and m(r), we find the "perturbation equations"

$$d\Delta m / dr = 4\pi r^2 \Delta \rho \tag{76}$$

and

$$- d\Delta \rho / dr = \Lambda (r) \Delta \rho + B(r) \Delta m. \qquad (77)$$

Here A and B are abbreviations for expressions which are fully determined by the properties of the limiting configuration (presumed known):  $m_{\infty}(r)$ ,  $p_{\infty}(r)$ ,  $(dp/d\rho)_{\infty}^{-1}$ , and  $(d^2p/d\rho^2)_{\infty}$ .

### PHASE TRANSITION EXCLUDED FOR SIMPLICITY

If the equation of state contains a point of condensation (finite jump in  $\rho$  as p passes a certain critical value), then the curve for density as a function of r will show a corresponding drop at a certain r value,  $r_{erit}$ . There will be a difference  $\Delta r_{erit}$  between the coordinate of the jump point in (1) the high- $\rho_0$  configuration and (2) the limiting configuration. In the interval of r values between  $r_{crit}$  and  $r_{crit} + \Delta r_{crit}$  there will be a finite difference in density between two configurations which otherwise may differ very little from each other in the region in question. This circumstance is no obstacle to a perturbation analysis of the relation between the two configurations. Neither does the presence of such a phase transition change the character of the conclusions that one may draw about  $\Delta \rho(r)$  and  $\Delta m(r)$ , provided only that the r-values of the two zone boundaries are so chosen as not to lie close to the point of transition. To carry through all the details of fitting inner and outer solutions at a point of transition nevertheless introduces complications. Therefore, any phase transition will be excluded for the sake of simplicity. In other words, it will be assumed that  $(dp^*/d\rho^*)^{-1}$  is everywhere finite so that the coefficients A(r) and B(r) are also finite throughout Zone III. That they are finite in Zone II follows automatically from the asymptotic  $\gamma$ -law that applies in that region:  $dp^*/dp^* = \gamma - 1.$ 

### THEORY OF OSCILLATIONS ABOUT LIMITING CONFIGURATION IN ZONE II

In Zone II the limiting configuration has a simple analytic character. In consequence the perturbation equations (76) and (77) can be solved at once. Measure the strength of the perturbation by a number Q (which will turn out to be complex). Then the density of the high- $\rho_0$  configuration in Zone II is

$$\rho^*(r) = \frac{2(\gamma - 1)}{(\gamma^2 + 4\gamma - 4)4\pi r^2} (1 + Qs^{\lambda} + Q^*s^{\lambda^*}). \tag{78}$$

Here  $Q^* s^{\lambda *}$  is the complex conjugate of  $Qs^{\lambda}$ . Also  $s = (4\pi \rho_0 */3)^{1/2} r$  is the same dimensionless measure of distance which was employed previously, and  $\lambda$  is a characteristic exponent, now to be found. For this purpose note, first, that the pressure differs from equation (78) only by the addition of one more factor  $(\gamma - 1)$ ; and, second, that the mass follows from equation (78) by integration:

$$m*(r) = \frac{2(\gamma - 1)r}{(\gamma^2 + 4\gamma - 4)} [1 + Q(\lambda + 1)^{-1}s^{\lambda} + \text{complex conjugate}].$$
 (79)

Finally, write the equation of small perturbations in equation (11) of hydrostatic equilibrium in the form

Fractional change in 
$$(-dp^*/dr)$$
 = Fractional change in  $(p^* + p^*)$   
+ Fractional change in  $(m^* + 4\pi r^*p^*)$  - Fractional change in  $(1 - 2m^*/r)$ .

This equation has to be satisfied independently by the terms in  $Q s^{\lambda}$  and by the terms in  $Q^* s^{\lambda*}$ . It is enough to demand equality of the coefficients of  $Q s^{\lambda}$  on both sides of the equation:

$$(1-\lambda/2) = (1) + [(\gamma-1)/\gamma + (\lambda+1)^{-1}/\gamma] + 4(\gamma-1)/\gamma^2(\lambda+1)].$$
 (81)

Solving this quadratic equation for  $\lambda$ , one finds

$$\lambda = -\alpha + i\beta$$
,  $\lambda^* = -\alpha - i\beta$ , (82)

where the positive quantities  $\alpha$  and  $\beta$  are listed in equations (60) and (61).

### DETAILS OF PROOF OF THEOREM 9 CONTINUED: FITTING ZONE II TO ZONE I

The form of the departure from the limiting configuration is thus fully determined in Zone II. The amplitude and phase are also fully determined in terms of the large but finite central density  $\rho_0$ . In other words, the complex quantity Q is fixed by joining the present perturbative solution onto the solution obtained by numerical integration (or otherwise) in Zone I.

In view of the oscillatory character of the solution in Zone II ( $\lambda$  complex), the join between the solutions in the two zones is best made by plotting (Fig. 3) two quantities which are so selected as (1) to have an amplitude of oscillation which is independent of r; (2) to have phases which differ by 90°; and (3) to have the same amplitude of oscillation. For one of these quantities it is natural, in the light of equations (78) and (82), to take the "pressure perturbation factor"

$$\begin{split} \xi(s) &= \left[ \frac{(\gamma^2 + 4\gamma - 4)}{2(\gamma - 1)^2} 4\pi r^2 p^*(r) - 1 \right] s^a \\ &= Q \exp(i\beta \ln s) + \text{complex conjugate(c.c.)}. \end{split}$$
 (83)

It is not equally appropriate to extract the other quantity in the same way out of expression (79) for the oscillations in mass,

$$\left[\frac{(\gamma^2 + 4\gamma - 4)}{2(\gamma - 1)} \frac{m^*(r)}{r} - 1\right] s^{\alpha} = \frac{Q[(1 - \alpha) - i\beta]}{(1 - \alpha)^2 + \beta^2} \exp(i\beta \ln s) + \text{c.c.}, \quad (84)$$

because this quantity does not have the desired 90° phase difference from  $\xi(s)$ . However, subtract out of equation (84) the in-phase component and renormalize what is left to arrive at the desired quantity,

$$\eta(s) = \beta^{-1}[(1-\alpha)^2 + \beta^2)](84) - \beta^{-1}(1-\alpha)(83)$$

$$= (Q/i) \exp(i\beta \ln s) + c.c.$$
(85)

For  $\gamma = \frac{4}{3}$  the two oscillating departures from the limiting configuration are the "pressure perturbation factor"

$$\xi(s) = [14(4\pi r^2 p^*) - 1][(4\pi \rho_0^*/3)^{1/2} r]^{3/4} = Q \exp[i(\frac{47}{16})^{1/2} \ln s] + \text{c.c.},$$

and the "adjusted mass perturbation factor"

$$\eta(s) = (47)^{-1/2} \left\{ 12 \left[ \frac{14}{3} (m^*/r) - 1 \right] - \left[ 14 (4\pi r^2 p^*) - 1 \right] \right\}$$

$$\times \left[ (4\pi \rho_0^*/3)^{1/2} r \right]^{2/4} = (Q/i) \exp\left[ i \left( \frac{47}{16} \right)^{1/2} \ln s \right] + \text{c.c.}$$
(86)

Figure 3 shows the behavior of these two oscillatory perturbation factors as evaluated in Table 4 from Bondi's numerical integration for the conditions in Zone I. The integration does not go quite far enough to see the full development of the limiting behavior as expected in Zone II (rotation on a circle of fixed radius |Q| with a phase  $\left[\frac{47}{16}l^{12}\ln s + \delta\right)$ . The analysis in Table 5 suggests for |Q| a value of the order of 0.4–0.5 and for  $\delta$  an angle of the order of  $\frac{1}{3}$  radian. Table 5 presents a tentative determination of the amplitude |Q| and the phase  $\delta$  of the oscillatory difference (Fig. 2) between (1) the high- $\rho_0$  density distribution and (2) the limiting density distribution, as described in Zone II by equation (78) with  $\gamma = \frac{4}{3}$ . The "pressure perturbation factor"  $\xi$  and the

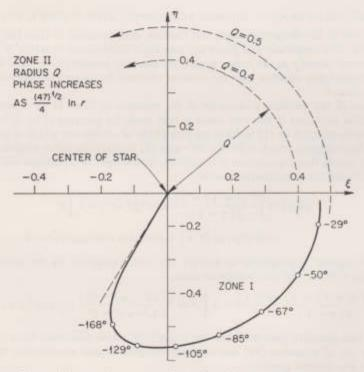


Fig. 3.—The oscillatory difference between a configuration of large central density and the limiting configuration of infinite central density. The plot is designed to show the relation between the solution in Zone I (start of oscillation; points taken from data in Table 4) and Zone II (fully developed oscillations as described by eqs. [78] and [79]: a circle of fixed radius Q centered on the origin in the present diagram). The curve for Zone I shows the "pressure perturbation factor"  $\xi$  of eq. (83) and the "adjusted mass perturbation factor"  $\eta$  of eq. (85) at successive points on the way from the center of the high- $\rho_0$  configuration to the point where the density has fallen to one-fifth the central value. In Zone II the oscillation is described by a point rotating in the  $(\xi, \eta)$  diagram on a circle of radius Q with phase  $\varphi = \beta \ln s + \text{const} = 1.717 \ln [(4\pi\rho_0/3)^{1/2}r] + \text{const}$ . Values of the quantity  $\beta \ln s$ , expressed in degrees, are shown for each point on the curve for Zone I—even though the oscillation is not yet fully developed at the point where Bondi's numerical integration breaks off—as a guide in tracing the transition to the ideal behavior in Zone II.

"adjusted mass perturbation factor"  $\eta$  were calculated as described in Table 4 from the last four points in Bondi's numerical integration in Zone I. The last digits of the numbers listed in the table are uncertain. The limiting form for the oscillations (eq. [78]) is not yet fully developed at s=0.9. Therefore any conclusions about |Q| and  $\delta$  have to be tentative, pending more extensive integrations. If the last point of Bondi were dropped—and if the  $\xi$  and  $\eta$  values derived from them were eliminated (last column in Table 5), a procedure for which there is no obvious warrant—then evidently one would be led to |Q|=0.47,  $\delta=17^\circ$  or 0.30 radian, for the amplitude and phase characteristic of the oscillations in Zone II. ( $Q\cong0.47$  exp i 0.30.)

This detail for the case of  $\gamma = \frac{4}{3}$  illustrates the following point that applies for every  $\gamma$ -value in the allowed range from 1 to 2. The complex amplitude Q of the oscillations in density  $\rho(r)$  and mass m(r) in Zone II, relative to the limiting configuration, has for each  $\gamma$  a unique non-zero value. It is not a drawback for the present purpose that we have

discovered no analytic means to calculate the function  $Q = Q(\gamma)$  for every  $\gamma$ !

 ${\bf TABLE~5}$  Tentative Determination of the Amplitude |Q| and the Phase  $\delta$  for  $\gamma=4/3$ 

$x = (4\pi \rho_0 */3)^{1/3}r$	0.505	0.603	0.747	0.909
Arctan $(\eta/\xi)$ = "actual phase".	-51.0°	-32.2°	-11.8°	+ 7.9° - 9.4° 17.2° (0.376)
$(47/16)^{1/2}$ In $s$ = "uncorrected phase"	-67.0°	-49.6°	-28.6°	
Tentative phase correction.	+16.0°	17.4°	16.8°	
$(\xi^2 + \eta^2)^{1/2}$ = tentative value of $ Q $	0.458	0.468	0.470	

## CONSERVATION OF NORMALIZED "AREA IN PHASE SPACE" IN "PROPAGATION" OF STATIC OSCILLATION FROM INTERIOR TO SURFACE

The static oscillations which arose in Zone I, and which have now been shown to follow a simple analytical law in Zone II, also propagate through Zone III all the way to the surface. There they produce an oscillatory dependence of the equilibrium mass upon the logarithm of the central density. It is the ultimate objective of this section to prove and evaluate this dependence. For this purpose it is now useful to show that there exists a conservation law for the propagation of the oscillations through Zones II and III. This conservation law has to do, not with the oscillations  $\Delta \rho(r)$  and  $\Delta m(r)$  (relative to the limiting configuration) for a single value  $\rho_0$  of the central density, but with a kind of "area in phase space" (Fig. 4) determined by the oscillations for two values,  $\rho_{01}$  and  $\rho_{02}$ , of the central density. This area is given by the determinant

$$D_{12}(r) = \begin{vmatrix} \Delta \rho_1^*(r) & \Delta \rho_2^*(r) \\ \Delta m_1^*(r) & \Delta m_2^*(r) \end{vmatrix}. \quad (87)$$

How does the area  $D_{12}(r)$  alter with increase of the distance from the center of the configuration? The changes in density and mass for any one solution individually are given, according to equations (76) and (77), by formulae of the type

$$\Delta \rho^*(r+dr) = [1 - A(r)dr]\Delta \rho^*(r) - [B(r)dr]\Delta m^*(r),$$
  
 $\Delta m^*(r+dr) = [4\pi r^2 dr]\Delta \rho^*(r) + \Delta m^*(r).$ 
(88)

Write the right-hand side as a square matrix multiplied into a column vector. Also note that the resulting vector relation applies to each solution, whence

$$\begin{pmatrix} \Delta \rho_1^* & \Delta \rho_2^* \\ \Delta m_1^* & \Delta m_2^* \end{pmatrix}_{r+dr} = \begin{pmatrix} 1 - A dr & -B dr \\ 4\pi r^2 dr & 1 \end{pmatrix} \begin{pmatrix} \Delta \rho_1^* & \Delta \rho_2^* \\ \Delta m_1^* & \Delta m_2^* \end{pmatrix}_r.$$
(89)

Every relation of the type (89) between square matrices translates immediately into the corresponding relation between determinants; or here,

$$D_{12}(r + dr) = (1 - A dr) D_{12}(r),$$
 (90)

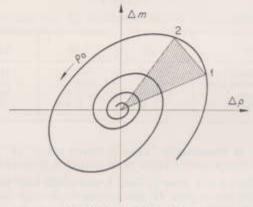
Rewrite this formula as

$$D_{12}(r + dr) \exp \int_{r}^{r+dr} A dr = D_{12}(r).$$
 (91)

Thus arrive immediately at the conservation law for "normalized area in phase space."

THEOREM 10.

$$D_{12}(r+dr) \exp \int_{-r+dr}^{-r+dr} A dr = D_{12}(r) \exp \int_{-r}^{r} A dr = P_{12}(r) = \text{constant}.$$
 (92)



Oscillations at r=5 km.

Fig. 4.—Schematic diagram of the oscillations in density and mass (relative to the limiting configuration) at a fixed value of r, as the central density is raised, showing the kind of "area in phase space" which is spanned by the vectors associated with two nearby central densities,  $\rho_{01}$  and  $\rho_{02}$ . The cross-hatched area is to be doubled (parallelogram) to obtain the quantity dealt with in the text.

Here the normalization factor (defined in terms of the limiting configuration,  $\rho_0$  infinite) has the value

$$\exp \int_{-r}^{r} A(r) dr$$

$$= \exp \int_{-r}^{r} \left( \text{coefficient of } \Delta \rho^* \text{ in expression for } -d\Delta \rho^* / dr \text{ obtained by} \right) dr$$

$$= \exp \int_{-r}^{r} \left[ \frac{d^2 p / d\rho^2}{dp / d\rho} d\rho - \frac{dp + d\rho}{p + \rho} - \frac{dp}{p + (m/4\pi r^3)} \right].$$
(93)

Here p,  $\rho$ , and m (asterisks and subscripts  $\infty$  have been omitted for simplicity;  $\rho \equiv \rho_{\infty}^*$  etc. —) are considered to be known as functions of r for the limiting configuration. The integral does not exist if the lower limit is taken to be zero. Therefore, it is reasonable to take the lower limit to be some standard point  $r = r_1$ . However, this procedure introduces an artificial element of arbitrariness into the normalization factor. For this reason

it is better to add and subtract inside the integrand a term  $dp/(p+\rho)$ . It compensates at the origin the term  $-dp/(p+m/4\pi r^5)$ , the only term in equation (93) which cannot be integrated explicitly. The integral of this new term is  $\ln (d\rho/dn)$ , where n is the number density of baryons (chaps. viii, ix). We arrive in this way at the following equivalent "canonical forms" for the normalization factor:

$$\exp \int_{\text{standard}}^{r} A dr = \frac{(dp_{\infty}^{*}/dp_{\infty}^{*})(dn_{\infty}/dp_{\infty}^{*})}{(p_{\infty}^{*} + p_{\infty}^{*})}$$

$$\times \left\{ \exp \int_{0}^{r} [(p_{\infty}^{*} + p_{\infty}^{*})^{-1} - (p_{\infty}^{*} + m_{\infty}^{*}/4\pi r^{2})^{-1}](dp_{\infty}^{*}/dr) dr \text{ (Form } \right\}.$$

$$\exp \int_{0}^{r} \frac{p_{\infty}^{*} - (m_{\infty}^{*}/4\pi r^{2})}{r - 2m_{\infty}^{*}} 4\pi r^{2} dr \text{ (Form 2)}$$

The integral in the exponent gives no contribution in Zones I and II, where the  $\gamma$ -law equation of state has been taken to apply. Write this asymptotic  $\gamma$ -law in the form

$$\rho_{\infty}^*(\text{cm}^{-2}) \equiv (G/\epsilon^{\pm}) \rho_{\infty}(g/\text{cm}^3) = L^{-2}(L^{\eta}n_{\infty})^{\gamma}$$

$$= \text{expression}(78) \text{ with } Q \text{ set equal to zero },$$
(95)

where L is some characteristic quantity with the dimensions of a length. Substitute equation (95) into equation (94). Then the canonical form of the normalization factor in the asymptotic  $\gamma$ -law region becomes

$$\begin{split} \exp & \int_{\rm standard}^{\tau} A \, d \, \tau = (\gamma - 1) \gamma^{-2} [\, 2\pi (\gamma^2 + 4\gamma - 4) / (\gamma - 1) \,]^{2 - (1/\gamma)} \\ & \times L (\tau / L)^{4 - (2/\gamma)} \, . \end{split} \tag{96}$$

This quantity is finite not only in Zones I and II, where equation (96) applies, but also all the way to the surface. It has the dimensions of length. In consequence the canonical "normalized area in phase space"  $P_{12}$  is dimensionless, as well as independent of r.

In Zones I and II, where a  $\gamma$ -law equation of state has been taken to apply, the normalization factor is proportional to  $r^{4-(2/\gamma)}$ ; or to  $r^{5/2}$  in the case  $\gamma = \frac{4}{3}$ . The conservation law (92) as it applies in Zone II,

$$r^{4-(2/\gamma)}D_{12}(r) = \text{constant},$$
 (97)

can be verified directly. For this purpose one only has to substitute into equation (97) from equations (78) and (79) the expressions for  $\Delta \rho_{1,\,2}$  and  $\Delta m_{1,\,2}$  in terms of the oscillating factors  $Q[(4\pi\rho_0^*/3)^{1/2}\ r]^{-\alpha} \exp\left[i\beta \ln\left[(4\pi\rho_0^*/3)^{1/2}\ r\right]\right]$ . All r-dependence indeed disappears from expression (97). Or referring back to equation (92), one finds the following explicit expression for the conserved "normalized area in phase space" in its dependence upon the central densities of the two configurations in question:

$$\begin{vmatrix} \Delta \rho_1 & \Delta \rho_2 \\ \Delta m_1 & \Delta m_2 \end{vmatrix}_{\text{at } r} \exp \int_{\text{standard}}^{\tau} A \, d \, r = P_{12} = 3 \left( \frac{3}{\pi} \right)^{1/2} \left( \frac{2}{3} \right)^{(1/\gamma)} \\ \times \frac{(\gamma - 1)^{1+(1/\gamma)} |Q(\gamma)|^2}{(5\gamma - 4)(\gamma^2 + 4\gamma - 4)^{(1/\gamma)}} \frac{\beta \sin \left[ (\beta/2) (\ln \rho_{02}^* - \ln \rho_{01}^*) \right]}{\left[ (\rho_{01}^* + \rho_{02}^*)^{1/2} L^2 \right]^{(3/2) - (1/\gamma)}}.$$
(98)

Now, as earlier,  $\beta$  is given by the expression  $[-(9/\gamma^2) + (11/\gamma) - \frac{1}{4}]^{1/2}$ . Through equation (98) the quantity which is propagated from the interior to the surface without change has at last been sorted out and evaluated.

### FINAL STEP IN PROOF OF DAMPED OSCILLATIONS: EFFECT ON SURFACE OF PERTURBATIONS IN INTERIOR

How do the static oscillations in the interior—"oscillations" defined relative to conditions in the limiting configuration—how do these oscillations affect the physics at the surface? Denote the mass of the limiting configuration by  $M_{\infty}^*$  and denote by  $R_{\infty}$  the radius, which by definition is the point where the pressure goes to zero. Consider now an equilibrium configuration of large but finite central density. At its surface, i.e., at the place where p vanishes for it, the radial coordinate is  $R_{\infty} + \Delta R$  and the mass is  $M_{\infty}^* + \Delta M^*$ . Or back at the point  $r = R_{\infty}$  we have in this configuration

$$m^*(R_\infty) = M_\infty^* + \Delta M^* - 4\pi R_\infty^2 \Delta R \rho_s^*$$
, (99)

with  $\rho_s = 7.8 \text{ g/cm}^2$  representing the surface density; and (from the equation of hydrostatic equilibrium)

$$p^*(R_\infty) = \rho_*^* M_\infty^* \Delta R / [R_\infty (R_\infty - 2M_\infty^*)],$$
 (100)

The departure from the limiting configuration at  $R_{\infty}$  is described by the "vector"

$$\Delta \rho^* = (d p^* / d \rho^*)_s^{-1} \rho_s^* M_{\infty}^* \Delta R / [R_{\infty} (R_{\infty} - 2M_{\infty}^*)],$$
  
 $\Delta m^* = \Delta M^* - 4\pi R_{\infty}^2 \Delta R \rho_s^*.$ 
(101)

Now consider alongside the one configuration of central density  $\rho_{01}$  a second configuration of central density  $\rho_{02}$ . Look at the expression for the "area in phase space" as defined by the cross-product of two vectors of the form (101):

$$\begin{vmatrix} \Delta \rho_1^* & \Delta \rho_2^* \\ \Delta m_1^* & \Delta m_2^* \end{vmatrix}_{B_\infty} = \left( \frac{d \, p^*}{d \, \rho^*} \right)^{-1} \frac{\rho_s^* M_\infty^*}{R_\infty (R_\infty - 2 M_\infty^*)} \begin{vmatrix} \Delta R_1 & \Delta R_2 \\ \Delta M_1^* & \Delta M_2^* \end{vmatrix} \,. \tag{102}$$

To normalize this expression, multiply by the canonical normalization factor (94), evaluated at the surface. There  $p^* = 0$ ,  $\rho^* = \rho_s^*$ , and  $(dn/d\rho^*)$  is the reciprocal of the baryon mass,  $\mu_s^* = \frac{1}{56}$  (mass\* of Fe<sup>56</sup> atom). Thus the normalized "area in phase space" is

$$P_{12} = (M_{\odot}^{*}/\mu_{s}^{*})R_{\odot}^{-1}(R_{\odot} - 2M_{\odot}^{*})^{-1} \times \exp \left[ \int_{Z_{\text{OBe III}}}^{R_{\odot}} \frac{\rho_{\odot}^{*} - (m_{\odot}^{*}/4\pi r^{3})}{r - 2m_{\odot}^{*}} 4\pi r^{2} dr \right] \begin{vmatrix} \Delta R_{1} & \Delta R_{2} \\ \Delta M_{1}^{*} & \Delta M_{2}^{*} \end{vmatrix}.$$
(103)

Equate the two expressions for the normalized "area in phase space": equation (98), obtained by working out from the center to the surface; and equation (103), based on conditions at the surface. In this way arrive at the equation

$$\begin{vmatrix} \Delta R_1 & \Delta R_2 \\ \Delta M_1^* & \Delta M_2^* \end{vmatrix} = \text{Constant}(\rho_{01}^* \rho_{02}^*)^{-(3/4)+(1/2\gamma)} \sin[(\beta/2)(\ln \rho_{02}^* - \ln \rho_{01}^*)], \quad (104)$$

where the constant is built up out of known or evaluable quantities. It follows from equation (104) that the perturbations in the surface conditions for any one configuration individually are of the form

$$\Delta R = C_R (\rho_0 * L^2)^{-(3/4) + (1/2\gamma)} \sin [(\beta/2) \ln (\rho_0 * L^2) + \delta_R],$$

$$\Delta M = C_M (\rho_0 * L^2)^{-(3/4) + (1/2\gamma)} \sin [(\beta/2) \ln (\rho_0 * L^2) + \delta_M],$$
(105)

with the character of damped harmonic oscillations in the variable  $\ln p_0$ , as was to be proved.

The amplitude factors  $C_R$ ,  $C_M$  and the phase factors  $\delta_R$  and  $\delta_M$  are not individually determinable from the law of conservation of normalized area in phase space. This law alone fixes only one combination of constants, the "vector product"

$$\begin{split} C_R C_M \sin(\delta_R - \delta_M) &= 3 \left( 3/\pi \right)^{1/2} \left( \frac{2}{3} \right)^{1/\gamma} \frac{(\gamma - 1)^{1+(1/\gamma)} |Q(\gamma)|^2}{(5\gamma - 4)(\gamma^2 + 4\gamma - 4)^{(1/\gamma)}} [-(9/\gamma^2) \\ &+ (11/\gamma) - (\frac{1}{4})^{1/2} \mu_s^* (R_{\infty}/M_{\infty}^*) (R_{\infty} - 2M_{\infty}^*) \\ &\times \exp \int_{2\alpha n_0}^{R_{\infty}} \frac{(m_{\infty}^* / 4\pi r^2) - \rho_{\infty}^*}{(r - 2m_{\infty}^*)} 4\pi r^2 dr \,. \end{split}$$
(106)

Here, as before, the integral goes over the limiting configuration, assumed known. That the "vector product" (106) does not vanish for  $\gamma$  in the allowed range from one to two shows that the oscillations in  $\Delta R$  and  $\Delta M$  are out of phase. Before examining the interesting implications of this circumstance, we turn back to the history of equilibrium configurations to see the meaning of the new oscillations in a wider context.

### REFERENCES

Bondi, H. 1964, Roy. Soc. London Proc., A, 281, 39.

Chandrasekhar, S. 1939, Introduction to the Study of Stellar Structure (Chicago: University of Chicago Press).

Harrison, B. K. 1965, Phys. Rev. (in press).

Sedov, L. I. 1959, Similarity and Dimensional Methods in Mechanics, trans. M. Friedman (New York: Academic Press).

Sommerfeld, A. 1960, Atombau und Spektrallinien, Vol. 2: Wellenmechanischer Erganzungsband (4th ed.; Braunschweig: Vieweg).
Tooper, R. F. 1964, Ap. J., 140, 434.

# MASS AND RADIUS OF EQUILIBRIUM chapter 6 CONFIGURATIONS: 1932–1964

That the mass of an equilibrium configuration is a damped periodic function of  $\ln \rho_0$  for large  $\rho_0$  does not seem to have been remarked heretofore. It was clear only recently that something unexpected was showing up in calculated curves for  $M^*$  as a function of central density. What is the history of this curve? And what points of principle had already come to light as one studied this curve in more and more detail?

### LANDAU'S PIONEERING ANALYSIS

In 1932 Landau gave a general argument that a sufficiently large collection of cold matter cannot sustain itself against gravitational collapse. His argument was based on the idea that electrons supply the pressure resisting collapse. The neutron was not discovered until after Landau had submitted his paper for publication. However, his arguments apply as well to a neutron gas as to an electron gas. Therefore, Landau's arguments will be rephrased here so as to bring out their full generality: Landau pointed to the known circumstance that with increasing mass the material is more strongly compacted. In consequence the Fermi gas, which resists the gravitational pull, is squeezed to a higher and higher energy per particle. Ultimately, this Fermi energy rises to a relativistic level. Thereupon this energy ceases to depend upon the rest mass of the particle. It then makes no difference in the energy per particle, and therefore no difference in the pressure, whether the Fermi gas consists of electrons (densities up to ~108 g/cm3) or whether it consists of neutrons (densities ~10th g/cm3). What counts is only the linear dimension of the region to which the particle is confined. On a simplified analysis one ascribes to the configuration an effective mean density, and an effective radius R. The linear dimension of the region to which one particle is confined is then of the order  $R/A^{1/2}$  in the case of an ideal neutron gas containing A baryons, almost all of which are neutrons. In the case of where the pressure arises from electrons, and where the nuclear composition is roughly half neutrons and half protons, then the number of electrons is only about half the baryon number, or  $\sim A/2$ .

The confinement distance gives in order of magnitude the de Broglie wavelength. Divide into  $\hbar$  to obtain the momentum. Then multiply by c to obtain the Fermi energy of compression per particle:

$$E_{\rm F} \sim (\hbar c/R) \left\{ \frac{A^{1/3} \text{ for neutrons}}{(A/2)^{1/3} \text{ for electrons}} \right\}$$
. (107)

In geometrized units the corresponding mass-energy per fermion is

$$M_{\rm F}^{*}({\rm cm}) \equiv (G/c^{2})(E_{\rm F}/c^{2}) \sim (L^{*z}/R) \left\{ \frac{A^{1/3}}{(A/2)^{1/3}} \right\},$$
 (108)

where  $L^* = (\hbar c/G)^{1/2} = 1.6 \times 10^{-33}$  cm is the Planck length (see Table 2).

The gravitational mass-energy per fermion is given in order of magnitude by the "standard mass" associated with one fermion,

 $\mu_s$  ( = baryon mass) in case of neutron gas,

~ 2 µ, (proton + neutron) in case of electron gas,

multiplied by the effective average gravitational potential,  $\sim -GA\mu_s/R$ . Translating this gravitation energy to geometrized units, one has

$$M_0^*(cm) \sim \begin{cases} 1 \text{ for } n\text{-gas} \\ 2 \text{ for } e\text{-gas} \end{cases} A \mu_s^{*z} / R,$$
 (109)

where  $\mu_s^* = (G/c^2)\mu_s = 1.2 \times 10^{-62}$  cm is the mass of a baryon, expressed in cm (see Table 2).

Both the compressional and the gravitational energy depend in the same way upon R, Landau pointed out. Therefore, the decisive question is the sign of the totalized coefficient of 1/R. When it is positive, it will decrease the total energy to increase R. Then the de Broglie wavelengths will increase. The Fermi energy will fall into the non-relativistic region. The energy of compression will then fall faster than 1/R. Equilibrium—and an equilibrium which is stable—will be obtained at some finite and natural value of R. Not so when the totalized coefficient of 1/R is negative. Then collapse will set in, Landau argued. The critical number of baryons at which the coefficient of 1/R changes sign is given in order of magnitude by the equation

$$L^{*1}A^{1/3} - A\mu_s^{*1} = 0$$
 for the neutron gas ;  
 $L^{*1}(A/2)^{1/3} - 2A\mu_s^{*1} = 0$  for the electron gas ;

or, overlooking details,

$$A \sim (L^*/\mu_s^*)^3 \sim (10^{-33} \text{ cm}/10^{-52} \text{ cm})^3 \sim 10^{57};$$
  
 $A \mu_s \sim 10^{57} \times 1.6 \times 10^{-24} \text{ g} \sim 2 \times 10^{33} \text{ g} (= M_{\odot}).$ 
(111)

In this way Landau arrived at a value for the critical mass of cold matter which in both cases is of the order of magnitude of the mass of the Sun, M<sub>☉</sub>. As reviewed in retrospect, Landau's reasoning indicates that there should be two separate regimes of collapse, one at densities a little over white-dwarf densities, the other a little above normal nuclear densities.

It is interesting to extend Landau's line of reasoning to estimate the effect of a change in the constant of proportionality  $L^2$  in the formula  $\rho^* = L^2 n^{4/3}$ . A 10 per cent increase in this constant means a 5 per cent increase in L itself and a 15 per cent increase in the critical mass and the critical baryon number (eq. [111]).

### THE CHANDRASEKHAR LIMIT

The 1935 Chandrasekhar added to Landau's order-of-magnitude discussion a detailed analysis of the approach to the first critical point predicted by Landau (the point where electron pressure is overwhelmed) based on the following assumptions: (1) Newtonian equation of hydrostatic equilibrium (eq. [43] in the limit " $c^2 \rightarrow \infty$ "), (2) cold matter, (3) pressure supplied by ideal degenerate electron gas, and by this gas alone. The Fermi energy of this electron gas starts at non-relativistic values for low compressions ( $\rho < 10^{\circ}$  g/cm²) and rises to values great compared to  $mc^2$  for high compressions. Chandrasekhar calculated in detail the equation of state valid throughout the entire range of Fermi energies (eq. [275]–[278] below). (4) The gravitating mass associated with one electron (the mass of the electron itself, plus the mass of the charge-neutralizing proton, and of

any accompanying [bound] neutrons) is taken to have a standard value  $\mu_{eff}$ , unaffected by compression (no relativistic increase of mass; no nuclear transmutations; no inverse

beta-decay of the type  $e^- + p \rightarrow n + \nu$ ).

Integrating the equation of hydrostatic equilibrium starting first with one central density  $\rho_0$ , then with another, and so on, Chandrasekhar obtained a curve from which one can read off for every central density—and therefore for every equilibrium configuration—the mass M of that configuration. This Chandrasekhar curve for M as a function of  $\rho_0$  shows no maximum. Instead, the calculated M approaches asymptotically a finite bound, the Chandrasekhar limit,

$$M_{\rm Chandra}^* = (3\pi)^{1/2} \frac{2.01824}{2} (L^*/\mu_{\rm eff}^*)^2 \mu_{\rm eff}^*,$$
 (112)

as the central density increases indefinitely to the point of "central crush." Apart from having a well-defined numerical coefficient, this result agrees with that of Landau (eq. [110]). The electron mass does not appear in the equation. The number 2.01824 is the solution of an eigenvalue problem; it is a dimensionless mathematical constant such as  $\pi$  or e. When one takes for the effective mass per electron

$$\mu_{\rm eff} = (\frac{1}{26})$$
 (mass of Fe<sup>16</sup> atom)

or (see chap. i, n. 4; and Table 2)

$$\mu_{\text{eff}}^* = \frac{56}{26} \frac{0.998838}{1.007825} (1.242 \times 10^{-52} \text{ cm}) = 2.65 \times 10^{-52} \text{ cm},$$
 (113)

he finds for the Chandrasekhar limit

$$M_{\text{Chandra}}^* = 1.860 \times 10^5 \,\text{cm} = 1.26 M_{\odot}^*$$
, (114)

a little more than the mass of the Sun. There is no equilibrium for a greater mass, according to this analysis. Of course the Sun and more massive stars are hot and enormously expanded relative to the cold configuration considered here and, therefore, are nowhere near this Chandrasekhar limit.

### THE COLD NEUTRON STAR OF OPPENHEIMER AND VOLKOFF

In 1938, further pursuant to Landau's considerations, Oppenheimer and Serber pointed out that electrons could not be compressed to indefinitely high Fermi energy, as contemplated in the approach to the Chandrasekhar central crush. Instead, they must react with protons to form neutrons. In a following paper, Oppenheimer and Volkoff (1939) analyzed numerically the equilibrium configurations of a star built up from an ideal neutron gas. For this purpose they employed for the first time the general-relativity equation of hydrostatic equilibrium. For equation of state of the neutrons they adopted (with appropriate mass change) the non-relativistic-through-relativistic equation of state which Chandrasekhar had derived for an ideal electron gas, maintained at absolute zero temperature. Their results for equilibrium configurations had no correspondence with those of Chandrasekhar for an obvious reason. They dealt with different physical conditions and much higher densities.

For central densities as low as  $10^{10}$  g/cm<sup>3</sup> and less, the calculated equilibrium mass was under  $\frac{1}{10}$  the mass of the Sun. With increase of the central density above  $10^{10}$  g/cm<sup>3</sup> the mass of the configuration continued to rise steadily. It reached a peak value of about 0.7 of the mass  $M_{\odot}$  of the Sun for a central density  $\rho_0$  in the neighborhood of  $10^{15}$  g/cm<sup>3</sup>. At higher density the mass appeared to fall gradually, approaching a limiting

<sup>&</sup>lt;sup>1</sup> Solution of the Lane-Emden equation of order n = 3; see Chandrasekhar (1939), p. 96, Table IV-

value of the order of 0.4  $M_{\odot}$  for infinite central density. Oppenheimer and Volkoff made it plausible that the equilibrium is stable for all configurations short of the peak at 0.7  $M_{\odot}$ ,  $\sim 10^{15}$  g/cm<sup>3</sup> and unstable for all the configurations of higher central density. Since this point corresponds to the second of the two points of instability estimated by Landau,

it may be called the Landau-Oppenheimer-Volkoff (LOV) point of instability.

In using the term "LOV point of instability" to designate the maximum in the curve for  $M^*$  as a function of central density, one has to be careful to distinguish this kind of configuration from the configuration of "central crush" ( $\rho_{\theta} = \infty$ ). There is nothing singular about the density distribution for the critical LOV configuration. The characteristic feature is only this, that here, Oppenheimer and Volkoff propose, the transition occurs from (1) configurations which undergo vibrations when subject to an arbitrary small perturbation to (2) configurations which, when perturbed, move further and further from equilibrium, in the direction of explosion or collapse.

INVERSE BETA-DECAY; A UNIVERSAL EQUATION OF STATE; THE FINAL REVELATION OF THE FIRST POINT OF INSTABILITY; THE 1964 HARRISON-WAKANO-WHEELER CURVES

What about the first point of instability predicted by Landau, the one at densities  $\sim 10^{\circ}$  g/cm<sup>3</sup>? The sequence of configurations calculated by Chandrasekhar marches all the way from low central densities to infinite  $\rho_0$  ("central crush") and yet does not show any such point of instability. Why not? In considering this question three of us (B. K. H., M. W., and J. A. W.) came to the conclusion that this point of instability can never show up unless the equation of state is physically reasonable, in the sense that it makes proper allowance for the occurrence of reactions of the type

$$e^- + p \text{ (bound)} \rightarrow n \text{ (bound or free)} + p$$
. (115)

The problem was made well defined by going to the idealized limit in which (1) all reactions are catalyzed to the absolute end point of thermonuclear evolution, and (2) matter is at absolute zero temperature. This double postulate means that one does not have many different equations of state to consider, for different materials, but one universal equation of state for cold, catalyzed matter. Happily, elementary considerations of statistical mechanics and standard data on nuclear masses together sufficed to determine this universal equation of state with acceptable accuracy for the whole range from  $\rho = 7.8$ g/cm<sup>3</sup> (uncompressed Fe<sup>54</sup>) up to  $\rho$  values approaching those of the nucleus ( $\sim 10^{14}$ g/cm<sup>3</sup>) (1958 work of B. Kent Harrison; results reported by B. K. H., M. W., and J. A. W. in SEU; details of derivation given for first time in present report, chap. x). For nuclear and supranuclear densities we accepted, for the sake of simplicity, the concept of an ideal cold degenerate gas of electrons, protons, and neutrons, in beta equilibrium, but with negligible particle-particle interactions. We had not seen at the time when we reported this work (1958) the results of Schatzman." He had adopted the Newtonian equation of hydrostatic equilibrium, an excellent approximation for densities of 1010 g/cm<sup>3</sup> and less. He had followed the early considerations of van Albada (1946, 1947; see also Burbidge, Burbidge, Fowler, and Hoyle [1957]) on the the crushing of electrons onto nuclei by pressure. From this foundation Schatzman calculated a correction formula in the Chandrasekhar analysis. He found that the equilibrium mass no longer increases indefinitely with central density (even if more and more slowly toward an asymptote) as in the Chandrasekhar results. Instead, it reached a maximum  $M \sim 1.29$  $M_{\odot}$  at  $R \sim 2.9 \times 10^{-3} R_{\odot}$ . The maximum differs from the LHWW maximum. Also

<sup>&</sup>lt;sup>3</sup> See Schatzman (1956), for a discussion of which we are indebted to Professor Schatzman; 1958a, b. Schatzman refers to still earlier work of Kaplan (1949), who had made assumptions just opposite to those of Schatzman: no inverse beta-decay processes (hence accepting the Chandrasekhar equation of state) but allowance for the general-relativity equation of hydrostatic equilibrium. On these quite different assumptions Kaplan also found a peak in the curve for mass as a function of central density, but at  $\rho_0 = 2.5 \times 10^{19} \, \text{g/cm}^3$ ,  $R = 1.1 \times 10^5 \, \text{cm}$ , M = 0.96 of the Chandrasekhar limiting mass.

Schatzman's maximum mass, at this finite density, is greater even than what Chandrasekhar's limiting formula (eq. [112], [114]) gives for  $\mu_{\rm eff} = (\frac{1}{26})$  (mass of Fe<sup>56</sup>) at infinite density; namely,  $M_{\rm m} = 1.26~M_{\odot}$ . This difference appears to be traceable to the circumstance that most of Schatzman's numerical calculations assume an average mass number  $\langle A \rangle = 16$  for the dominant nuclear species. The philosophy in the present work is different. What will be the dominant nuclear species is not specified in advance. Neither is it dependent upon any special assumption about the past history of the system.

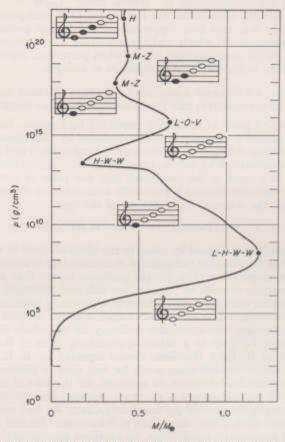


Fig. 5.—Harrison-Wakano-Wheeler (HWW) catalogue of all equilibrium configurations of cold, catalyzed matter. HW equation of state. Integrations to central density of 10<sup>18</sup> g/cm³, M. W.; integrations to 10<sup>28</sup> g/cm³, B. K. H. Masses (after assembly) in units of the mass of the Sun, M☉ = 1.987 × 10<sup>28</sup> g (M☉\* = 1.474 × 10<sup>3</sup> cm). Black dots: points of change of stability. L stands for Landau, who predicted the existence of the two most important of these critical points. The HWW curve agrees closely in the range 10<sup>18</sup> to 10<sup>17</sup> g/cm³ with the 1939 curve of Oppenheimer and Volkoff, who were the first to determine the position of the LOV critical point (model of ideal neutron gas). From low densities up to ~10<sup>7</sup> g/cm³ the HWW curve for M(ρ<sub>0</sub>) agrees in its general run with the curve calculated by Chandrasekhar in 1935 for a substance deriving its pressure from an ideal electron gas, and with an effective mass per electron μ<sub>eff</sub> equal to ½ of the mass of an Fe<sup>36</sup> atom. However, the Chandrasekhar curve shows no maximum; it approaches an asymptote M∞/M☉ = 1.26 as the central density goes to infinity. When one allows for the crushing of electrons into combination with protons (HW equation of state) he arrives (1958) at the LHWW critical point. MZ, critical points discovered by Misner and Zapolsky (1964); H, by Harrison (1964). The musical scales show which among the acoustical normal modes of oscillation (purely radial; spherical symmetry) are unstable (black notes) between one critical point and the next (discussion in text).

Instead, the present treatment assumes as a matter of principle the unique and universal equation of state of cold, catalyzed matter. For each pressure there is then a uniquely determined nuclear species which is dominant at that pressure (cf. the derivation of the

HW equation of state in chapter x and especially Table 14).

This HW equation of state can be inserted into the TOV general relativity equation (11) of hydrostatic equilibrium. One of us (Masami Wakano, also in 1958) integrated the resulting differential equation for forty-five values of the central density, going up to 1018 g/cm3. This range has since been extended (by Harrison in 1964) to 1022 g/cm3. The earlier HWW results and the HW equation of state have appeared in print in several places (Harrison et al. 1958; Wheeler 1962; Wheeler 1964). The newly extended results (1964) appear in Figures 5, 6, and 7.

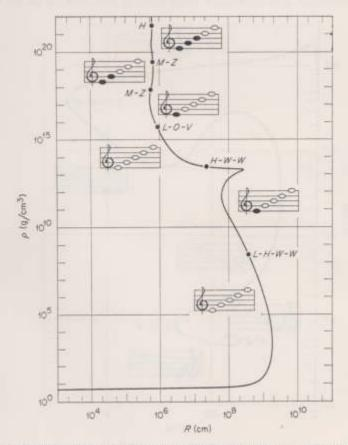


Fig. 6.—Radius as a function of the central density for the equilibrium configurations of cold, catalyzed matter. Integrations of  $10^{16}$  g/cm<sup>2</sup>, M. W.; to  $10^{10}$  g/cm<sup>3</sup>, B. K. H. The black dots denote the critical points of Fig. 5, where both  $M^*$  and A are extremal with respect to change in  $\rho_0$ . Though  $M^*$  is stationary at a critical point, R is not. Consequently the "gravitational potential"  $(1-2M^*/R)^{1/2}$  is changing. A bigger R on one side of a maximum than on the other means a higher gravitational potential, a non-so-tight binding, and therefore instability with respect to nearby configurations on the other side of the critical point. See Fig. 5 for further details.

<sup>&</sup>lt;sup>5</sup> Thanks are expressed to Dr. H. T. Maehly and Mrs. Barbara Weymann of the staff of the Institute for Advanced Study's MANIAC for kind collaboration in this work.

The Harrison-Wakano-Wheeler curve for equilibrium mass as a function of central density (Fig. 5) showed in 1958 for the first time both of the critical points whose existence had been predicted by Landau. At this LHWW4 point the system becomes unstable against a collapse in which electrons are crushed into union with baryons. This instability occurs at a point well short of the ideal Chandrasekhar limit and for an obvious reason: a cold gas which has lost some of its electrons by inverse beta-reactions cannot provide as much pressure as a gas which has all its electrons. When the central density increases further, this "softness" is replaced by "hardness." The system transforms largely into a neutron gas. A return to stability takes place. This return to stability is marked by another critical point, at  $\rho_0 \sim 3 \times 10^{13} \, \mathrm{g/cm^3}$  (HWW, 1958). Then comes the LOV critical point ( $\rho_0 \sim 6 \times 10^{16} \, \mathrm{g/cm^3}$ ). In 1964, Misner and Zapolsky brought to light a further minimum and maximum. These features also show up on the extended

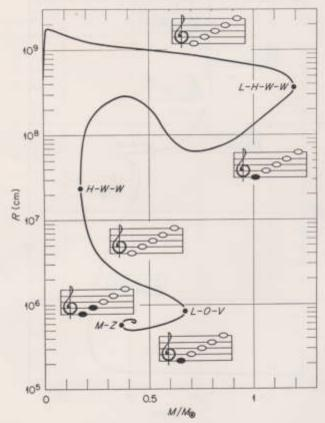


Fig. 7.—Connection between mass and radius for the equilibrium configurations of cold, catalyzed matter. Integrations to  $10^{18}\,\mathrm{g/cm^3}$ , M. W.; to  $10^{29}\,\mathrm{g/cm^3}$ , B. K. H. Objects with the size of meteorites and planets lie so far to the left that they can hardly be made out. The winding-up of the curve for high  $\rho_0$  values, first brought to light by B. K. H., is proved in chap. v to be a general feature of all asymptotically  $\gamma$ -law equations of state. Consequently there are infinitely many critical points (extrema of M; black dots in diagram). Acoustical modes which are unstable are indicated on the musical scale by black notes; stable ones, by white notes.

<sup>&</sup>lt;sup>4</sup> Landau-Harrison-Wakano-Wheeler.

Note added in proof: Tsuruta (1964) has independently found this maximum and minimum.

HWW curve, along with still another minimum at  $\rho_0 \sim 3 \times 10^{21} \,\mathrm{g/cm^3}$  found by Harrison in 1964.

#### REFERENCES

Albada, G. B. van. 1946, Bull. Astr. Inst. Netherlands, 10, 161.

— 1947, Ap. J., 105, 393.

Burbidge, E. M., Burbidge, G. R., Fowler, W. A., and Hoyle, F. 1957, Rev. Mod. Phys., 29, 547.

Chandrasekhar, S. 1935, M.N., 95, 207.

Chandrasekhar, S. 1935, M.N., 95, 207.

Chandrasekhar, S. 1935, M.N., 95, 207.

1939, Introduction to the Study of Stellar Structure (Chicago: University of Chicago Press).

Harrison, B. K., Wakano, M., and Wheeler, J. A. 1958, in Onzième Conseil de Physique Solvay, La Structure et l'évolution de l'univers (Brussels: Stoops).

Kapian, S. A. 1949, Notes Savantes Université Luów, 15, 110.

Landau, L. D. 1932, Phys. Zs. Savjetunion, 1, 285.

Misner, C. W., and Zapolsky, H. S. 1964, Phys. Rev. Letters, 12, 635.

Oppenheimer, J. R., and Serber, R. 1938, Phys. Rev., 54, 530.

Oppenheimer, J. R., and Volkoff, G. 1939, Phys. Rev., 55, 374.

Schatzman, E. 1956, Astr. Zh., 33, 800.

1958b, White Dwarfs (New York: Interscience).

1958b. "Théorie des naines blanches," in Hdb. d. Phys., ed. S. Flügge, Vol. 51 (Berlin: Springer-Verlag).

Benjamin), chap. x.

# THEORY OF THE STABILITY OF chapter 7 EQUILIBRIUM CONFIGURATIONS

#### THE FREQUENCY OF THE ACOUSTICAL MODES OF SPHERICAL SYMMETRY

What is the explanation of these strange features in the curve for M as a function of  $\rho_0$ ? As the central density increases, does each maximum in M mark the passage from stability to instability, and does each minimum signal the return from instability to stability? That generalization, like the generalization that all odd numbers are prime, is borne out only by the first few examples! HWW already in 1958 reasoned that the LHWW maximum marks the onset of instability, and that the HWW minimum shows the return of stability—a stability which Oppenheimer and Volkoff in 1939 made it plausible to consider as disappearing at the LOV maximum. To allow a definitive stability analysis, Chandrasekhar (1964a, b) and also Misner and Zapolsky (1964) have recently formulated a variational principle with the help of which one can determine the circular frequency,  $\omega$ , of the lowest purely radial mode of vibration of the system (acoustical mode;  $\omega$  in radians per unit change in the group-theoretically defined Schwarzschild time coordinate t, a coordinate which agrees asymptotically for large r with proper time). For this purpose one picks that trial function,  $\xi(r)$  (amplitude of radial displacement in the oscillation), which minimizes the expression<sup>2</sup>

$$\omega^{\pm} = (c \mu_s^*)^2 (1 - 2M^*/R)$$

$$\times \frac{11 - (111 + 1) - 1V}{\int_0^R (1 - 2m^*/r)^{-3/2} (\rho^* + p^*) (d \rho^*/dn) \, \xi^2 r^2 dr}.$$
(116)

Here we use the abbreviations

$$\begin{split} \Pi &= \int_0^R (\,1 - 2\,m^{\,*}/\,r\,)^{\,-1/2} n^{\,2} (\,d\,n/\,d\,\rho^{\,*}\,)^{\,2} (\,d^2\,\rho^{\,*}/\,d\,n^2\,) \\ &\qquad \qquad \times [\,(d/\,d\,r\,) (\,r^2\,\xi\,d\,\rho^{\,*}/\,d\,n\,)\,]^{\,2} r^{\,-2} d\,r\,\,, \\ (\,\Pi\Pi + \Pi\,) &= \int_0^R (\,1 - 2\,m^{\,*}/\,r\,)^{\,-1/2} n\,(\,8\pi\,r^2\,\rho^{\,*} + 4\,m^{\,*}/\,r\,)\,\xi^2 d\,r\,\,, \end{split}$$

<sup>&</sup>lt;sup>1</sup> This variational principle is derived from energy considerations in Appendix B, just as the TOV equation of hydrostatic equilibrium was derived from energy considerations in chap. iii.

<sup>&</sup>lt;sup>2</sup> This expression has been obtained by transforming Chandrasekhar's formula for  $ω^3$  in such a way that every quantity which appears at a given point r will be directly expressed in terms of the physical variables at that point. Thus, wherever  $e^{b_0/2}$  appears in his formula we write  $(1-2m^*/r)^{-1/2}$ , and wherever  $e^{b_0/2}$  appears we put (cf. eq. [28])  $(1-2M^*/R)^{1/2}$   $μ_e^*/μ^*$ . We also replace the pressure gradient  $dp^*/dr$  by  $-(p^* + ρ^*)(m^* + 4π^2ρ^*)/r(r - 2m^*)$ ; and the chemical potential  $μ^*$  by  $(p^* + ρ^*)/n$  or  $dρ^*/dn$ , as appropriate (eq. [14]). We understand by  $μ_e^*$  the standard baryon mass; that is,  $\frac{r}{k^*}$  of the mass of a free atom of Febt (as in Table 2); and by n, the number density of baryons. Finally, where Chandrasekhar specializes to a γ-law equation of state and writes in one of his terms (corresponding to H above) the quantity γρ, we replace this by its proper generalization  $(ρ^* + ρ^*)(dρ^*/dρ^*) = n dρ^*/dn = n^2d^2ρ^*/dn^2$ . The numbering I, II, III, IV has been employed so that one can, if he wishes, check each term as so transformed against the corresponding term on the right-hand side of Chandrasekhar's eq. (15').

and

$$IV = \int_0^R (1 - 2m^*/r)^{-1/2} n (4\pi r^2 p^* + m^*/r)^2 \xi^2 dr.$$

The function  $\xi_1(r)$  which produces the lowest value of the fraction (116) is the "normal mode" or "lowest mode" of oscillation of the system. This known, let one start anew minimizing expression (116). This time, however, demand that the trial function  $\xi(r)$  be orthogonal to  $\xi_1(r)$  in the sense

$$\int (1 - 2m^*/r)^{-1/2} (\rho^* + p^*) (d\rho^*/dn) \xi(r) \xi_1(r) r^2 dr = 0. \quad (118)$$

In this case the extremum problem defines another function,  $\xi_2(r)$ , the "second mode," Similarly one can define and calculate higher modes, one by one, until one has a complete set of modes,  $\xi_1(r)$ ,  $\xi_2(r)$ , . . . ,  $\xi_n(r)$ , . . . , which—for convenience—one has multiplied by such factors that they are not only orthogonal but also normalized:

$$(\xi_m, \xi_n) = \int (1 - 2m^*/r)^{-1/2} (\rho^* + p^*) (d\rho^*/dn) \xi_m(r) \xi_n(r) r^2 dr = \delta_{mn}$$

$$= \begin{cases} 0 \text{ for } m \neq n \\ 1 \text{ for } m = n \end{cases} .$$
(119)

In the special case of a sphere of iron of modest dimensions, where the density is practically the same at the center as at the surface, the modes under discussion have a well-known and simple form,

$$\xi(r) = (\Delta \rho_0 / k \rho_0) \begin{cases} -(kr)/3 \text{ for small } r \\ [(kr)^{-1} \cos kr - (kr)^{-2} \sin kr] \text{ for all } r \end{cases} \cos \omega l,$$

$$\Delta \rho(r) = \Delta \rho_0 (kr)^{-1} \sin kr \cos \omega l.$$
(120)

Here the wavenumber k is such as to make the density and pressure perturbations vanish at the surface, r = R:

$$k_n = n \, (\pi/R) \qquad \qquad (n=1, \, 2, \, 3, \, \ldots),$$
 
$$\omega_n^2 = k^2 (\, d \, p / d \, \rho \,)_0 = {\rm constant} \, \, n^2 \, . \eqno(121)$$

In the following we consider the dynamics of the individual normal modes at a moment

when the central density is increasing.

For the lowest mode, n=1, the density change  $\Delta \rho(r)$  falls monotonically from  $\Delta \rho = \Delta \rho_0$  at the center to  $\Delta \rho = 0$  at the surface. The material undergoes a simple breathing oscillation. The displacement  $\xi(r)$  vanishes at r=0, by reason of symmetry, but everywhere else is directed inward. For the next mode, n=2, the material moves inward between r=0 and r=0.581 R, and outward from that nodal surface to r=R. For the mode n=3 there are two nodal spheres which divide the two regions where the fluid moves inward from the one intervening region where it moves outward. More generally, in the nth mode the displacement  $\xi(r)$  vanishes at the origin and in addition on (n-1) spherical surfaces, or at a total of n points.

When the mass of the configuration is increased, the density at the center rises. In the course of this change each normal mode of oscillation gradually changes in  $\omega^2$ . Also the amplitude  $\xi(r)$  ceases to be given by a formula as simple as equation (118). However, each mode remains clearly identified. The displacement  $\xi(r)$  has the same number, n, of zeroes, as did the ancestral mode from which it was derived. The amplitudes for different modes satisfy the condition (119) of orthogonality. Also the quantities  $\omega_n^2$  remain in monotonic

sequence,

$$\omega_1^2 < \omega_2^2 < \omega_3^2 < \dots$$
 (122)

Theorem 11. The configuration is stable against arbitrary small perturbations of spherical symmetry if and only if  $\omega_1^2$  is positive.

By way of illustration, consider the case where  $\omega_1^2$  is negative (call  $\omega_1^2 = -\alpha_1^2$ ; thus the amplitude factor multiplying  $\xi_1$  depends upon time as  $e^{\pm \alpha_1 t}$ ) and all the other  $\omega_n^{2}$ 's are positive (amplitude factor periodic in  $\omega_n t$  with period  $2\pi$ ). Let the actual configuration differ from the equilibrium configuration for that same number of baryons, A, by a small initial static radial displacement  $\xi_i(r)$ . Then at any later time at which the small amplitude approximation makes sense, the displacement is

$$\xi(r, t) = (\xi_i, \xi_1) \xi_1(r) \cosh \alpha_1 t + \sum_{n=2}^{m} (\xi_i, \xi_n) \xi_n(r) \cos \omega_n t,$$
 (123)

The first term, if it differs from zero at all, eventually comes to dominate the motion. The increasingly rapid inward flow of matter throughout the entire system becomes more important than any of the vibratory displacements associated with  $n = 2, 3, \ldots$ . This is the situation when the "Fourier coefficient"  $(\xi_i, \xi_1)$  of the original displacement is positive; that is, when the original displacement itself is "predominantly inward." When the initial displacement is predominantly outward, and  $(\xi_i, \xi_1)$  is negative, then an

outward flow becomes stronger and stronger as time advances.

When not only  $\omega_1^2$  but also  $\omega_2^2$  is negative, then *two* modes of motion grow essentially exponentially with time. However, the growth constant for the first of these modes,  $\alpha_1$ , exceeds the growth constant,  $\alpha_2$ , for the second mode (cf. eq. [122]). Therefore, the first mode, when it has any significant amplitude at all to begin with (non-negligible value of  $[\xi_i, \xi_1]$ ), will eventually dominate. Thus a system with both  $\omega_1^2$  and  $\omega_2^2$  negative can be compared with a pencil standing on its tip, on top of which there is *another* pencil standing on its tip. When an arc light projects onto a screen the motion of the two-pencil system, two modes of instability show up. In the slower-growing mode the angle of inclination of the upper pencil to the vertical is 1.43 times as great as the angle of inclination of the lower pencil, and has the same sign. In the other mode the upper pencil has -2.10 times the inclination of the lower one; and the exponential growth constant is 2.68 times larger. This faster growing mode dominates in the case of the pair of pencils; and likewise in the case of an equilibrium distribution of mass in which the two lowest acoustical modes of spherical symmetry are both unstable.

Misner and Zapolsky (1964), employing the variational principle of Chandrasekhar, calculate the value of  $\omega^2$  for the lowest acoustical mode near the LOV critical point. They find that  $\omega_1^2$  changes from positive (stability) to negative (instability) as  $\rho_0$  increases through the characteristic value,  $\sim 6 \times 10^{16}$  g/cm<sup>3</sup>, associated with this critical point. This circumstance means that configurations are unstable for values of  $\rho_0$  for at least

some distance past this point.

What about the further critical point marked MZ in Figure 5, located near  $\rho_0 \sim 3 \times 10^{19}$  g/cm<sup>3</sup>? There, as at the LOV critical point, the curve for M as a function of  $\rho_0$  shows a maximum. In the neighborhood of this maximum Misner and Zapolsky again calculated  $\omega_1^2$ . However, in this case they found no change in the sign of  $\omega_1^2$  at or near the maximum in  $M = M(\rho_0)$ . They report that the lowest acoustical mode is unstable throughout this region. They quote one of us (J. A. W.) as reasoning that it is not the lowest mode but a higher mode which becomes unstable at the MZ critical point. We shall see shortly that the third acoustical mode becomes unstable at this point.

So much for what has been learned previously about the stability of the equilibrium configurations by calculating the frequencies of acoustical modes. Now for another preliminary step toward understanding stability, this time focusing attention on energy.

<sup>3</sup> For the familiar arguments that justify this stability theorem, see any summary of the theory of small departures from equilibrium (work of Poincaré, Liapounoff, and Morse [1934, 1939, 1951]) as, e.g., Ledoux (1958); Lyttleton (1953); or Geronimus (1954).

### ZEL'DOVICH ON SOLUTIONS WITH ENERGY EXCESS

Zel'dovich (1962) compares the configurations just before the LOV mass maximum ( $\rho_0 < \rho_{LOV} \sim 6 \times 10^{15} \, \mathrm{g/cm^2}$ ) with those just beyond that maximum ( $\rho_0 > \rho_{LOV}$ ). For each baryon number A, less than the peak value  $A_{LOV}$ , and greater than some unspecified lower limit, there are two configurations. The high- $\rho_0$  one of these two configurations, as Zel'dovich can show from the results of the numerical integrations of Oppenheimer and Volkoff, has a greater mass-energy than does the low- $\rho_0$  arrangement. Moreover, for A values sufficiently low in comparison with  $A_{LOV}$  the high- $\rho_0$  configuration even has a higher mass-energy than that corresponding to A free baryons. This point can be summarized and stated with a little more precision in Theorem 12.

Theorem 12. There exist solutions of the general-relativity equation of hydrostatic equilibrium which have excess energy relative to dispersed Fe<sup>56</sup> atoms at rest at infinite separation.

Figure 8 shows mass-energy as a function of baryon number (schematic only, in order to show all the important features on one and the same diagram). The heavy line, leading

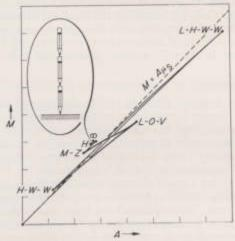


Fig. 8.—Mass-energy as related to baryon number (schematic). Dashed straight line: For baryons in the standard form of free Febb atoms ( $\mu_* = \frac{1}{2} \pi$  mass of Febb). Heavy lines: As additionally deduced here from the numerical results of Oppenheimer and Volkoff. Lighter lines: As additionally deduced here from the HW integrations, See Fig. 5 for identification of critical points. Here "\widtharpoonup" denotes the limiting configuration of infinite central density. The infinitely many zigzags leading to this point are not shown. When two sectors of the curve meet at a critical point, the configurations on the higher lying of these two sectors have (n+1) unstable acoustical modes (purely radial; spherical symmetry) when the configurations on the lower-lying sector have n unstable acoustical modes. The slope gives the chemical potential,  $\mu_*^*e^{i\eta_*}$  of a baryon anywhere in the interior of the configuration, and at its surface (r=R), in the form  $dm^*/dA = \mu_*^*(1-2M^*/R)^{1/R}$ . The difference in this slope between the higher-lying configurations and the lower-lying configurations near a point in the diagram where two sectors meet is directly connected with the operation of "pumping up the energy of the system." This operation takes place in a cycle in which one adds baryons and then takes them away (points LOV and LHWW) or takes them away and then adds them (MZ and H points). This "pumping action" is the foundation for an important point noted by Zel'dovich: There are configurations which are collectively unstable against breakup into free Febb atoms even though any individual particle is well bound to the configuration in every instance (chemical potential less than the standard value  $\mu_*$ ; or a value of the general-relativity gravitational potential at the surface,  $[1-2M^*/R]^{1/R}$ , which in all cases is less than unity). This instability is analyzed more deeply in the text in terms of the changing stability of individual modes of acoustical vibration. The three pencils standing tip-to-top symbol

from the HWW to the LOV critical point, and from the LOV point back to the MZ point, is taken with modifications from the paper of Zel'dovich (1962). The upper of these two heavy lines crosses the straight line  $M = A\mu_s$  corresponding to the mass-energy of baryons in the form of dispersed Fe<sup>36</sup> atoms. To the left of this crossing point the equilibrium configurations on the (LOV)-(MZ) branch have excess energy.

A configuration with excess energy is unstable in principle against a collective transformation in which it disperses into free Febs atoms. However, as Zel'dovich points out, the

same configuration at the same time is stable in another sense.

Theorem 13. Every equilibrium configuration is stable against any one-at-a-time removal of Fe<sup>56</sup> atoms.

Proof.—(Zel'dovich; see also Theorem 4 and eq. [28] above): The mass-energy ("injection energy") needed to create a baryon at the surface of the configuration—or in its interior—is  $\mu_*(1-2M^*/R)^{1/2}$ . This is less than the energy  $\mu_*$  needed to create a baryon ( $\frac{1}{26}$  of a free Fe<sup>36</sup> atom) far from all gravitational attraction. Therefore it costs energy to remove a single baryon (or a small number of baryons) from the system to infinity.

Zel'dovich invites attention to the analogy between the orbits of individual baryons in the massive system and the orbits of electrons in the Fermi-Thomas atom model. He makes the analogy more lively by imagining the idealized situation in which the baryons have a practically unlimited mean free path through the configuration, as do the electrons through the atom. None of these orbits ever reaches an r-coordinate larger than R. Every orbit is bound in the self-consistent gravitational field of force of all the other particles.

### EINSTEIN ON SOLUTIONS WITH ENERGY EXCESS

It is interesting that long ago Einstein (1939) also showed the existence of self-consistent solutions with energy excess for a system of particles held together by their mutual gravitational attraction. He was concerned not directly with gravitational collapse but with the Schwarzschild singularity. Is it possible, he asked, to build up a field containing such a singularity "with the help of actual gravitating masses"? He excluded in this connection the incompressible fluid of Schwarzschild (cf. Fig. 1 and associated discussion in the text) as giving a speed of sound exceeding the speed of light. With this one equation of state violating causality, Einstein was concerned about accepting any equation of state lest in it, too, "assumptions have been made which contain physical impossibilities." Therefore he focused attention on "a system resembling a spherical star cluster . . . a great number of small gravitating bodies which move freely under the influence of the field produced by all of them together"—what in atomic physics would be called a "self-consistent solution." He limited attention to motion in circular orbits. He showed that "the Schwarzschild singularity does not appear for the reason that the matter cannot be concentrated arbitrarily," thus answering the question he had set himself.

Our interest here in Einstein's models arises from a different cause—their exhibition of the phenomenon of energy excess. To bring this effect into view, it is enough to consider his simplest model: flat space inside  $r_0 - \Delta r$ ; Schwarzschild geometry from  $r_0$  to  $\infty$ ; and particles in the thin shell between  $r_0 - \Delta r$  and  $r_0$  occupying orbits, with all orientations of these orbits equally probable. Particles near the inside of this shell are subject to almost no gravitational pull; therefore, their centripetal acceleration is very small; consequently they must move with low velocity if they are to remain in circular

<sup>&</sup>lt;sup>4</sup> Fig. 2 of Zel'dovich shows only the one LOV critical point. The lower branch on his curve is shown as leading back to the origin, rather than to the HWW critical point indicated in the present Fig. 8.

<sup>\*</sup> Einstein considered a spherically symmetric array of particle orbits. The same question of binding has been examined in the case of a collection of orbits of full cylindrical symmetry by Raychaudhuri and Som (1962). We are indebted to Dr. Raychaudhuri for illuminating discussions of these two papers.

orbits. Particles at the outside of the shell move with the highest velocities. When this velocity is a sizable fraction of the speed of light, the relativistic contributions to the energy per particle and to the gravitational attraction become significant. This is the only complication in the problem. Otherwise a Newtonian analysis would suffice. Moreover, the Newtonian analysis shows some of the main features that are of interest.

In the Newtonian treatment the gravitational potential outside is  $-G(A\mu_s)/r$  and

inside is  $-G(A\mu_*)/r_0$ . The gravitational energy is

$$\frac{1}{2}\int (\text{gravitational potential}) d(\text{mass}) = -G(A\mu_s)^2/2r_0$$
. (124)

The totalized kinetic energy, according to the virial theorem, is opposite in sign to the potential energy and of half the magnitude. The sum of the kinetic and potential energies can be translated into mass and added to the mass before assembly,  $A\mu_s$ , to get the Schwarzschild mass-energy as sensed externally. In geometrized units (see Table 2) one has for this quantity the formula

$$M^*$$
 (Newtonian approximation) =  $(A \mu_s^*) - (A \mu_s^*)^2/4r_0$ . (125)

Einstein's result agrees with this quasi-Newtonian formula for large  $r_0$  (low velocity!). For general values of  $r_0$ , including the case of compact configurations and high velocities, where relativistic corrections become important, his expression for the mass-energy is given less readily in terms of  $r_0$  itself than in terms of a "radius parameter,"  $\theta$ , connected with  $r_0$  by the equation

$$r_0 = (A \mu_s^*) 2^{1/2} [(\tan \theta_0 - \theta_0) - (\tan \theta - \theta)]^{-1}.$$
 (126)

Here  $\theta_0$  is defined as arc tan  $2^{1/2} = 0.95530$  radian =  $54^{\circ}44'7''$ . When  $\theta$  is 0, the Schwarzschild radius  $r_0$  of the shell has its minimum value

$$r_0(\text{minimum}) = 3.082(A\mu_s^*).$$
 (127)

The particles moving in the outer region of the shell have the maximum permissible velocity, the speed of light itself. For a larger  $\theta$ , one has a configuration of a greater  $r_0$ . When  $\theta$  approaches  $\theta_0$ , the quantity  $r_0$  goes to infinity. The speeds of the particles in their orbits become smaller and smaller (Newtonian limit). In terms of this radius parameter  $\theta$  the mass-energy of the configuration in the general case is

$$M^* = (A \mu_s^*) 2^{-1/2} \frac{1 - (\cos^2 \theta_0) / (\cos^2 \theta)}{(\tan \theta_0 - \theta_0) - (\tan \theta - \theta)}.$$
 (128)

Values calculated from equation (128) are compared in Table 6 with the quasi-Newtonian values. Table 6 gives the mass-energy,  $M^*$ , for a fixed number of particles, A, of

<sup>6</sup> For the sake of compactness the expressions of Einstein, containing an algebraic parameter  $\sigma$  in a rather complicated way, have been translated here into terms of the trigonometric parameter  $\theta$ , connected with  $\sigma$  by the relation  $\sigma = (\cos \theta - 3^{-1/2})/(\cos \theta + 3^{-1/2})$ . Also Einstein uses conformal coordinates and a corresponding coordinate radius  $r_R$ , whereas the quantity r (or  $r_0$ ) in the text is the Schwarzschild coordinate r, defined by the circumstance that  $r d\theta$  gives directly, without any correction factor, distance along a great circle. Note that  $r = r_R (1 + M^*/2r_R)^2$ . In terms of the r employed here and elsewhere in the present article, the metric outside Einstein's cluster of particles is

$$- (1 - 2M^*/r) dl^2 + (1 - 2M^*/r)^{-1} dr^2 + r^2 (d\theta^2 + \sin^2\theta d\phi^2)$$
and inside is
$$- (1 - 2M^*/r_0) dl^2 + dr^2 + r^2 (d\theta^2 + \sin^2\theta d\phi^2).$$

The coefficient of  $dr^2$  changes rapidly but smoothly over the thickness  $\Delta r$  of the shell from 1 inside to  $(1-2M^*/r_0)^{-1}$  outside (extreme value  $[1-(2/3)]^{-1}=3$  for last row in Table 6). Through the analysis of this change—and of the accompanying change in particle velocities—Einstein is led to the formulae of his paper, formulae reported here in the  $\theta$  notation.

rest mass  $\mu_r$ , when these particles move in circular orbits confined to a thin spherical shell located at a value  $r_0$  of the Schwarzschild coordinate r. Here  $M_{QN}^+$  denotes the quasi-Newtonian approximation for the mass (eq. [125]) and  $M_B^+$  denotes Einstein's full general-relativistic value (eq. [128]). The quantity  $\theta$  is the "radius parameter" defined above. The configurations which, according to Einstein's analysis, have excess energy (over and above the same number of free particles at rest at infinite separation) are marked with asterisks for ease of identification.

From the numbers in Table 6 one sees that Einstein's value for the mass-energy of the system agrees closely with the quasi-Newtonian value for a cluster of large radius and low velocity, as expected. However, for more compact configurations, where velocities approach the speed of light, and relativistic corrections become important, Einstein's formula gives results systematically higher than equation (125). For a sufficiently compact configuration the increase is great enough to make the total mass-energy greater

TABLE 6

Mass-Energy,  $M^*$ , for a Fixed Number of Particles, A, of Rest Mass,  $\mu_0$ , Moving in Circular Orbits at  $r=r_0$ 

.0	*6/(Aµe*)	$M_{QN}*/(A\mu_z*)$	$M \pi^*/(A \mu_c^*)$
0 95530 95 90 80 70 60 50 40 30 20 10 0 00	135 14.30 6.17 4.47 3.77 3.43 3.24 3.146 3.100 3.084 3.082	1-(Aµ,*/4r <sub>0</sub> ) 0.998 0.982 0.959 0.944 0.934 0.927 0.923 0.921 0.919 0.919	1-(Aµ,*/4r <sub>0</sub> 0.998 0.984 0.966 0.961 0.963 0.972 0.984 0.998 1.012* 1.023* 1.027*

than that for the same number of free particles at rest at infinite separation (last three rows of table). Thus we must conclude that the system is in principle unstable against a collective change leading to breakup into free particles. Yet the orbit of any one particle is stable against small perturbations. The particle is bound. It cannot escape to infinity by itself. This "stability in the small and instability in the large" is thus a property not only of certain of the equilibrium configurations of cold, catalyzed matter, but also of certain of Einstein's clusters of particles. Furthermore, it is a feature of a third kind of organized system, a "geon."

### A GEON AS A THIRD EXAMPLE OF A SOLUTION WITH ENERGY EXCESS

A geon is a collection of electromagnetic radiation, or gravitational radiation, or both, held together by its own mutual gravitational attraction. The concept arose directly out of concern about the issue of gravitational collapse. The high densities encountered in late stages of collapse presented, and still present, issues about the equation of state of highly compressed matter. These issues in turn demand for their solution information about elementary-particle physics that is not available. In looking for a way to sidestep these issues, one naturally recalled that some stars derive their energy almost exclusively from particles; others, from a mixture of particles and radiation. The extreme limit of a

<sup>&</sup>lt;sup>3</sup> J. A. Wheeler, Richtmyer Memorial Lectures, New York, January, 1954 (unpublished); for simple spherical geons see Wheeler (1955); for thermal geons see Power and Wheeler (1957) (these both reprinted in Wheeler [1962]); and for gravitational geons see Brill and Hartle (1964a).

system deriving its mass-energy from radiation alone therefore suggested itself. However, with no matter to provide opacity and to dam up the radiation against escape, stability could only be maintained by excluding all photon orbits in which the motion is purely radial or even largely radial. This requirement is easily satisfied, and a large class

of geons turns out to be open for investigation.

to

One of the simplest of these gravitation-electromagnetic entities is an elementary spherical geon. Here the motion of the photons (apart from zero-point radial oscillation) is purely tangential. The electromagnetic energy is confined to a shell of minimal thickness located at some definite distance R from the center. In terms of the massenergy of the system this distance is  $R=2.25~M^*$ . The system as a whole is in equilibrium against any change in dimensions. Moreover, the individual photons are well bound. Any escape is possible only by a physical-optical tunneling process. The number of vibration periods required for escape by this mechanism becomes large exponentially fast with increase in the ratio

$$R/\lambda = 2\pi R/2\pi \lambda = \frac{\text{(Proper circumference of the active region)}}{\text{(Wavelength of the trapped radiation)}}$$

Therefore the system can be made as stable as one pleases against escape of individual photons by making up the geon out of radiation of sufficiently short wavelength.

Stability against escape of individual photons, yes; stability against a collective deformation, leading either to collapse or explosion, no. Consider a slow change in which the proper circumference of the active region changes from  $2\pi R$  to  $2\pi a$ . The tangential wavenumber of a typical photon (standing wave) is altered from

$$\begin{split} k_{\rm tang} &= 1/\lambda = (R/\lambda)/R = [\,l\,(l+1)\,]^{\,1/2}/R \\ k_{\rm tang} &= [\,l\,(l+1)\,]^{\,1/2}/a = (R/a\,\lambda\,)\,. \end{split} \eqno(129)$$

The radial component of the wavenumber ("zero-point oscillation" in the thin spherical shell) is negligible by comparison. Therefore the energy of the individual photons can be calculated directly from  $k_{\rm tang}$ . The sum of their energies, that is, the total electromagnetic mass-energy of the system, is increased from its original value, E, by the same factor of change as multiplies  $k_{\rm tang}$ . It becomes (R/a)E. The gravitational mass-energy of the system can be estimated well enough for the purposes of a qualitative discussion by the quasi-Newtonian approximation of equation (124); thus,

$$M_{\rm gray}^{*} \simeq - ({\rm electromagnetic \ mass-energy})^{*2}/2a$$
. (130)

Combining electromagnetic and gravitational contributions, one has for the total massenergy of the geon in the present approximation the result

$$M^* \simeq (ER)/a - (ER)^{\ddagger}/2a^{\ddagger}$$
. (131)

This expression peaks at  $a^2=1.5$  ER. The peak value represents the equilibrium mass-energy of the system. It is connected with the equilibrium radius by the standard formula for simple spherical geons,  $M^*=(4/9)a$ . However, the mass-energy is evidently a maximum at  $a^2=1.5$  ER. There is equilibrium, but it is unstable equilibrium. The system is unstable against a collective motion in which the dimensions of the geon either grow ("system running downhill on the outside slope of the potential hill toward disintegration into free radiation") or contract ("running down the inner slope of the potential hill toward collapse"). The analysis of the equilibrium and its instability, given here in terms of quasi-Newtonian reasoning, has been justified by Brill and Hartle (1964a-c) on the basis of general relativity and first principles.

<sup>\*</sup> The following discussion is adapted from the 1963 Les Houches lectures of Wheeler (1964).

### THREE KINDS OF SYSTEM WITH ENERGY EXCESS: A COMPARISON AND CONTRAST

The geon differs from Einstein's cluster of particles and from the equilibrium configurations of cold, catalyzed matter in two respects. First, equilibrium for the geon is always unstable; for the cluster and the star, sometimes unstable, sometimes stable. Second, when the geon explodes and all the energy is extracted from the products of explosion, nothing is left. In contrast, let the cluster or the star be in a configuration of energy excess. Let it explode. Again extract all the energy from the products of explosion. The energy made available in this way for use is only a small fraction of the total massenergy of the original system. The bulk of that mass-energy is unavailable. It appears as the sum of the masses of the dispersed particles, at rest and at infinite separation.

Despite these two differences between the geon and the two kinds of particulate systems, there is at the end an even more important point of similarity: All three types of system possess configurations with energy excess. Moreover, this energy excess traces back in every case to the same source: to particles or radiation traveling close to or at the speed of light. Neither Einstein's clusters of particles nor the equilibrium configurations of cold, catalyzed matter manifest energy excess except when the configuration is so compact that the velocities of a sizable fraction of the particles are relativistic. It does not matter that in Einstein's cluster the particles with the highest velocities are at the outside of the configuration, whereas in the cold star the highest pressures and greatest Fermi energies and fastest velocities are at the center. The important point is that these velocities should be relativistic. Under these conditions the pressure-density relations for a collection of particles approximate those for a collection of photons. That only a fraction of the particles are relativistic in Einstein's cluster or in a configuration of cold, catalyzed matter, even for very high central density, is responsible for the limited magnitude of the energy excess in these two instances. Only a fraction of either kind of system is comparable to a geon. Therefore, it is natural that neither should show the phenomenon of energy excess in such extreme measure as does a geon!

L. Gratton has noted in a private discussion (December, 1964) that there exists in principle a way to pass from a cluster with energy excess to a geon with energy excess; Let the cluster contain as many particles as antiparticles. Let it be arranged, by the spacing of the orbits, so that a particle has a good chance to annihilate an antiparticle only if the two momenta are nearly equal in magnitude and opposite in direction. Then the two annihilation photons will travel preferentially nearly tangentially. This is the direction of motion most favorable for retaining the photons in the resulting geon. Thus a configuration with an energy excess of a few per cent at most will be transformed into a system with 100 per cent energy excess.

# BARYONS ADDED AND BARYONS TAKEN AWAY IN REPEATED CYCLES TO "PUMP UP" THE CENTRAL DENSITY AND THE EXCESS ENERGY TO MAXIMUM VALUES

"Energy excess" and acoustical modes, stable and unstable: What have these ideas to do with the infinite number of maxima in the curve of equilibrium mass  $M^*$  as a function of the central density  $\rho_0$ ? Answer: As the central density increases without limit, a larger—if nevertheless restricted—region of the deep interior comes to pressures so high, and Fermi energies so great, that conditions are effectively relativistic or "geon-like." The energy excess of the system increases relative to the same number of baryons at rest at infinite separation. However, this steady augmentation of the energy excess and steady rise of the central density does not come about by steady addition of baryons to the system. Instead, the fractional energy excess  $[(M^* - A\mu_n^*)/A\mu_n^*]$  and the central density are both "pumped up" toward their limiting values by an infinite series of oscillatory changes in the baryon number A. Moreover, at each stage of the pumping process the system develops a higher order of instability.

This concept of "pumping up" the central density may be reviewed appropriately in

broad outline before one turns to any detail about the energy changes and the orders of

instability.

Any given cycle of the "pump" consists of two opposite strokes. The first stroke proceeds to the right in Figure 8; that is, proceeds by adding baryons. An example is the change from point HWW ("starting configuration" for the second cycle of the pump) to point LOV. The added baryons augment both A and  $M^*$ . However, the increase in  $M^*$  is not as great as the increase in A multiplied by the mass of a free baryon. The baryons are bound. The tighter the baryon binding, the lower is the slope  $dM^*/dA$  compared to the free baryon value  $\mu_*$  (dashed, straight line in Fig. 8). The stroke stops when the system comes to a critical point (maximum in  $M^*$ ). This point marks the beginning of a new branch in the curve for  $M^*$  versus A (Fig. 8).

Starting from the newly attained critical point, the second stroke of the pump proceeds to the left—or, in the example, from point LOV to point MZ, on a branch of lower slope,  $dM^*/dA$ . In this stroke baryons are removed from the system. For a given change,  $-\Delta A$ , in the baryon number the mass-energy  $M^*$  does not drop as much in this stroke as it rose in the preceding stroke. Consequently there is a net gain in  $M^*$ —and gain in the fractional energy excess. This net gain is a little analogous to climbing a mountain on a zigzag road of a special kind. On each sector of this road heading to the right the slope is steep and the gain in elevation substantial. On the next sector to the left the road appears to be abandoning its purpose, for it loses altitude. However the downward slope is modest. From each point on this sector one can still look down on the track previously

covered and note the gain!

Only by this zigzag course can  $M^*$  mount to values greater than  $\mu_*A$  along a roadway where everywhere dM\* is less than \(\mu\_\* dA\). This important observation one owes to Zel'dovich (1962). However, he contemplated a roadway with only two sectors in it, meeting at the LOV critical point. We see from Figure 8 that the actual situation is considerably more complicated. First, infinitely many sigzags must be traversed to attain the "summit" where central density is infinite. Second, the earliest zigzags lose elevation rather than gaining it. The reason is simple. The first zigzag has to do with configurations of densities considerably less than nuclear densities. Here electrons provide the dominating contribution to the pressure. The binding is only modest. In other words, the effective mass per baryon in the system,  $M^*/A$ , is less than the "standard mass of a baryon," \( \mu\_s^\* \) (see Table 2), only by an energy of an electronic order of magnitude (see tables in Appendix A for details). In contrast, the next uphill segment (HWW to LOV) carries the system to specific energies, M\*/A, which (1) are lower and (2) are lower by an energy of a nuclear order of magnitude. This energy lowering is reasonable because a substantial part of the system has now become one giant nucleus. Only in the outer region are individual Fe56 nuclei to be seen.

Theorem 14. The binding at the LOV critical point is the tightest binding which can be achieved—according to the HW equation of state—in any equilibrium configuration of cold, catalyzed matter held together by its own mutual gravitation.

By the wording of this theorem we exclude any system which is undergoing gravitational collapse, for it is not in equilibrium. Figure 8 shows qualitatively the superior binding at the LOV critical point. However, it is not obvious from that diagram that the binding at the LOV switchback is greater than that at the earlier LHWW switchback. The electronic order of magnitude at the binding at that earlier critical point had to be exaggerated in the drawing in order that it should even be visible! The most reliable indication of the binding is to be seen in the tables in Appendix A, giving both  $M^*/A\mu_s$  and  $\mu_s^{-1}dM^*/dA$ . There the content of Theorem 14 is obvious.

\* If one examines not the average energy per particle but the energy per last added particle, or the quantity  $\mu_e^{-1} dM^*/dA$ , one finds that it reaches its minimum value of 0.842 a little beyond the LOV switchback, as expected. This minimum value can be read either (1) from the tables in Appendix A or

Once the system has become essentially nuclear in character, with nuclear stiffness and the corresponding ability to be worked upon by the pump, then each pair of backand-forth strokes does at last steadily raise up the average mass-energy per baryon,  $M^*/A$ . The limiting value is reached only after an infinite number of strokes. At this limit the central density is infinite and the calculated (HW equation of state) ratio of mass to mass before assembly is  $M^*/A\mu_i = 1.068$ . (The calculated limiting value of  $\mu_i^{-1} dM^*/dA$  is  $[1-2 \times 0.100]^{1/2} = 0.894$ .)

### STABILIZATION REQUIRED TO REACH UNSTABLE CONFIGURATIONS

All but two of the "strokes of the pump" (origin in [M, A] diagram to LHWW maximum, and HWW minimum to LOV maximum) run through configurations for which the equilibrium is unstable. For the leftward strokes HWW ← LHWW and MZ ← LOV the instability is as simple as that of a ladder standing on end without support. One can imagine a contraint which artificially stabilizes the system at this otherwise unstable position of equilibrium. Moreover, insofar as this stabilizer maintains the system exactly at the equilibrium point, it does not have to supply any stabilizing force, Only perturbations introduced from outside have to be resisted. The smaller they are, the smaller the demand imposed on the stabilizer. Therefore it is appropriate to consider the ideal limit in which the stabilizer (1) can be neglected as a mass-carrying system in comparison with the configuration which it stabilizes but (2) converts unstable equilibrium to stable equilibrium. Similarly at higher modes of stability one sees no obstacle in principle to an arrangement in which one traverses all the zigzags of the (M, A) diagram. One slowly adds baryons to approach one critical point and takes them away to get to the next critical point. Without the stabilizer, the instability of the system in the course of the later strokes of the pump is to be compared with that of a sequence of ladders standing one on top of another. The final limiting configuration  $(\rho_0 = \infty)$  is in effect reached by a tower of infinitely many ladders which, without the stabilizer, would teeter in an infinitely precarious equilibrium.

### The coupled rates of change of $M^*(\rho_0)$ and $A(\rho_0)$

Turn now from the meaning and measure of energy excess to the mathematics of massenergy and its bearing on the stability of the acoustical modes.

Theorem 15. The mass-energy of an equilibrium configuration changes on adiabatic addition or removal of baryons at a rate given by the formula

$$dM^*/dA = \mu_s^* (1 - 2M^*/R)^{1/2}$$
. (132)

This theorem is a direct consequence of Theorem 4 and equation (27) (see also eq. [54]). The word "equilibrium" is of course understood here in the legalistic sense of that term: the matter is assumed to be cold, so that there is no energy flow to the outside; and catalyzed, so that all thermonuclear reactions have gone to the absolute end point appropriate to the given pressure and temperature (0° K). The word "adiabatic" implies that the removal or addition of a particle is to be carried out so slowly that the system transforms smoothly from the state of equilibrium appropriate to A baryons to that

<sup>(2)</sup> by recalling that  $low \ \mu_s^{-1} \ dM^*/dA = (1-2M^*/R)^{1/3}$  means  $high \ redshift$  and  $high \ M^*/R$ . Thus, on a graph showing the pair of values  $(M^*,R)$  for all equilibrium configurations (Fig. 7 transposed to a linear scale), draw a straight line through the origin with the largest slope,  $M^*/R = \text{const}$ , which will make contact with the curve. This point of tangency lies between the LOV maximum and the MZ minimum. The slope of the line is 0.146, whence  $|\mu_s^{-1} dM^*/dA|_{\min} = (1-2 \times 0.146)^{1/2} = 0.842$ . Thus an added iron atom adds 84 per cent of its mass to the system, the other 16 per cent being radiated away. Contrast these extremal numbers with those for additions to Schwarzschild's critical mass of a fluid with the impossible property of incompressibility: 33 per cent of atomic mass added, 67 per cent radiated away (eq. [54]).

appropriate to  $(A \pm 1)$  baryons, with no heating or other departure from equilibrium along the way, and with an idealized stabilizer used where appropriate.

Theorem 16. M\* and A for equilibrium configurations reach their maxima and minima at identical po values ("critical points").

That  $dM^*/d\rho_0$  and  $dA/d\rho_0$  vanish at identical points follows from the finiteness of the chemical potential on the right-hand side of equation (132) (Zel'dovich 1962).

#### INFINITE DIMENSIONAL CONFIGURATION SPACE AND NEUTRAL STABILITY

In the first-order change of central density from  $\rho_{0, \text{ crit}} - \frac{1}{2}\Delta\rho_0$  to  $\rho_{0, \text{ crit}} + \frac{1}{2}\Delta\rho_0$  there is no first-order change in mass-energy or in baryon number. However, there is a first-order shift in the position of the material,

$$\Delta r(a) = \left[ \frac{\partial r(a, \rho_0)}{\partial \rho_0} \right] \Delta \rho_0. \qquad (133)$$

Here the "particle label" a tells how many baryons are surrounded by the thin spherical shell of matter under consideration  $(0 \le a \le A)$ , and r(a) gives the Schwarzschild coordinate of this shell. Not only this special displacement  $\Delta r(a)$  but also every small displacement  $\delta r(a)$  from a specified configuration may be regarded as a contravariant vector (or, today, a "tangent vector") in the infinite dimensional configuration space. The particle label a distinguishes one component of this vector from another. The quantity  $M^*$  (for a fixed number of baryons, A) is a function of position in this configuration space. The gradient of  $M^*$ , otherwise known as the first variational derivative,  $\delta M^*/\delta r(a)$ , is a covariant vector (or a "one-form"). It is so defined that its scalar product with the displacement vector gives the first-order change in M:

$$\delta M^*$$
 (calculated to first order in  $\delta r[a]$ , eq. [21])  $\equiv \int [\delta M/\delta r(a)] \delta r(a) da$ . (134)

Here the integration over a takes the place of the summation over indices that is so familiar when one evaluates the scalar product  $\Sigma_i P_i \delta r^i$  of two vectors in a finite-dimensional space.

Theorem 17. An equilibrium configuration possesses a characteristic mode of "vibration" of zero frequency (ω² = 0) when and only when dM\*/dρ0 = 0; that is, only at a critical point. Moreover, the displacement in this characteristic mode is given by the special movement (133) associated with the increase of the density at the center.

Discussion and proof. A system is said to possess a mode of motion of zero frequency when, starting from a configuration of equilibrium, it is carried by a first-order displacement to another equilibrium configuration. The absence of forces both at the beginning and at the end of the first-order displacement means that no work is done in the displacement, even to second order. Therefore no energy is stored up or set free such as is needed to drive the displacement. An example out of mechanics in a two-dimensional space may not be out of place to illustrate the qualitative situation in infinite-dimensional coordinate space. The point x = 0, y = 0 is a point of equilibrium for the motion of a particle under the influence of the potential  $V = (j/2)x^2 + (k/2)y^2$  because all components of the force,  $F_x = -jx$ ,  $F_y = -ky$ , vanish at this point. The same is not so after this special displacement: (x, y) from (0, 0) to  $(\Delta x, 0)$ ! The new point  $(\Delta x, 0)$  is not in general a point of equilibrium. However, in the special case in which j is zero (V =ky2/2) the new point is a point of equilibrium, though removed by a first-order displacement  $(\Delta x, 0)$  from the original point of equilibrium. In this case the equations of motion permit a motion of the type  $x(t) = x_0 + v_0 t$  ("zero frequency limit" of  $x_0 \cos \omega t +$  $(v_0/\omega)$  sin  $\omega t$ ). In the example all components of the force vanish at the new point as at the old point. However, not all displacements from the original point lead to an acceptable second point; only displacements leading in a particular characteristic direction lead to points which are also equilibrium points. The situation is similar in the

infinite-dimensional system.

All "components"  $(0 \le a \le A)$  of the force  $-\delta M^*/\delta r(a)$  vanish for any equilibrium configuration. However, when the system is subjected to an arbitrary small first-order displacement  $\delta_1 r(a)$ , it is carried to a configuration for which all components of the force  $-\delta M^*/\delta r(a)$  may or may not vanish. When they do vanish, the new configuration, like the old one, is an equilibrium configuration for the same number of baryons, A. In this case the force vanishes at the beginning and at the end of the displacement to first order. Therefore, the work vanishes to second order. Consequently the displacement  $\delta_0 r(a)$  is a characteristic mode of the system of zero frequency. But this situation of having an equilibrium configuration for A baryons near another equilibrium configuration for the same number of baryons is ordinarily impossible. This one can see from an inspection of the chart of the equilibrium configurations (see Fig. 5), Or equivalently one can note (1) that the one monotonic increasing parameter  $\rho_0$  catalogues all equilibrium configurations, each with its own baryon number and (2) that the derivative  $dA/d\rho_0$  differs from zero everywhere except at a critical point, so that (3) nearby equilibrium configurations contain different numbers of baryons-except at a critical point. So only at a critical point does there exist a displacement  $\delta_{ir}(a)$  (= the  $\Delta r(a)$  of eq. [133]) which carries the system from an equilibrium configuration to a nearby equilibrium of the same baryon numberthe necessary and sufficient condition for a mode of zero frequency, as was to be proved,

### THE CONTRASTING STABILITY OF THE TWO BRANCHES OF $M^*(A)$

For a baryon number A a little less than a maximum in  $A(\rho_0)$  or a little more than a minimum in  $A(\rho_0)$  there are two branches in the curve for  $M^*(A)$  which meet at the relevant critical point. On one of these branches near the critical point the mass-energy is higher than it is on the other branch ( $M^*$  being compared for the two branches for identical A values).

Theorem 18. That mode which acquires "zero frequency" ( $\omega^2 = -\alpha^2 = 0$ ) at the critical point is stable ( $\omega^2 > 0$ ) on the lower branch and unstable ( $\alpha^2 > 0$ ) on the upper branch.

Proof.—The how and why of this relationship appears more clearly in Figure 9 than in any one formula which one can easily write down. The drawing and the following analysis apply to the case where the critical point is a maximum of  $A(\rho_0)$ ; it is easily modified to apply to the converse case of a minimum. Denote the maximum by  $A_{\rm crit}$ . Pick a value of A only a very little less than  $A_{\rm crit}$ . For this baryon number there are two near-critical equilibrium configurations. Denote the one with with the higher massenergy by G; the other, by E. Denote by r(a, E) and r(a, G) the Schwarzschild coordinates of the successive baryon "shells"  $(0 \le a \le A)$  in the two equilibrium states. Then

$$\Delta(a) \equiv r(a, G) - r(a, E) \tag{135}$$

is the displacement which carries the lower-energy configuration, E, to the higher-energy one, G. Let the successive stages in this displacement be designated by a parameter x which runs from  $O(\rho_0 = \rho_E)$  to  $I(\rho_0 = \rho_B)$ ; thus,

$$\delta \tau(a) = x\Delta(a)$$
, (136)

Write the mass-energy of the system in the course of this displacement in the form

$$M^{\pm}(x) = M_R^{\pm} + (M_G^{\pm} - M_R^{\pm}) f(x).$$
 (137)

Then the derivative df(x)/dx must vanish at x=0 and at x=1, because both points are equilibrium points. The lowest-order expression which vanishes at x=0 and x=1 can be written in the form

$$df(x)/dx = 6kx(1-x),$$
 (138)

where k is some constant. Integrating, we have

$$f(x) = k(3x^2 - 2x^3) + c, (139)$$

where c is another constant. These two constants are fixed by the requirement that f(0) = 0 and f(1) = 1; thus,

$$M^*(x) = M_E^* + (M_G^* - M_E^*)(3x^2 - 2x^3).$$
 (140)

This result presupposes that the difference  $A_{\rm crit} - A$  is sufficiently small that one can neglect terms in x of the fourth and higher orders ("limiting behavior near normal critical point"). On this understanding the second derivative of the energy is

$$d^{2}M^{*}(x)/dx^{2} = (M_{a}^{*} - M_{B}^{*})(6 - 12x), \tag{141}$$

positive on the lower branch (x = 0 at E), corresponding to stability, and negative on the upper branch (x = 1 at G), implying instability, as was to be proved.

Theorem 19. The difference in mass-energy between the two branches of the curve M\* = M\*(A) which meet at a given normal critical point is given by the formula

$$M^*$$
 (higher  $\rho_0$  value)  $-M^*$  (lower  $\rho_0$  value) =  $q (A_{wit} - A)^{8/2}$  (142)

in the limit where A is close to a maximum, Acrit.

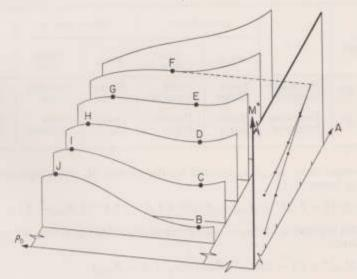


Fig. 9.—Mass-energy  $M^*$  as a function of baryon number and compaction in the neighborhood of a critical point, showing the relation between equilibrium configurations (black dots) and non-equilibrium configurations (remainder of the contours). The diagram is schematic only. The one degree of freedom called compaction, and plotted as central density  $\rho_0$ , should in principle be replaced (if only one could on a single sheet of paper) by an infinite number of degrees of freedom. In the neighborhood of any dot these degrees of freedom are most naturally conceived as the amplitudes of the distinct acoustic modes of the system. Of these infinitely many configuration coordinates, however, only one is important near the critical point: the one which carries the system in the general direction from E to G. At the same time it raises the central density (cf. eq. [133]). The system at G (and at H, I, I) is untiable against this mode of deformation; at E (and at D, C, B) it is stable against this deformation. Evidently an equilibrium is unstable or stable against this mode according as the configuration in question lies on the upper or lower branch of the  $M^*(A)$ -curve—"upper" or "lower" being defined in case of ambiguity by which lies higher when the two branches meet at the casp (projection of point F of contour diagram onto the  $M^*$ , A plane).

Here the constant q has the value

$$q = (-2M_{erit}*R_{erit}'/3R_{erit}^2)(-2/A'')^{1/2}(1-2M_{erit}*/R_{erit})^{-1/2}\mu_**.$$
 (143)

In this formula the primes denote derivatives with respect to the central density evaluated at the critical point; thus,  $A'' \equiv [d^{3}A(\rho_{0})/d\rho_{0}]^{2}_{crit}$ .

Proof.—Expand A in a Taylor series about the point  $\rho_0 = \rho_{crit}$  through terms of the third order:

$$A = A_{crit} + \frac{1}{2}A''(\rho_0 - \rho_{crit})^2 + \frac{1}{6}A'''(\rho_0 - \rho_{crit})^3 + \dots$$
 (144)

Furthermore use the relation

$$dM^* = (1 - 2M^*/R)^{1/2}\mu_*^* dA$$
 (145)

to evaluate  $M^*$  to the same order in terms of the coefficients in the expansion of A:

$$M^* = M + \frac{1}{2} (1 - 2M/R_{\text{crit}})^{1/2} \mu_s^* A^{\prime\prime} (\rho_0 - \rho_{\text{crit}})^2 + [(1 - 2M/R_{\text{crit}})^{1/2} A^{\prime\prime\prime} + (1 - 2M/R_{\text{crit}})^{-1/2} M R_{\text{crit}}^{-2} R^{\prime} A^{\prime\prime}] (\mu_s^* / 6) (\rho_0 - \rho_{\text{crit}})^2 + \dots$$
(146)

TABLE 7

Change in Radius near a Critical Point as Criterion for the Relative Stability of the High- $\rho_0$  and Low- $\rho_0$  Branches of the Function  $M^*(A)$  near that Point

NATURE OF		Low-pe Branch		High-po Branch		
CRITICAL POINT	Τ Κ (ρε)	M*(A)	Critical Mode	M*(A)	Critical Mode	EXAMPLES (Figs. 5-8)
Maximum in M*	Decreasing Increasing	Lower Higher	Stable Unstable	Higher Lower	Unstable Stable	LHWW; LOV None
Minimum in M*	Decreasing Increasing	Higher Lower	Unstable Stable	Lower Higher	Stable Unstable	HWW MZ

Here, for compactness,  $M_{\text{crit}}^*$  is denoted by the symbol M. Solve equation (144) for  $(\rho_0 - \rho_{\text{crit}})$  in terms of A,

$$\rho_0 - \rho_{\text{crit}} = \pm \left[ (-2/A'')(A_{\text{crit}} - A) \right]^{1/2} + (A'''/3A''')(A_{\text{crit}} - A) + \dots$$
 (147)

Substitute this expression for  $(\rho_0 - \rho_{crit})$  into equation (146) to obtain  $M^*$  as a function of A, as desired:

$$\begin{split} M^* (A) &= M_{\rm crit}^* + (1 - 2M_{\rm crit}^* / R_{\rm crit})^{1/2} \mu_s^* (A - A_{\rm crit}) \\ &\mp (M_{\rm crit}^* R_{\rm crit}' / 3R_{\rm crit}^2) (1 - 2M_{\rm crit}^* / R_{\rm crit})^{-1/2} \mu_s^* (-2/A^{\prime\prime})^{1/2} (A_{\rm crit} - A)^{3/2} \end{split}$$
(148)

+ terms of second and higher order in (  $A_{
m crit}-A$  ).

This expansion completes the proof of the theorem.

### CHANGES IN STABILITY DIAGNOSED BY CHANGES IN RADIUS

From equation (148) one sees that, near any maximum in  $M^*(\rho_0)$  at which the radius of the configuration is decreasing, the high- $\rho_0$  branch (+ sign in eq. [147]!) has the

higher mass-energy for a given A. Conclusions of this type about energy, also about stability of the critical acoustical mode, are spelled out in detail in Table 7 not only for a maximum in  $M^*(A)$  (to which eq. [148] applies) but also for a minimum. These conclusions can be deduced most easily by noting that near a maximum in  $M^*(A)$ , for example, the branch of higher energy must have the lower slope,  $dM^*/dA = \mu_s^*(1-2M^*/R)^{1/2} =$  "injection energy" (in order to meet the lower branch at the critical point!) and must therefore have the lower R value. The "critical mode" is that one among the purely radial modes (modes of spherical symmetry) for which  $\omega^2 = -\alpha^2$  vanishes at the given critical point.

### FINAL SURVEY OF THE CHANGES IN STABILITY

The foregoing analysis gives the tools unambiguously to say which acoustical mode is changing stability at which critical point throughout the curve  $M^* = M^*(\rho_0)$  (Fig. 10).

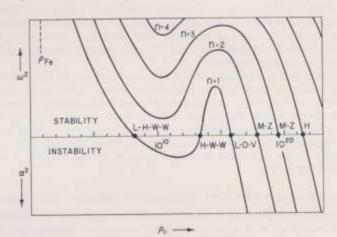


Fig. 10.—Square of the circular frequency,  $\omega^z$ , or square of the exponential growth constant,  $\alpha^z$ , as functions of the central density for the lowest modes of purely radial and spherically symmetric oscillation of equilibrium configurations of cold, catalyzed matter. The diagram is purely schematic and has no computational basis. Only the points of change of stability (black dots) have actually been calculated. The direction of change of stability at each of these points is completely determined, however, by the considerations summarized in Table 7.

Start at spheres little enough that the increment  $\rho_0 - \rho_{Fe}$  in the central density is small compared to the normal density of iron. In this domain of sizes the rise in the central density goes as the square of the radius,

$$\rho_0 - \rho_{V_0} = (d \rho / d p) p_0 = (d \rho / d p) (2\pi G / 3) \rho_{V_0}^2 R^2$$
. (149)

We shall use Poincaré's term "stability parameter" to represent the quantity which in the regime of stability is the square of the circular frequency,  $\omega^2$ , and in the regime of instability is the negative square of the exponential growth constant,  $-\alpha^2$ . The stability parameters of all the modes are positive for little spheres and given, according to equation (121), for the present idealization of zero rigidity, by the relation

$$\omega_{n}{}^{2} = \left( \, n^{2} \pi^{2} / R^{2} \, \right) d \, p \, / \, d \, \rho \, \, , \label{eq:omega_n}$$

or (from eq. [149], and in geometrized units)

$$\omega_n^2 = (2\pi^2/3) n^2 [(\rho_{F_0}^+)^{-1} - (\rho_0^+)^{-1}]^{-1},$$
 (150)

The fall of the stability parameters with central density continues as the mass of the sphere goes up, although the simple law (150) ceases to hold when the central density is comparable to twice the density of iron or more. Eventually the LHWW critical point is reached. Theorem 17 states that one of the modes changes stability at this point. Equation (122), on the ordering of the modes, says that  $\omega_1^2$  must be the first quantity to change sign. Wakano's calculations (see Fig. 6) show that R is decreasing at this point. Table 7 shows that the mode in question, n = 1, is changing from stability to instability—as is also obvious from the fact that this mode was stable to begin with!

An elementary property of the mode n=1 provides the simplest way to see that this is the mode which dominates the changes, not only at this critical point, but also at the next two (HWW and LOV) critical points. In this simple breathing mode the medium moves inward everywhere—also at the surface—when the central density rises. In accordance with this feature of the dominating mode (the mode that changes stability) the radius is decreasing as the central density rises at each one of the first three critical points. In agreement with this diagnosis, one confirms from Table 7 that the dominating mode changes from unstable to stable at the HWW minimum (matter crushed to a substantial fraction of nuclear density and consequently more rigid than previously) and—for the last time—from stable to unstable at the LOV maximum (gravitational forces finally dominant even over nuclear rigidity).

That the mode n=2 is dominant at the MZ minimum can be checked from Table 7, but can be seen still more directly from *outward* movement of the radius with increase of the central density at this point. This is one of the most outstanding elementary features associated with the motion in the mode n=2 (cf. discussion following eq. [121]).

The higher modes become unstable one by one at the higher critical points, critical points which approach moreover more and more closely the standard spacing  $\Delta lnp_0$  of equation (63). These and other principal features of the stability parameters are sketched out in Figure 10.

### QUANTITATIVE ANALYSIS OF RATE OF CHANGE OF STABILITY AT CRITICAL POINT

In a more nearly complete analysis one would evaluate quantitatively the rate of change of the relevant  $\omega_n^2$  with  $\rho_0$  as this stability parameter changes sign. For this purpose one represents the kinetic energy in a slow departure from equilibrium in the form of an integral

(Kinetic energy) = 
$$\int_{0}^{A} f(a) [d\delta r(a)/dt]^{2} da$$
 (151)

(see Appendix B for the function f[a] and its derivation). Furthermore, one contemplates a periodic variation of  $\delta r$  with the time (Schwarzschild time coordinate, defined group-theoretically, and normalized to agree asymptotically with proper time at infinity) with circular frequency  $\omega$ , in which the kinetic energy agrees on the time average with the potential energy. This agreement gives an equation for the stability parameter,

$$\omega^2 = \frac{\text{(Potential energy, expressed as a functional of the second order in } \delta r [a])}{\int_0^A f(a) [\delta r(a)]^2 da} \ . \tag{152}$$

Let  $\delta r(a)$  be a displacement which goes a small fraction x of the way from the minimum E in Figure 9 to the maximum G, so that the concept of harmonic oscillations makes sense. Then the potential energy in the numerator of (152) is given, according to equations (140) and (142), by the expression

(Potential energy) = 
$$(M_0^* - M_E^*) 3x^2 = 3q (A_{crit} - A)^{3/2}x^2$$
. (153)

The displacement in the denominator of equation (152) is given by equations (136), (135), (133), and (147) in the form

$$\delta r(a) = x\Delta(a) = x(\rho_G - \rho_E)\partial r(a, \rho_0)/\partial \rho_0$$
  

$$= 2x[(-2/A'')(A_{crit} - A)]^{1/2}\partial r(a, \rho_0)/\partial \rho_0.$$
(154)

The amplitude, x, of the departure from equilibrium cancels out of the final expression for  $\omega^2$ , as expected; and, with a little reduction, the expression for the relevant stability parameter becomes

$$\omega_n^{*i} = -\alpha_n^{*i} = K(R_E - R_{crit}).$$
 (155)

Here the constant has the dimensions of cm-1 and the value

$$K = \left[ \frac{-\frac{3}{4} (\partial^2 M^* / \partial \rho_0^2) (M^* / R^2)}{(1 - 2M^* / R) \int f(a) [\partial r(a, \rho_0) / \partial \rho_0]^2 da} \right]_{\text{crit}},$$
 (156)

All the quantities needed to evaluate K can be found from a few integrations of the equations of hydrostatic equilibrium near the critical point. The term in the stability parameter  $(\rho_R - \rho_{\rm crit})(dR/d\rho_0)$  was replaced by  $(R_E - R_{\rm crit})$  in deriving equation (155) to bring out as clearly as possible that it is the change of the radius near the critical point which governs the stability or instability of the dominant acoustical mode.

# PRESENT STABILITY ANALYSIS COMPARED AND CONTRASTED WITH ONE THAT MAKES DETAILED CALCULATIONS OF FREQUENCIES

It will be noted that no knowledge of the kinetic-energy term in the denominator of equation (156) was required in any of the foregoing assignments of specific modes to specific critical points. Nor was any actual numerical evaluation of frequencies ever needed, whether by use of Chandrasekhar's variational principle or otherwise. Only if one wants to know more than the nature of the stability on each branch of the curve  $M^*(A)$  (see Fig. 8) and asks for detailed values of the  $\omega_n^2$  or  $\alpha_n^2$  is it necessary to resort to equation (156) (for the dominant mode near a critical point) or to equation (116) (for any mode at any po). It is no accident that the analysis turned out this way. Any detailed calculation of frequency goes back to an examination of evolution of the dynamics with time. But the central feature of the foregoing study of the mass-energy of stationary configurations was that it did not look at any variation with time. Therefore there was no way for inertia to show up-nor any way for the inertia-proportional denominator of equation (116) or equation (156) to make an appearance. Appendix B shows how one can extend the first-order variational analysis of chapter iii to give the energy to second order to provide an alternative foundation for the stability analysis of the present section. It also derives the kinetic energy denominator of equation (152) and traces the correlation between these potential and kinetic energy terms and the numerator and denominator of Chandrasekhar's variational expression for ω".

### WHY MORE MODES BECOME UNSTABLE AS THE CENTRAL DENSITY RISES

It is the principal finding of this chapter that more and more modes become unstable as the central density rises higher and higher. Why? One can state the situation qualitatively in these terms. For any given high central density  $\rho_0^*$  there is an inner region of extension  $r_0 \sim (\rho_0^*)^{-1/2}$  (see Fig. 2) which is teetering on the verge of collapse. An acoustical mode of high order has many alternating zones of density increase and density decrease inside this critical region. Therefore, it has no effective coupling to the decisive

degree of freedom. To excite this mode is to excite a vibration, not to promote a collapse! On the other hand, to excite an acoustical mode of low order is to make a density increase throughout the critical region, and to initiate collapse; hence the instability of the acoustical modes of lower order. The demarcation between unstable modes (low n) and stable modes (high n) therefore comes at that order n at which the location of the innermost nodal sphere in the vibration first penetrates well into the critical sphere, of radius ~ (00\*)-1/2.

### REFERENCES

. 1964c, Bull. Am. Phys. Soc., 9, 425.

Chandrasekhar, S. 1964a, Phys. Rev. Letters, 12, 114, 437.

. 1964b, Ap. J., 140, 417.

Einstein, A. 1939, Ann. Math., 40, 922. Geronimus, J. L. 1954, Alexander Michailowitsch Ljapunow-Stabilitätsprobleme der Bewegung, trans. from

Russian by H. Mänzel (Berlin: VEB Verlag Technik).

Ledoux, P. 1958, "Stellar Evolution," in Hdb. d. Phys., Vol. 51, ed. S. Flügge (Berlin: Springer-Verlag).

Lyttleton, R. A. 1953, The Stability of Rotating Liquid Masses (Cambridge: Cambridge University Press). Misner, C. W., and Zapolsky, H. S. 1964, Phys. Rev. Letters, 12, 635.

Morse, M. 1934, The Calculus of Variations in the Large (Providence, R.I.: American Mathematical

Society) . 1939, Functional Topology and Abstract Variational Theory (Paris: Gauthier-Villars).

1951, Introduction to Analysis in the Large (2d ed.; mimeographed notes; Princeton: Institute for Advanced Study).

for Advanced Study).

Oppenheimer, J. R., and Volkoff, G. 1939, Phys. Rev., 55, 374.

Power, E. A., and Wheeler, J. A. 1957, Rev. Mod. Phys., 29, 480.

Raychaudhuri, A. K., and Som, M. M. 1962, Cambridge Phil. Soc. Proc., 58, 338.

Wheeler, J. A. 1955, Phys. Rev., 97, 511.

— 1962, Geometrodynamics (New York: Academic Press).
— 1964, "Geometrodynamics and the Issue of the Final State," in Relativity, Groups and Topology, ed. C. and B. DeWitt (New York: Gordon and Breach).

Zel'denich V. B. 1963, Then the Tore Fig. (USS) 43, 1667 (English translation in Sected Phys.

Zel'dovich, Ya. B. 1962, Zhur. eksp. Teor. Fiz. (USSR), 42, 1667 (English translation in Soviet Phys.— J.E.T.P., 15, 1158).

### chapter 8 NO ESCAPE FROM COLLAPSE

### FOUR REASONS FOR CONSIDERING CONFIGURATIONS OF UNIFORM DENSITY

In an equilibrium configuration of high central density,  $\rho_0^*$ , the central critical region, of extension  $\sim (\rho_0^*)^{-1/2}$ , volume  $\sim (\rho_0^*)^{-3/2}$ , and mass  $\sim (\rho_0^*)^{-1/2}$ , dominates the discussion of the stability. The oscillations in total mass and onter radius are only a minor accompaniment to this central development. For this reason one would like to see the key factor in the instability brought out from under the complicating covering of the outer layers and into the light of day. This is one reason for focusing attention now on massenergy M\* for a fixed number of baryons A for spherical configurations in which the density is uniform throughout, and in which only this density is adjustable. For small A values  $(A \ll 10^{67})$  the energy will be found to possess a maximum for a particular density (dependent upon A!) and to fall off both for higher compactions (gravitational contraction!) and for more dispersed configurations (explosion!) Thus the instability basic to a high- $\rho_0$  equilibrium configuration will become apparent from examining energy for a family of

non-equilibrium configurations.

There are three other reasons for investigating the energy of uniform configurations. (1) For large A values, corresponding in order of magnitude to the baryon content of the Sun ( $A \sim 10^{67}$ ), the energy of uniform configurations, as a function of the degree of compaction, is found to have two minima and two maxima. The configurations associated with these extrema correspond reasonably well, both in density and in radius, to equilibrium configurations of maximal or minimal mass, as given by the detailed solution of the equations of hydrostatic equilibrium in the same range of masses for the same equation of state. Thus the "uniform model" predicts the main features of the dwarf star and the neutron star without predicting-or even being able to predict-the rest of the infinite sequence of higher and relatively unimportant critical points. (2) For the uniform model, as for no other model, one can sort out and separate cleanly from each other those features of the calculation of critical mass which have to do with long-range forces (gravitation and general relativity) and those which have to do with short-range forces (equation of state). In this way one can see at a glance (cf. the "slide rule" below) the effect of changes in the equation of state upon the stability. (3) Finally, most important of all, this separation of factors in stability for uniform configurations allows one to see and to prove that no equation of state compatible with causality and with stability of matter against microscopic collapse can save a system from having a configuration which is unstable against collective gravitational collapse.

### SEPARATION OF LONG- AND SHORT-RANGE FORCES; THE "SLIDE RULE"

The separation of long- and short-range effects is essential to the following analysis. It is accomplished by focusing in the study of short-range forces upon the logarithm of the number density of baryons,  $\log n$ ; and in the analysis of the long-range forces, upon the logarithm of the proper volume,  $\log V$ . However either of these quantities individually is changed in squeezing or expanding an A-baryon system, their sum keeps always the fixed value

 $\log n + \log V = \log n V = \log A = \text{const} . \tag{157}$ 

Equation (157) links two very different kinds of quantity: n, having to do with the microscopic physics of the system; and V, having to do with macroscopic physics, the fitting of the geometry inside the system to the geometry outside. In addition to these two magnitudes, so different in kind, employed in analyzing the equation of state and the gravitational forces, respectively, another magnitude will make its appearance in both the microscopic and the macroscopic physics: the logarithm of the density  $\rho(g/cm^3)$  or  $\rho^*(cm^{-2}) = (G/c^3)\rho$ , of mass-energy. This quantity measures, on the one hand, the density of mass-energy stored up by reason of work done against the short-range forces. On the other hand, it governs the curvature of geometry inside the volume V. Therefore it determines (together with V) the geometry that will join on the outside. Thus finally it fixes the mass-energy  $M^*$  of the system as it will be sensed by an outside observer who measures the period of a planet or the deflection of a light ray.

In summary, the microscopic physics will be contained in a graph of  $\log \rho^*$  as a function of  $\log n$ . The macroscopic physics will appear on a chart where again the ordinate is  $\log \rho^*$ , but the abscissa is  $-\log V$  (later to be recognized as identical with  $\log n - \log A$ ). On this chart will appear contour lines for many different values of  $N^*$ . With the help of these contour lines one can read off the mass-energy associated with any given pair of values ( $\log \rho^*$ ,  $\log V$ ). The superposition of the ( $\log \rho^*$ ,  $\log n$ )-curve onto the contours of the ( $\log \rho^*$ ,  $\log V$ ) or ( $\log \rho^*$ ,  $\log n$ - $\log n$ -log n)-plane calls for a horizontal transposition of the ( $\log \rho^*$ ,  $\log n$ )-curve by a distance ("slide-rule" operation) equal to  $\log n$ , where n is the fixed number of baryons under consideration. Picked out by the curve of the equation of state in this way will be all those pairs of values ( $\log \rho^*$ ,  $\log V$ ), that is to say, all those uniform configurations which possess this specified number of baryons. Moreover, one can immediately read off for each configuration from the appropriate contour line the massenergy of that configuration. In this way it will be possible to verify that the massenergy sinks down toward zero ("gravitational collapse") along this one-parameter family of configurations of fixed A-value as the compaction increases to a finite limiting value.

So much for the operation of the "slide rule" in broad outline. The rest of this section deals with the construction of that part of the "slide rule" which has to do exclusively with the long-range forces—that is, the contour diagram for  $M^*$  as a function of  $\rho^*$  and V. Also taken up at the end of this section is the operation of the slide rule and the conclusions drawn from it about gravitational collapse. Here the treatment draws on those features of the equation of state (other half of "slide rule") which are developed in more detail in chapters ix and x.

### VOLUME-DENSITY RELATION FOR UNIFORM CONFIGURATIONS OF SPECIFIED TOTAL MASS-ENERGY

Theorem 20. Every momentarily static and homogeneous and spherically symmetric configuration of a given mass  $M^*$  is characterized by a pair of values  $(\rho^*, V)$  which lie on the curve of Figure 11.

Here  $\rho^*(\text{cm}^{-2}) = (G/c^2) \rho$  (g/cm<sup>3</sup>) is the density of mass-energy in the local Lorentz frame (tangent flat space) and V (cm<sup>3</sup>) is the proper volume.

Discussion and proof.—The configuration is being viewed at a moment of time symmetry (cf. Theorems 1 and 2). The mass factor  $m^*(r)$  which appears in the radial part of the metric is given by the elementary integral

$$m^*(r) = \int_0^r \rho^* 4\pi r^2 dr = (4\pi \rho^*/3) r^3,$$
 (158)

inside the configuration, and by  $M^*$  at the surface and outside, continuity at the surface being of course demanded. The 3-geometry has the Schwarzschild form

$$d\,s^2 = (\,1 - 2M^*/\,r\,)^{-1}d\,r^2 + \,r^2(\,d\,\theta^2 + \sin^2\,\theta\,d\phi^2) \eqno(159)$$

outside; and inside the form

$$ds^2 = (1 - 8\pi \rho^* r^2/3)^{-1} dr^2 + r^2 (d\theta^2 + \sin^2\theta d\phi^2),$$
 (160)

One recognizes that the geometry inside is that of Friedmann (that is, a section of a closed spherical universe at the phase of maximum expansion) either from the elementary fact that density means curvature and uniform density (plus spherical symmetry!) means uniform curvature, or from the following mathematics: Define the length a by the equation

 $a^2 = 3/8\pi \, a^*$  (161)

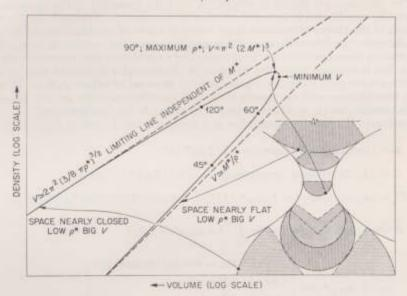


Fig. 11.—Relation between density  $\rho^*$  and proper volume V for momentarily static and homogeneous and spherically symmetric configurations of a given mass-energy  $M^*$  (\*\*mooth curve\*\*). The lower dashed line represents the relation  $V=M^*/\rho^*$  between density and volume when the curvature of space is negligible (matter occupying only a small sector of the Friedmann 3-sphere; upper illustration in insert). The upper dashed line corresponds to the opposite limiting case, where the volume of the occupied region fills out almost the entirety of the Friedmann 3-sphere (lower illustration in insert). In this case one recognizes that the radius of curvature is  $(3/8\pi\rho^*)^{1/2}$ . Also the volume of a 3-sphere is  $2\pi^2$  (radius)<sup>2</sup>. Thus one has approximately (neglecting the missing volume)  $V=2\pi^2$   $(3/8\pi\rho^*)^{3/2}$ , independent of  $M^*$ . The angles marked here and there on the curve give the value of the hyperspherical angle  $\chi_2$  at the boundary of the region occupied by the matter in selected configurations. Further details are given in the text.

Introduce the "hyperspherical angle"  $\chi$  through the equation

$$r = a \sin \chi$$
. (162)

Then the metric (160) inside takes the standard form of the 3-geometry on the surface of a hypersphere,

$$d s^2 = a^2 [d\chi^2 + \sin^2 \chi (d\theta^2 + \sin^2 \theta d\phi^2)], \tag{163}$$

and a represents the radius of this 3-sphere. The point  $\chi = 0$  represents the center of the configuration.

The insert in Figure 11 shows schematically the join between the spherical geometry inside and the Schwarzschild geometry outside for selected cases. In each case the mass

as sensed externally (M\*) has been taken to have the same value. Thus one and the same Schwarzschild geometry makes an appearance in all the examples. What differs from example to example is the place where the join is made to the spherical geometry inside. When this place is far out (big R) the density inside is small, and where it is close in the density inside is large. The point of join, as described in terms of the geometry inside. is located at a certain value,  $\chi = \chi_0$ , of the hyperspherical angle. All values of  $\chi_0$  are possible, from small  $\chi_0$  (small sector out of a big 3-sphere; upper insert in Fig. 11) through  $\chi_0 = \pi/2$  (configuration of maximum density) to  $\chi_0$  closer and closer to  $\pi$ (nearly complete universe of huge radius and low density; mass as sensed outside still M\*). The diagrams are meant to emphasize that the geometry is the important concept, not the coordinates in terms of which that geometry is expressed. In this respect one thinks of the theory of operator rings, where the laws of combination and commutation of the operators determine everything, and the particular matrices in terms of which one represents those operators are irrelevant. The r-coordinate has, moreover, the disadvantage that it conceals from view in many of the examples (examples with  $\chi_0 > \pi/2$ ) that there are two points which have one and the same set of values  $(r, \theta, \phi)$ . If one is to use any coordinates—and the inserts show that coordinates really are not necessary then the coordinates  $(\chi, \theta, \phi)$  are to be preferred inside the configuration.

In summary, the principal properties of a configuration of uniform density  $\rho^*$  (cm<sup>-2</sup>)

are

$$a = (\text{radius of curvature}) = (3/8\pi\rho^*)^{1/2};$$

$$R = (1/2\pi)(\text{proper circumference}) = (3/8\pi\rho^*)^{1/2} \sin \chi_0;$$

$$M^* = (\text{mass-energy}) = (4\pi\rho^*/3)R^3 = (4\pi\rho^*/3)(3/8\pi\rho^*)^{3/2} \sin^3 \chi_0;$$

$$V = (\text{proper volume}) = 4\pi \int_0^{\chi_0} (a \sin \chi)^2 (a d\chi)$$

$$= (3/8\pi\rho^*)^{3/2} \begin{cases} 2\pi (\chi_0 - \sin \chi_0 \cos \chi_0)(\text{general } \chi_0) \\ (4\pi/3)\chi_0^3(\text{small } \chi_0) \\ \pi^2(\text{half of 3-sphere}) \end{cases}$$
(165)

Of interest here are not configurations of a given density, however, but of a given mass-energy  $M^*$ . Therefore, solve equation (164) for  $\rho^*$  in terms of  $M^*$ ; also express V in terms of  $M^*$ : thus,

$$\log p^* = -2 \log M^* + \log [(3/32\pi)\sin^6 \chi_0], \tag{166}$$

and

$$\log n - \log A = -\log V = -3 \log M^* + \log[(1/16\pi)\sin^9 \chi_0/(\chi_0 - \sin \chi_0 \cos \chi_0)].$$
(167)

For fixed  $M^*$  let  $\chi_0$  be increased gradually from 0 to  $\pi$ . Then  $\rho^*$  and V run through a curve, the curve shown in Figure 11. This completes the proof of Theorem 20.

One can deduce almost all of the important features of Figure 11 without any detailed calculation by focusing attention on the two limiting cases (1) where the matter occupies only a very small fraction of the 3-sphere and (2) where it occupies almost all of the 3-sphere, as shown by the two dashed lines in Figure 11 and the accompanying discussion in the caption. Other key points on the curve are described in Table 8 and stated in Theorems 21 and 22. Table 8 summarizes the limiting cases of special simplicity in the relation between density and volume for momentarily static and spherically symmetric

configurations of uniform density, when the total mass-energy has some specified value M\*. The numbers in the second row of the table are found by solving the transcendental equation  $\chi = \tan \chi \left[1 - \frac{\pi}{6} \sin^2 \chi\right]$ . The quantity  $\rho^*V$  which is listed in the last column represents the mass-energy which the system would have had, had it been dispersed into small parts, each perhaps about to decompress explosively, but nevertheless momentarily static at the originally chosen density  $\rho^*$ . For the collected configuration the total mass-energy (as it will, e.g., be observed from outside) has in every case the value  $M^*$ . How much less this is than the number in the last column shows how important is the negative mass-energy of gravitational interaction of the matter with itself.

Theorem 21, No momentarily static and spherically symmetric and homogeneous object of mass M\* (cm) can have a volume less than

$$V_{min} = 0.895\pi^2(2M^*)^3$$
. (168)

Comment.—This is slightly less than half the volume of a hypersphere which has exactly the characteristic Schwarzschild radius 2M\* (cf. Table 8 or the insert in Fig. 11).

TABLE 8 THE RELATION BETWEEN DENSITY AND VOLUME FOR MOMENTARILY STATIC, SPHERICALLY

SYMMETRIC CONFIGURATIONS OF UNIFORM DENSITY

Special Feature	χe	p*	· V	**V
Very small sector of sphere Minimum V Maximum p* Nearly closed universe	≪1	Small	$\sim M^*/\rho^*$	∞M*
	80.0+°	1/36.8 M*1	$70.7 M^{*3}$	1.92 M*
	π/2	1/33.5 M*2	$79.0 M^{*3}$	2.36 M*
	∞π	Small	$\sim 2\pi^2(3/8 \pi \rho^*)^{3/3}$	≫M*

THEOREM 22. No momentarily static and spherically symmetric and homogeneous object of mass-energy  $M^*$  can have a density  $\rho^*$  (cm<sup>-2</sup>) = (G/c<sup>3</sup>)  $\rho$  (g/cm<sup>3</sup>) greater

$$\rho_{\text{max}}^* = (3/32\pi M^{*1}).$$
 (169)

Comment.—This maximum occurs when the matter fills out exactly half of the Friedmann 3-sphere.

### THE SLIDE RULE, ITS USE, AND THE INTERPRETATION OF THE RESULTS

Now for the gravitational part of the promised "slide rule"! It appears in Figure 12, constructed in an obvious way out of many single curves like the curve shown in Figure This construction ends the present analysis of the long-range forces.

Next, imagine superposed on Figure 12 the other half of the slide rule, the sliding half. Let it consist of a sheet of glass on which is engraved in black the equation of state, in the form of a single curve for the density of mass-energy,  $\rho^*$ , as a function of the number density of baryons, n (with log scales employed for both quantities). For low values of n one is dealing with dispersed granules of Fe<sup>in</sup>. In this regime  $\rho^*$  is given by

$$\rho^* \cong \mu_s^* n$$
, (170)

where  $\mu_s^*$  is the standard mass per baryon (see Table 2;  $\frac{1}{56}$  of the mass of an atom of Fe<sup>56</sup>). At modest compressions  $\rho^*$  is a little greater than  $\mu_s^*n$  by reason of the mass equivalent of the work of compression. For very high values of n, on any asymptotic  $\gamma$ -law equation of state, the density of mass-energy is given by an expression of the form

$$\rho^* \sim L^{-2} (nL^2)^{\gamma}$$
, (171)

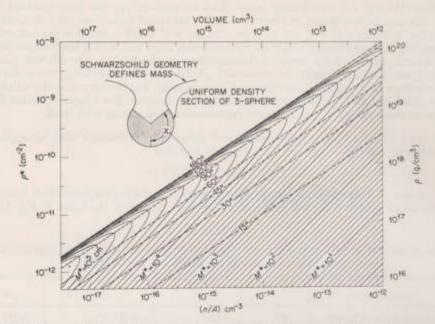


Fig. 12.—Contour diagram giving mass-energy as a function of density and volume for spherically symmetric configurations of uniform density at moment of time symmetry (neither implosion nor explosion yet underway). Diagram deduced exclusively from general relativity from the central principle connecting space curvature with density of mass-energy,  ${}^{(3)}R = 16\pi\rho^*$ ; quite independent of form of relation connecting density  $\rho^*$  of mass-energy with number n of baryons per cm³ (or with pressure  $\rho$ ). Units: for volume, cm² (= total number of baryons, A, divided by the number of baryons per cm³, n); for reciprocal of volume (n/A), cm⁻¹; for density of mass-energy,  $\rho^*$  (cm⁻³) =  $(G/e^2)\rho(g/cm³)$  with  $G/e^3 = 0.742 \times 10^{-20}$  cm/g; for mass,  $M^*$  (cm) =  $(G/e^3)M(g)$ . The mass contours are drawn at 1-db intervals (factor  $10^{6.4} = 1.260$ ); e.g., between  $M^* = 10^4$  cm and  $M^* = 10^5$  cm there appear contours belonging to the following mass values (with  $M\odot$  = mass of Sun =  $1.987 \times 10^{32}$  g):

logis M*	M*(cm)	M(g)	M/M <sub>O</sub>
4 0.	1 .000×104	1_347×10m	0.0678
4 1.	1 .260×104	1_697×10m	.0854
4 2	1 .584×104	2_13_×10m	.1074
4.9	7.94 ×104	1.069×10 <sup>13</sup>	.537
5.0	1.000×108	1.347×10 <sup>13</sup>	0.678

The region where the matter is located occupies a section of a 3-sphere. It extends from hyperspherical angle  $\chi=0$  out to the value of  $\chi$  indicated by the appropriate dashed line in the  $(\rho^*,n/A)$ -plane. For small values of  $\chi$  the departure from flatness is almost negligible. Then one has very nearly  $\rho^*=M^*/$  volume =  $M^*n/A$  (straight line of unit slope in this log-log diagram). However, for any given value of the volume (or of n/A) there is a maximum allovable value of the density, given by  $\rho^*=(3\pi^{1/3})^{2/12}/(n/A)^{3/3}$  (configuration indefinitely near to closed universe;  $\chi=180^\circ$ ; mass zero as seen from outside). Hence the uppermost straight line with its slope  $\frac{3}{2}$  in the log-log diagram. It separates allowable configurations from configurations incompatible with Einstein's standard general relativity. If one desires to increase all  $M^*$  labels in the diagram by the factor  $10^n$ , he should multiply all  $\rho^*$  labels by  $10^{-2n}$ .

where L is a quantity with the dimensions of a length. Here the asymptotic exponent  $\gamma$  must be no less than unity if matter is not to collapse already on a microscopic scale, quite apart from any gravitationally induced collapse. On the other hand,  $\gamma$  can be no greater than 2 without violating causality (chap, ix). If highly compressed material behaves as an ideal Fermi gas, then a has the asymptotic value of 4.

haves as an ideal Fermi gas, then  $\gamma$  has the asymptotic value of  $\frac{4}{3}$ .

With no more than these simple features of the equation of state to draw upon, what conclusions can one reach as he sets the glass slider into place above Figure 12? Let some definite displacement  $\log A$  be selected between the  $\log n$  scale on the slider and the  $(\log n - \log A)$  scale on Figure 12. Follow the trace made on Figure 12 by the equation of state. In this way obtain the mass-energy of every single momentarily static and spherically symmetric configuration of uniform density which contains the fixed number of baryons, A.

Look first at the low  $\rho^*$  end of the curve for the equation of state. There the curve degenerates to the straight line (170) with unit slope in the (log  $\rho^*$ , log n)-plane. But also the contours of Figure 12 degenerate in this same low  $\rho^*$  limit to straight lines, again with unit slope. Therefore the lower portion of the curve for the equation of state coincides with one and only one  $M^*$  contour; the contour  $M^* = \mu_* A$ . This result for the mass-energy of A widely dispersed baryons is hardly surprising. It merely serves to

check the operation of the slide rule.

For modest compressions, that is, for somewhat higher  $\rho^*$  values on the curve for the equation of state, allowance must be made for two effects: (1) the  $\rho^*$  values lie slightly higher than the straight line  $\mu_s$ \*n (compressional energy); and (2) the M\* contours also bend upward (see Fig. 12) as compared to ideal straight lines of unit slope on the loglog diagram (gravitational energy). According to whether gravitational or compressional energy dominates, the curve for the equation of state is now slowly switching to contours of lower or higher mass-energy M\*. All this is as it should be. If we were concerned solely with the non-relativistic domain, we could find a simpler graphical means to bring this story into evidence, However, we wish to go all the way from non-relativistic to relativisitic compressions, and therefore use the diagram in its present form. For example, employing the Harrison-Wheeler equation of state on the "slider" part of the slide rule, we construct curves for mass-energy as a function of compression for three selected choices of the baryon number A, as shown in Figure 13. In that diagram one can see at once the approximate correspondence between the predictions of the uniform model and the detailed integrations of the accurate general relativity equation of hydrostatic equilibrium, as depicted in Figures 5-7.

# continuous sequence of configurations with fixed A but mass-energy going to zero

Now follow the curve for the equation of state to higher and higher densities, as it is traced on the imaginary glass slider we have placed over Figure 12. Recognize that it can never have a slope less than unity on the log-log diagram; otherwise matter would collapse spontaneously. Recognize, on the other hand, that the limit for gravitational collapse (the upper border of the contour diagram in Fig. 12;  $\chi_0 = 180^\circ$ ; matter curving up space into a closed universe) has a log-log slope of only two-thirds. Therefore the curve for the equation of state cannot help but cross this border. Here the sequence of configurations of A baryons (A fixed) comes to a decisive end with  $M^* = 0$ . Thus one establishes in the most direct way possible the important Theorem 23.

Theorem 23. Provided that matter does not undergo collapse at the microscopic level at any stage of compression, then—regardless of all other features of the equation of state—there exists for each fixed number of baryons A a continuous sequence of configurations leading to a "gravitationally collapsed configuration," in which the mass-energy M\* as sensed externally is zero.

### NO BARRIER TO COLLAPSE OF A SUPRASOLAR MASS

In Figure 12 there is an "energy ridge" running downhill from the lower left-hand side of the diagram to the upper right. Theorem 23 states there is a continuous sequence of configurations traversing this ridge, quite apart from the details of how the crossing takes place. To be more concrete, consider a few special cases. In one case the baryon number is so great (some powers of ten greater than the baryon number of the Sun) that the entire sequence of configurations is traversed while the matter is still at low density. The matter has the form of dust all the way to the collapse limit. In this case there is no pressure at any stage of the way. The equation of state keeps the form  $\rho^* = \mu_* n$  through the entire sequence. The "curve" on the glass slide of the slide rule reduces throughout its attainable length to a straight line with a logarithmic slope of unity. Project this line onto Figure 12, the stationary part of the slide rule, and follow that line from low densities to the critical density of a completely collapsed configuration. The contours which are cut along the way have successively lower and lower mass-energies,

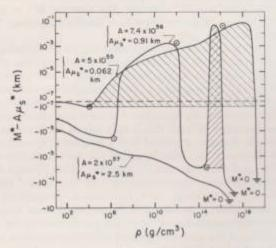


Fig. 13.—Mass-energy  $M^*$ , as sensed externally, as a function of density  $\rho$ , for momentarily static and spherically symmetric configurations of uniform density. The curves were determined by use of the "slide rule" of chap. viii, with Fig. 12 constituting one-half of the slide rule, and the HW equation of state of chap. x constituting the other, and no actual computation whatsoever being required. For  $A < 10^{16}$  (5 ×  $10^{16}$  representative) there is just one minimum in the mass-energy curve; for  $10^{16} < A < A_{\rm eff} \sim 10^{16}$  (2 ×  $10^{16}$  representative) there are two minima and two crushing points; for  $A \ge A_{\rm eff} \sim 10^{16}$  (2 ×  $10^{16}$  representative), the mass-energy curve is monotonic decreasing (no equilibrium configurations; collapse inevitable). For comparison with the uniform model, one has in Figs. 5, 6, and 7 the results of numerical integrations of the general relativity equation of hydrostatic equilibrium employing the same equation of state. Those equilibrium configurations have central densities indicated here by circled dots. The usefulness of the uniform model is evident from the comparison. Diagram prepared by Kip S. Thorne.

dropping monotonically to  $M^* = 0$ . This result is reasonable. The effective energy of the gravitational field becomes more and more negative, There is no energy of compression on hand even to make a try at compensating this negative quantity.

It is easy to give expressions in this case of dust for the density and mass-energy at each stage of the contraction in terms of the value of the mass,  $M_0^*$ , when the dust is infinitely dispersed. The proper volume expresses itself as the ratio  $M_0^*/\rho^*$ . On the other hand, the proper volume is also given by equation (165) in terms of the density and the hyperspherical angle,  $\chi_0$  (shown in Fig. 12). Equating the two expressions for V, one can solve for the density, finding

$$\rho^* = (27/128\pi M_0^{*1})(\chi_0 - \sin \chi_0 \cos \chi_0)^2. \tag{172}$$

The density increases continuously through the sequence of configurations to a finite limit at the final collapsed state ( $\chi_0 = 180^{\circ}$ ):

$$\rho^* (\text{maximum}) = (27\pi/128M_0^{*1}).$$
 (173)

The mass falls steadily to zero for the same sequence of configurations:

$$M^*/M_0^* = \frac{2}{3} \sin^3 \chi_0 / (\chi_0 - \sin \chi_0 \cos \chi_0)$$
 for general  $\chi_0$   
= 1 for small  $\chi_0$  (dispersed dust)  
=  $\frac{4}{3\pi} = 0.424$  for  $\chi_0 = \pi/2$   
= 0 for  $\chi_0 = \pi$  ("collapse").

Some illustrative values have been calculated from equation (173) and are collected in Table 9. This table gives the density,  $\rho_{\text{max}}$ , for a cloud of dust in the collapsed configura-

TABLE 9

DENSITY OF A DUST CLOUD AT COLLAPSE AS FUNCTION OF MASS BEFORE ASSEMBLY

Ma/M <sub>☉</sub>	$M_{\theta}(g)$	Me*(cm)	ρ <sub>mia</sub> *(cm <sup>-2</sup> )	$\rho_{\rm max}({\rm g/cm^2})$
10 <sup>12</sup> 10 <sup>11</sup> 10 <sup>10</sup> 6.41×10 <sup>8</sup>	1.987×10 <sup>46</sup> 1.987×10 <sup>46</sup> 1.987×10 <sup>46</sup> 1.274×10 <sup>46</sup>	1.474×10 <sup>17</sup> 1.474×10 <sup>18</sup> 1.474×10 <sup>18</sup> 0.945×10 <sup>14</sup>	3.05×10 <sup>-28</sup> 3.05×10 <sup>-28</sup> 3.05×10 <sup>-21</sup> 7.42×10 <sup>-29</sup>	4.11×10 <sup>-1</sup> 4.11×10 <sup>-1</sup> 4.11×10 <sup>-1</sup>

tion as a function of the mass of the cloud before assembly (the table is based on eq. [173]; maximum density where concept of "dust" makes sense is taken to be 1 g/cm², as indicated by last row in table). In every case the mass as sensed *outside* is indefinitely close to zero. From these numbers one sees, as William Fowler has also pointed out on numerous occasions, that an object containing as many baryons as a galaxy ( $\sim 10^{11}$   $M_{\odot}$ ) in a state of gravitational collapse is still at a density lower than the density of air, where any resistance of matter to being compressed can have nothing to do with the situation!

The lower the number of baryons, the higher the density at which the mass-energy of gravitational interaction first becomes important. Thus as one shifts his attention from a galaxy to a star, the critical density goes from less than that of air to the order of magnitude of nuclear densities. In this domain mass-energy no longer decreases monotonically for configurations of a given A as the compaction is increased—although ultimately this universal behavior does dominate (Theorem 23). But first the special features of the equation of state make themselves felt. Thus, when the number of baryons is  $0.74 \times 10^{67}$  (or the mass  $M_0$  before compaction is  $0.62~M_{\odot}$ ) and one follows the line of the equation of state upward through the contour diagram of Figure 12, he finds (Fig. 13) that the total mass-energy  $M^*$  decreases through the sequence of configurations to a shallow minimum (shallow on a nuclear scale of energies!) at  $\sim 10^{6}$  g/cm<sup>3</sup>; reaches a maximum at  $\sim 10^{16}$  g/cm<sup>3</sup>; reaches a deeper minimum at  $\sim 10^{14}$  g/cm<sup>3</sup>; goes through a final maximum at  $\sim 10^{16}$  g/cm<sup>3</sup>; and thereafter decreases monotonically to  $M^* = 0$  at the configuration of collapse.

### COLLAPSE BARRIER FOR SUBSTELLAR SYSTEMS

Now let the number of baryons be very small (kilograms or tons) compared to the baryon content of a star. Then the sequence of configurations has a fantastically shallow minimum. This dip measures the gravitational potential energy of attraction of the iron atoms in this sphere of everyday dimensions. The corresponding density is negligibly higher than the standard density of Fe<sup>36</sup>. Further progress along the sequence of configurations takes one to higher and higher densities. More and more work is done along the way against compressional forces. Densities are still too low for gravitation to give any help, until at last one comes to very high densities. Here one is finally traversing the "energy ridge" in Figure 12. The densities are so extreme that it is reasonable to ask for an account of the traversal in terms of the simple asymptotic  $\gamma$ -law equation of state (171). In this case one can trace the variation of density and energy across the ridge to the configuration of collapse by way of equations like (172) and (174) except for the change in the equation of state:

$$\rho^* = L^{-2} \left[ (27/128\pi)^{1/2} (\chi_0 - \sin \chi_0 \cos \chi_0) / A \right]^{2\gamma/(3\gamma - 2)}, \quad (175)$$

$$\rho_{\text{max}}^* = L^{-2} [(27\pi/128)^{1/2}A]^{2\gamma/(3\gamma-2)},$$
(176)

$$M^* = (3/32\pi)^{1/2} L[(128\pi/27)^{1/2} A/(\chi_0 - \sin\chi_0 \cos\chi_0)]^{\gamma/(3\gamma-2)} \sin^3\chi_0. \quad (177)$$

These equations reduce for  $\gamma = 1$  ("dust") to the results previously given. The case  $\gamma = \frac{4}{3}$  is particularly interesting because it corresponds to the case of an ideal Fermi gas com-

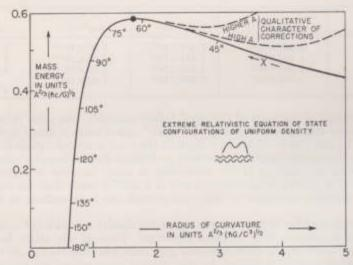


Fig. 14.—Potential barrier against gravitational collapse for configurations of uniform density. Here A is kept fixed. It is taken to be much smaller in order of magnitude than  $10^{37}$ . Consequently the density to which one must go before gravitational energies become significant is enormous. The calculations assume that a  $\gamma$ -law equation of state applies in this high density regime, with  $\gamma=\frac{\pi}{4}$  and with the constant of proportionality appropriate to an ideal Fermi gas. The abscissa in the diagram is a simple measure of the degree of compaction of the configuration. It is the radius of curvature of the Friedmann geometry (3-sphere) inside the region occupied by the matter. It is given in terms of the density eq. (175) by the equation  $a=(3/8\pi\rho^*)^{1/2}$ . The angles marked on the curve mark the extent of the ideal complete 3-sphere occupied by the matter (cf. insert in Fig. 12). For low compaction, low density, and high radius of curvature, greater and greater departures from the ideal  $\gamma=\frac{\pi}{4}$  equation of state are to be expected. These departures set in the sooner on the diagram, the higher is the A value (dashed lines at upper right). For more detail in this region for very high A values ( $\sim 10^{37}$ ) see Fig. 13. The unit in the diagram is  $(hc/G)^{1/2}=L^*=1.616\times 10^{-32}$  cm, equivalent to  $2.177\times 10^{-6}$  g or  $1.955\times 10^{16}$  erg or the energy set free by 0.467 tons of conventional explosive. At the maximum of the curve the mass-energy is 0.5837  $A^{1/2}$  ( $h_C/G)^{1/2}=A^{2/3}$   $1.3\times 10^{-3}$  g; the hyperspherical angle  $\chi$  subtended by the spherical collection of matter at its center is 63.173°; the radius of curvature is 1.6426  $A^{2/3}$  ( $h_C/G)^{1/2}=A^{3/3}$   $2.68\times 10^{-23}$  cm; and the density is  $A^{-4/2}$   $2.24\times 10^{92}$  g/cm<sup>2</sup>.

pressed to densities so great that the Fermi energy is large compared to the rest energy of the particles. In this case the characteristic length L in the equation of state (171) has the value (cf. eq. [36], chap. ix, and Table 2)

$$L = (3^{2/8}\pi^{1/8}/2)(\hbar G/c^3)^{1/2} = 1.524L^* = 2.46 \times 10^{-83} \text{ cm}$$
, (178)

independent of the rest mass of the fermion, as is to be expected.

Figure 14 shows in this case,  $\gamma = \frac{4}{3}$ , the potential barrier against gravitational collapse. Figure 15 shows selected configurations before and after the passage of the barrier

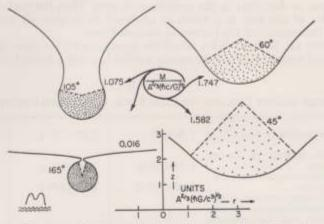


Fig. 15.—Geometry for four configurations of uniform density, each containing the same number of baryons A, and differing only in degree of compaction. The calculations assume  $\rho$  is proportional to  $n^{4/8}$  (extreme relativistic limit of ideal Fermi gas). The region of uniform curvature where the matter is located joins on smoothly in every case to the exterior Schwarzschild geometry. However, the mass associated with the Schwarzschild geometry differs from case to case as shown in Fig. 14. In the case where the matter has almost pinched off from the surrounding space the mass as sensed by an external observer is almost zero. Points on the typical surface in the drawing have significance; off, none. The surface has symmetry with respect to rotations about the vertical axis. It is shown here as if imbedded in a Euclidean space of one higher dimension, hence the s-axis in the diagram (the extra dimension having nothing whatsoever to do with time). The density of dots indicates qualitatively the density of matter. This matter is depicted for ease of representation as occupying a cone in the purely mathematical space of one higher dimension. In reality it is to be conceived as confined to a 3-sphere; that is, to the "surface" in the diagram. Contrast the present sequence, in which A is fixed and M\* varies, with the sequence in the insert of Fig. 11, where M\* is fixed and A varies.

summit. Table 10 summarizes principal features of the barrier against gravitational collapse of selected substellar masses as calculated from equations (175)–(178), which assume an ideal Fermi gas in the limit of densities very high in comparison with nuclear density. The mass-energy at the summit increases as  $A^{2/3}$ ; or, relative to the *initial* mass, as  $A^{-1/3}$ . Thus the supplementary energy which must be supplied goes to zero as A

approaches values small compared to stellar magnitudes.

The table is confined to a limited range of densities (last row). When the density falls to nuclear values or less, complications set in, in the equation of state. These consequences have already been examined (Figs. 5–7 and esp. Fig. 13). On the other hand, the very concept of equation of state becomes questionable when the radius of curvature of space approaches the Compton wavelength,  $4 \times 10^{11}$  cm. The density required to produce such a curvature is  $\sim 10^{20}$  cm<sup>-2</sup> or  $10^{48}$  to  $10^{48}$  g/cm<sup>2</sup>. If any good reason is discovered to think that the equation of state of an ideal Fermi gas makes sense at still higher densities, then one can consider seriously the compaction of smaller masses to the point where gravitational collapse sets in.

### NOT TECHNOLOGICALLY FEASIBLE TO PUT IN ENOUGH ENERGY TO PUSH A SUBSTELLAR MASS OVER THE BARRIER

To take a sphere of the smallest mass listed in Table 10 and to raise it slowly to the summit of the collapse barrier (density ~10<sup>48</sup> g/cm²; energy increased ~10<sup>45</sup> fold by the work of compression) is, of course, possible in principle. Place the sphere at the center of a configuration of cold matter of mass a little less than the mass of the Sun. Go through the operation of "pumping up" the central density to higher and higher values. Take the cold star through successive cycles in which one adiabatically adds and subtracts baryons, as described in the preceding chapter. Then the goal will be achieved. The instability of the star as a whole as analyzed in chapter vii traces back to the teetering on the summit of the barrier as discussed here.

In discussion Dr, Richard Eden raised the question whether there is not some more nearly practical means to supply the energy needed to crush a limited amount of matter.

TABLE 10

BARRIER AGAINST COLLAPSE FOR IDEAL FERMI GAS IN HIGH-DENSITY LIMIT

Mass before compaction $(=A \mu_i) \dots$	1.60×10° g	3.09×10 <sup>13</sup> g	9.76×10 <sup>st</sup> g
Mass-energy at summit of barrier against collapse. Equivalent of this energy in tons of con-	1.24×10 <sup>17</sup> g	1.92×10 <sup>n</sup> g	1.92×10 <sup>26</sup> g
ventional explosive	2.66×10 <sup>m</sup> T	4.12×10 <sup>ss</sup> T	4.12×10 <sup>30</sup> T
Factor by which energy required to trig- ger gravitational collapse exceeds any possible output from that reaction even assuming 100 per cent efficiency	7.74×10°	6.22×10 <sup>6</sup>	1.97×10 <sup>1</sup>
Schwarzschild radial coordinate of com- pacted configuration at top of barrier Radius of curvature of the Friedmann	2.31×10 <sup>-11</sup> cm	3.58×10 <sup>-7</sup> cm	3.58×10 <sup>-2</sup> cm
geometry within the configuration	2.59×10 <sup>-11</sup> cm	4.01×10 <sup>-7</sup> cm	4.01×10⁻² cm
Density of mass-energy in it, in geom- etrized units	1.79×10 <sup>20</sup> cm <sup>−2</sup>	7.42×10 <sup>11</sup> cm <sup>-8</sup>	7.42×101 cm <sup>-2</sup>
Density at barrier summit in conven- tional units	2.40×1048 g/cm <sup>2</sup>	1040 g/cm <sup>2</sup>	10 <sup>20</sup> g/cm <sup>2</sup>

In response it was suggested that in principle the matter could be propelled inward in pieces with such speeds and such times of dispatch that all came together in a very small space at a very high density. For this purpose, however, each particle has to be supplied with an energy ~10\* times its own rest energy! (This factor increases, moreover, if one extrapolates the considerations of Table 10 to smaller masses, where the densities at the summit are higher, and the concept of an equation of state is questionable). One finds himself trying to imagine a machine which is at the same time a combination of accelerators of previously unimagined size, a focusing device better than any electron microscope, and a resolver of time superior to that of any nanosecond counter. Then one turns from this design problem and looks at the total energy requirement (Fig. 16). At this point one becomes all the more convinced that it is beyond the bounds of technology to drive matter over the collapse barrier at a density of order of 10<sup>49</sup> g/cm³! One will not look for gravitational collapse in masses like those listed in Table 10. At stellar masses, yes; at the level of elementary particles, maybe; but not in between.

It is worth emphasizing that the requirement of ~10<sup>17</sup> g of mass-energy equivalent (or ~10<sup>21</sup> tons of TNT equivalent) to get to the top of the barrier at ~10<sup>49</sup> g/cm<sup>3</sup> density is independent of the details of the equation of state. The reasoning goes in the following steps: (1) the very concept of equation of state cannot be trusted when the radius of curvature of space is comparable to or less than the Compton wavelength. On this ac-

count this length sets a natural limit to the extension of a barrier-surmounting configuration about which one can talk classically. (2) In addition it does not make sense in terms of devices conceivable today to compact great amounts of matter into a domain orders of magnitude smaller than a Compton wavelength,  $X = \hbar/mc$ . (3) This dimension for the radius of curvature of space inside the configuration determines a density  $\rho \sim 10^{49} \, \mathrm{g/cm^3}$  via the equation  $(3/8\pi \, \rho^*)^{1/2} = X$ . (4) A density of this magnitude multiplied by a volume of this extension together determine a mass-energy

$$M^*(cm) \sim \rho^* \lambda^2 \sim (\lambda/8)$$
 or  $M(g) \sim (c^2/G)(\lambda/8) \sim 10^{16} g$ . (179)

This result is independent of whether the  $\gamma$  in any asymptotic  $\gamma$ -law equation of state has the value of  $\frac{4}{3}$  (as for radiation or an extreme relativistic Fermi gas) or the maximum value of 2, at which the speed of sound becomes equal to the speed of light. Let us adopt  $\gamma = 2$  instead of  $\gamma = \frac{4}{3}$ . Let us repeat the calculations in the first column of Table 10. Keep fixed the density at the summit of the barrier. Then the mass-energy at the barrier

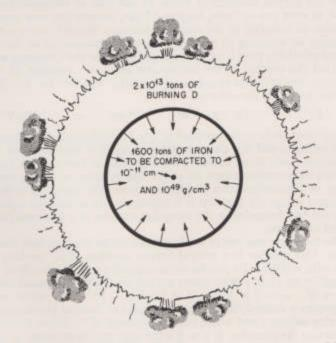


Fig. 16.—The difficulty with gravitational collapse as an energy source at a terrestrial level. The output from the 1600 tons, assuming the limiting efficiency of 100 per cent conversion of the collapsed matter into energy, is equivalent to  $3 \times 10^7$  megatons of high explosive. However, to get this energy out, one has to activate the iron. For this purpose it must be compressed into a region with dimensions of the order of the Compton wavelength, or—allowing for mass-energy put in during compression—to a density of the order of  $10^{49}$  g/cm³. The energy required for this activation process is  $\sim 10^8$  times as much as the energy which one can hope to extract from the 1600 tons with 100 per cent collapse! Moreover, the tailoring of the compaction is far beyond the capability of technology, even apart from the difficulties of localizability associated with the exclusion principle. Furthermore, conversion of the kinetic energy of compaction into heat and radiation before the critical condition is reached (top of potential barrier against gravitational collapse) would spoil the possibility of completing the activation. Even if the tailoring were perfect and these thermal losses were made negligible, the total energy of activation, if supplied by thermonuclear combustion of deuterium, would require an amount of this fuel which—by a numerical coincidence—happens to be the same as the entire deuterium content of the ocean,  $\sim 2 \times 10^{13}$  tons. These numbers assume an equation of state which asymptotically for high densities reads  $\rho \sim$  constant  $\pi^{\gamma}$ , with  $\gamma = \frac{\pi}{2}$ . A change in  $\gamma$  alters the 1600-ton figure but leaves unchanged the  $\sim 2 \times 10^{-11}$  cm and the  $\sim 10^{49}$  g/cm³ and  $2 \times 10^{14}$  tons of D (discussion in text).

summit is also altered by less than a factor 2. The only important change occurs in the number of baryons into which that energy of compression is fed. The matter now being assumed harder to compress, a smaller number of particles is required to sop up the requisite energy. Accordingly, the calculated mass before assembly will be reduced—and reduced very much below 1600 tons if the asymptotic value of  $\gamma$  is close to 2. The technical difficulties of going over the barrier—energy and compaction—are unchanged.

### THE BARRIER FALLS AT BIG A AND LOW A AND HAS A MAXIMUM AT INTERMEDIATE A

The barrier against collapse is zero for configurations of cold, catalyzed matter containing as many baryons as the Sun or more. The barrier comes into being and increases when the baryon number drops to 0.4 of the baryon number of the Sun and a little less. At some lesser fraction of the baryon number of the Sun the barrier has its greatest value. When the baryon number drops to the substellar values of Table 10, the barrier is already decreasing with baryon number. Why not drastically extrapolate this law of decrease below the baryon numbers of Table 10 and look at configurations containing only a handful, or even two or three, baryons? First, because the very concept of equation of state loses all meaning at the relevant densities. Second—even if one nevertheless goes on using an equation of state—because any calculation of the "barrier" by classical general relativity puts it at dimensions far below the Compton wavelength of a baryon, so that the concept of the barrier also loses any meaning. If, despite these powerful warnings, one still goes ahead to calculate the "barrier" for A=2 or 3, he gets from Figure 14 a height of the order of

$$(\hbar c^3/G)^{1/2} \sim 10^{-5} \text{ g}$$
 or  $10^{16} \text{ erg}$  or  $10^{28} \text{ eV}$  (180)

-not an energy soon likely to be attained in any Earth-bound accelerator!

It would be wrong to end this chapter without a word of caution about the nature of the energy analysis made here. Taking a fixed number of baryons, we have compared the energy of different configurations all at the one moment of time symmetry, rather than the energy of one configuration at different times. The questions of dynamics have yet to be examined (chap. xi). But first it is appropriate to go into the equation of state, on which so much has depended in the foregoing analysis of static configurations, both

equilibrium and otherwise.

Out of all the foregoing analysis of static configurations two numbers and two conclusions stand out. One number is a critical baryon number,  $A_{\rm crit}$ , marking the limit of configurations with stability. Its precise value depends upon the details of the equation of state at densities near and a little above nuclear densities. Its general order of magnitude is  $A_{\rm crit} \sim M_{\odot}/\mu_{*} \sim 2 \times 10^{33} \ g/2 \times 10^{-24} \ g \sim 10^{67}$ . The other is a number,  $A_{\rm quantum}$ , less precisely defined, below which the ideas of classical physics no longer make sense in analyzing collapse, and where even the concept of "collapse barrier" is not the best way to describe the situation. If  $\gamma = \frac{4}{3}$  is the appropriate exponent in an asymptotic  $\gamma$ -law fit to the equation of state at densities very high compared to nuclear density, then this baryon number is calculated (Table 10) to be of the order of magnitude of  $A_{\rm quantum} \sim 1.6 \times 10^{8} \ g/1.6 \times 10^{-24} \ g \sim 10^{23}$ . Changes in  $\gamma$  in the allowable region change  $A_{\rm quantum}$  by a modest number of powers of 10. In terms of these two numbers the two conclusions are these:

Theorem 24. No cold, catalyzed configuration of A baryons is stable against gravitational collapse when A exceeds A<sub>crit</sub>.

Theorem 25. A system of A baryons, with A > Aquantum but A < A<sub>crit</sub>, constrained to uniform density possesses at least one cold, catalyzed configuration of equilibrium which is unstable against gravitational collapse.

These two statements together exhaust the cases to which one can apply classical physics.

## EQUATION OF STATE OF COLD, chapter 9 CATALYZED MATTER

#### THE END POINT OF THERMONUCLEAR EVOLUTION

What is the state of lowest energy of a system of A baryons? This question has motivated all of the foregoing analysis. Some of the configurations considered were configurations of equilibrium. Others were not, but were examined because they threw light on the theory of equilibrium. But all of the configurations were static—at least momentarily—because in the last analysis the question raised has to do with a concept in-

trinsically static: the final energy state of an A-baryon system.

This concept of final energy state is so central to the discussion that it is appropriately spelled out in a little detail. The idea has already become well established in chemical thermodynamics, though not without struggles at the time many decades ago when it was first introduced. That one could analyze the possibilities for a reaction by comparing the free energies of the initial and final states, without study or even knowledge of the perhaps dozens of intermediate stages, was in the end a principle too powerful to be overlooked. In the study of many important problems this principle short-circuited immense complexities of chemical-reaction-rate theory. Those complexities are called to mind again as one looks with admiration at the complications being unraveled step by step today in the theory of thermonuclear reactions in stars. Clearly there is no substitute for this undertaking insofar as one is concerned with understanding the evolution of actual stars, in the actually available time scale. However, one is permitted to ask other questions, too; and among them this question of principle: Granted indefinitely long time, and indefinitely effective means to catalyze thermonuclear reactions, and granted exactly A hydrogen atoms to start with, what will be the final output of energy from the system?

In terms of the energy principle, one translates this question to the form: What is the difference between the energy of the initial state and the energy of the final state? This formulation leads directly to the issue in this section: What is the final state of matter? Here we speak of matter as one conceives of it within the framework of standard nuclear physics; that is to say, looking apart (until chap. xi) from the issues opened up by gravi-

tational collapse.

In asking for the final state of an A-baryon system, first sharpen the question, by defining more clearly what is meant by an "A-baryon system."

### SYMMETRY AGAINST $A \rightarrow -A$

When we deal with an A-baryon system, we understand the number A to have sign as well as magnitude. Thus a negative A implies a system built out of antiprotons and antineutrons. We accept the observed symmetry between antiparticles and particles as

<sup>&</sup>lt;sup>1</sup> For a recent comprehensive review, see Hayashi, Höshi, and Sugimoto (1962). See also Schwarzschild (1958); Burbidge, Burbidge, and Fowler (1957); and Salpeter (1957). For the Urca process see Gamow and Schönberg (1941).

implying complete symmetry between systems with positive A and systems with negative A even when A is very large.

#### ELECTRICAL NEUTRALITY

We shall also understand the term "baryon" to imply electrical neutrality; that is, a baryon is either a neutron, or a proton-plus-electron, or any hyperon derived from a neutron by any of the standard transformations of elementary-particle physics, accompanied by whatever electronic muonic or mesic satellite is required for consistency with the law of conservation of charge.

Is such electrical neutrality really maintained when gravitational fields are as power-

$$g \sim GM/R^2 \sim (.7 \times 10^{-8} \text{ cm}^3/\text{g sec}^2)(1.4 \times 10^{33} \text{ g})/(.10^6 \text{ cm})^2 \sim 10^{16} \text{ cm/sec}^2$$
, (181)

as they are calculated to be in a neutron star? This gravitational pull is concentrated almost exclusively upon the nuclei. However in the outer reaches of the star the material is held up practically entirely by the pressure of the electrons. Will not the protons and electrons be entirely separated from each other by the countervailing action of these two forces? No! Rudkjøbing (1952) has pointed out that the star will be endowed with an electric field that points radially outward. It transmits to the protons the sustaining influence of the electron pressure. This field is greatest in the outermost region of the object. There an entire Fe<sup>36</sup> nucleus has to be sustained by the elastic forces coming from something of the order of only one electron per atom, responsible for lattice binding. Even in that extreme case the calculated electric field,

$$E \sim m_{Fe} g / \epsilon \sim 6000 \text{ V/cm}$$
, (182)

is negligible both in its direct effects and in its contribution to the energy density of the system. That the electrical potential at the center of the neutron star is of the order of  $(6000 \text{ V/cm})(10^6 \text{ cm}) \sim 10^{10} \text{ V}$  is no source of concern; physics has to do after all with fields, not potentials! Therefore electrical neutrality will be assumed in all analysis of the local nuclear physics.

#### DEFINITION OF NEUTRINO NEUTRALITY

Not only electrical neutrality but also "neutrino neutrality" will be taken to be included in the term "final state of an A-baryon system," In other words, the system will be taken to be labile with respect to the emission of neutrinos or antineutrinos, whether this system is an isolated baryon, or a nucleus, or a collection of baryons as great as a neutron star. There exist of course some beta-decay processes which have very long halflives. Of whatever length the half-life of any such process may be, the term "final state" will be taken to imply that all beta-transformations have gone to completion. Examined more closely, this assumption consists of two parts. First, it tacitly takes space itself to be "neutrino-neutral"; second, it assumes the system to be in neutrino equilibrium with space. We shall explicitly adopt the idealization in which the neutrino field pervading all space is taken to be in thermodynamic equilibrium at absolute zero temperature and to have a Fermi energy of zero. Weinberg (1962) and Zel'dovich (1962) have examined some of the physical consequences for beta-decay processes which have very low energy release if this Fermi energy is not equal to zero—that is, if the universe contains a surplus of neutrinos of one kind-but no efforts to detect such effects have succeeded.2 However, the absorption of neutrinos from a plutonium plant has been detected (Reines and Cowan 1953, 1959; Cowan, Reines, Harrison, Kruse, and McGuire 1956; Carter,

<sup>&</sup>lt;sup>3</sup> Professor L. Langer kindly communicated personally in June, 1964, the null results to date of experiments carried on at the University of Indiana designed to detect such effects.

Reines, Wagner, and Wyman 1959). Therefore, we know that effects such as Weinberg has discussed cannot be escaped if one surrounds the A-baryon system under study with an ideal membrane impermeable to neutrinos and artificially pumps up the Fermi energy of this radiation to some substantial level. In this way, according as one pumps in neutrinos or antineutrinos, one can in principle push the beta-equilibrium of nuclear matter in the direction of protons or neutrons. By invisible means a most visible change can thus be produced in something so substantial as a solid sphere of Fe<sup>56</sup>. Moreover, just as one can produce on Earth temperatures of  $10^{7.0}$  K, for short times in substantial amounts of matter, so in a star collapsing from  $\rho \sim 10^8$  g/cm<sup>3</sup> to  $\rho \sim 10^{14}$  g/cm<sup>3</sup> via inverse beta-processes of the type

$$e^- + p \rightarrow n + \nu , \qquad (183)$$

one has for a time an effective change in the Fermi energy of the neutrino sea over a still larger amount of material. It is quite beyond present technology to achieve such effects on Earth. Nevertheless, the very conceivability of changing the Fermi energy of the neutrino sea reminds one anew of a point of principle: To specify the state of thermodynamical equilibrium of matter it is not enough to give the temperature and the pressure. One must also specify the Fermi energy E, of the neutrino sea. We are interested here in an A-baryon system which is not itself undergoing collapse or the electron-capture reaction (183), and which also is far away from any other system that might undergo collapse. Therefore, we shall assume zero density both for neutrinos and for antineutrinos in the space where the A-baryon system is located; or more briefly, a zero Fermi energy,  $E_s = 0$ . We specify in addition that the A-baryon system is in beta-equilibrium with a surrounding space of this kind. We summarize the two ideas of (1) zero temperature and energy for the neutrinos of space, and (2) beta-equilibrium with this space, in the one term, "a neutrino-neutral system."

In the present state of ignorance about the ultimate constitution of elementary particles, it is necessary to be open to the possibility of some error concealed in the concept of a neutrino-neutral system. Not the slightest indication has ever been found that a proton is unstable with respect to such a complete imaginary transformation as

$$p \rightarrow e^{+} + 6 \nu + 10 \hat{\nu}$$
. (184)

Nor is there any reason whatsoever to believe that such a process ever does or ever might take place. Nevertheless, any discussion which deals with an issue so fundamental as gravitational collapse has to be open to the possibility that the law of baryon conservation may fail under such conditions of extreme density. Moreover, if the law of baryon conservation fails at all, then there is some finite non-zero probability that a baryon will break down spontaneously in a special kind of radioactive transformation in which neutrino emission is only one of the many conceivable outcomes. In this event baryons admit two quite different types of neutrino transformations; beta-decay, where the rate is reasonable and the concept of equilibrium makes sense; and baryon disintegration, with a transmutation inhibited, not by any approach to thermodynamical equilibrium, but by the fantastic smallness of the spontaneous transformation rate itself. One is reminded of a stick of dynamite. It can be warmed up. It can then be allowed to cool down into apparent thermodynamic equilibrium with its surroundings. It gives up its heat. Yet while giving back this energy it keeps hidden the much greater stockpile of energy latent within it. Do elementary particles have a hidden internal store of neutrinos analogous to the energy concealed in the dynamite? Whatever the answer to this question, we shall overlook this possibility here and shall assume that the concept of "a neutrino-neutral A-baryon system" in its elementary formulation makes sense,

<sup>&</sup>lt;sup>3</sup> For further detail, see, e.g., Wheeler (1962), pp. 3-6.

To use the term "neutrino-neutral" does not imply that the system gives off no neutrinos or antineutrinos. On the contrary, as pressures are raised, and electrons are crushed into combination with protons according to the reaction (183), neutrinos are necessarily emitted. As a portion of matter deep in a star is imagined to be squeezed from one pressure,  $p_1$ , to a higher pressure,  $p_2$ , the rate at which that collection of baryons gives off neutrinos depends upon the rate at which the pressure is raised. If the pressure change is very fast, the beta-decay will lag far behind. In consequence the density will come to its equilibrium value only after some delay. Moreover, the energy excess in the inverse beta-decay will be substantial. Consequently, the neutrinos themselves will carry away a significant part of the work of compression. Similarly, in a rapid decompression, the antineutrinos given off will carry away appreciable energy. The existence of a rate-connected energy excess in beta-decay affects the density-pressure relation in a cycle of compression and decompression after the manner of other hysteresis phenomena (Fig. 17). However, in the present considerations of changes from one near-

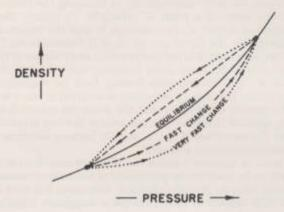


Fig. 17.—Equilibrium relation between pressure and density compared and contrasted with relation when changes occur so rapidly that neutrino and other processes of energy dissipation become important (hysterisis-curve).

equilibrium configuration to another, the time available for the transformation will be taken to be very long. Accordingly a very slight energy excess in the reaction (183) will be sufficient to guarantee that the ratio of neutrons to protons keeps in step with the changing pressure. In such slow changes it is appropriate to neglect any output of energy in the form of neutrinos or antineutrinos, important though one knows neutrino processes to be in the case of rapid changes. Naturally the net number of neutrinos emitted is independent of the rate, and is completely fixed by the initial and final conditions.

A last idea implicit in the notion of the "final state of an A-baryon system" is zero excitation: no heat, no lattice vibration, no electronic excitation, no nuclear excitation. In other words, we idealize the matter as being at the absolute zero of temperature, T=0, and endowed with zero entropy, s=0. All of the foregoing ideas together we summarize in the phrase "cold matter, catalyzed to the end point of thermonuclear evolution."

#### THE FINAL STATE WHEN A IS SMALL

It may be useful to specify still more concretely the final state of an A-baryon system in the case when A is small, even at the expense of looking at old chapters out of elementary nuclear physics! Not only nuclear physics enters, however. After nuclear forces

<sup>4</sup> Gamow and Schänberg (1941); for a recent review see, e.g., Chiu (1964).

have had their say, electronic binding, or chemical forces, come on the scene; and then finally gravitational forces have to be considered—if they have any effect. The magnitudes of the contributions from these three kinds of interactions differ by many powers of ten. Therefore it may seem at first sight quite out of place even to look at all three energies together at the same time. However, the energies that are so nearly negligible when A is small eventually come to dominate when A is  $\sim 10^{62}$ . Therefore, it helps in seeing the situation as a whole to look at some of the relevant numbers for all three contributions even in the small A domain.

For A values less than about 90, nuclear forces are most fully satisfied by putting all of the baryons into a single nucleus. There are only two exceptions to this rule, one at A = 5, the other at A = 8. For the normal case (with A < 90) then, the solution of the problem is simple: (1) One looks up in a table of nuclear masses that nuclear species with the given A which has the lowest mass (for A = 1, e.g., a hydrogen atom rather than a neutron). (2) The nuclear charge now being fixed, one looks up the lowest electron state of an atom containing this number of electrons (1s<sup>2</sup>S<sub>1/2</sub> for hydrogen). (3) One looks up the nuclear spin and magnetic moment. He couples the nucleus to the electronic system in such a way as to achieve the hyperfine state of lowest energy (F = 1 for H). This is the absolutely lowest state of the A-baryon system.

# An aside on A = 5, A = 8, and fluctuations in Geometry

The two special cases deserve some discussion because of the interesting points of principle which they raise. The lowest state of the A=5 system consists of a helium atom and a hydrogen atom. Nuclear forces being satiated, one might think of electronic binding as coming next on the list in determining the answer to the original question: What is the absolutely lowest energy state of the 5-baryon system? In other words, one might be tempted to ask for the binding of the two atoms in the lowest electronic state of the HeH molecule. But in this system the van der Waals force is too weak, and falls off with distance too rapidly, to give any bound state at all. It would be a mistake to conclude that there is therefore no bound state. The correct conclusion would seem to be that there is binding, a fantastically weak binding, but nevertheless a binding. This binding is produced, not by the van der Waals potential at all—for it falls off with distance too fast to have any significant volume average—but by the gravitational interaction of the two atoms. To determine the Bohr radius and the energy of the bound state, apply the elementary quantum mechanics of the hydrogen atom. Replace the electron mass by the reduced mass of the H and He:

$$m \to \mu = m_1 m_2 / (m_1 + m_2) \simeq \frac{4}{5} \mu_u$$
. (185)

Replace the Coulomb-coupling constant by the gravitational-coupling constant

$$e^2 \rightarrow G m_1 m_2 \simeq 4G \mu_s^2$$
. (186)

Thus find

(Bohr radius) = 
$$(\hbar^2/m e^2) \rightarrow \frac{5}{16} (\hbar^2/G\mu_*^2) = 1.1 \times 10^{24} \text{ cm} = 1.2 \times 10^6 \text{ l.} - \text{yr}$$
  
and

(Binding energy) = 
$$m e^4 / 2 \hbar^2 \rightarrow \frac{3}{5}^2 (G^2 \mu_e^5 / \hbar^2)$$
  
=  $3.2 \times 10^{-79} \text{ g cm}^2 / \text{sec}^2 = 2.0 \times 10^{-67} \text{ eV}$ .

<sup>&</sup>lt;sup>5</sup> For the estimation of van der Waals forces and of the critical strength needed to produce one bound state in other situations, see, e.g., Kihara (1953, 1955); see also discussions of the law of fall-off of the van der Waals force at large distances by Wheeler (1941), Casimir and Polder (1948), Casimir (1948), Sparnay (1958), Derjaguin (1960), and Lifshitz (1954 and 1955a, b).

The energy (187) is too small to be interesting in its own right, but it is very interesting for the point of principle which it raises. The gravitational field is an aspect of geometry, according to Einstein's theory. This geometry, like all fields, according to the quantum principle, must undergo characteristic fluctuations. A simple estimate shows that the magnitude of these fluctuations in the effective gravitational potential in a region of extension L (see, e.g., Wheeler [1962], pp. 77 ff.)—big or small—is of the same order as the static gravitational potential created at this same distance L by a particle of the Planck mass.

 $M^* = (\hbar c/G)^{1/2} = 2.2 \times 10^{-5} \text{ g}$ , (188)

In other words, the static gravitational potential created by the He atom at the location of the H atom, and supposedly responsible for the binding energy (187), is actually smaller in a ratio

$$\sim 4\mu_s/M^* = 6.4 \times 10^{-24} \text{ g}/2.2 \times 10^{-3} \text{ g} \sim 10^{-19}$$
 (189)

than these fluctuations. Therefore it is not at all clear whether the calculation (187) of the binding energy has any meaning. This point of principle is not important for any calculation of the total energy of the A=5 system. However, it does recall—along with the lower limit in Table 10 to the masses for which the classical idea of a collapse barrier makes sense—the many ways in which the quantum principle finds itself linked up with elementary-particle physics and general relativity when one discusses gravitational collapse.

The situation for A=8 (final state two helium atoms) is so similar to that for A=5

that it does not require a special discussion.

Table 11 summarizes the energetics in the low A region, up to  $A = 1008 \, (= 18 \, \text{Fe}^{56})$ . It lists the lowest state only for selected A values in the range 1 to 1008. Also given in each case for comparison with the lowest energy state is an alternative energy state, selected for its general interest or for its illustrative value. At A values up to 1008, and even at A values greater by many powers of 10, nuclear forces completely dominate the binding. Apart from the exceptional cases A = 5 and A = 8, where the state of lowest energy consists of two nuclei bound together fantastically weakly by gravitation, the lowest state for A less than about 90 consists of a single nucleus. For larger A values the preferred partition is two nuclei; for still larger A, three nuclei; and so on. The values of nuclear masses, molecular binding energies, and solid-state cohesive energies used in the construction of the table were taken from Gray (1957). According to the numbers given there, Niez is calculated to have a packing fraction -8.58 × 10-4 as compared to -8.45 × 10<sup>-4</sup> for Fe<sup>36</sup>; however, it is assumed here and in the discussion of the text, that Fe<sup>36</sup> is actually the nucleus with the tightest binding. The packing fraction tabulated here is defined by  $M_A$  (in mass units, on the O<sup>16</sup> scale) = (1+f) A, with f = $f_{\text{nuclear}} + f_{\text{chemical}} + f_{\text{cohesive}} + f_{\text{gravitational}}$ . Energy releases are calculated from  $\Delta E =$ 931 MeV A Δf.

The minimum in the packing fraction curve occurs near A=56. It will be assumed here and hereafter to occur exactly at A=56. In other words, require that modest amounts of matter (grams or kilograms; gravitational energies still negligible!) be created out of empty space in the cheapest possible way. Let only a specified supply of electromagnetic or other non-material energy be available. Then the greatest number of baryons compatible with this supply of energy will be created by employing a cycle of

transformations equivalent to the reaction

$$(Energy) \rightarrow (Fe^{bb}) + (anti-Fe^{bb}).$$
 (190)

If the matter is subsequently wanted in some other form, such as hydrogen or oxygen, additional energy must be supplied. Thus the basic unit of mass-energy per baryon is the quantity referred to earlier in the text,

$$\mu_s = \frac{1}{56}$$
 (Mass of Fe atom) = 1.659 × 10<sup>-24</sup> g.

 $\mbox{TABLE 11} \label{eq:table 11}$  Lowest Energy State of A-Baryon System for  $A \leq 1008$ 

A	State	Investment	februiesi	fechasive*	favor, totar f	farme, inten-	ΔE (alternative-+lowest)
1	Hi n1	+81.4 ×10 <sup>-4</sup> +89.9 ×10 <sup>-4</sup>					Lowest 0.78 MeV (β-decay)
2	H <sup>2</sup> (H <sup>1</sup> ) <sub>2</sub>	+73.9 ×10 <sup>-4</sup> +81.4 ×10 <sup>-4</sup>	-240×10 <sup>-11</sup>		- 8 ×10 <sup>-48</sup>	- 4×10 <sup>-44</sup>	Lowest 1.44 MeV ("β-fusion")
4	He <sup>4</sup> (H <sup>2</sup> ) <sub>2</sub>	$^{+\ 9.69\times 10^{-4}}_{+73.9\ \times 10^{-4}}$	-120×10 <sup>-ij</sup>		- 17 ×10 <sup>-46</sup>	- 10×10 <sup>-40</sup> - 4×10 <sup>-40</sup>	Lowest 23.8 MeV (fusion)
8	$(\mathrm{He}^{\epsilon})_{2}$ $\mathrm{Be}^{8}$	$^{+\ 9.69\times10^{-4}}_{+\ 9.84\times10^{-4}}$			- 1.4×10 <sup>-13</sup>	- 10×10 <sup>-46</sup> - 19×10 <sup>-46</sup>	Lowest 0.10 MeV (fission)
16	(u)14 O18	$^{0.00\times10^{-4}}_{+89.9~\times10^{-4}}$			- 1.2×10 <sup>-18</sup>	- 32×10 <sup>-46</sup>	Lowest 134 MeV ("condensation")
40	A <sup>40</sup> K <sup>40</sup>	$^{-\ 6.22\times 10^{-4}}_{-\ 5.87\times 10^{-4}}$				- 61×10 <sup>-46</sup> - 61×10 <sup>-46</sup>	Lowest 1.3 MeV (β-decay)
56	$Fe^{24}$ $[(H^{1})_{2}]_{24}$	$^{-\ 8.45\times 10^{-4}}_{+81.4\ \times 10^{-4}}$	-240×10 <sup>-11</sup>	-0.3 ×10 <sup>-11</sup>	- 62 ×10 <sup>-44</sup>	- 77×10-4	Lowest 468 MeV (fusion)
80	Se <sup>80</sup> (A <sup>40</sup> ) <sub>2</sub>	$^{-7.24\times10^{-4}}_{-6.22\times10^{-4}}$	- 27×10 <sup>-ii</sup>			- 98×10 <sup>-60</sup> - 61×10 <sup>-60</sup>	Lowest 7.7 MeV (fusion)
90	Fe <sup>16</sup> S <sup>14</sup> Zr <sup>50</sup>	$^{-7,61\times10^{-4}}_{0$	- 5×10 <sup>-11</sup> §		- 250 ×10 <sup>-63</sup>	- 68×10 <sup>-40</sup> -106×10 <sup>-40</sup>	Lowest 1.5 MeV (2-fission)
68	$\frac{(Fe^{56})_{1}}{Er^{166}}$	$^{-\ 8.45\times 10^{-4}}_{-\ 0.90\times 10^{-4}}$		-2 ×10 <sup>-11</sup> §	- 520 ×10 <sup>-45</sup>	- 77×10 <sup>-40</sup> -165×10 <sup>-40</sup>	Lowest 118 MeV (3-fission)
38	$\begin{array}{c} Fe^{16}(Ni^{00})_{\pm} \\ Sn^{118}Sn^{120} \\ U^{238} \end{array}$	- 8.40×10 <sup>-4</sup> - 5.03×10 <sup>-4</sup> + 5.40×10 <sup>-4</sup>		-3 ×10 <sup>-11</sup> § -1 ×10 <sup>-11</sup> §	700 ×10 <sup>-46</sup> - 590 ×10 <sup>-46</sup>	- 80×10 <sup>-66</sup> -128×10 <sup>-66</sup> -204×10 <sup>-66</sup>	Lowest 75 MeV (2×2-fission) 306 MeV (4-fission)
08	(Fe <sup>56</sup> ) <sub>18</sub> (O <sup>18</sup> ) <sub>58</sub>	- 8.45×10 <sup>-4</sup> + 2.71×10 <sup>-4</sup>	- 15×10-11	-4 ×10 <sup>-11</sup> § -0.02×10 <sup>-11</sup>	-2000 ×10 <sup>-46</sup> - 970 ×10 <sup>-46</sup>	- 77×10 <sup>-40</sup> - 35×10 <sup>-40</sup>	Lowest 10500 MeV (rearrangemen

<sup>\*</sup> $f_{\rm cohomics}$  calculated from the expression [(heat of fusion, in kcal/mole) + (heat of vaporization)]  $\times$  [4.65  $\times$  10<sup>-14</sup> to convert to atomic mass units per atom or molecule]  $\times$  [(1 - 1.3  $N^{-1/2}$ ) to correct approximately for incomplete bonding when number N of atoms or molecules is limited]/[mass of the atom or molecule in atomic mass units].

and for systems containing N atoms or molecules of mass number A from  $f_{\text{grav}, \text{inter}} = -0.966$   $(N-1.63)^{3/2} [\mu^{+} (A_1\mu_{+}^{+})^{2}]^{1/2}$ .

§ Denotes estimate made when necessary physical constant was not available in Gray (1957).

 $<sup>\</sup>dagger f_{erw}$ , interaction calculated as in eq. (187) for HeH and He;; for 16s system via model of a neutron gas (Appendix C); for diatomic molecules from  $f_{erw}$ ,  $_{total} = -(G/c^2)m_1m_1/(m_1 + m_2)r_{16}$ 

<sup>‡</sup> Gravitational energy interior to a nucleus calculated from standard approximation of nucleur physics for the electrostatic energy of the nucleus, 0.625 MeV  $Z(Z=1)/A^{1/2}$ , by changing  $e^z$  to  $G_{\rm Ha}^2$ , Z to A; thus,  $f_{\rm even} = 5.35 \times 10^{-40} \, (A=1)/A^{1/2}$ .

Other masses are greater than  $A\mu_s$  by a packing fraction factor f'. This factor is similar in its definition and use to the familiar packing factor f used with the  $O^{10}$  or  $C^{12}$  mass scale,

$$M = A \mu_s (1 + f') = A (M_{O^{12}}/16)(1 + f),$$
 (191)

with one exception: f is negative from a little beyond  $O^{16}$  to a little short of  $Hf^{180}$ , whereas f' is positive for all kinds of matter other than  $Fe^{56}$ , and zero only for  $Fe^{56}$ . However, the familiar quantity f is listed in Table 11 because of its well-established status in the literature.

#### THE REGIME OF SCALLOPS IN THE OVER-ALL PACKING PRACTION

When A exceeds about 90, the state of lowest energy is not one nucleus but two. For greater A, it is profitable to divide the system into many distinct nuclei, provided that

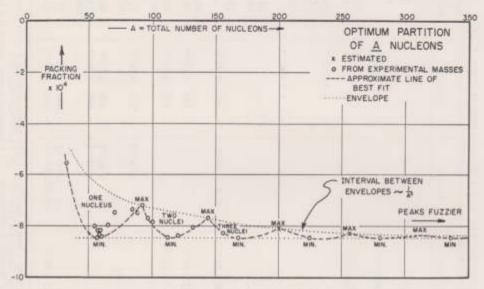


Fig. 18.—Lowest energy state of A baryon system for A < 350, showing the approach to the packing fraction of pure Fe<sup>16</sup>.

the mass numbers of the individual nuclei do not depart widely from 56. The greatest stability is achieved for A values which are integral multiples,  $A = n \cdot 56$ , of the optimum number. When A differs from such a value, then the individual nuclei cannot all have mass number 56. However, the departures from 56 in the pieces of the system ("fluctuations") will be smaller and smaller as the total baryon number A rises above 56 by more and more powers of 10. Thus one is led to the limit in which the system is almost entirely solid Fe<sup>36</sup>; only a few inclusions of other nuclei are needed to make up the difference between the actual A value and an integral multiple of 56.

The approach to the limit of pure iron (Fig. 18) can be analyzed semi-quantitatively. Represent the packing fraction in the neighborhood of the minimum by a smooth parabolic curve of the form

$$f = f_{\min} + (4f_1/A_{\min}^2)(A_p - A_{\min})^2$$
, (192)

where  $A_p$  is the mass number of a piece and the values of the constants adopted here are

$$f_{\min} = -8.45 \times 10^{-4}$$
,  $A_{\min} = 56$   $f_1 = 2.7 \times 10^{-4}$ . (193)

Let A represent the total mass number. Let n be the number of separate nuclei into which it is most profitable to divide the system for baryon numbers a little less than A. Let A be such that it has just become equally favorable energetically to divide the system into (n + 1) parts; thus,

$$\begin{pmatrix} \text{Packing fraction for} \\ \text{division into parts of} \\ \text{mass number } A_p = A/n \end{pmatrix} = \begin{pmatrix} \text{Packing fraction for division into} (n+1) \\ \text{parts of mass number } A_p = A/(n+1) \end{pmatrix}.$$

or

$$(A/n) - A_{\min} = A_{\min} - A/(n+1),$$

or

$$A = [2n(n+1)/(2n+1)] A_{min} \simeq (n+\frac{1}{2}) A_{min}$$
. (194)

This condition locates the scallops in Figure 18 as halfway between minima. The individual nuclei have mass numbers

$$A_p = A/n \simeq A_{\min}(1 + 1/2n),$$

when A is divided into n parts; and

$$A_p = A/(n+1) \simeq A_{\min}(1-1/2n),$$
 (198)

when A is divided into (n + 1) parts. Evidently the composition approaches closer and closer to Fe<sup>in</sup> as n (and A) becomes larger and larger! So does the packing fraction. The packing fraction at the scallop peak is

$$f_{\text{scallep peak}} \simeq f_{\min} + f_1/(n + \frac{1}{2})^2$$
, (196)

## NEW TYPE OF PERIODICITY FOR A OF ORDER OF 10<sup>4</sup> AND MORE

According to this broad analysis, the packing fraction for the optimum structure of the A-baryon system will show the scallop-shaped pattern of Figure 18, with the magnitude of the rises above  $f_{\min}$  going inversely as the square of A. In actuality this idealized pattern will not hold exactly at the peaks of the scallops, owing to the small fluctuation of the packing fractions of actual nuclei about the general trend indicated by the parabolic formula (192). For this reason there will be a scattering as one changes A gradually in the neighborhood of a scalloped peak, sometimes division into n parts being favored, sometimes into n+1. Consequently the scalloped-shaped pattern will be well defined only if the number of parts, n, is not too large. As the number of parts gets larger and larger the size of this region of fluctuations gets larger and larger compared to the whole width of one scallop,  $\Delta A = A_{\min}$ . At the same time, the size of the fluctuations of the packing fraction throughout a scallop zone ceases any longer to fall off with the law which one can deduce from the foregoing analysis,

$$f(A) \simeq f_{\min} + P_1(A) / A^2$$
 ("intermediate  $A^{**}$ ), (197)

where  $P_1(A)$  is a function which is periodic in A with period  $\Delta A = A_{\min} = 56$ . Instead, the particularities of the packing fractions of the very few nuclei which lie closest to the bottom of the packing fraction "curve" dominate the whole discussion from this point onward. The packing fraction for the system no longer follows equation (197) but instead varies according to the formula

$$f(A) \simeq f_{\min} + P_2(A) / A \text{ ("large } A").$$
 (198)

Here  $P_2(A)$  is a new periodic function of A, again with period  $\Delta A = A_{\min} = 56$ . In illustration of this argument, consider Table 12 for the optimum way to put A baryons into

individual nuclei when A is around 56000. The table is schematic only. No pretense is made to having sufficiently precise data on packing fractions to pick the critical few nuclei near the bottom of the packing fraction curve; hence the numbers "57," "50," "64," etc., are to be regarded as illustrative only. The conclusion to be drawn from the table is unaffected by this uncertainty. The optimum partition of  $A = (56n + \Delta A)$  baryons into separate nuclei follows this pattern to  $A \sim 10^4$  or more: (1)  $(n - n_1)$  nuclei of Fe<sup>18</sup>, (2) a pattern which is a complicated function of  $\Delta A$ —but a periodic function of  $\Delta A$ , with period  $\Delta A = A_{\min}$ .

As illustrated in Table 12, the sequence of nuclei repeats itself cycle after cycle. Only at the beginning and end of each cycle does one have absolutely pure Fe<sup>16</sup>. Elsewhere in the cycle there is a scattering of other nuclei. In consequence the packing fraction varies with A as indicated by equation (198). The "impurity" nuclei are always limited in number to a handful. Therefore, as A becomes larger—10<sup>6</sup>, 10<sup>8</sup>, 10<sup>10</sup>, etc.—it becomes

### TABLE 12

## OPTIMUM PARTITION OF A BARYONS INTO INDIVIDUAL NUCLEI FOR A ~ 56000 (SCHEMATIC)

Commencement of a period:	
A = 56000	1000×56
56001	999×56, 1×57
56002	
56002	999×56, 1×58
56003	999×56, 1×59
56004	999×56, 1×60
56005	999×56, 1×61
56006	999×56, 1×62
56007	998×56, 1×57, 1×62
56008	998×56, 2×60
Etc	270/30, 2/00/
A new period begins:	
A = 56056	1001×56
56057	$1000 \times 56, 1 \times 57$
56058	1000×56, 1×58
Etc	
	PRINCIPLE AND PRINCIPLE OF THE PRINCIPLE

more and more appropriate to regard the composition of matter of minimum energy content as essentially 100 per cent pure Fe<sup>56</sup>,

# The long-range forces begin to affect local conditions When $A \sim 10^{50}$ ("compression")

For the A-values considered so far, nuclear energies are of course enormously larger in order of magnitude than energies of electronic binding. The electronic or "chemical" energies in turn are of enormously larger order of magnitude than the energies of gravitational cohesion. However, the electronic energies have a saturation character whereas the gravitational energy mounts with the number of attracting nucleons. The A-value eventually comes at which these gravitational energies are of the same order of magnitude as chemical energies. How great is this chemical energy; and how high must A be to make the gravitational energy equally large? The packing fraction associated with the solid body forces in Fe<sup>30</sup> is

$$f_{\rm cohesion} = -\frac{(\,9\,4.6\;{\rm k\;cal/mole})\,(\,4.1\,8\,\times\,10^{10}\,{\rm erg/k\;cal})}{(\,5\,5.9\,5\;{\rm g/mole})\,(\,8.9\,9\,\times\,10^{20}\,{\rm erg/g})} = -\,7.9\,\times\,10^{-11}\,. \eqno(199)$$

The gravitational energy of a sphere of uniform density, mass M, and radius R is

$$E_{\text{grav}} = -\frac{3}{5}(GM^2/R),$$
 (200)

Divide by  $Mc^2$  to obtain the corresponding packing fraction. Also express the A-dependent terms directly in terms of A; thus,

$$M = A \mu_{\star}$$
, (201)

and

$$R = [M/(4\pi\rho/3)]^{1/3} = (3A\mu_s/4\pi\rho)^{1/3}. \qquad (202)$$

In this way find

$$\begin{split} f_{\rm grav} &= -\tfrac{3}{5} (GM/\,c^2R) = -\,0.966\,A^{2/3} (\,\rho^*\mu_s^{\,\,*\,*})^{\,1/3} \\ &= -\,0.966\,A^{\,2/3} (\,0.742 \times 10^{-28}\,{\rm cm/g}) [\,(7.8\,{\rm g/cm^3}) (\,1.659 \times 10^{-24}\,{\rm g}\,)^{\,2}\,]^{\,1/3 \,(203)} \\ &= -\,1.99 \times 10^{-44}A^{\,2/3} \,. \end{split}$$

The gravitational packing as calculated from equation (203) becomes of the same order as the cohesive packing for

$$A = 2.50 \times 10^{50}$$
,  
 $M = 4.14 \times 10^{26}$  g = (Mass of Earth) / 14.4, (204)  
 $R = 2.33 \times 10^{8}$  cm = (Radius of Earth) / 2.74.

For values of the baryon number of this order and more, gravitational pressures squeeze

matter to significantly more than normal density.

At  $A \sim 10^{10}$  is a decisive point. Here the force of gravitation begins to contribute as much to the energy as do the elastic forces; and when A reaches  $\sim 10^{10}$ , the gravitational forces contribute as much as do nuclear forces. Moreover, the gravitational forces introduce a long-range element into the energy analysis which is completely different in character from the short-range influence of the nuclear and elastic forces. The two kinds of forces have to be treated for practical purposes in entirely different ways. The short-range forces are described by an equation of state connecting the local density with the local pressure as induced by the long-range forces. The long-range forces are treated by the general relativity equation of hydrostatic equilibrium. The foundations of that Einsteinian equation and its consequences have already been examined. Now the point has come to analyze the foundations of the idea of an equation of state (this chapter) and the details of the derivation of the HW equation of state (chap. x).

# FRAME IN WHICH FLOW OF BARYONS AND FLOW OF ENERGY BOTH VANISH

We arrive at the idea of an equation of state by dividing up an A-baryon system (with A very large) into parts. Each part is small enough so that conditions do not change significantly through its interior (change in density/density  $\ll 1$ ). At the same time the parts are large enough to contain many baryons, and to allow one to define a number

density of baryons and an energy density, as follows.

If shocks were running back and forth through the interior, and radiation were streaming through the matter at an energy density comparable to that of the matter itself, the motions could be so chaotic that there would be no natural reference system with respect to which to describe the matter in a simple way. However, attention has been focused here on a particular question: What is the ground state of an A-baryon system when A is large? The system is electrically neutral. It is neutrino-neutral: all beta-decay has come

to its end point. And the system is at absolute zero temperature, endowed with zero entropy. To demand that the system be in the final state as so defined (not possible for  $A > A_{\rm crit} \sim 10^{87}$ ) is not to require that velocities in the system shall be zero. At high pressure the Fermi energy may be in the relativistic domain, and the individual particles may be moving at nearly the speed of light. However, the hypothesis that the A-baryon system is in its lowest state does imply Theorem 26.

Theorem 26. Nowhere in the system do there exist any relative motions out of which one can extract energy. Otherwise the system could be brought into a state of still lower energy!

From Theorem 26 follows Theorem 27.

THEOREM 27. For each portion of the medium and for each moment of time there exists a natural local Lorentz frame with respect to which to observe the matter in that region at that time: natural in the sense that with respect to this frame the flow of baryons and the flow of energy both vanish at that place and at that time.

We think of an idealized hollow tube which has been thrust through the material at the given point. It serves as the shaft in which a small-scale lattice work of clocks and measuring rods can rise freely. That reference system comes to momentary rest with respect to the portion of matter under study and then falls back toward the center of attraction. In this local Lorentz reference frame at the summit of its flight there is a well-defined meaning to speaking of the proper volume of the specified nearby region, as well as of the number of baryons in it. The quotient of these two quantities defines the number density

(Number of baryons per unit of volume) = 
$$n$$
. (205)

This quantity varies smoothly with position throughout any system which will be of interest here. Moreover, granted the law of conservation of baryons, one concludes that the quantity

$$A = n \ d \text{ (proper volume)}$$
 (206)

has a well-defined value for the system, independent of time.

## THE UNIVERSAL CHARACTER OF THE EQUATION OF STATE

The division of the system into parts has as its consequence that one can ascribe to each part not only a number of baryons  $n\,d$  (proper volume) but also an amount of massenergy

$$d \text{ (mass-energy)} = \rho d \text{ (proper volume)}.$$
 (207)

Theorem 28. The density p of mass-energy of cold, catalyzed matter defined by equation (207) depends only on the number density of baryons, n, according to a universal law,

$$\rho = \rho(n). \tag{208}$$

If this were not so, otherwise identical subsystems, dA, of the same total system (or of different total systems), when confined to the same element of proper volume dV, would have different mass-energies. But there is no known conservation law which would forbid the transformation from the state of higher energy to the state of lower energy. The law of conservation of baryon number is automatically satisfied by the transformation:  $dA \rightarrow dA$ . Initial and final states are electrically neutral and neutrinoneutral. Therefore, with enough time, the transformation must take place. In this way one arrives at the unique configuration of lowest energy, zero temperature, and zero entropy—and the unique equation of state (208).

#### PRESSURE BUT NO SHEARING STRESS

The same line of reasoning excludes the existence of shear in the system. Imagine the opposite. Conceive of the A-baryon system as rigid, as capable of supporting shear, and as having shears build into it dependent upon the history of its construction. Then one has to admit the possibility of a different "lowest energy state" for an A-baryon system, according as these shear stresses have one or another value. But a system with internal shears is not really in its lowest state. Whether a system behaves as a solid or a liquid, whether rocks flow, and whether iron yields are governed by the time scale available for relaxation. On the indefinitely long time scale assumed in the present discussion of questions of principle, every substance behaves as a fluid. Therefore:

Theorem 29. In cold matter catalyzed to the state of lowest energy, the off-diagonal components of the stress tensor vanish and the diagonal components have a common value, the pressure, p.

Moreover p, like  $\rho$ , depends only on the number density of baryons, according to a universal law,

p = p(n), (209)

## THREE WAYS TO GIVE OPERATIONAL MEANING TO THE ENERGY DENSITY

What procedure makes most sense for evaluating the density of mass-energy depends upon the circumstances. In case (1) the forces are weak and the mean free paths of the particles are long. The energy is almost exclusively kinetic. It is obtained by adding up the mass-energies of the individual particles as determined, e.g., by their velocities  $\beta_k c$ and rest masses  $M_k$ :

$$\rho dV = d \text{ (mass-energy)} = \sum_{k \text{ in } dV} m_k (1 - \beta_k^2)^{-1/2}$$
. (210)

In this same simple case the pressure is given by the expression

$$\rho dV = \sum_{k \text{ in } dV} \left( m_k \beta_k^2 c^2 / 3 \right) \left( 1 - \beta_k^2 \right)^{-1/2}. \tag{211}$$

In the opposite case (2), the forces are strong and the mean free paths short. Thus there is a considerable time in which the same baryons move tortuously about in the same small element of volume. It is appropriate here (as also in case [1]) to think of that element of volume inclosed in walls. The inclosure is lifted out of the system and allowed to expand slowly and adiabatically. The contents are catalyzed at every step of the way to the nuclear state of lowest energy. Ultimately an unlimited volume is achieved. The matter is dispersed in this volume as a dust made of particles of iron. During the expansion both the pressure and specific volume per baryon,

$$v = dV/dA = 1/n$$
, (212)

remain well defined and in principle measurable. Consequently the mass-energy per baryon in the compressed state can be evaluated from the work done in the expansion

$$\rho/n = (\text{mass-energy per baryon}) = \mu_s + \int_{n=n}^{n=0} p(n) d(1/n). \tag{213}$$

How does it come about that baryon number makes so important an appearance in the analysis of energy? Because, in an expansion conducted without benefit of walls, the baryons provide markers by which to identify the motion of the medium. They tell what new volume (after expansion) is to be identified with what old volume (before expan-

sion). Only by following the change in volume does one have a well-defined means to

evaluate the work done and the change in the density of mass-energy.

Different kinds of markers, protons and electrons, for example, might be imagined to give different pictures for the movement of the boundaries of this volume. In principle there is such a difference. For example, if one imagines himself as carrying out adiabatically the transformation from a dwarf star to a neutron star, then he is in effect slowly switching on an electric field of the order of 6000 V/cm (eq. [182]). Associated with such a field is an excess of ~3 × 10° electrons/cm² at the surface. There are of the order of ~8 × 10° free electrons/cm² in the iron near the surface. Accordingly, the adiabatic transformation to high densities has moved the protons inward more than the electrons. However, the calculated difference in displacement is only of the order of 3 × 10° cm²/8 × 10° cm² ~4 × 10<sup>-14</sup> cm, as compared to the many km of inward motion of both kinds of particles in shrinking from a dwarf star to a neutron star—a negligible difference!

As there is a difference in the motions marked out by protons and electrons, so there is a difference in the volume change as indicated by protons and by neutrons in a shrinking or growing star of near-nuclear density. Such a system is partly stellar and partly nuclear in character. The inner part is effectively one giant nucleus. The outer shell is iron, made up of well-separated and quite distinct nuclei. Elsewhere there is a gradation between the two extremes. In the inner part there is the nuclear force equivalent of an electric field. It has to do with the relative displacement of the neutrons and protons. Again the

calculated amount of this relative displacement is negligible.

It follows from this analysis that one kind of particle is as good as another in marking out volume change. However, in the course of some of the changes of interest, electrons combine with protons to make neutrons. Therefore, neither electrons nor protons nor neutrons individually—which can be created and destroyed—are as convenient as baryons for following the motion of the medium. Hence the emphasis on the average volume per baryon or the number density of baryons, n, in the formulation of the equa-

tion of state,  $\rho = \rho(n)$ .

To determine  $\rho$  one can sum up the rest plus kinetic energies of the particles when they are nearly free; or in the general case one can evaluate the energy change in expansion to infinite dilution; or one can follow a third procedure, based on general relativity: (1) investigate the local geometry; (2) measure its curvature; (3) employ the fundamental relation of equation (2) between curvature and density; thus (4) find the density of mass energy,  $\rho$ , for the given number density of baryons, as desired.

# LIMITATION ON CURVATURE OR DENSITY AT WHICH THE CONCEPT OF EQUATION OF STATE MAKES SENSE

The concept of equation of state, now defined and given operational significance, loses its meaning when space is too strongly curved; that is, when the local components of the Riemann curvature tensor, or the local components of the tide-producing force, or the gradients of the gravitational field are too large. A stronger restriction might at first sight seem indicated: that the gravitational field itself must not be too great. Two reasons suggest themselves for this preliminary reaction; first, the possible influence of a strong gravitational field upon the properties of space; second, the possible influence of a strong gravitational field upon the properties of matter.

Any concern that space itself might be affected by a strong gravitational field is countered by a general consideration. Einstein's principle of equivalence states that the gravitational field apparent at any point can be annulled by looking at what goes on there from an appropriately moving frame of reference: a local inertial or Lorentz frame (small-scale lattice work of meter sticks and clocks falling freely in an idealized hollow pipe thrust through the system). The local physics in such a reference frame differs not at all from physics in flat space. Therefore the equation of state derived from consid-

erations of flat-space physics applies immediately to a specimen of matter located on the local Lorentz frame. Now for the second point: Is there any difference between this specimen and the surrounding matter? The comparison is carried out at the instant when the specimen is momentarily at rest with respect to the system. Moreover, the specimen has the same baryon density as the immediately neighboring matter. Any difference arises from this circumstance: that the matter in the system is being accelerated outward with respect to the local Lorentz frame by the differential of pressure between the center of the system and the surface. The specimen in the tube experiences no such acceleration. It is under the same pressure as the surrounding matter, but under zero pressure gradient. How important is the acceleration caused by the pressure gradient? Is it great enough to put in question the policy of using the same equation of state for the "accelerated" matter (stationary in the star) as for the "unaccelerated" specimen (located on the Lorentz frame)? No, this acceleration is not normally enough to make a difference. Even in the extreme case of a neutron star this acceleration is only ~10<sup>14</sup> cm/sec<sup>2</sup> (eq. [181]). In contrast, the K-electron in a plutonium atom experiences an acceleration,

$$g \sim e^2/m r^2 \sim (4.8 \times 10^{-10}/6 \times 10^{-10})^2/10^{-27} \sim 10^{27} \text{ cm/sec}^2$$
, (214)

without ceasing to follow elementary physical law. Moreover, within a nucleus the accelerations run to still higher orders of magnitude:

$$g \sim v^2/r \sim (10^{10} \text{ cm/sec})^2/10^{-13} \text{ cm} \sim 10^{33} \text{ cm/sec}^2$$
, (215)

with no known problem thereby being created.

In accordance with this order-of-magnitude analysis we neglect the effect of the acceleration and analyze the equation of state as if we were always dealing with physics in a local Lorentz frame. In this sense there is a clean separation between two kinds of issues. Those of one kind have to do with the constitution of matter and are local. Those of the other kind have to do with the production of gravitational fields by this matter. They are non-local ("gravitational action at a distance"; determined by solving Einstein's field equations). The issues of the first kind can be treated entirely within the framework of special relativity. General relativity comes in only in the issues of the second kind.

The helpful separation between local and non-local issues breaks down when there is too much difference from point to point in the local Lorentz frames required to annul the gravitational field. This breakdown occurs when the inhomogeneity in the gravitational field is great, or when-in Newtonian language-the local "tide-producing force" is large. In relativity language the corresponding quantity is the Riemann curvature tensor. Both the Newtonian and the Einsteinian quantities have the order of magnitude  $M^*/r^2$  at the Schwarzschild coordinate r outside of a mass  $M^*$  (cm) =  $GM(g)/c^2$ . Inside the mass, at points where the density  $\rho$  is of the order of the average density or higher, the typical component of the Riemann curvature tensor is of the same order as the typical component of the Ricci curvature tensor which in turn—according to Einstein's field equations—is of the same order as the density itself, as translated to geometrical units:  $\rho^*(cm^{-2}) = (G/c^2)\rho$  (g/cm<sup>2</sup>). This curvature or tide-producing force would seem to have no effect insofar as the particles responsible for energy and pressure have welldefined positions. However, with a particle of mass m(g) or  $m^*(cm)$  is associated a characteristic localizability distance h/mc (reduced Compton wavelength). Referred to this distance the inhomogeneity in the effective gravitational potential—and therefore the consequent fractional disturbance in the mass-energy of the particle-is of the order

$$\delta m/m \sim \begin{pmatrix} M^*/r^3 & \text{outside} \\ \rho^* & \text{inside} \end{pmatrix} (\hbar/mc)^2$$
. (216)

This measure of disturbance will be small compared to unity for the most critical particles, electrons, when the density is restricted by a limit of the order

$$\rho^* < (m c/\hbar)^2 \sim 10^{21} \text{ cm}^{-2}$$
 (217)

Ol

$$\rho = (c^2/G) \rho^* < 10^{40} \text{ g/cm}^2$$
, (217')

a condition that ordinarily will be satisfied!

Only when trying to trigger the gravitational collapse of some tons of matter or less (Table 10 and the last part of chap, viii) does one come to a calculated density at the top of the collapse barrier of the order of the critical limit (217) or more. Then the idea of an equation of state begins to lose sense. The physics of passage from the normal state to the collapsed state under these conditions would seem to require a deeper type of analysis in which quantum considerations show up much more pervasively than they did in chapter viii.

There is another argument that new considerations are needed to deal with a situation as extreme as that contemplated in equation (217). The calculated mass-energy at the point of passage over the barrier,

$$M \sim \rho (\hbar/m c)^2 \sim [(c^2/G)(m c/\hbar)^2](\hbar/m c)^3$$
  
 $\sim (\hbar c/G)/m \sim (10^{-5} g)^2/(10^{-27} g) \sim 10^{17} g$ , (218)

is no greater in order of magnitude than the mass of a large Arctic ice island. However, this mass is so narrowly localized that it creates an enormous gravitation field in its immediate vicinity:

$$g \sim (GM)/(R)^2 \sim (\hbar c/m)/(\hbar/mc)^2 \sim mc^3/\hbar \sim 10^{33} \text{ cm/sec}^2$$
. (219)

Thus gravitational accelerations have at last mounted to the magnitude of intranuclear accelerations (eq. [215]). Under these conditions it is out of the question to say that the equation of state can be calculated as if the gravitational field were not there! The physics of "local" forces and of "long-range" forces are no longer separable. It is remarkable that gravitational accelerations become comparable to accelerations in a nucleus for the same conditions at which the radius of curvature of space becomes comparable to the Compton wavelength of an electron. This circumstance is a double indication that physics of a new kind comes in when the density limit of ~10<sup>49</sup> g/cm<sup>2</sup> is surpassed.

## AN ASIDE: UNIVERSE SHARPLY CURVED AS VIEWED FROM FAST PARTICLE

Space curved up nearly into closure, and the radius of curvature of this space of the same order as the Compton wavelength: this is the extreme which, contemplated long enough, one may hope, can lead into new ways of thinking about the relation between geometry and particles. To achieve such conditions two alternative idealized experiments suggest themselves, neither of them technologically feasible. (1) Curve space the requisite amount, over the requisite region, by putting  $\sim 10^{17}$  g of mass-energy into a region with an extension of the order of  $4 \times 10^{-11}$  cm. The difficulties of this task are only too clear from Figure 16 and the associated discussion in the text. Or (2) take space as it is and make its radius of curvature appear to the electron as short as the Compton wavelength by imparting to it a sufficiently great energy. For an order-of-magnitude estimate of this energy, take space to have a radius of curvature of the order of  $(10^{10} \text{ light-years}) \times (10^{10} \text{ cm/light-year}) = 10^{20} \text{ cm}$ . To bring this down to the Compton wavelength, the Lorentz contraction factor must be of the order of  $(4 \times 10^{-11} \text{ cm})/(10^{28} \text{ cm}) \sim 1/(2 \times 10^{28})$ . Therefore the electron should have a mass-energy of the order of

$$\sim (2 \times 10^{38}) \times (10^{-27} \text{ g}) = 2 \times 10^{11} \text{ g}$$
 (220)

An energy of this magnitude will be set free by the thermonuclear combustion of  $4\times10^{\circ}$  tons of deuterium, so that the supplying of the energy presents no problem of principle. To put that energy into the electron is another matter. If the entire universe is reduced in thickness to a Compton wavelength, then any Earth-bound accelerator is seen by the electron as an unbelievably small fraction of the Compton wavelength! Thus there is a fundamental question of principle as to whether one can speak sensibly of the process of acceleration under such conditions. Against speaking of velocities and energies close to the limit (220) no such objection of principle is evident. This accepted, then the limiting energy given by equation (220) would seem to mark the point beyond which the principle of Lorentz covariance, as normally formulated for electrons, must break down. All reference frames are no longer equivalent when an electron is going so fast that it can feel the curvature of space. It is not possible at this point to say that the physics in the tangent flat space is the same as the physics in the actual curved space.

# THE FUNCTION $\rho(n)$ AS A THERMODYNAMIC POTENTIAL

So much for the conditions of extreme curvature where the concept of an equation of state breaks down. Now for the case of greater immediate interest, where all the conditions are satisfied for speaking of the number density of baryons, n, and the density of mass-energy,  $\rho = \rho(n)$ , of cold matter catalyzed to the end point of thermonuclear evolution. (Throughout this section we shall use geometrized units but omit the asterisks for notational convenience.)

The function  $\rho(n)$  serves in effect as a potential from which to derive the other quantities of interest: the pressure and the chemical potential. The pressure is obtained by comparing the change in energy in a small expansion with the change in volume:

$$\begin{split} \rho\left(n\right) &= (\text{Pressure}) = -\frac{d\left(\text{energy per particle}\right)}{d\left(\text{volume per particle}\right)} \\ &= -d\left(\rho/n\right)/d\left(1/n\right) = nd\rho/dn - \rho \;. \end{split}$$

The chemical potential  $\mu(n)$  is defined for the present purpose as the mass-energy which is added to the system by bringing in one more particle from infinity. The energy consists of two parts. Of these the first is the work required to ready a space for the particle in the already existing medium by pushing aside matter at the pressure p:

$$(Work) = (Pressure)(volume) = p/n$$
. (222)

The second part is the mass-energy,  $\rho/n$ , of the particle which is inserted into this slot. Thus one has the result that the chemical potential is

$$\mu = \left( p + \rho \right) / n . \tag{223}$$

As an alternative way to evaluate the chemical potential, note that the addition of dn particles to a unit volume increases the mass-energy in that volume by the amount  $d\rho$ , whence

 $\mu = d \rho / d n . \tag{224}$ 

The agreement of equations (223) and (224) is guaranteed by equation (221) for the pressure. The product of the chemical potential by the relativistic generalization,  $e^{\nu/2}$ , of the gravitational potential gives the injection energy which, according to Theorem 4, is constant throughout the interior of an equilibrium configuration. In the special case of an ideal Fermi gas the chemical potential is identical with the Fermi energy.

#### ALTERNATIVE CHOICES FOR THE THERMODYNAMIC POTENTIAL

The quantities p and  $\mu$  are in some sense complementary to  $\rho$  and n. They can equally well serve as the primary variables in describing the conditions in the medium. More-

over, the "potential"  $p = p(\mu)$  is as comprehensive in its summarizing powers as the "potential"  $\rho = \rho(n)$ . To lead into the use of  $p = p(\mu)$  as a "potential," consider the change in pressure in a small alteration of conditions:

$$d p = d (n d \rho / d n - \rho) = n (d^2 \rho / d n^2) d n = n (d \mu / d n) d n = n d \mu$$
, (225)

This relation gives one the means to derive the density of baryons and of mass-energy from the function  $p(\mu)$ ; thus

$$n = d \phi / d \mu \tag{226}$$

(analogous to eq. [224]) and

$$\rho = n\mu - p = \mu dp/d\mu - p = -d(p/\mu)/d(1/\mu)$$
 (227)

(analogous to eq. [221]),

In addition to the options of taking  $\rho(n)$  as the starting point, or using  $p(\mu)$  as the basic potential, one could deduce everything from a knowledge of the pressure as a function of the density of mass-energy,  $p = \rho(\rho)$ . Thus the chemical potential is

$$\mu = \mu_e \exp \int n d\mu / n \mu = \mu_e \exp \int_0^p dp / (p + \rho),$$
 (228)

where  $\mu_s$  is the chemical potential of a baryon at infinite dilution,  $\mu_s = \frac{1}{5 \cdot 6} m(\text{Fe}^{56})$  (see Table 2). Similarly the number density of baryons is

$$n = n_1 \exp \int dn / n = n_1 \exp \int_{\rho_1}^{\rho} d\rho / (p + \rho),$$
 (229)

where "1" denotes some standard state of very great dilution. Any reference to this state can be eliminated at the expense of a slight complication in the formula. Write

$$\rho = \rho_1 \exp \int_{\rho_1}^{\rho} d\rho / \rho \qquad (230)$$

and divide this equation into the preceding equation. Go to the limit where the state "1" has infinite dilution. Here one has  $\lim_{n \to \infty} (\rho_1/n_1) = \mu_s$ . Thus find the desired formula for n:

$$n = (\rho/\mu_*) \exp - \int_0^\rho \frac{p d\rho}{\rho(p+\rho)}$$
 (231)

Note that the product  $n\mu$ , with  $\mu$  from equation (228) and n from equation (231), gives  $(p + \rho)$ , as expected (eq. [223]).

BARYON NUMBER AS DEDUCED FROM PRESSURE AND DENSITY MEASUREMENTS.

The content of formula (231) is summarized in Theorem 30.

THEOREM 30. Up to the fixed normalizing factor μ<sub>s</sub>, one can determine the number of baryons in the cold, catalyzed matter contained in a specified volume V by way of measurements limited exclusively to the pressure-density correlation during adiabatic decompression.

Equation (231) is remarkable not only because it makes the distinction between amount of matter (as measured by the number of baryons) and amount of mass (as measured by inertia or gravitational attraction). It is also remarkable because it expresses the quantity n, having to do with the microscopic particulate structure of matter, in terms of measurements on two quantities, p and  $\rho$ , which are so far as anything could

well be from probing into that particulate structure.

How is this conclusion to be reconciled with Bondi's (1964) recent comment that "any attempt to deduce particle number from a relativistic integral over a static configuration is doomed to failure"? In reaching that conclusion one considered two configurations. The two systems were identical not only in total mass, but also in distribution of pressure and density. Yet they differed because they arose by contraction from configurations of complete dissociation which contained different numbers of baryons. The final apparent identity of the two systems came about because energy was allowed to escape during the contraction in the one case, but not in the other.

In agreement with this reasoning one knows very well that the relation between density and pressure differs between hot matter and cold matter. It also differs between matter that is, and matter that is not, catalyzed to the end point of thermonuclear evolution. However, in the derivation of Theorem 30 attention focused exclusively on matter which is so catalyzed, and which is cold, and which is neutrino-neutral, and which is given time to adjust to changes in pressure (see Fig. 17). Under these conditions the energy required to compress a mole of baryons from infinite dispersion to a given particle density is uniquely determined by the physics of matter as a standard and universal function of that density. Then equation (231) supplies a rational means to evaluate this particle density. Furthermore, the integral of this particle density with respect to proper volume then gives the total baryon number A, as it entered, for example, into the variational analysis of chapter iii. Thus the conceptual advantage is apparent of dealing with matter which is both cold and catalyzed to the end point of thermonuclear reactions.

# $\gamma$ -Law in the relativistic and non-relativistic domains: Comparison and Contrast

About the detailed course of the universal equation of state a great deal is known at low densities and very little at supranuclear densities. However, at any density, low or high, it is appropriate to describe the dependence of  $\rho$  upon n over a limited region by a " $\gamma$ -law." Here the value of  $\gamma$  is defined by the logarithmic derivative

$$\gamma \equiv d \ln \rho / d \ln n . \tag{232}$$

When one expresses the same relation between  $\rho$  and n in integral form, he requires in addition to  $\gamma$  a constant of proportionality. It is conveniently taken to have the dimension of a length; thus, over a limited range of n,

$$(G/c^2) \rho(g/cm^3) \equiv \rho^*(cm^{-2}) = L^{-2}(L^3n)^{\gamma}$$
. (233)

In the same range the pressure is given, according to equation (221), by the formula,

$$p^* = (\gamma - 1) \, \rho^* \, . \tag{234}$$

There is an important distinction between  $\gamma$ -laws as employed in the relativistic and non-relativistic domains. In non-relativistic theory not the total mass-energy  $\rho$ , but only the part

$$\epsilon = \rho - n \mu_s$$
 (235)

over and above the rest mass, comes into discussion as the dependent variable. As for the independent variable, one is not accustomed to distinguish between number density n and mass density  $\rho$  except insofar as the standard mass  $\mu_{\sigma}$  is used to transform from the one to the other. Thus one writes

$$\epsilon = O \rho^{\gamma *}$$
, (236)

Here the asterisk on the exponent distinguishes the non-relativistic  $\gamma$  from the relativistic one. Expressed in the relativistic language of the equation  $\rho = \rho(n)$ , equation (236) reads

$$\rho = \mu_s n + \text{constant}^* n^{\gamma*}$$
 (237)

to be compared and contrasted with

$$\rho = \text{constant } n^{\gamma}$$
. (238)

The pressure calculated from equation (237) is

$$b = nd \rho/dn - \rho = \text{constant}^* (\gamma^* - 1) n^{\gamma^*} = (\gamma^* - 1) \epsilon$$
, (239)

to be distinguished from equation (234) despite their superficially identical form,

A few additional points of comparison and contrast between the relativistic and the non-relativistic formulations of the equation of state are to be noted. Go back to the relativistic formula (221), or (dropping asterisks for notational convenience)

$$d\rho/(\rho + p) = dn/n, \qquad (240)$$

and approximate:

$$d\rho/\rho - \rho d\rho/\rho^2 + \dots = dn/n. \qquad (241)$$

Integrate to find

$$\ln(\rho/n) - \ln(\rho/n)_{\text{standard}} = -\int \rho d(1/\rho) + \dots \qquad (242)$$

Note that  $(\rho/n)_{\text{standard}} = \mu_s$ . Thus have

$$\rho = n \mu_s \exp[-\int \rho d(1/\rho) + ...];$$
 (243)

or, to the same order of approximation,

$$\epsilon = -\rho \int \rho d(1/\rho). \tag{244}$$

Assume that one knows the Newtonian energy density  $\epsilon$  as a function of  $\rho$ , so that it can serve as a "potential" for the non-relativistic equation of state. Then one obtains at once from (244) first the pressure

$$\dot{p} = -\frac{d\left(\epsilon/\rho\right)}{d\left(1/\rho\right)} = \rho d\epsilon/d\rho - \epsilon \tag{245}$$

(to be contrasted with the accurate eq. [221]) and—to the same level of approximation—

$$\mu - \mu_s = (p + n\mu_s + \epsilon)/n - \mu_s = \mu_s(p + \epsilon)/\rho = \mu_s d\epsilon/d\rho$$
 (246)

(to be compared with the relativistic relation  $\mu = d\rho/dn$ ). When one wishes to know the chemical potential in the non-relativistic domain starting, not from a knowledge of the energy density  $\epsilon$  as a function of  $\rho$ , but from a knowledge of the *pressure* as a function of  $\rho$ , he can use the Newtonian formula

$$\mu - \mu_s = \mu_s \int d p / \rho , \qquad (247)$$

derived from equations (244) and (246), and to be compared with the relativistic equation (228).

## γ ONE OR GREATER FOR STABILITY AGAINST THE COLLAPSE OF MATTER

What limitations on the equation of state can one deduce from general principles, without entering into the microscopic physics behind the pressure-density relation? Two.

The first has to do effectively with a lower limit on  $\gamma$ ; the second, with an upper limit.

The one concerns stability against collapse; the other, causality.

The equation of state of van der Waals forced one to consider a pressure-volume relation of the form shown in Figure 19. The section of the curve where pressure decreases with decreasing volume signifies instability. A weighted piston exactly balanced on a cylinder-full of such a substance may be adjusted to equilibrium, but the equilibrium is unstable. Nor is it only the collection of matter as a whole which is unstable against the slightest up or down excursion of the piston from the equilibrium point. Each elementary portion of the medium is similarly unstable with respect to expansion or contraction away from its equilibrium volume. This instability is notification that the medium will

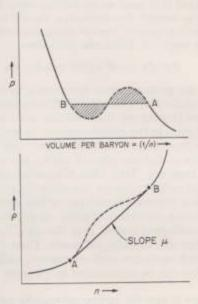


Fig. 19.—Passage from "analytic form" of equation of state to the true physical form of the equation of state in a zone of phase transition. Above: Standard argument that net work  $\int \rho dV$  between A and B should be the same for the analytic and for the true equations of state. Below: Transcription of the same reasoning to the  $\rho = \rho(n)$  formulation of the equation of state. The slope  $d\rho/dn$  (which may be written alternatively as the chemical potential  $\rho$  or as the ratio  $([\rho + \rho]/n)$  must have the same values at A and B as along the straight line connecting A and B ("condition of tangency").

develop two phases. Of these, one in the example of van der Waals is gaseous; the other, liquid. In consequence the actual equation of state follows, not the dashed line AB, but the straight line. The height of this line is such that the work done in the compression from A to B at constant pressure is identical with the work which would have been done

had one followed the unstable ideal equation of state.

This familiar consideration about the pressure during a change of state is readily translated into a statement as to how  $\rho$  varies as a function of n (lower portion of Fig. 19). Rather than go through the mathematics, one can follow the physics, using words that have in mind the example of van der Waals. Throughout the region where the two phases are in equilibrium with each other, the energy to inject a mole of material must be the same whether that mole is in the form of gas or in the form of liquid. Therefore the slope  $\mu = d\rho/dn$  is constant throughout the region of the change of phase, and agrees with the slope at each end point:

$$(d\rho/dn)_A = (d\rho/dn)_B = (\rho_B - \rho_A)/(n_B - n_A),$$
 (248)

Here equation (248) amounts to two implicit equations to determine the two points of transition,  $n_A$  and  $n_B$ . How to solve graphically by applying a straight edge to the curve of the equation of state is evident at once from the lower portion of Figure 19. It is also clear why matter at a number density between  $n_A$  and  $n_B$  coagulates into matter at the number density  $n_A$  and matter at the number density  $n_B$ . In this way it lowers the mass-energy per unit volume from the higher value of the dashed curve to the value indicated by the straight line. In other words, the dashed line does not represent the absolutely lowest energy state, whereas the full line does. Therefore, the full line describes the true equation of state and the dashed line does not.

The characteristic feature that distinguishes the allowed equation of state from the unphysical one can be stated in at least six equivalent ways. First, the slope  $d\rho/dn$  never decreases with increasing n. Second, the derivative,  $d^2\rho/dn^2$  is never negative. Third, the chemical potential ("injection energy") never decreases with increasing n. Fourth, the

derivative  $d\mu/dn$  is never negative. Fifth, the derivative

$$d p / dn = n d^2 \rho / dn^2 = n d \mu / dn$$
 (249)

is never negative. Sixth, the pressure never decreases with increasing density.

One can imagine a curve for  $\rho(n)$  which starts off from the point A as does the dashed curve in the diagram, first turning up, then starting to turn down, but then departing from the curve in the diagram in the following sense: It never turns up again. Its slope continues to decrease, decreasing more and more slowly, but always remaining positive. In this case it is impossible to find any point B nor to draw any straight line AB which satisfies the condition of tangency (248). Then the material is unstable against coagulation into two phases, one of ordinary matter, the other of a completely collapsed medium. Moreover, this collapse is a microscopic collapse; it has nothing whatsoever directly to do with any long-range forces, curvature of space, or gravitational collapse. If gravitational collapse leads to a collapsed system, then the quite distinct kind of collapse considered here may be said to lead to collapsed matter. There is not the slightest evidence to indicate that matter undergoes any such microscopic collapse.

This analysis of stability can be summarized in Theorem 31.

Theorem 31. Either matter is unstable against microscopic collapse, or there exist positive constants  $\rho_A$ ,  $n_A$  and  $\mu_A > \mu_S$ , such that the density of mass-energy for  $n > n_A$  satisfies the inequality

 $\rho \ge \rho_A + (n - n_A) \mu_A . \tag{250}$ 

Here  $n_A$  represents the highest particle density at which one has reliable information about the function  $\rho = \rho(n)$ ; and  $\rho_A$  and  $\mu_A = (d\rho/dn)_A > \mu_s$  represent the value and slope at that point. The theorem says that the straight-line extrapolation from the point A represents a lower limit to the curve for the equation of state. From Theorem 31 follows Theorem 32.

Theorem 32. Granted absence of microscopic collapse, then the asymptotic value of the logarithmic derivative cannot be less than unity:

$$\gamma_{\rm asymptotic} = d \ln \rho / d \ln n \ge 1$$
 . (251)

This theorem has already been used in conjunction with the contour diagram of Figure 12 in chapter viii. In this way one could prove for every baryon number A greater than  $A_{\rm quantum}$  the existence of a continuous sequence of configurations leading to gravitational collapse (Theorems 24 and 25). For this purpose it was vital to have a lower limit on  $\gamma_{\rm asymptotic}$ 

### > TWO OR LESS FOR CONSISTENCY WITH CAUSALITY

Contrary to what one might have thought, no upper limit on the stiffness of matter, no upper bound to  $\gamma_{\text{saymptotics}}$  was required in chapter viii to establish the theorem about gravitational collapse. If matter is difficult to compress, then much energy must be pumped into it in accomplishing the compression. Consequently the A baryons have a greater mass than they would have had otherwise. This greater mass only assists the collapse when the critical compression is reached. Nevertheless, it is still of interest to look at the upper limit on γ<sub>asymptotie</sub>.
The speed of sound, measured in units of the speed of light, is

$$\beta_{\text{sound}} = (d p^* / d \rho^*)^{1/2},$$
 (252)

and in the asymptotic limit is  $\beta_{\text{sound}} = (\gamma_{\text{asymptotis}} - 1)^{1/2}$ . Result (252) is well known in Newtonian theory. Curtis (1950) has proved that the same formula is a consequence of Einstein's general relativity. If the speed of sound from A to B exceeded the speed of light in one Lorentz reference system, then another Lorentz reference system could be found in which the acoustic wave reached B before it started from A. But this effect would violate the principle which one knows under the name of causality. Therefore:

THEOREM 33. The value of y cannot exceed two.

It is to be noted that the  $\gamma$  under discussion here is the  $\gamma$  in the relativistic form (233) of the equation of state, not the \( \gamma^\* \) of the non-relativistic formulation (236).

It has been urged as plausible by one of us<sup>6</sup>—and by others—that  $p^* \le \rho^*/3$  is a more appropriate asymptotic limit on the pressure  $(\gamma = \frac{4}{3})$  than the limit  $p^* \le \rho^*$  given by the causality condition and  $\gamma = 2$ . The stronger limit would insure that the trace of the stress-energy tensor in a local Lorentz system,

$$T_{\mu}^{\mu} = \rho^* - 3 \rho^*$$
, (253)

is never negative, and only vanishes for the special case of pure radiation. However, in a valuable contribution Zel'dovich (1961) has supplied a counterexample; a simple ideal-

See Wheeler (1964), p. 202. In the older literature (Eddington; and also Curtis [1950]) the thought is occasionally expressed that the trace of the stress-energy tensor,

$$T = T_0^0 + T_1^1 + T_2^2 + T_2^3 = \rho^* - 3\rho^*$$

measures the particle density. For an ideal Fermi gas Chandrasekhar's (1935) formulae (see eqs. [275]-(278) below) give

$$\rho^* - 3p^* = 2\pi (Gm/c^2)(mc/h)^3 \begin{cases} \sinh(t/2) - (t/2) & \text{(general)} \\ (t^3/48) & \text{(small } t) \\ \frac{1}{2} \exp(t/2) & \text{(large } t) \end{cases}.$$

The high density form of this expression ( $\sim$ exp t/2) is altogether different from that for the particle density ( $\sim$ exp 3t/4). Therefore there is no reason to think of the trace, T, of the stress-energy tensor as

providing any direct measure whatever of the particle density,

Both in earlier discussions and today the (idealized) concept of "incompressibility" is of course under-Both in earner discussions and today the (localized) concept of incompressionity is of course understood to mean—by definition—a particle density which is not subject to being increased. However, a fixed particle density and a fixed value of T are evidently very different ideas. Thus one will not uphold today the view that "incompressible matter corresponds to T = constant" nor the view that the Curtis equation of state  $\rho^* = \rho_0^* + 3\rho^*$  corresponds to incompressible matter. Whatever this equation of state does not represent, it does describe an idealized situation of interest in its own right. His integration of the equations of hydrostatic equilibrium for this equation of state is instructive, especially for the way in which it confirms the original particle of the particle of which it confirms the existence of a limiting configuration in which the pressure goes to infinity at the center. It would be interesting to see precise integrations made for this equation of state of Curtis for lesser values of the central pressure. One would like to know whether the equilibrium configurations change from stable to unstable when the central pressure first exceeds a certain critical value short of infinity, as one expects on physical grounds.

ized physical model for an equation of state with the property that p\* agrees asymptoti-

cally with  $\rho^*$  not  $\rho^*/3$ , in the limit of very high density.

Zel'dovich puts forward his analysis, not with the aim of giving a detailed account of the equation of state of real matter at high densities, but rather as a pure model, illustrating a point of principle. As such it is nevertheless most interesting, because it throws new light on concerns often expressed about the so-called "hard-core" model of the nucleonnucleon interaction, and its bearing on the compressibility of matter at very high density.

THE SOFT "HARD CORE"

The often-used terminology "hard core" would seem at first sight to rule out any separation between the two nucleons which is less than some characteristic distance b. This idea is clear enough for stationary centers. Yet stationary centers one does not have even when, as here, the medium under discussion is deprived of all excitation and maintained at absolute zero temperature. There is zero-point motion. Moreover, the zero-point kinetic energy goes up indefinitely with compaction. In a medium so compressed, a nucleon of high momentum collides with another nucleon, also of high momentum. After the collision the particles are moving in new directions with new velocities. In which of the four obvious Lorentz frames is the distance b to be measured? And if no one choice of frame is compatible with the symmetry between the particles, as is normally the case, then what covariant way is there to describe the exclusion distance? And how can any definition of exclusion distance be compatible with causality and the simple demand that information should not propagate from one place to another with a speed in excess of the speed of light? No satisfactory answer to these questions has ever been given. Moreover, viewing the medium in the large, one sees still another objection to the idea of the hard core: Hard core means incompressibility; and incompressibility means a speed of sound in excess of the speed of light, in violation of causality; ergo, no hard core!

Zel'dovich finds a model to describe baryon-baryon repulsion which is compatible with special relativity. The model considers the interaction to be mediated by a vector field which resembles the vector field of electromagnetism except in two points: its quanta have a non-zero rest mass; and the charge on the sources is not  $\pm e$ , but always +g. In consequence the potential energy of interaction of two of these baryon charges is

$$(g^2/r_{12})\exp(-r_{12}/a),$$
 (284)

where the range a is

$$a = \hbar / (\text{rest mass of quantum of the vector field}) \cdot c$$
. (255)

When the baryon density is so high that there are many baryons within the range a, then, Zel'dovich shows, elementary statistical considerations apply. The potential energy of interaction per unit of volume becomes

$$\rho_{\text{pot}}^* = (G/c^2)(n^2/2)\int (g^2/r)e^{-r/a}4\pi r^2 dr = 2\pi G(g^2a^2/c^2)n^2$$
. (256)

For an otherwise ideal Fermi gas compressed to a relativistic Fermi energy the kinetic energy rises as a lesser power of the baryon density:

$$\rho_{\rm kin}^* = (3^{4/3}\pi^{2/3}/4)L^{*3}n^{4/3}$$
. (257)

Therefore the potential-energy term dominates at great compressions. The total density of mass-energy in the model follows an asymptotic  $\gamma$ -law with  $\gamma = 2$ . Therefore the pres-

<sup>&</sup>lt;sup>7</sup> An investigation of an ideal hard-core Fermi gas in the high-density limit had been carried out, but not yet published in September, 1964, according to a kind personal communication of L. Gratton at that time.

sure p\* is asymptotically equal to ρ\*. The speed of sound approaches indefinitely close to the speed of light, not the (speed of light)/31/2. The material has the maximum rigidity permitted by the principle of causality. This example shows that the limit  $\gamma = \overline{2}$  is in principle an achievable limit.

So much for general considerations about the equation of state; now for the pressure-

density relationship employed in the detailed calculations.

#### REFERENCES

Bondi, H. 1964, Nature, 202, 275.
Burbidge, E. M., Burbidge, G. R., and Fowler, W. A. 1957, Rev. Mod. Phys., 29, 547. Carter, R. E., Reines, F., Wagner, J. J., and Wyman, M. E. 1959, Phys. Rev., 113, 280. Casimir, H. B. G. 1948, Nederlandsche Akademie von Welenschappen, 51, 793. Casimir, H. B. G., and Polder, D. 1948, Phys. Rev., 73, 360. Chandrasekhar, S. 1935, M.N., 95, 207. Chiu, H. Y. 1964, Ann. Phys., 26, 364.

Cowan, C. L., Jr., Reines, F., Harrison, F. B., Kruse, H. W., and McGuire, A. D., 1956, Science, 124, 103. Curtis, A. R. 1950, Proc. R. Soc. London, A, 200, 248.

Derjaguin, B. V. 1960, Sci. Am., 203 (No. 1), 47. Gamow, G., and Schönberg, E. 1941, Phys. Rev., 59, 539.

Gray, D. E. (ed.) 1957, American Institute of Physics Handbook (New York: McGraw-Hill Book Co.). Hayashi, C., Hoshi, R., and Sugimoto, D. 1962, Prog. Theor. Phys. Suppl., No. 22, p. 1. Kihara, T. 1953, Rev. Mod. Phys., 25, 831.

1955, ibid., 27, 412.

Lifshitz, E. M. 1954, Doklady Akad. Nauk S.S.S.R., 97, 643.

1955a, Doklady Akad. Nauk S.S.S.R., 100, 879 (1955).

1955b, Zhur. Eksp. Teor. Fiz., 29, 94 (1955); translation, Soviet Phys.—J.E.T.P., 2, 73.

Reines, F., and Cowan, C. L., Jr. 1953, Phys. Rev., 90, 492.

Redkjøbing, M. 1952, Pub. Copenhagen Obs., No. 60.
Salpeter, E. E. 1957, Rev. Mod. Phys., 29, 244.
Schwarzschild, M. 1958, Structure and Evolution of the Stars (Princeton, N.J.: Princeton University

1964, in Gravitation and Relativity, ed. H. Y. Chiu and W. F. Hoffmann (New York: W. A. Benjamin).

Zel'dovich, Ya. B. 1961, Zhur. Eksp. Teor. Fiz., 41, 1609 (English translation in Soviet Phys. - J.E.T.P., 14, 1143, 1962).

1962. Zhur. Ehst. Teor. Fiz., 43, 1561 (English translation in Soviet Phys.-J.E.T.P., 16, 1102, 1963).

# THE HARRISON-WHEELER EQUATION

# chapter 10 OF STATE

### EQUATION IN FORM OF TABLE OF VALUES AND ANALYTICAL FITS TO THEM

This equation of state has been presented in graphical form by Harrison, Wakano, and Wheeler (1958), and by Wheeler (1962, 1964). The same publications reported general-relativity calculations of equilibrium configurations based on this pressure-density relation, as well as successive steps in the analysis of the results—now brought up to date and summarized here in chapters vi and viii and Appendix A. Neither Harrison's 1957 table of pressure for 47 values of the density, nor his 1957 analytical fits to these numbers, nor the derivation have been reported heretofore. The analytical fits present the pressure-density relation in the most compact form and are therefore given first; then the table; then the derivation.

Regime I, 
$$\rho$$
 from 7.86 to  $1.00 \times 10^6$  g/cm<sup>3</sup>,  

$$\rho(g/cm sec^2) = 3.0271 \times 10^{12} (\rho^{1/2} - 1.4415)^4 - 1.50319 \times 10^{11}.$$
(258)

Regime II, 
$$\rho$$
 from  $1.00 \times 10^6$  to  $3.22 \times 10^{11}$  g/cm<sup>3</sup>,

$$p(g/\text{cm sec}^2) = 2.4616 \times 10^{15} \rho^{5/4} (1 + 2388.8 \rho^{-1/2})^{-5/6}$$
. (259)

Regime III, 
$$\rho$$
 from  $3.22 \times 10^{11}$  to  $4.63 \times 10^{12}$  g/cm<sup>3</sup>,

$$p(g/\text{cm sec}^2) = 3.1134 \times 10^{21} \rho^{2/3} (1 + 0.0031822 \rho^{1/6})^6$$
. (260)

Regime IV. 
$$\rho$$
 from  $4.63 \times 10^{12}$  g/cm<sup>3</sup> to infinity.

$$p(g/\text{cm sec}) = 2.9959 \times 10^{20} \rho^{5/2} (9.1208 \times 10^8 + \rho^{5/9})^{-6/5},$$
 (261)

approaching for  $\rho > 5 \times 10^{29}$  g/cm<sup>3</sup> the limiting form

$$p \simeq (c^2/3) \rho$$
, (262)

The formula listed in one region joins onto that listed for the next region to about four significant figures at the point of transition. There are no serious discontinuities in the derivatives at each point of join. Equations (258)–(261) were employed in the 1957 integrations of the general relativity equation of hydrostatic equilibrium (M. W.). In the 1964 integrations (B. K. H.) a table of pressure for 47 values of the density, analogous to Table 13 of primary values and obtained from that table by graphical interpolation, was used directly in the electronic computer. Interpolation was made between one point and the next assuming a constant logarithmic derivative between; thus,

$$\frac{\log p - \log p_j}{\log \rho - \log \rho_j} = \frac{\log p_{j+1} - \log p_j}{\log \rho_{j+1} - \log \rho_j}.$$
 (263)

The results obtained from the integrations of the TOV equation (11) using Table 13 were essentially identical to those obtained using equations (258)-(261).

TABLE 13

PRESSURE FOR 47 VALUES OF THE DENSITY (B. K. H.)\*

p(g/cm sec <sup>2</sup> )	$\mu(g/cm^2)$	p*(cm-1)	ρ*(cm <sup>-1</sup> )	w(cm-s)	$\rho^{+}/\pi - \mu_{z}^{+}$ (cm
≤1.01E9	7.86	≤8.37E −41	5.83E -28	4.73E24	0
5.07E9	7.88	4.19E −40	5.85E -28	4.75E24	1.50E -67
1.01E10	7.90	8.37E −40	5.86E -28	4.76E24	3.67E -67
5.07E10	8.06	4.19E −39	5.98E -28	4.85E24	9.13E -66
1.01E11	8.15	8.37E -39	6.05E -28	4.91E24	2.35E -65
1.21E12†	1.16E1	1.00E -37	8.61E -28	6.99E24	2.11E -63
1.40E13	1.64E1	1.16E -36	1.22E -27	9.90E24	1.92E -62
4.41E13	2.60E1	3.64E -36	1.93E -27	1.57E25	9.63E -62
1.70E14	4.51E1	1.40E -35	3.35E -27	2.72E25	2.92E -61
8.46E14	8.82E1	6.99E -35	6.55E -27	5.32E25	8.64E -61
5.82E15	2.12E2	4.81E -34	1.57E -26	1.27E26	2.90E -60
7.23E16	7.05E2	5.97E -33	5.23E -26	4.25E26	1.23E -59
1.90E17	1.15E3	1.57E -32	8.54E -26	6.93E26	2.12E -59
5.61E17	2.06E3	4.63E -32	1.53E -25	1.24E27	3.83E -59
2.85E18	4.99E3	2.35E -31	3.70E -25	3.00E27	8.71E -59
2.45E19	1.66E4	2.02E -30	1.23E -24	9.98E27	2.44E -58
4.10E20	8.30E4	3.39E -29	6.16E -24	5.00E28	8.79E - 58
4.45E21	3.31E5	3.68E -28	2.46E -23	2.00E29	2.49E - 57
2.80E22	1.00E6	2.31E -27	7.42E -23	6.02E29	5.49E - 57
1.21E23†	2.41E6	1.00E -26	1.79E -22	1.45E30	1.01E - 56
8.96E23	8.00E6	7.40E - 26	5.94E -22	4.82E30	2.28E -56
6.50E24	4.61E7	5.37E - 25	3.42E -21	2.77E31	5.30E -56
1.21E25†	7.56E7	1.00E - 24	5.61E -21	4.55E31	6.32E -56
3.18E26	1.02E9	2.63E - 23	7.59E -20	6.15E32	1.44E -53
1.74E27	3.15E9	1.44E -22	2.34E -19	1.90E33	2.09E - 55
2.22E28	2.32E10	1.83E -21	1.72E -18	1.39E34	4.11E - 55
8.50E28	6.93E10	7.02E -21	5.14E -18	4.15E34	5.75E - 55
2.03E29	1.41E11	1.68E -20	1.05E -17	8.47E34	7.05E - 55
3.55E29	1.74E11	2.93E -20	1.29E -17	1.04E35	7.54E -55
5.95E29	3.22E11	4.91E -20	2.39E -17	1.93E35	9.19E -55
8.55E29	6.79E11	7.06E -20	5.04E -17	4.06E35	1.08E -54
1.27E30	1.18E12	1.05E -19	8.74E -17	7.03E35	1.17E -56
2 . 28E30	2.07E12	1.88E -19	1.54E -16	1.24E36	1.25E -54
	2.79E12	2.76E -19	2.07E -16	1.66E36	1.30E -54
	3.88E12	4.32E -19	2.88E -16	2.31E36	1.36E -56
	4.63E12	5.63E -19	3.44E -16	2.76E36	1.39E -54
1.90E31	8.73E12	1.57E -18	6.48E -16	5.19E36	1.55E - 54
1.21E32†	2.70E13	1.00E -17	2.00E -15	1.60E37	2.05E - 54
1.99E33	1.48E14	1.64E -16	1.10E -14	8.65E37	3.98E - 54
2.09E34	6.47E14	1.73E -15	4.80E -14	3.65E38	8.43E - 54
1 .66E35	2.51E15	1.37E -14	1.86E -13	1.32E39	1.76E -53
	2.16E16	2.59E -13	1.60E -12	9.16E39	5.16E -53
	2.44E17	4.63E -12	1.81E -11	6.86E40	1.41E -52
	5.05E17	1.00E -11	3.75E -11	1.22E41	1.84E -53
3.87E38†	1.52E18	3.20E -11	1.13E -10	2.90E41	2.66E -52
1.21E39†	4.47E18	1.00E -10	3.32E -10	6.68E41	3.73E -52
4.50E39	1.55E19	3.72E -10	1.15E - 9	1.72E42	5.45E -52

<sup>\*</sup> A quantity such as  $5.95 \times 10^{-28}$  is listed in the table as 8.95E - 23 to follow computer language (E = "exponent") and to simplify typography. The conversion factors  $G/e^2 = 0.742 \times 10^{-28}$  cm/g and  $G/e^2 = 8.26 \times 10^{-28}$  sec<sup>2</sup>/cm g, respectively, were used to translate from density  $\rho$  and pressure  $\rho$  to the geometrized values of these quantities  $\rho^2$  and  $\rho^2$ . The number density of baryons, n, was calculated, after the construction of the rest of the table, from  $n = (\rho/\mu_0) \exp{[-\int \rho^{2-1} (\rho^2 + \rho^2) - \frac{1}{2} \theta^2 d\rho^2]}$ , with  $\mu_0 = 1.659 \times 10^{-28}$  g. All of the pressure-density values in this table are primary (calculated by B. K. H. as described below) except those marked by daggers; they were interpolated from a log-log plot (errors of order of 5 per cent or less). Equations (258)—(261) are more convenient than the table in most numerical calculations.

Harrison (1965) has given the following analytic fit to n, with n in cm<sup>-3</sup> and  $\rho$  in g/cm<sup>3</sup>:

$$n = 6.0228 \times 10^{23} \rho (1 + 7.7483 \times 10^{-10} \rho^{9/16})^{-4/9}$$
, (264)

Thus n varies linearly with  $\rho$  at low densities and with the  $\frac{3}{4}$  power of  $\rho$  at high densities,

## DERIVATION: REGION UP TO 104 ATMOSPHERES

International Critical Tables gives information2 on the volume compressibility of iron,

$$k = -(1/V)(\partial V/\partial p)_T = (1/\rho)(\partial \rho/\partial p)_T, \qquad (265)$$

expressed up to 104 atm in the form

$$k = a - 2b \, b \, , \tag{266}$$

with

$$a = 0.606 \times 10^{-4} \text{ atm}^{-1}$$
  $b = 2.2 \times 10^{-12} \text{ atm}^{-2}$ . (267)

Integration gives

$$\rho(g/cm^2) = 7.86 \exp(a p - b p^2 - a p_0 + b p_0^2), \qquad (268)$$

with  $p_0 = 1$  atm = 1.0133 × 10<sup>8</sup> g/cm sec<sup>2</sup>, and the density running from 7.86 to a little over 8 g/cm<sup>3</sup>.

# FEYNMAN, METROPOLIS, AND TELLER FROM 15 g/cm3 TO 104 g/cm3

Feynman, Metropolis, and Teller (1949) consider densities of iron high enough so that the specificities of the normal solid-state forces are overcome ( $p > 10^{12}$  g/cm sec<sup>2</sup>,  $\rho > 15$  g/cm<sup>3</sup>). Then they can apply the Fermi-Thomas statistical atom model, with the Dirac exchange corrections, to an individual iron atom located in a cell, idealized as spherical, and characterized by a radius

$$R = (9\pi^2/128Z)^{1/3} (\hbar^2/m e^2) x_0, \qquad (269)$$

Here x is Fermi's dimensionless radius parameter. The electrical potential at the distance r from the nucleus is written as  $(Ze/r)\psi(x)$ , with  $\psi(x)$  taken to satisfy the equation

$$d^2\psi/dx^2 = x(\epsilon + \psi^{1/2}/x^{1/2})^{\frac{1}{2}}$$
. (270)

<sup>1</sup> This analytical expression reproduces to better than 1 per cent the HW value of  $n(\rho)$  for all values of  $\rho$ . It is well suited to describe the pressure-density relation near the second and more important (LOV) critical point, and at higher pressures. At lower pressures, however ( $\rho < 10^{12}$  g/cm<sup>3</sup>), what counts in the prediction of critical points is the small difference between  $\rho$  and  $\mu_s n$ , a difference which measures the work of compression. This difference, as given by the HW equation of state, allows for the effects associated with crushing of electrons onto nuclei near the first (LHWW) critical point. The analytical expression (264), despite its 1 per cent limit of error, does not allow for these effects and therefore does not predict the existence of this first critical point. For a similar reason Oppenheimer and Volkoff (1939) did not see the first critical point.

<sup>2</sup> International Critical Tables (New York: McGraw-Hill Book Co., 1928), 3, 47–48. We have not taken into account the following publications which have appeared since the present work was done, primarily because this region of pressures plays no critical part in our analysis of equilibrium configurations: the paper by Knopoff (1963) on "Equations of State of Matter at Ultra-High Pressures"; McQueen and Marsh (1960) (equation of state for nineteen elements, including Fe); Birch (1963); Takehashi and Bassett (1964) (room-temperature measurements on iron; starting with zero pressure, 7.85 g/cm², 7.10 cm²/mole, a-lattice, body-centered cubic; with increasing pressure gradual decrease in volume; at 130 kb iron suffers phase change to e-lattice, hexagonal close-packed, with volume alteration d −0.20 ± 0.03 cm²/mole; at 200 kb, 6.10 cm³/mole, 9.1 ± 0.01 g/cm³); Boyd and England (1963, p. 135) (melting of iron at high pressure). (We express our appreciation to Dr. Howard Young of Du Pont Central Research, Wilmington, Delaware for bringing these last three references to our attention.)

Here  $\epsilon$  is the Dirac correction (known). The integration starts with  $\psi(0) = 1$ . Different choices are made for the starting slope. For each, equation (270) is integrated numerically out to the cell boundary  $x = x_0$ . There the potential gradient  $(d/dx) [\psi(x)/x]$  is evaluated. That solution for which this gradient vanishes is accepted. From it Feynman et al. evaluate a "pressure correction factor,"

$$F(x_0) = (x_0^5/3^{5/3}) \left\{ [\psi(x_0)/x_0]^{1/2} + \epsilon \right\}^5 \left[ [1 - (5\epsilon/4) \{\epsilon + [\psi(x_0)/x_0]^{1/2}\}^{-1}] \right]. \quad (271)$$

Denote by  $p_{uniform}$  the pressure which one would expect from the electrons if they acted as a Fermi gas uniformly distributed through the cell volume; thus,

$$p_{\text{uniform}} = n_e \frac{\dot{p}_F^2}{5 m} = \frac{8 \pi}{15 m h^3} \left( \frac{3 h^3 n_e}{8 \pi} \right)^{5/8} = (2 \pi)^{1/3} \frac{256}{15 \pi^4} \frac{Z^{10/3}}{x_0^5} \frac{m^4 e^{10}}{h^8}.$$
 (272)

The pressure is

$$p = F(x_0) p_{uniform}, \qquad (273)$$

and the density is

$$\rho = \frac{56\,\mu_s}{4\,\pi R^2/3} = \frac{3\,2}{3\,\pi^3} \, \frac{26}{3\,\pi^3} \, \frac{56\,\mu_s}{(\,\hbar^2/\,m\,e^2)^3}. \tag{274}$$

In the range from  $\rho$  a little more than 8 g/cm<sup>3</sup> (eq. [268]) to  $\rho \sim 15$  g/cm<sup>3</sup> (eq. [273]), the pressure was obtained by graphical interpolation.

# CHANDRASEKHAR FROM 104 g/cm2 to 107 g/cm2

As the density reaches the order of  $10^4$  g/cm³, the "pressure correction factor"  $F(x_0)$  of equation (271) approaches so close to 1 that the electrons constitute effectively an ideal Fermi gas. Moreover, the Fermi momentum,  $p_F$ , is still in the non-relativistic domain ( $p_F \sim mc/6$ ). However, the point is approaching where relativistic effects will have to be considered. Therefore it is appropriate to use Chandrasekhar's (1934, 1935, 1939) formula for an ideal degenerate electron gas, which is valid for relativistic as well as non-relativistic Fermi energies. It is not possible to express pressure in terms of density, or density in terms of pressure, in closed form; but both allow themselves to be expressed in closed form in terms of the Fermi energy; or, more simply, in terms of a parameter t, defined by

OF

(Fermi momentum) = 
$$m \epsilon$$
 
$$\begin{cases} \sinh(t/4) \text{ (general)} \\ (t/4) \text{ (small } t) \\ \frac{1}{2} \exp(t/4) \text{ (large } t) \end{cases}$$
 (275)

The number density of baryons is

$$n = (A/Z)(8\pi m^3 c^3/3h^3) \begin{cases} \sinh^3(t/4)(\text{general}) \\ t^6/64(\text{small } t) \\ \frac{1}{8} \exp(3t/4)(\text{large } t) \end{cases}$$
(276)

The mass density is

$$\rho = \mu_s n + m \left( \pi m^2 c^2 / 4 h^2 \right) \begin{cases} (\sinh t - t) (\text{general}) \\ t^2 / 6 (\text{small } t) \end{cases} . \tag{277}$$

The pressure is

$$p = m c^{2} (\pi m^{3} c^{3} / 12h^{3}) \begin{cases} [\sinh t - 8 \sinh(t / 2) + 3t] (\text{general}) \\ t^{6} / 160 (\text{small } t) \\ \frac{1}{2} \exp t (\text{large } t) \end{cases}$$
(278)

The Chandrasekhar equation continues to apply, with fixed Z=26, A=56, until the Fermi kinetic energy of the electrons rises to a value of the order of 1  $mc^2$ . Then the neutron-proton equilibrium is pushed by inverse beta reactions toward a significantly decreased Z/A ratio. The Fermi energy reaches  $mc^2$  when the number density of electrons is

$$n_e = (3^{1/2}/\pi^2)(m c/\hbar)^3 = 3.03 \times 10^{30}/\text{cm}^3$$
, (279)

corresponding to a mass density of Fe<sup>56</sup> equal to  $1.08 \times 10^7$  g/cm<sup>3</sup>.

SEPARATED NUCLEI IN BETA-EQUILIBRIUM WITH A RELATIVISTIC ELECTRON GAS:  $\sim\!10^7~{\rm g/cm^3}$  to  $\sim\!4\times10^{12}~{\rm g/cm^3}$ 

The effect of the inverse beta reactions was considered qualitatively by Landau (1932) and by Oppenheimer and Serber (1938). It was considered in more detail by van Albada (1946, 1947) in connection with the origin of the heavy elements, and by Schatzman (1958) and by Auluck and Mathur (1959) in connection with the theory of the first critical point in the curve of equilibrium mass as a function of central density. It has also been considered by Salpeter (1960, 1961). Happily, as van Albada had pointed out in 1947, and as we found in the more detailed 1958 investigation reported here, essentially no nuclear physics is required for the treatment of the present regime. One has only to know nuclear masses and to apply the most elementary principles of statistical mechanics to obtain the equation of state.

The qualitative situation is easily outlined. If it were not for the electrostatic repulsion between protons, nucleons would aggregate into nuclei of unlimited size. In actuality, however, the Coulomb energy is so great in a heavy nucleus that it undergoes fission. If Coulomb forces alone were relevant, the lowest packing fractions would be found for the lowest A-values. If nuclear forces alone counted, the packing fraction would go down indefinitely with increasing A. When the two conflicting effects are considered together and the total packing is minimized, then A has a value as low as 56. The balance changes when the electron pressure is raised to relativistic values. The nucleus contains a higher proportion of neutrons to protons. Consequently the Coulomb forces play a smaller role. Greater rein is given to the natural tendency of the specifically nucleonic attraction to favor agglomeration into systems containing large numbers of baryons.

At any one electron pressure there is one nucleus which (1) has the requisite neutron to proton ratio to be in beta-equilibrium with the electrons and (2) has the most favorable packing fraction compatible with the neutron-proton ratio. For low pressure this nucleus is  ${}_{28}\text{Fe}^{56}$ . As the electron pressure is raised the mass goes up. At a certain stage of the compression the best bound nucleus is calculated to be at or near  ${}_{29}\text{Y}^{129}$ . Here, at a density  $\sim 3 \times 10^{11} \, \text{g/cm}^3$ , the neutron-proton ratio has reached a critical level. Any further augmentation leads to what has been called "neutron drip." Not nuclei of one species alone are present (with still larger mass number), but nuclei of one species plus free neutrons. One has what is in effect a two-phase system.

With further increase of the electron pressure the (Z, A)-values of the favored nucleus move beyond the line of neutron drip, to higher and higher A-values, and to higher and

<sup>&</sup>lt;sup>3</sup> See Werner and Wheeler (1958) for a first plot of the line of neutron drip in the (Z, A)-plane, and Brandt, Fuller, Wakano, Werner, and Wheeler (1960). For related issues see Goeppert-Mayer and Teller (1949).

<sup>\*</sup> See Salpeter (1960) for considerations on the idea that the neutrons might aggregate into drops, and for plausible indications that this will not take place.

higher neutron-to-proton ratios. At a sufficiently high pressure one calculates, for example,  $_{43}\mathrm{Cd^{187}}$  to be the favored nucleus. Of course, the favored nucleus is evaporating neutrons; but at the same time new neutrons are condensing on it from the surrounding neutron gas. Equilibrium is preserved. In the example the conditions have become so extreme ( $\rho \sim 4 \times 10^{12} \mathrm{ g/cm^3}$ ) that at last more of the pressure is being provided by neutrons than by electrons. Moreover, only a minor fraction of the nucleons is present in the form of  $_{48}\mathrm{Cd^{187}}$ . The neutron gas so dominates the situation that one can say that the medium has in effect become one vast nucleus, with a lower-than-normal nuclear density.

So much for the qualitative situation; now for the quantitative analysis, substantial parts of which will already be found in the papers of van Albada (1946, 1947). Many different nuclei come into consideration, from Fe<sup>36</sup> onward, as the pressure is raised. Therefore it is reasonable to represent nuclear masses by a semi-empirical mass formula. We

employed a formula of the usual type with the constants of Green (1955):

$$M(Z, A)/[M(O^{16})/16] = b_1A + b_2A^{2/3} - b_3Z + b_4A(0.5 - Z/A)^2 + b_5Z^2/A^{1/3};$$

$$b_1 = 0.992064$$
,  $b_2 = 0.019120$ ,  $b_3 = 0.000840$ ,  
 $b_4 = 0.10178$ ,  $b_6 = 0.000763$ ,  $M_n = 1.008982[M(O^{16})/16]$ .

Beta-equilibrium is obtained when the atom with (Z-1) protons and mass number A has the same mass-energy as the atom with the same mass number, with charge Z, and with one more electron. In the normal beta-decay this electron comes off with the lowest possible energy. This energy puts the electron into the last and most weakly bound state in the atom. The mass-energy of this electron is already included, along with the masses of the other (Z-1) electrons, in the usual mass value for a free atom. In the present case, however, the lowest state available to the electron lies at the top of the Fermi sea. Call the energy of this state

$$E_F = (\text{Rest plus kinetic energy at top of Fermi sea}) \equiv m c^2 + m_K c^2$$
. (281)

This represents a promotion of energy of  $E_F - mc^2 = m_K c^2$  over that required in normal beta-decay. Therefore one condition on the equilibrium is

$$M(Z-1, A) = M(Z, A) + m_K.$$
 (282)

Hereafter we take the mass equivalent,  $m_K$ , of the kinetic energy to be expressed in the familiar unit  $M_1 = M(O^{16})/16$ . In the statistical approximation, this first requirement for equilibrium takes the form

$$(\partial M/\partial Z)_A = -m_K \tag{283}$$

when expressed in terms of mass values. When expressed in terms of packing fractions, defined by  $M = AM_1(1+f)$ , this condition becomes

$$\partial f/\partial Z = -\left(1/A\right)(m_K/M_1). \tag{284}$$

In addition to equilibrium with respect to changes in Z one has to consider equilibrium with respect to changes in A. Let (Z, A-1) and (Z, A) be the two nuclei (with Z/A-values governed by eq. [284]) which lie closest to the bottom of the packing-fraction curve. In other words, let these two nuclear species be in equilibrium with respect to the baryon-conserving rearrangement reaction

$$(A-1)$$
Atoms of type $(Z, A) \rightleftharpoons A$  Atoms of type $(Z, A-1)$ . (285)

There is no concern about charge conservation in this reaction, because the atoms are neutral. Thus, as the reaction slowly goes to the right the totalized nuclear charge rises from (A-1)Z to AZ, but at the same time Z electrons are slowly injected into the lowest unfilled states in atoms of type (Z,A-1). The mass-energies of these electrons are already included in the standard atomic mass values. Not so when the electron gas is under high pressure. Then the additional mass  $Zm_K$  of the kinetic energies of these Z electrons must be understood to be inserted on the right-hand side of the reaction equation. Thus find as the second condition for equilibrium

$$(A-1)M(Z, A) = AM(Z, A-1) + Zm_K$$
. (286)

In the continuum approximation employed in the statistical treatment of atomic masses, this requirement takes the form

$$\partial f / \partial A = (Z / A^2) (m_K / M_1),$$
 (287)

Equations (284) and (287) constitute two equations to the solved for the two unknowns, Z and A, for each value of the Fermi kinetic energy,  $m_E$ .

There is a simple way to summarize the equilibrium conditions. Define a variationeffective packing fraction.

$$F = \binom{All \text{ of the mass associated with one baryon}}{\text{at the top of the Fermi distribution}}/M_1 - 1$$
$$= f + (Z/A)(m_K/M_1).$$
 (288)

(This cannot be used in calculating *energy* any more than a Lagrange function directly gives energy.) Then equations (284) and (287) are equivalent to extremizing F with respect to adjustment both of Z and of A.

The computation of the equation of state proceeds in the following way. (1) Pick an A-value between A = 56 and A = 122. (2) Calculate Z from the requirement

$$A(\partial f/\partial A) + Z(\partial f/\partial Z) = 0 (289)$$

(a linear combination of eqs. [284] and [287]). In terms of the semi-empirical mass formula with the constants of equation (280), this condition gives an equation for Z:

$$Z = (b_2/2b_1)^{1/2}A^{1/2}$$
(290)

(locus of the minimum in the packing fraction curve in the (Z, A)-plane as the electron pressure is changed). (3) Calculate the Fermi kinetic energy  $m_K$  of the electrons needed to stabilize the atom (Z, A) against beta-decay:

$$m_K/M_1 = b_3 + b_4 - (2b_2b_5)^{1/2}(A^{-1/2}b_4/b_5 + A^{1/6}).$$
 (291)

Also calculate the packing fraction f. (4) Knowing the Fermi energy of the electrons, evaluate the parameter t defined by

$$m_K = m \left[ \cosh(t/4) - 1 \right].$$
 (292)

(5) Find the pressure (all electronic in origin) from equation (278), the number density of baryons, n, from equation (276), and the mass density, p, from

$$\rho = n_e (A/Z) M_1 (1+f) + (\pi m^4 c^3 / 4h^3) \left( \sinh t - t - \frac{32}{5} \sinh^3 t / 4 \right). \quad (293)$$

#### REGIME OF STABILIZED NEUTRON DRIP

The analysis proceeds in this way until the neutron-proton ratio reaches a limit, the line of neutron drip in the (Z, A)-plane. Here a nucleus is unstable against loss of a neutron. A

neutron atmosphere forms. As the electron pressure is further increased, the neutronproton ratio rises still higher by a double process: the A-value of the dominant nuclear species rises; and the density of the neutron atmosphere goes up. In consequence there are now two contributors to the pressure, which becomes

$$p = p_o + p_n. \qquad (294)$$

Each contribution is given by an expression of the form (278). The parameter t employed to specify the Fermi energy and momentum of the electrons is replaced in the case of the neutrons by a corresponding parameter T. For these particles one writes

(Rest energy plus Fermi kinetic energy) = 
$$(M_n + M_K) c^2 = M_n c^2 \cosh(T/4)$$
. (295)

The neutron pressure stabilizes a nucleus that would not ordinarily be stable. Or put the same point in other words. The nucleus in question, though much heavier than He<sup>5</sup>, is like He<sup>5</sup> in this respect; it undergoes a decay process similar to the breakup

$$He^5 \rightarrow He^4 + n$$
 . (296)

However, there are sufficiently many neutrons present that reactions going to the right are balanced by equally many reactions going to the left. Thus there is a well-defined way to talk of a nucleus (Z,A) which lies beyond the line of neutron drip. Moreover, this nucleus extremizes the effective packing fraction F of equation (288), with respect to small adjustments of Z and A, as before. In consequence all of the preceding analysis applies (eqs. [281]–[292]), with the exception of the final step, the evaluation of pressure, baryon density, and mass density (eq. [293]). All three quantities have to be supplemented with contributions from the neutrons.

The Fermi energy of the neutrons must be such as to supply the necessary stabilization; thus,

$$M(Z, A) = M(Z, A-1) + M_n + M_K$$
. (297)

This condition can be written in the continuum approximation as

$$(\partial M/\partial A)_{s} = M_{n} + M_{K}$$
(298)

OF

$$M_1(1 + f + A \partial f / \partial A) = M_1(1 + f_0 + M_K/M_1)$$
 (299)

or-in view of equation (287)-as

$$f + (Z/A)(m_K/M_1) = f_n + (M_K/M_1) = f_n + (1 + f_n) 2 \sinh^2(T/8)$$
. (300)

In determining the equation of state in the two-phase region we supplement steps (1), (2), (3), (4) as described previously (ca. eqs. [289]–[292]) by these: (5) Determine the energy parameter T of the neutrons from equation (300), (6) Calculate the neutron pressure  $p_n$  from equation (278) with the neutronic  $M_n$  and T substituted for the electronic m and T. Add to the electron pressure to obtain the total pressure (294), (7) Evaluate the number density of baryons as the sum of two contributions, one from bound nucleons, the other from free neutrons. The first contribution is T0 times the number density of electrons T1 is reasonable here as before to think of this number density as being uniform—the same inside nuclei as outside. In contrast to the free electrons, the free neutrons are located, not everywhere but only outside the nucleus. Their contribution to the number density of baryons is therefore not T2, but

$$n_{\rm s} \left[ 1 - \frac{\text{(Volume occupied by nuclei)}}{\text{(Total volume)}} \right] = n_{\rm s} \left( 1 - \frac{n_e}{Z} \frac{4\pi r_0^3}{3} A \right). \tag{301}$$

Here  $(4\pi r_0^3/3)$  is the volume per baryon in standard nuclear matter. However, for the conditions under discussion here, the volume inside nuclei is still small enough compared

to the volume outside that this correction is neglected. The total number of baryons per unit volume is calculated from the formula as thus simplified.

$$n = (8\pi/3)(M_nc/h)^3 \sinh^3(T/4) + (A/Z)(8\pi/3)(mc/h)^3 \sinh^3(t/4)$$
, (302)

(8) Similarly, the mass density is written as

$$\rho = \rho_n + (\rho_{\text{nuclei}} + \rho_{\text{electrons}})_{\text{eq.}} (293), \qquad (303)$$

with

$$\rho_n = (\pi M_n^4 c^3 / 4h^3) (\sinh T - T), \qquad (304)$$

again neglecting the volume-occupation factor in the second term of equation (301). Table 14 gives representative numbers from the one-phase region as well as the two-phase region. The table gives also the contributions to number density of baryons and to mass density, as calculated from the formulae in the text. In the calculations  $r_0$  was taken to be  $1.25 \times 10^{-13}$  cm, corresponding to a baryon density of  $1.22 \times 10^{38}$ /cm³, somewhat lower than the value of  $1.74 \times 10^{38}$ /cm³ deduced for the central regions of nuclei from the Stanford experiments on the scattering of electrons. More significant figures are given in the table than are justified, in order to facilitate interpolations. The calculation—based as throughout this table on the model of "dominant nucleus in equilibrium with electrons and neutrons"—is cut off beyond A = 187 in favor of the model of three ideal Fermi gases (n, p, e) in electrical and beta-equilibrium. At the pressure in question,  $p = 6.63 \times 10^{30}$  dynes/cm², the two models agree not only as to density,  $\rho = 4.54 \times 10^{12}$  g/cm³ (compare last two columns) but also very nearly as to the derivative,  $dp/d\rho$ .

The numbers in the next to the last column of Table 14 show that at a density of

$$\rho_{\text{transition}} \sim 4.54 \times 10^{12} \text{ g/cm}^3$$
 (305)

the free neutrons have taken over from the electrons most of the burden of supplying the pressure. The principal function of the electrons is to make the neutrons remain neutrons. A most modest electron pressure would have been enough to restrain the free neutrons from changing to protons. A considerably larger pressure is actually needed, according to the calculations, to restrain bound neutrons from changing to protons. Were that change to take place, the nuclei would become much more attractive sites for the condensation of neutrons. Then the pressure of the free neutrons would go down or disappear. Despite all these details, the end result, from the point of view of the equation of state is a pressure originating primarily from free neutrons. In other words, so far as the pressure-density relation is concerned, one can practically forget the nuclei and almost forget the electrons. Moreover, it is all the more appropriate to drop the nuclei out of the analysis from A = 187 onward by reason of two developments. First, the nuclei are calculated to contain only a small fraction (cf. Table 14) of all baryons. Second, the neutron-proton ratio has become too extreme, and is too far removed from the region where one has good mass values, for one any longer to be able to trust the semi-empirical mass formula as a reliable means of extrapolation.

MIXTURE OF IDEAL ELECTRON, PROTON, AND NEUTRON FERMI GASES FROM  $p = 4.54 \times 10^{18} \text{ g/cm}^3 \text{ TO } 10^{15} \text{ g/cm}^3$ , AND FROM  $10^{15} \text{ g/cm}^3$ TO THE HIGHEST DENSITIES; ALTERNATIVES

We did what would seem better than to treat the source of the pressure and density as a pure neutron gas from  $\rho_{\text{transition}} \sim 4.54 \times 10^{12} \, \text{g/cm}^3$  onward. We treated it a as mixture of three ideal Fermi gases—neutrons, protons, and electrons—not interacting with each other except insofar as they are required to fulfil the condition of electrical neutrality,

$$n_e = n_p$$
, (306)

TABLE 14 DOMINANT NUCLEUS FOR SELECTED PRESSURES\*

A of Dominant Nucleus	78	122	144	187	Mixed Guses
Z of dominant nucleus Its packing fraction, f Fermi kinetic energy of e's. Fermi kinetic energy of n's. Number density of e's.	31.3 -0.000559 9.2 MeV None 4.03×10 <sup>33</sup> cm <sup>-3</sup>	39.1 +0.000853 23.6 MeV 0.01 MeV 6.14×10 <sup>31</sup> cm <sup>-3</sup>	42.5 +0.001552 28.1 MeV 1.38 MeV 1.03×10 <sup>th</sup> cm <sup>-3</sup>	48.4 +0.002776 34.4 MeV 3.14 MeV 1.88×10 <sup>m</sup> cm <sup>-2</sup>	None None 4.64 MeV 3.84 MeV 5.90×10 <sup>28</sup> cm <sup>-3</sup>
Number density of nuclei,	1.29×10 <sup>22</sup> cm <sup>-3</sup>	1.57×10 <sup>aa</sup> cm <sup>-a</sup>	2.42×10 <sup>33</sup> cm <sup>-3</sup>	3.88×10 <sup>13</sup> cm <sup>-3</sup>	None
Volume occupation factor,  (n <sub>s</sub> /Z) 4πr <sub>0</sub> <sup>2</sup> A/3  Number density of free n's  Number density of free p's  Free baryons/bound baryons  Total baryon density  Electron pressure  Neutron pressure  Total pressure  Mass density (nuclei)  Mass density (n's)  Total mass density	0.818×10 <sup>-4</sup> None None 0 1.01×10 <sup>24</sup> cm <sup>-2</sup> 1.56×10 <sup>28</sup> g/cm sec <sup>2</sup> None 1.56×10 <sup>28</sup> g/cm sec <sup>2</sup> 1.67×10 <sup>29</sup> g cm <sup>-2</sup> None 1.67×10 <sup>29</sup> g cm <sup>-2</sup>	1.56×10 <sup>-1</sup> 10 <sup>32</sup> cm <sup>-2</sup> None 0.001 1.91×10 <sup>36</sup> cm <sup>-2</sup> 5.82×10 <sup>26</sup> g/cm sec <sup>2</sup> 10 <sup>24</sup> g/cm sec <sup>2</sup> 5.82×10 <sup>26</sup> g/cm sec <sup>2</sup> 3.18×10 <sup>31</sup> g cm <sup>-2</sup> 10 <sup>3</sup> g cm <sup>-2</sup> 3.18×10 <sup>31</sup> g cm <sup>-2</sup>	2.88×10 <sup>-2</sup> 0.583×10 <sup>36</sup> cm <sup>-2</sup> None 1.67 0.931×10 <sup>36</sup> cm <sup>-3</sup> 1.18×10 <sup>39</sup> g/cm sec <sup>2</sup> 0.516×10 <sup>30</sup> g/cm sec <sup>3</sup> 1.70×10 <sup>30</sup> g/cm sec <sup>3</sup> 0.580×10 <sup>15</sup> g/cm <sup>-2</sup> 0.975×10 <sup>35</sup> g/cm <sup>-3</sup> 1.56×10 <sup>35</sup> g/cm <sup>-3</sup>	5.94×10 <sup>-3</sup> 1.99×10 <sup>28</sup> cm <sup>-8</sup> None 2.74 2.71×10 <sup>28</sup> cm <sup>-8</sup> 2.62×10 <sup>28</sup> g/cm sec <sup>3</sup> 4.00×10 <sup>20</sup> g/cm sec <sup>2</sup> 6.62×10 <sup>28</sup> g/cm sec <sup>3</sup> 1.20×10 <sup>28</sup> g cm <sup>-3</sup> 3.34×10 <sup>28</sup> g cm <sup>-3</sup> 4.54×10 <sup>28</sup> g cm <sup>-3</sup>	None 2.71×10 <sup>28</sup> cm <sup>-2</sup> 5.93×10 <sup>28</sup> cm <sup>-3</sup> 2.71×10 <sup>28</sup> cm <sup>-2</sup> 1.20×10 <sup>27</sup> g/cm sec <sup>2</sup> 6.62×10 <sup>28</sup> g/cm sec <sup>3</sup> 6.62×10 <sup>28</sup> g/cm sec <sup>3</sup> None 4.54×10 <sup>28</sup> g cm <sup>-2</sup> 4.54×10 <sup>28</sup> g cm <sup>-2</sup>

<sup>&</sup>lt;sup>8</sup> Table constructed by K. S. T. <sup>9</sup> The free proton pressure is  $5.29\times10^{64}$  g/cm sec<sup>2</sup>. <sup>8</sup> The free proton mass density is  $0.989\times10^{9}$  g/cm<sup>3</sup>.

and neutrino neutrality,

$$E_e + E_p = E_n$$
, (307)

Here the symbol E implies rest energy plus kinetic energy. We found that this model, which we had originally introduced to describe matter at densities three times nuclear  $(\sim 3 \times [3 \times 10^{14}] \text{ or } 10^{15} \text{ g/cm}^3)$  and higher, gave also down at densities  $\sim 70$  times smaller than nuclear levels, at  $4.54 \times 10^{12} \text{ g/cm}^3$ , a pressure-density correlation identical to that obtained by use of the semi-empirical mass formula as indicaed in Table 14. Also the derivative  $dp/d\rho$  very nearly agreed between the two models at this point. Therefore we employed this three-gas model as a simple means to extrapolate the pressure-density relation from  $4.54 \times 10^{12} \text{ g/cm}^3$  to nuclear levels, in addition to using it to predict pressures at

nuclear and supranuclear levels.

At higher densities it is no longer possible to deduce the equation of state from simple arguments of thermodynamical equilibrium plus mass values estimated from the semiempirical mass formula. The substance becomes one giant nucleus. Compression to higher densities means compression of this nucleus. All of nuclear physics comes into play. To estimate the pressure-density relation in detail is out of the question at this time when it is difficult even to give a theoretical account good to 50 per cent of the absolute binding energy of nuclear matter at normal density! Salpeter (1960), Skyrme (1959), Cameron (1957, 1959a, b) and Hoyle (1946) have given some consideration to the equation of state at densities ranging from nuclear levels (3 × 1014 g/cm3) to 10 or 100 times that magnitude. Skyrme's equation (Skyrme 1959; Cameron 1959b) gives  $b = 7.8 \times$  $10^{34} \,\mathrm{g/cm} \,\mathrm{sec^2 \,at} \,\rho = 10^{15} \,\mathrm{g/cm^3} \,\mathrm{and} \,\rho = 6.4 \times 10^{37} \,\mathrm{g/cm} \,\mathrm{sec^2 \,at} \,\rho = 10^{16} \,\mathrm{g/cm^3}$ , and in between a nearly constant value of 2.9 for the logarithmic derivative d ln p/d ln p. The calculated speed of sound at the higher of these densities is thus  $(dp/d\rho)^{1/2} = (2.9 \times$  $6.4 \times 10^{87}/10^{16}$  = 4.3 times the speed of light. The obvious conflict with causality indicates some of the difficulty in describing repulsive nuclear interactions by an elementary instantaneous action at a distance (see discussion at end of chap, ix). Before the conflict with causality had become apparent, Cameron 1959b had employed Skyrme's equation of state in the general relativity equation of hydrostatic equilibrium to calculate the LOV critical point, finding  $M=2.01~M_{\odot},~R=8.1\times10^5~{\rm cm},~\rho_0=4\times10^{15}~{\rm g/cm^3}$  (cf. Figs. 5-7).

At high densities, and therefore high Fermi energies, a new kind of effect develops. Nucleons are promoted to hyperons. Also, more and more hyperonic states beome accessible as the Fermi energy rises. One can suppose that this increase in the number of accessible hyperonic states, makes it possible to accommodate more baryons than could be fitted into the same volume at the same Fermi energy if only the proton and neutron states were available. In other words, for a given and very high baryon density this effect might be thought greatly to lower the pressure. Following this line of reasoning in all strictness, and treating the various states as distinct and independent ideal Fermi gases, Ambartsumyan and Saakyan (1960) arrive at an asymptotic equation of state of the form  $\rho \sim \text{constant } n^{14/13}$ , or  $p^* \sim p^*/13$ . One cannot deny the conceivability of an asymptotic  $\gamma$  as low as  $\frac{1}{13}$ , and this value may even be correct. However, it is not obvious that baryons can evade the action of the Pauli principle by changing from a neutron to a  $\Lambda$ -hyperon or a  $\Xi$ -hyperon. It is not clear that these states are as nearly independent as that proposition would require. At ordinary nuclear densities it does not save neutrons and protons for the requirements of the exclusion principle to agglomerate into alpha-

particles!

In our calculations of an equation of state (Table 13 and eqs. [258]–[261]) at densities three times nuclear and higher (10th g/cm² and up) we have assumed for simplicity (and because we found no decisive indication favoring any alternative procedure) (1) that the

<sup>\*</sup>These effects have been considered by Cameron (1957, 1959a, b); by Ambartsumyan and Saak-yan (1960); and by Wheeler (1964).

pressure can be calculated as if it originated exclusively from electrons, protons, and neutrons, even at the very highest densities; and (2) the contributions of the nucleon-nucleon interactions themselves to the pressure are negligible at these densities compared to the contributions of the zero-point kinetic energies of the particles (see eq. [256] for the alternative assumption that the "soft hard core" dominates).

Specifically, our model assumed that nuclear matter at very high densities can be treated for the purpose of a pressure calculation as if it were an ideal mixture of three ideal Fermi gases, electrons, protons, and neutrons in statistical equilibrium at absolute zero temperature. Three conditions govern the equilibrium.

 Electrical neutrality demands that the number densities of electrons and protons be equal.

$$n_x = n_y$$
. (308)

But the number density is given by  $(8\pi/3h^3)$  times the cube of the Fermi momentum. Consequently the Fermi momenta of these two particles must agree:

$$p_{F_0} = p_{F_D}$$
, (309)

or

$$m c \sinh(t/4) = M_E c \sinh(\tau/4)$$
. (310)

Here  $\tau$  is the energy parameter for the protons. At very high energies the Fermi energy is given by  $cp_F$ . The rest mass drops out. Therefore the Fermi energies of electrons and protons come into agreement at very high compressions on the present elementary model.

2. The system must be neutrino-neutral; that is, beta-equilibrium must obtain; or

$$E_{Fe} + E_{Fp} = E_{Fn}$$
, (311)

where E includes in every case the rest energy. In terms of the energy parameter T of the neutrons this equation takes the form

$$m c^2 \cosh(t/4) + M_p c^2 \cosh(\tau/4) = M_n c^2 \cosh(T/4)$$
. (312)

The sum of the pressures of the three kinds of particles must balance the external pressure; or

$$\begin{split} p &= \frac{\pi \, m^4 c^5}{1 \, 2 \, h^3} \left( \sinh \, t - \, 8 \, \sinh \, \frac{t}{2} + \, 3 \, t \right) + \frac{\pi M_p^4 \, c^5}{1 \, 2 \, h^3} \left( \sinh \, \tau - \, 8 \, \sinh \, \frac{\tau}{2} + \, 3 \, \tau \right) \\ &\quad + \frac{\pi M_n^4 \, c^5}{1 \, 2 \, h^3} \left( \sinh \, T - \, 8 \, \sinh \, \frac{T}{2} + \, 3 \, T \right). \end{split}$$

The three conditions (310), (312), (313) for the three unknown energy parameters t,  $\tau$ , and T we dealt with parametrically, as follows: (1) A t-value is chosen. (2) Then the energy parameter for the protons is found from equation (310), and (3) the energy parameter for the neutrons is found from equation (312). (4) The pressure is calculated from equation (313), (5) The mass density is calculated from

$$\rho = \frac{\pi \, m^4 \, c^3}{4 \, h^3} \, \left( \sinh \, t - t \right) + \frac{\pi M_p^4 \, c^3}{4 \, h^2} \, \left( \sinh \, \tau - \tau \right) + \frac{\pi M_n^4 \, c^3}{4 \, h^3} \, \left( \sinh T - T \right). \tag{314}$$

(6) The number density of baryons is computed from

$$n = \frac{8\pi M_p^2 c^3}{3h^3} \sinh^3 \frac{\tau}{4} + \frac{8\pi M_n^3 c^3}{3h^5} \sinh^3 \frac{T}{4}.$$
 (315)

Where Equation 1s Relevant	Pressure in Terms of Density of Mass-Energy	Density of Mass-Energy in Terms of Baryon Density	Pressure in Terms of Baryon Density
<ol> <li>Fe<sup>86</sup> at ~10<sup>8</sup> g/cm<sup>3</sup> (free electron gas, non-relativistic)</li> </ol>	$b = \frac{8\pi}{15mh^3} \left(\frac{3h^3}{8\pi} \frac{26\rho}{56\mu_s}\right)^{5/3}$	$\rho = n\mu_x + \frac{8\pi}{10mc^2h^3} \left(\frac{3h^3}{8\pi}  \frac{26n}{56}\right)^{5/2}$	$p = \frac{8\pi}{15mh^3} \left(\frac{3h^3}{8\pi} \frac{26n}{56}\right)^{5/3}$
<ol> <li>Fe<sup>86</sup> at ~10<sup>6</sup> g/cm<sup>2</sup> (free electron gas, relativistic)</li> </ol>	$b = \frac{2\pi c}{3 h^3} \left( \frac{3h^3}{8\pi} \frac{26 \rho}{56 \mu_s} \right)^{4/3}$	$\rho = n\mu_s + \frac{2\pi}{h^3 c} \left( \frac{3h^3}{8\pi} \frac{26n}{56} \right)^{4/3}$	$p = \frac{2\pi c}{3h^2} \left( \frac{3h^3}{8\pi} \frac{26n}{56} \right)^{4/3}$
relativistic region	At a second control of the second control of	$\rho^* = \frac{GMn}{c^2} \left[ 1 + \left( \frac{3h}{4Mc} \right)^2 \left( \frac{3n}{8\pi} \right)^{2/3} \right]^{1/2}$	$p^* = \frac{GMn}{3c^2} \frac{(3h/4Mc)^2 (3n/8\pi)^{2/3}}{[1 + (3W/4Mc)^2 (3n/8\pi)^{2/3}]^{1/3}}$
<ol> <li>Ideal gas composed of neutrons (or any one fermion!) at relativistic energies (speed of sound=c/3<sup>1/9</sup>)</li> </ol>	CONTRACTOR CONTRACTOR	$\rho^* = (3^{4/2}\pi^{2/2}/4)L^{*2}n^{4/2}b$	$p^* = (3^{1/3}\pi^{2/3}/4)L^{*3}n^{4/3}b$
<ol> <li>Maximum pressure con- ceivable for highly com- pressed matter (speed of sound=e)</li> </ol>	$\rho^* = \rho^*$	$\rho^* = 4\pi \left(\frac{G}{\varepsilon^2}\right) g^2 \left(\frac{\hbar}{m_\pi c}\right)^2 n^2$	$p^* = 4\pi \left(\frac{G}{c^2}\right) g^2 \left(\frac{\hbar}{m_\pi c}\right)^2 n^2$
5. Opposite limiting case of zero pressure (dust; ideali- zation of Friedmann uni- verse)	b* = 0	$\rho^* = n\mu_s^*$	$p^* = 0$
<ol> <li>Simple analytic expression reducing to ρ=ρ<sub>0</sub> at zero pressure and to form 4 at high pressure</li> </ol>	$\phi^* = (\rho^* - \rho_0^*)/3$	$\rho^* = (\rho_0^*/4) [3(n\mu_s^*/\rho_0^*)^{4/3} + 1]$	$p^* = (\rho_0^*/4)[n\mu_s^*/\rho_0^*)^{4/3} - 1]$
<ol> <li>Simple analytic expression reducing to ρ = ρ<sub>0</sub> at zero pressure and to form 5 at I high pressure</li> </ol>	$b^* = (\rho^* - \rho_0^*)$	$\rho^* = (\rho_0^*/2)[(n\mu_s^*/\rho_0^*)^2 + 1]$	$p^* = (\rho_0^*/2)[(n\mu_s^*/\rho_0^*)^2 - 1]$

<sup>\*</sup> The equation of state is known or calculable at densities from 7.8 g/cm² up to nuclear densities,  $\sim 3 \times 10^{16}$  g/cm². Of the numerous regimes in this range, (details in text) only those two regimes for which the analytic expressions are simplest are listed in the present table (rows I and 2). At supranuclear density the equation of state is unknown—hence the variety of conceivable limiting forms (4, 5, 6) for the equation of state listed here, ranging from  $p^{2n} = p^{2n}$  (speed of sound equal to speed of light) down to zero pressure. Rows 7 and 8 give simple analytic expressions which (a) have the limiting forms of 4 and 5 at high compression and yet (b) reduced to  $p = p_0$  at zero pressure. Notation,  $p(g, \text{cm}^2) = p^2 / \text{cm}^{2n} = (G/e^2)p_0$ , pressure; n, number of baryons per cm<sup>2</sup>, m, mass of electron;  $p_0$ , mass of neutral atom of  $F(e^n, \text{divided by } 56$ ;  $p^2 \text{(cm)} = (G/e^2)p_0 / \text{(m)} = (G/e^2)p_0 /$ 

pointed out by Zel'dovich to be conceivable at very great compressions; gt (dimensions g cmt/sect), the square of the charge-like coupling constant in this theory.

b When the ideal neutron gas is replaced by a mixture of three ideal Fermi gases—electrons, protons, and neutrons—with extreme relativistic Fermi energies (rest plus kinetic!) as required for charge neutrality  $(E_0 - E_0)$  and beta-equilibrium  $(E_0 - E_0)$  and the three kinds of particles have number densities  $n_s = n_P = n/9$  and  $n_B = 8n/9$  (for neutrons right times the volume in phase space, twice the Fermi momentum, and twice the Fermi energy of protons!). Then an extra factor  $(1/9)^{1/2} + (1/9)^{1/2} + (8/9)^{1/2}$  is to be inserted on the right-hand side of these expressions for  $s^*$  and  $s^*$  in terms of n (pressure lowered 4 per cent by permitting ideal neutron gas to transform to neutrino-neutral equilibrium!).

This is how the numbers were calculated which appear in Table 13 from  $p = 4.54 \times 10^{12}$ 

g/cm3 to the highest densities.

At very high densities the model gives Fermi energies and momenta for electrons and protons which are equal to each other and equal to half the Fermi energy and momentum, respectively, of a neutron (cf. eq. [312]). In consequence, the calculated number densities of the three kinds of particles stand to each other asymptotically in the ratio  $n_s:n_p:n_a::1:1:8$ . This and other limiting situations and alternatives are summarized in Table 15, which gives simple expressions for the "universal equation of state" of cold, neutrino-neutral matter catalyzed to the end point of thermonuclear evolution.

This ends the summary, regime by regime, of the methods used in calculating the pressure-density relation of Table 13. That numerical equation of state, summarized in the analytical fits of equations (258)–(261), was used in the 1957 (M. W.) and 1964 (B. K. H.) calculations of equilibrium configurations which are presented in Figures 5–7 and Appendix A. We do not know how to make any improvement in this equation of state which will be at the same time substantial and reliable. However, we do offer a simplification of the equation of state which is appropriate for calculations that are willing to overlook the first critical point in the critical mass diagram (the critical point which has to do with the crushing of electrons onto nuclei). This simplified equation of state idealizes the medium to be a neutron gas. It differs from the rather complicated but exact equation of Chandrasekhar (cf. eqs. [276]–[278]) which describes the full range of behavior, non-relativistic and relativistic, in this respect: It gives a pressure which is too low by the factor \(\frac{15}{16}\) (7 per cent error) in the non-relativistic domain, but is asymptotically correct in the relativistic domain. To obtain this formula, one notes that the relation between number density and density of mass-energy in the extreme relativistic domain is (eq. [36]; limiting form of eqs. [276]–[278])

$$\rho^* (\text{cm}^{-2}) = (3^{4/3}\pi^{2/3}/4)L^{*2}n^{4/2},$$
 (316)

with  $L^*$  equal to the Planck length of Table 2. In the opposite limiting case of dispersed granules of Fe<sup>36</sup>, the appropriate formula is

$$\rho^* (\text{cm}^{-1}) = \mu_s^* n$$
, (317)

with  $\mu_s$  ( $\frac{1}{56}$  of mass of Fe<sup>56</sup>) given in Table 2. From two different sides steps have been taken to get a simpler equation to cover the entire region (Zel'dovich [1961], eq. [6.5]; Wheeler [1964], eq. [127]). We combine the features of both approaches and write

$$\rho_{ZW}^{*} = \left[ \mu_{*}^{*2} n^{2} + \left( 3^{8/3} \pi^{4/3} / 16 \right) L^{*4} n^{8/2} \right]^{1/2}. \tag{318}$$

This is the suggested approximation for dealing with equilibrium configurations when one is willing to look apart from electron crush and concentrate on the equilibrium configurations with central densities of 10<sup>13</sup> g/cm<sup>3</sup> or more.

In the non-relativistic domain equation (318) gives

$$\rho_{ZW}^* \simeq \mu_s^* n + (3^{8/2}\pi^{4/8}/32)(L^{*4}/\mu_s^*)n^{5/3}$$
(319)

and

$$p_{ZW}^* \simeq (3^{5/3}\pi^{4/3}/16)(L^{*4}/\mu_s^*)n^{5/3}$$
 (320)

as compared to the correct formula (cf. appropriate limiting cases of eqs. [276] and [278]) for an ideal cold neutron gas in the low-pressure limit,

$$p^* = (3^{5/3}\pi^{4/3}/15)(L^{*4}/\mu_s^*)n^{5/3}$$
. (321)

As an alternative to equation (318) with its semi-theoretical background one can employ the formula  $\rho = \rho(n)$  given in equation (264). It has no such simple derivation as equation (318). It is obtained from equation (318) by changing the exponents and con-

stants. These numbers are selected to give the best fit achievable by an expression of this form to the values for  $\rho = \rho(n)$  of Table 13 in the domain where  $\rho$  departs from close proportionality to n. The values in Table 13 are based on an analysis of the situation more detailed than that which led to equation (318). Therefore, equation (264) is preferable to equation (318) for computational work.

The theory and details of the equation of state have been reviewed in the last two chapters; the theory and details of equilibrium configurations, in chapters vi and vii. Out of the combined analysis it is appropriate to pick out one or two representative points in Table 16. They recall the original objective—to find the lowest energy state of an

#### TABLE 16

#### FEATURES OF EQUILIBRIUM CONFIGURATIONS FOR SELECTED A-VALUES\*

Mass Number, Mass, Radius, and Central Density

A from 1 to  $\sim 10^5$ M from  $1.6 \times 10^{-24}$  g to  $\sim 10^{-19}$  g R from  $10^{-8}$  cm to  $\sim 10^{-4}$  cm  $\rho_0$  at first fluctuating, then settling down to 7.85 g/cm<sup>3</sup>

A from  $\sim 10^5$  to  $\sim 3.2 \times 10^{38}$ M from  $\sim 10^{-19}$  g to  $\sim 5.3 \times 10^{14}$  g R from  $\sim 1.7 \times 10^{-7}$  cm to  $\sim 2.5 \times 10^4$  cm  $\rho_0$  close to 7.85 g/cm<sup>3</sup> except near upper limit of this regime, where  $\rho_0$  increases slightly

A from  $\sim 3.2 \times 10^{18}$  to  $\sim 7.3 \times 10^{16}$ M from  $\sim 5.3 \times 10^{14}$  g to  $\sim 1.2 \times 10^{23}$  g R from  $\sim 2.5 \times 10^{4}$  cm up to  $\sim 1.8 \times 10^{8}$  cm and back down to  $\sim 9 \times 10^{7}$  cm  $\rho_0$  from a little more than 8 g/cm<sup>3</sup> up to  $4.5 \times 10^{12}$  g/cm<sup>3</sup>

A from 7.3 × 10<sup>101</sup> down to 2.2 × 10<sup>101</sup>, up to Neutron gas forms beyond Y<sup>122</sup>. With increas-8 × 10<sup>101</sup>, then oscillations of decreasing amplitude approaching 5 × 10<sup>101</sup> more of the pressure. For all A between

M from  $1.2 \times 10^{33}$  g down to  $0.4 \times 10^{33}$  g, up to  $1.3 \times 10^{33}$  g, then oscillations of decreasing amplitude approaching  $0.8 \times 10^{23}$  g

R reaches maximum of 3 × 10<sup>8</sup> cm, minimum of 5 × 10<sup>8</sup> cm, then oscillates with decreasing amplitude approaching 6 × 10<sup>5</sup> cm ρ<sub>0</sub> from 4.5 × 10<sup>12</sup> g/cm<sup>3</sup> to ∞

A greater than  $A_{\rm em} \sim 1.4 \times 10^{57}$ 

Features of Ground-State Configuration

Individualistic collection of atoms, all Fe<sup>50</sup> only if A is an integral multiple of 56, otherwise individual mass numbers fluctuate about 56 by an amount which is the smaller the greater A is. These atoms held together by chemical forces

Mass of practically pure Fe<sup>36</sup> held together primarily by chemical forces,  $6.6 \times 10^{-12}$  erg/atom or  $7.1 \times 10^{10}$  erg/g or  $5.5 \times 10^{11}$  erg/cm<sup>2</sup>. Central pressure caused by gravitational forces,  $p_0 = (2\pi/3)$   $Gp^2R^2$ , is negligible by comparison for small radius R but grows as  $R^2$  and compares with energy density of chemical forces at upper limit of this regime

Pressure of gravitational forces squeezes down atomic volume at center of system, raising electronic energy, until at upper limit of this regime, electrons gain relativistic energies, combine with more loosely bound nuclear protons to form neutrons, alter equilibrium nuclear constitution step-by-step away from Fe<sup>36</sup> to Y<sup>125</sup>, on line of neutron drip

Neutron gas forms beyond Y<sup>127</sup>. With increasing central density this gas carries more and more of the pressure. For all A between  $A_{\text{quantum}}$  (some tons) and  $A_{\text{eff}} \sim 1.4 \times 10^{10}$  there exists a potential energy barrier which must either be tunneled (fantastically low probability) or surmounted (by supplying energy to the system through implosion or otherwise) to initiate collapse

No equilibrium configuration No barrier against collapse No escape from collapse

These features of the configurations of equilibrium for cold, catalyzed matter are deduced from the equation of state of this chapter and the numerical integrations of the general relativity equation of hydrostatic equilibrium reported in chap, vi and Appendix A.

A-baryon system—and the warning which has emerged from the investigation up to this point: none of these configurations represents the truly lowest energy state of an Abaryon system. For that, it is necessary to look at collapsing configurations,

#### REFERENCES

Albada, G. B. van. 1946, Bull. Astr. Inst. Netherlands, 10, 161.

1947, Ap. J., 105, 393.
Ambartsumyan, V. A., and Saakyan, G. S. 1960, Astr. Zhur., 37, 193 (English translation in Soviet Astr.,

Auluck, F. C., and Mathur, C. S. 1959, Zs. f. Ap., 48, 28.

Birch, F. 1963, in Solids under Pressure, ed. W. Paul and D. M. Warschauer (New York: McGraw-Hill Book Co.).

Boyd, F. R., and England, J. L. 1963, in Annual Report of the Director of the Geophysical Observatory for 1962-1963 (Washington, D.C.: Carnegie Institution of Washington).
 Brandt, W., Fuller, R., Wakano, M., Werner, F. G., and Wheeler, J. A. 1960, in Proceedings of the International Conference on Nuclidic Masses (Toronto: University of Toronto Press).

Cameron, A. G. W. 1957, Canadian J. Phys., 35, 1021.

Cameron, A. G. W. 1957, Canadian J. Phys., 35, 1021.

1959a, Ap. J., 129, 676.
1959b, Ibid., 130, 884.

Chandrasekhar, S. 1934, Observatory, 57, 373.
1935, M.N., 95, 207.
1939, Introduction to the Study of Stellar Structure (Chicago: University of Chicago Press).

Feynman, R. P., Metropolis, N., and Teller, E. 1949, Phys. Rev., 75, 1561.

Goeppert-Mayer, M., and Teller, E. 1949, Phys. Rev., 76, 1226.

Green, A. E. S. 1955, Nuclear Physics (New York: McGraw-Hill Book Co.).

Harrison, B. K. 1965, "Asymptotic Behavior of Cold Superdense Stars," Phys. Rev. (to be published).

Harrison, B. K., Wakano, M., and Wheeler, J. A. 1958, in Onzième Conseil de Physique Solvay, La Structure et l'évolution de l'univers (Brussels: Stoops).

Hoyle, F. 1946, M.N., 106, 343.
Knopoff, L. 1963, in High Pressure Physics and Chemistry, ed. R. S. Bradley (New York: Academic Press).

Landau, L. D. 1932, Phys. Zs. Sowjetunion, 1, 285.

McQueen, R. C., and Marsh, S. P. 1960, J. Appl. Phys., 31, 1253. Oppenheimer, J. R., and Serber, R. 1938, Phys. Rev., 54, 530. Oppenheimer, J. R., and Volkoff, G. M. 1939, Phys. Rev., 55, 374. Saipeter, E. E. 1960, Ann. Phys., 11, 393.

. 1961, Ap. J., 134, 675. Schatzman, E. 1958, Hdb. d. Phys., ed. S. Flügge, Vol. 51 (Berlin: Springer-Verlag).

Skyrme, T. H. R. 1959, Nuclear Phys., 9, 665.

Takehashi, T., and Bassett, W. A. 1964, Science, 145, 483.
Werner, F. G., and Wheeler, J. A. 1958, Phys. Rev., 109, 126.
Wheeler, J. A. 1962, Geometrodynamics (New York: Academic Press).

1964, in Gravitation and Relativity, ed. H. Y. Chiu and W. F. Hoffmann (New York: W. A. Benjamin).

Zel'dovich, Ya. B. 1961, Zhur. Eksp. Teor. Fiz., 41, 1609 (English translation in Soviet Phys.—J.E.T.P., 14, 1143, 1962).

### chapter 11 GRAVITATIONAL COLLAPSE-TO WHAT?

#### CURVATURE NEARLY TO CLOSURE THE THEME OF THE ANALYSIS

Curvature, curvature, curvature! Curvature is the key to the statics of gravitational collapse, to the dynamics of infall, and to the quantum world of collapse and post-collapse phenomenology.

Curvature at a moment of time symmetry, extending over a volume sufficiently close to  $V_{\rm crit} = 2\pi^2$  (radius of curvature)<sup>3</sup> (Fig. 15 and chap, viii) makes an arbitrarily large number of baryons manifest to the outside world an arbitrarily small amount of mass-

energy.

Curvature evolving classically with time according to classical theory from a moment of time symmetry reaches in a finite proper interval an infinite magnitude—the nub of

all concern about the issue of gravitational collapse.

Finally, curvature the intensive quantity—and 3-geometry, <sup>(3)</sup> G, the extensive object and the carrier of curvature—do not evolve deterministically with time and do not reach infinite values. This is the message of quantum physics, however far one is today from unraveling its consequences. One is not permitted to say that the 3-geometry has this, that, or the other form. One speaks instead of the probability amplitude  $\psi = \psi(^{(3)} G)$  for this, that, or the other  $^{(8)} G$ . One does not forecast an outcome for gravitational collapse any more than one predicts the angle of emergence of an electron from a collision with a hydrogen atom! Instead one seeks in both cases to calculate the probability distribution of outcomes,

This final section of the report takes up those two of these three topics that have not been dealt with so far. It reviews the evolution of curvature with time up to the stage where the system becomes strongly quantum in character. Then it analyzes the possible outcomes. It ends with the conclusion that gravitational collapse is an inescapable phenomenon, not in large-scale physics alone, but also in elementary-particle physics; that matter has its own low but characteristic and non-zero radioactive decay rate for spon-

taneous transformation to the collapsed state.

Inescapable? Inescapable unless what is wrong with the principles of analysis that have been adopted? The decisive point in the reasoning is the idea that mass-energy curves space according to the simple elementary law of equation (2), a principle as simple as the law div  $E=4\pi\rho$  in electrostatics. This granted, a distribution of matter which is uniform in density and which is sufficiently extensive cannot fail to curve space up arbitrarily close to closure; it cannot fail to manifest to the outside an arbitrarily small gravitational pull. Curvature really comes into its own in the subject of gravitational collapse. Except for the prediction of Einstein's theory about the expansion and recontraction of the universe, all the other applications of general relativity (precession of perihelion, redshift, bending of light, gravitational radiation) as normally envisaged have to do with small departures from flatness. Not so here. Collapse produces geometries almost as far as can be from flatness. Any perturbation-theoretic expansion in powers of the departure from flatness is out of place. If one intends to abandon relativity, here is the place to do so. Otherwise he is on the way into a new world of physics, both classical and quantum. Here we go!

#### TIME SYMMETRY AND COLLAPSE FROM INFINITY RECONCILED

Let us first examine the dynamics of collapse. Already at the start an issue of principle presents itself. The geometry will develop infinite curvature as time advances, according to classical theory. Yet it started static. The initial conditions were taken to be time-symmetric (chaps, ii-viii). Therefore the entire past is the time-reversed image of the future. When classical geometrodynamics predicts physically impossible conditions at a finite time in the future, it must therefore predict equally violent curvatures at a finite time back in the past. Then how could the system even have got started off in the first place on its way to explosion, the instant of rest, and reimplosion? And therefore, why bother to deal with a problem that can never arise?

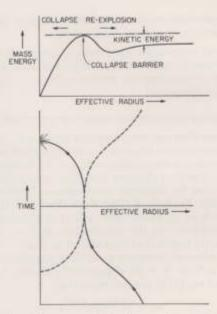


Fig. 20.—A motion which is not time symmetric (solid curve for effective radius of configuration as a function of time) obtained from an analysis of the equations of motion that deals with solutions which are time symmetric. In the transition zone at the summit of the barrier the motion departs slightly from time symmetry. However, the behavior near this point of equilibrium is so standard  $(R = R_0 - \epsilon \sinh at)$  that no issues of principle arise in the analysis.

A closer look (Fig. 20) shows that there are two ways into collapse in one of the principal cases of interest ( $A_{\rm quantum} < A < A_{\rm crit}$ ). Here a barrier—the "collapse barrier"—separates the normal position of equilibrium from the collapsing state. The top of the barrier corresponds to a configuration of unstable equilibrium. When the system has slightly less than this critical energy ( $E = E_0 - \epsilon$ ) and a lesser than critical size, the calculated dynamics is expansion, momentary rest just short of the summit, and reimplosion. Small displacements x to the left of the summit are connected with the time t by an equation familiar from elementary mechanics,

$$(dx/dt)^2 = -\epsilon + \alpha^2 x^2, \qquad (322)$$

with a solution of the form

$$x = (\epsilon^{1/2}/2\alpha)(e^{at} + e^{-at})$$
 . (323)

When the system has slightly more than the critical energy  $(E = E_0 + \epsilon)$ , implosion all the way from a condition of infinite dilution is a possible motion. The velocity of passage over the summit is very low. It is given for small x by an equation of the form

$$(dx/dt)^2 = \epsilon + \alpha^2 x^2, \qquad (324)$$

with the solution

$$x = (e^{1/2}/2a) (e^{at} - e^{-at})$$
. (325)

The conditions of motion on the way in after passing the summit differ from those in the case  $E = E_0 - \epsilon$  by an amount that can be made as small as one pleases (for all x greater than some fixed  $x_0 > 0$ ) by making  $\epsilon$  sufficiently small. Therefore:

Theorem 34: The time-symmetric motion, after the moment of time symmetry, gives an arbitrarily good representation of collapse from infinity.

More generally, it is not necessarily legitimate to object on principle to a motion, which ends in puzzling physical conditions, on the ground that it also starts from a fog. For example, the mystery surrounding the earliest minutes of the universe is no bar to the study of its subsequent dynamics!

#### GEOMETRIC DESCRIPTION OF COLLAPSE OF CLOUD OF DUST; THE FRIEDMANN REGION

Only in one idealized case does one have an exact solution for expansion to an instant of time symmetry and recontraction; the case of a cloud of dust of uniform density. Here there is no pressure to complicate the problem  $(A_{crit} = 0; A \text{ always greater than } A_{crit}!)$ . How the radius of the cloud of dust changes with time, and with it the density and the geometry, has been analyzed by different investigators (Tolman 1934; Oppenheimer and Snyder 1939; Klein 1961; Beckedorff 1962; Beckedorff and Misner 1962). Most useful for the present purpose is an approach close to that of Tolman and of Beckedorff and Misner, with minimum emphasis on the coordinates, and maximum attention to the geometry itself. The geometry inside the cloud of dust is identical to that in Friedmann's spherical universe, The radius of curvature  $a_0$  at the moment of time symmetry is connected with the density  $\rho_0^*(\text{cm}^{-2}) = (G/c^2)\rho_0(g/\text{cm}^3)$  at that instant by the relation (based on the fundamental eq. [2] of general relativity)

$$a_0 = (3/8\pi \rho_0^*)^{1/2}$$
, (326)

The radius varies with time according to the equation of a cycloid; in parametric form,

$$a = (a_0/2)(1 + \cos \eta)$$
,  
 $t = (a_0/2)(\eta + \sin \eta)$ .
(327)

The 4-geometry is described by the formula

$$ds^{2} = a^{2}(\eta)[-d\eta^{2} + d\chi^{2} + \sin^{2}\chi (d\theta^{2} + \sin^{2}\theta d\phi^{2})]$$
 (328)

for the proper distance between each point and its immediate neighbors.<sup>3</sup> In the complete Friedmann universe the hyperspherical angle  $\chi$  runs from 0 to  $2\pi$ . Here it runs from  $\chi=0$  (center of the cloud of dust) to  $\chi=\chi_0$  (surface of the cloud; proper circumference  $2\pi R=2\pi a\sin\chi_0$ ). As time goes on, each point keeps its hyperspherical coordinates  $\chi$ ,  $\theta$ ,  $\varphi$  and keeps its place on the hypersphere. The motion of the particles relative to

<sup>&</sup>lt;sup>1</sup> For an illuminating commentary on Tolman's approach and significant additional conclusions see Zel'dovich (1962).

<sup>\*</sup> For an interesting review of this topic, see Zel'dovich (1963).

<sup>\*</sup> For a review as to how this local information relates to the over-all geometry, see, e.g., Marzke and Wheeler (1964).

each other is most conveniently visualized in terms of the 3-sphere being first blown up and then deflated. The quantity t measures the proper time, after the phase of the maximum, as sensed by any of these particles. The interval of time, dt, (cm), is connected with the increment of the time parameter,  $d\eta$ , by the relation

$$dt = a(\eta)d\eta. (329)$$

In contrast to the dust particles, a photon moves from place to place on the hypersphere. When the photon is traveling radially outward from the center of the cloud of dust,  $\theta$  and  $\varphi$  stay constant, and  $\chi$  increases in such a way as to annul the element of proper distance ds; thus,

$$d\chi = d\eta = dt/a. \qquad (330)$$

A photon starting at the point  $\chi=0$  in the complete Friedmann universe can just make its way around to the antipodal point  $\chi=\pi$  in the time from the phase of maximum  $(\eta=0)$  until final collapse  $(\eta=\pi)$ . In the case of the cloud of dust, the same photon emerges from the matter at  $\chi=\chi_0$  at the earlier value of the time parameter  $\eta=\chi_0$ . Thus radial light rays appear on a  $(\chi,\eta)$  diagram as lines inclined at 45° (left-hand portion of Fig. 21). In such a diagram the dynamics of the particles does not appear on the

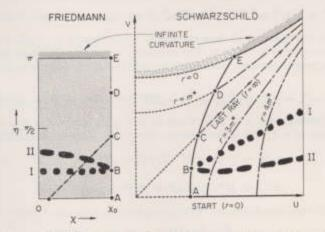


Fig. 21.—Join between the Friedmann geometry interior to a cloud of dust and the Schwarzschild geometry exterior to it, along the world line of the outermost particle (ABCDE). In both regions such coordinates are used that radial light rays have  $45^\circ$  slope. In the inner region (sector of angular opening  $\chi_0$  cut out of the expanding and recontracting spherical universe of Friedmann) every dust particle—and in particular the outermost one, at  $\chi_0$ —keeps its coordinates,  $\chi$ ,  $\theta$ ,  $\varphi$ , as the recontraction gathers speed (radius of curvature shrinking according to the law  $a|\eta| = |a_0/2|[1 + \cos\eta]$ ; here  $\eta$  is a time coordinate such that  $d\chi^2 - d\eta^2 = 0$  for light rays). In the outer region the coordinates, u, v of Kruskal are employed ( $du^2 - dv^2 = 0$  for light rays) so as to show the entirety of the spacetime geometry, although the Schwarzschild (r,t) coordinates are also shown where they are applicable. A spacelike hypersurface which in the Schwarzschild representation has constant t coordinate shows here as a straight line which projects back to the origin of the (u,v) diagram. The outermost particle, despite the appearance of its world line as one first looks at the Kruskal diagram, is evidently falling inward as it ages. After stage C of its history it can no longer send retarded radiation to a faraway observer. The curved-space geometry in which this particle moves is perfectly regular up to the stage E, where the curvature finally becomes infinite. I: Spacelike slice through geometry taken at constant value of time coordinate  $\eta$  in Friedmann region and constant value of I in Schwarzschild region. Outside the dust, the 3-geometry on this slice is  $(1-2M^*/r)^{-1}dr^2 + r^2(d\theta^2 + \sin^2\theta d\varphi^2)$ , where  $M^*$  represents the mass-energy of the system, a constant of the motion. II: Spacelike slice with these remarkable properties. (1) The 3-geometry outside has Schwarzschild character, but with a different and smaller mass-energy  $M_1$ , the difference  $M^* - M_1$ , being the general-rela

drawing. One has to remind himself of their motion by recalling that the scale factor a between angle,  $d\chi$ , and distance,  $ad\chi$ , is shrinking as the time parameter increases. A particle on the surface is by no means stationary with respect to its neighbors just because it has the same coordinates  $\chi = \chi_0$ ,  $\theta$ ,  $\varphi$  at successive instants, A, B, C, D, E in its life-history!

The particle A, B, C, D, E lives at the boundary between two geometries and belongs to both of them.

THEOREM 35: For particles at the interface between two 4-geometries to follow simultaneously the geodesic laws of motion appropriate to the two separate geometries is a necessary and sufficient condition that the geometries should join smoothly at the interface.

The basic ideas for a proof are given by Lindquist and Wheeler (1957); see also Beckedorff (1962) and Beckedorff and Misner (1965).

#### GEOMETRIC DESCRIPTION OF COLLAPSE OF CLOUD OF DUST; THE SCHWARZSCHILD REGION

The geometry outside the cloud is spherically symmetric. No radiant energy is flowing in or out, by assumption. Therefore, the mass-energy keeps the constant value

$$M^* = (4\pi/3)\rho_0^* R^3 = (4\pi/3)\rho_0^* a_0^3 \sin^3 \chi_0 = \frac{1}{2}(3/8\pi\rho_0^*)^{1/2} \sin^2 \chi_0$$
, (331)

appropriate to the moment of time symmetry, even though the radius and the density thereafter both change with time. The geometry outside is therefore that of Schwarzschild, with a proper distance from event to event which in Schwarzschild's coordinates is given by

$$ds^2 = -(1 - 2M^*/r)dt_{Sch}^2 + (1 - 2M^*/r)^{-1}dr^2 + r^2(d\theta^2 + sin^2\theta d\phi^2)$$
, (332)

In conformal coordinates  $x = \rho \sin \theta \cos \varphi$ ,  $y = \rho \sin \theta \sin \varphi$ ,  $z = \rho \cos \theta$ —or, more simply, in terms of  $\rho$ ,  $\theta$ , and  $\varphi$  themselves—the proper distance takes the form

$$\begin{split} ds^2 &= -(1 - M^*/2\rho)^2 (1 + M^*/2\rho)^{-2} dt_{\rm lich}^2 \\ &+ (1 + M^*/2\rho)^4 (d\rho^2 + \rho^2 d\theta^2 + \rho^2 \sin^2 \theta d\varphi^2) \;. \end{split} \tag{333}$$

Kruskal (1960) (see also Fronsdal [1959]) employs coordinates u and v, with

$$u^{z} - v^{z} = [(r/2M^{*}) - 1] \exp(r/2M^{*})$$
 (334)

and

$$2uv/(u^2+v^2) = \tanh(t_{Sch}/2M^*)$$
 (whenever  $t_{Sch}$  is defined). (335)

He defines a function f of  $(u^2 - v^2)$  through the equation

$$f^2 = (32M^{*3}/r) \exp(-r/2M^*)$$
. (336)

<sup>4</sup> Birkhoff (1923) proves that every centrally symmetric geometry which is free of mass-energy is static and identical up to a coordinate transformation with the geometry defined by the Schwarzschild metric. Petrov (1963) gives counterexamples where gravitational shock waves satisfy the condition of spherical symmetry but produce substantial departures from the Schwarzschild geometry. It is not clear what is the relation between these shock waves of Petrov and ordinary gravitational radiation which, like electromagnetic radiation, can never be spherically symmetric (no way to have amplitude constant and polarization smoothly varying in direction over the surface of a sphere). However, all forms of transport of energy, including radiation and shocks, are explicitly excluded from the present example, so Birkhoff's result applies. How far the Schwarzschild metric, nevertheless, is from being "static" appears from the discussion in the text. Note added in proof: Petrov's solution has now been shown (Hamoui [1964], Komar [1965]) to be nothing more than the Schwarzschild solution itself, expressed in terms of non-analytic coordinates.

In Kruskal's coordinates the proper distance from point to point is given by

$$ds^2 = f^2(-dv^2 + du^2) + r^2(u, v)(d\theta^2 + \sin^2\theta d\phi^2).$$
 (337)

Of special interest is the 3-geometry at the moment of time symmetry,  $l_{Seh} = 0$ , or v = 0. The nature of this geometry shows most clearly in the conformal coordinates. The proper circumference of a circle with the coordinate  $\rho$  is

$$2\pi r = 2\pi \rho (1 + M^*/2\rho)^2. \tag{338}$$

This quantity is big for large  $\rho$ , but also again for small  $\rho$ . The minimum value, obtained for  $\rho = M^*/2$ , is—after division by  $2\pi$ —

$$r_{\min} = 2M^*$$
. (339)

The geometry consists of two nearly Euclidean spaces connected by a throat. This geometry is illustrated in Figure 15 and in the insert in Figure 11. One and the same triplet of numbers r,  $\theta$ ,  $\varphi$  (with  $r > r_{\min} = 2M^*$ ) corresponds to two points in the 3-geometry, one on the "upper" quasi-Euclidean space, the other on the "lower" portion. Despite this disadvantage, the r coordinate of Schwarzschild has one important advantage. When multiplied by  $2\pi$  it gives directly the proper circumference which is run through in a rotation (a mathematical rather than a physical operation, because the successive displacements  $rd\theta$  are spacelike, not timelike). For this reason the diagrams in Figures 11 and 15 are so constructed that r appears as distance from an axis of rotation.

To obtain proper distance in a rotation  $d\theta$  it is correct to evaluate  $rd\theta$  but not correct to calculate the product  $\rho d\theta$ . Nevertheless  $\rho$  is a useful coordinate in this sense: it tells whether the point in question is on the lower ( $\rho$  from 0 to  $M^*/2$ ) or upper ( $\rho$  from  $M^*/2$  to  $\infty$ ) quasi-Euclidean space, as well as telling indirectly the proper distance  $rd\theta$  in a rotation, through the formula

$$r = \rho + M^* + (M^{*2}/4\rho)$$
, (340)

The identity in character of the parts of the 3-geometry above and below the throat shows through the possibility of labeling points with a new coordinate,

$$\rho' = (M^{*2}/4\rho)$$
, (341)

symmetrically related to  $\rho$ ,

$$r = (M^{*2}/4\rho') + M^* + \rho',$$
 (342)

but such that  $\rho'$  on the upper part of the geometry is less than  $M^*/2$ .

The mirror relationship of the upper and lower portions of the "hypersurface of time symmetry" shows still more clearly when one uses the Kruskal coordinate u (eqs. [334]–[337]). It is zero at the throat itself. This coordinate has equal magnitudes but opposite signs for two symmetrically related points on the upper (u positive) and lower (u negative) portions of the hypersurface.

# A TWO-DIMENSIONAL MODEL FOR THE SCHWARZSCHILD GEOMETRY AT A MOMENT OF TIME SYMMETRY

Imagine a long, thin-walled tube of soft copper and of substantial diameter. Further, picture as inked onto the outer surface of this tube a family of lines parallel to the axis, marked  $\theta = 30^{\circ}$ ,  $\theta = 60^{\circ}$ , ...,  $\theta = 360^{\circ} \approx 0^{\circ}$ , and in addition a family of circles,  $u = \dots, -2, -1, 0, 1, 2, \dots$  The tube is now gripped halfway along its length, at u = 0; and both ends are flared out with the help of a spinning tool, almost to flatness, like the bell

<sup>5</sup> For a more detailed discussion of this geometry and its time development with diagrams, see Fuller and Wheeler (1962).

of a trumpet. One ends up with a tangible model for the hypersurface in question. It has one deficiency. There is only one angle of rotation,  $\theta$ , in the model, whereas there are two,  $\theta$  and  $\varphi$ , on the hypersurface. This use of a two-dimensional model to represent a three-dimensional space will serve as introduction for still a further step in schematizing the geometry. Now let the entire 3-geometry of Schwarzschild at the moment of time symmetry be represented by the single line which runs from  $u=-\infty$  (big r!) to  $u=+\infty$  (again big r!) with the throat ( $r=2M^*$ ) at u=0. The two angles  $\theta$  and  $\varphi$  are to be supplied in one's imagination, as similarly in the model *one* of the two angles was to be provided.

Referring now to the right-hand portion of Figure 21, one has in the line v=0, that is, in the u axis itself, a schematic representation in the foregoing sense of the 3-geometry at the moment of time symmetry. More precisely, this line, extending from  $u=-\infty$  to  $u=\infty$ , is a section,  $\theta={\rm const}$ ,  $\varphi={\rm const}$ , of the 3-geometry. To gain some feeling for what it means to change  $\varphi$  or  $\theta$ , say by making the change  $\theta\to\theta+d\theta$ , one can note that one has shifted his attention by the proper distance  $rd\theta$ , where some values of r are marked on the diagram. It will be seen u=0 by no means implies r=0. Rather,  $r=2M^*$  at the throat. As one goes to negative u-values (not shown on the present incomplete Kruskal diagram), he finds  $r=3M^*$ ,  $r=4M^*$ , etc., an ever enlarging domain

("lower" portion of 3-geometry).

What about the development of the Schwarzschild 3-geometry with time? The Kruskal (u, v)-plane (Fig. 21) is a spacetime diagram. Light rays traveling radially  $(\theta = \text{const}, \varphi = \text{const}!)$  are described by lines with a slope of  $\pm 45^{\circ}$ . In contrast, a spacelike hypersurface has a slope less in magnitude than  $45^{\circ}$ . Therefore, any curve v = v(u) running through the Kruskal diagram with slope between  $+44.999...^{\circ}$  and  $-44.999...^{\circ}$  describes a possible spacelike hypersurface, a hypersurface which moreover possesses spherical symmetry (same section for all  $\theta$ ,  $\varphi$ ). In the model, the geometry in question may be typified by a tube which has been flared out more at some places than at others, perhaps more for positive u than for negative u, but which still preserves its rotational symmetry. This symmetry is not important as a matter of principle, However, it simplifies the discussion, by allowing the one line v = v(u) to represent an entire 3-geometry.

#### THE NATURE OF TIME IN GENERAL RELATIVITY

Time in general relativity has a character to which one is not accustomed in classical mechanics. In Newtonian theory one has his choice of one numerical value of the time coordinate, or another, or another. Each is as appropriate as another for an instant at which suddenly to observe and record the state of the system. In geometrodynamics one selects instead of a single parameter t an entire spacelike hypersurface and asks for the physical conditions on it. To state the matter differently, one has  $\infty^3$  space points, and at each a selection of the time to be made. The totality of these selections specifies a hypersurface. That each point should be out of causal connection with its neighbors demands that this hypersurface should in addition be spacelike, with the angle of slope at each point less in absolute magnitude than 45°. Consistently with this condition, to select some line, or any line, v = v(u), is thus to do what is the relativistic generalization of picking a time, some time, any time, in Newtonian mechanics. Non-relativistic theory is said to be successful when it can predict the state of the system for any choice of its one time coordinate, Similarly, a problem in general relativity has been solved when for every choice of a spacelike hypersurface one can state what is the 3-geometry (the geometrodynamical version of "the state of the system") upon that hypersurface.

#### THE EVOLUTION OF THE SCHWARZSCHILD GEOMETRY WITH TIME

The initial state of the geometrodynamical system has already been specified in the Schwarzschild geometry by giving the initial-value geometry on the spacelike hypersurface of time symmetry. This geometry is fully described by a formula for the distance between each point and its immediate neighbors on this three-dimensional manifold:

$$\begin{split} ds^{z} &= (1 - 2M^{*}/r)^{-1}dr^{2} + r^{2}(d\theta^{2} + \sin^{2}\theta d\varphi^{2}) \\ &= (1 + M^{*}/2\rho)^{4}(d\rho^{2} + \rho^{2}d\theta^{2} + \rho^{2}\sin^{2}\theta d\varphi^{2}) \\ &= f^{2}(u)du^{2} + r^{2}(u)(d\theta^{2} + \sin^{2}\theta d\varphi^{2}) \; . \end{split}$$
(343)

Happily, the "evolution of the geometry with time" is completely known. Schwarzschild's 4-geometry completely solves Einstein's field equations and reduces to equations (343) when  $t_{\rm Sch}=0$  or v=0. Therefore any spacelike slice through this 4-geometry gives at once a 3-geometry which "represents the state of the system" at that "time;" that is to say, upon that hypersurface. In brief, proceed as follows: (1) Pick a "time," or a spacelike hypersurface, by selecting any functional dependence of v upon u with |dv/du| < 1. (2) Calculate from the Schwarzschild 4-metric (332) or (333) or (337) the 3-geometry on this hypersurface, as

$$ds^2 = f^2[u, v(u)][-(dv/du)^2 + 1]du^2 + r^2[u, v(u)](d\theta^2 + sin^2 \theta d\varphi^2). \tag{344}$$

(3) Then one has in equation (344) the complete description of the configuration of the

3-geometry at this "time."

How does it come about that so many textbooks describe the geometry of the Schwarzschild solution as *static?* Because they limit attention to hypersurfaces of one particular type, a hypersurface represented in the Kruskal diagram by a straight line passing through the origin; thus,

$$v = v(u) = \gamma u , \qquad (345)$$

where  $\gamma$  is a constant. A little inspection of the relation of equation (335) between the Kruskal coordinates and the Schwarzschild coordinates shows that a constant value for the ratio  $\gamma = v/u$  implies a constant value for the Schwarzschild time  $t_{Sch}$ :

$$\gamma = v/u = \tanh (I_{Sch}/4M^*)$$
, (346)

In the Schwarzschild coordinates one sees from equation (332) that a constant value for  $t_{Seb}$ , that is, a zero value for  $dt_{Seb}$ , implies the same 3-geometry on the new hypersurface as one has upon the initial hypersurface.

There are interesting group-theoretical consequences for the invariance of the Kruskal

diagram under something like a Lorentz transformation,

$$v = v' \cosh \alpha + u' \sinh \alpha \qquad u = v' \sinh \alpha + u' \cosh \alpha$$
, (347)

which follow from this analysis, but they are not immediately relevant here. It is more useful to note simply these points: (1) The locus of points with constant  $t_{5\text{ch}}$  is a straight line through the origin. (2) The larger the Schwarzschild time coordinate, the greater this slope. (3) The starting time  $t_{8\text{ch}} = 0$  corresponds, as seen before, to the line of zero slope, v = 0. (4) An indefinitely large value of the coordinate  $t_{8\text{ch}}$  corresponds to indefinitely close approach to the hypersurface v = u (45° slope). (5) No matter how close the spacelike hypersurface  $v = \gamma u$  approaches to a unit slope, it nevertheless does not have unit slope. Moreover, however close  $\gamma$  is to unity, that line can be given a slope of zero by referring it to a Kruskal coordinate system (u', v') which differs from the present

<sup>\*</sup> Among these consequences one of the most interesting is this: that free particles starting out together at the throat at the phase of maximum distention, and traveling in the direction of increasing u with the most varied velocities, all go through identical histories. They end up after identical lapses of proper time in final approach to different points on the line r=0, but subject to tide-producing forces increasing at identical rates to unlimited values.

Kruskal frame by a sufficiently large value of the parameter  $\alpha$  in expression (347). Yet the slope of a light ray has the same unit value in the new frame, v'/u' = 1, which it has

in the old frame, v/u = 1.

Instructive as are these group-theoretical features of the Schwarzschild 4-geometry, they are taken in the wrong spirit, one knows today, if they are used to reason that the 3-geometry is not dynamic! In describing to Achilles the approach of the hare to the tortoise, one can use a time coordinate which has the value 1 when the separation is 1 meter, 2 when the separation is  $\frac{1}{2}$  meter, . . . , and n when the separation is  $(\frac{1}{2})^n$  meter. On this basis one has to wait an infinite time for the hare even to catch up, and he will never succeed in overtaking the tortoise. So with the family of hypersurfaces which have just been examined. They move ahead freely (with increasing values of the slope  $v/u = \gamma$ , or with increasing values of the Schwarzschild time coordinate  $l_{\text{Sch}}$ ) in some regions of the Kruskal diagram, but less and less near the origin, and at the origin itself not at all. As in speaking to Achilles, so in describing the development of the geometry with time, one has artificially restricted the discussion to a limited portion of the entire history.

#### THE TWO CONNECTED QUASI-EUCLIDEAN SPACES DEFORMED TO A "CYLINDER"

The freedom of choice that exists in choosing spacelike hypersurfaces is nowhere so clearly shown as on the Kruskal diagram itself. As an example, take that line in the (u, v)-plane which is marked  $r = m^*$  (or in the present notation,  $r = M^*$ ). Its slope being everywhere less than 1, it is plainly spacelike. Thus one has exercised that freedom of choice in the selection of "time," or in the selection of a spacelike hypersurface, to which one is rightfully entitled in studying the dynamics of geometry. One has broken loose from the restriction to the origin (u = 0, v = 0) which is hidden in the usual Schwarzschild coordinate system. What then is the 3-geometry on this spacelike hypersurface? One immediately has the answer by substituting  $r = M^*$ , and dr = 0, into expression (332):

$$ds^2 = +dt_{Sch}^2 + M^{*2}(d\theta^2 + \sin^2\theta d\varphi)^2$$
, (348)

This formula is nothing but the generalization to 3-space of the expression for the geometry on the surface of the copper cylinder. The quantity dls.h measures not time, but proper distance, and this distance parallel to the axis of the cylinder. The radius of the cylinder is M\*. Of course, the cross-section of the cylinder is not a circle, as in the analogy of the copper pipe, but a 2-sphere. The dynamics is clear. To return to the analogy with the soft metal tube, one thinks of it at the initial moment of time symmetry as flared out at each end into a quasi-Euclidean geometry. At some chosen later time, which is to say, on some other spacelike hypersurface of one's choosing, the geometry has undergone dynamic change. As viewed on the hypersurface just now selected, the flares have moved inward to undo the spinning operation by which they were imagined to have been formed in the first place. In addition the whole tube has shrunk, The effective radius of the throat to begin with was 2M\*. Now not only at the throat but everywhere the proper circumference, divided by  $2\pi$ , has shrunk to  $M^*$ , half the original value. Moreover the shrinkage continues as the hypersurface is pushed forward in the Kruskal diagram. One comes after the lapse of a finite proper time to a singular condition. The geometry itself collapses. The intrinsic curvature of the 3-geometry goes to infinity. In this sense there is a close parallelism with the Friedmann geometry, where also the curvature goes to infinity in a finite proper time.

The spacelike hypersurface  $r = M^*$  was taken as an illustration for the nature of time in general relativity, not because one was forced to any such special choice, but only because the 3-geometry on this hypersurface lent itself to simple analysis. One will

<sup>&</sup>lt;sup>7</sup> Appreciation is expressed to Professor Charles Misner for discussions giving insight into the Schwarz-schild geometry. See also Petrov (1963) for citation of work on this topic by Novikov (1962); see also Kruskal (1960).

recall once again that the person studying the 4-geometry has entire freedom in the choice of the hypersurface; it is fixed by him, not by the dynamics. The dynamics tells only what the geometry will be on the chosen hypersurface; that is, "at" the chosen "time."

#### JOIN BETWEEN SCHWARZSCHILD AND FRIEDMANN GEOMETRIES

So much for the full Schwarzschild geometry, its throat, the dynamics of the throat and of the rest of this geometry, and ultimate development of infinite curvature. Now for the join between a portion of this geometry (drawn in full line in Fig. 21) and that portion of the Friedmann geometry which is occupied by dust. The problem of join at the initial instant of time symmetry has been treated already in chapter viii. A particle of dust at the interface between the two geometrics (A in Fig. 21) has—and keeps—the coordinates ( $\chi_0$ ,  $\theta$ ,  $\varphi$ ) in the Friedmann geometry. In the Schwarzschild geometry its initial coordinates are  $r=a_0\sin\chi_0$ ,  $\theta$ ,  $\varphi$ . However, to know r is not by itself enough to tell whether the dust particle lies on the "upper" portion or the "lower" portion of the Schwarzschild geometry. For that purpose one looks at  $\chi_0$  itself. A value less than  $\pi/2$  implies less than half a Friedmann hypersphere, and tangency to the "upper" portion of the Schwarzschild geometry;  $\chi_0$  more than  $\pi/2$  implies a baglike geometry, with tangency to the "lower" portion of the Schwarzschild geometry. Both cases were illustrated in Figures 11 and 15. Here we take for definiteness the case  $\chi_0 < \pi/2$ . Then the point A lies as indicated in Figure 21. So much for the location of the dust particle at the initial moment of time symmetry.

As its proper time advances the dust particle, at rest for an initial instant, starts to fall and drops inward through a decreasing sequence of r-values:  $r \sim 2.6M^*$  at A;  $r = 2M^*$  at C;  $r = M^*$  at D; and r = 0 at E. For a detailed description of the motion a supplementary parameter  $\eta$  is useful. This parameter is identical in meaning and value with the parameter  $\eta$  employed to describe the motion of the same particle in the Friedmann geometry. Of course, one will never know this identity if he confines his attention entirely to the Schwarzschild geometry. In that case he will only realize that this parameter simplifies the solution of the geodesic equation of motion in the Schwarzschild geometry. In terms of the Schwarzschild coordinate  $r = r_0$  at the start of the fall, the solution has the form

$$r = (r_0/2)(1 + \cos \eta),$$

$$t_{Sch} = 2M^* \left\{ \ln \frac{(r_0/2M^* - 1)^{1/2} + \tan(\eta/2)}{(r_0/2M^* - 1)^{1/2} - \tan(\eta/2)} + (r_0/2M^* - 1)^{1/2} [\eta + (r_0/4M^*)(\eta + \sin \eta)] \right\},$$
(Proper time) =  $(r_0/2M^*)^{1/2}(r_0/2)(\eta + \sin \eta).$ 

Now identify this motion with the motion of the same particle as analyzed in the Friedmann geometry, when all three of the coordinates  $\chi$ ,  $\theta$ ,  $\varphi$  stay fixed in value and the radius of curvature of the space changes in accordance with equation (327):

$$r = (\sin \chi_0)(a_0/2)(1 + \cos \eta)$$
,  
(Proper time) =  $(a_0/2)(\eta + \sin \eta)$ .

From the comparison of equations (349) and (350) one finds

$$r_0 = a_0 \sin \chi_0$$
, (351)

$$M^* = r_0^2/2a_0^2$$
, (352)

Of these results, the first is already known from matching the two time-symmetric initial value geometries. There, one also found that the radius of curvature  $a_0$  had to be  $(3/8\pi\rho_0^*)^{1/2}$ , where  $\rho_0^*(\text{cm}^{-2}) = (G/c^2)\rho_0(g/\text{cm}^3)$  is the initial density. From this result one sees that equation (352) is also an equation familiar from the study of the initial value problem,

$$M^* = (4\pi \rho_0^*/3)r_0^3$$
, (353)

Thus, the most obvious features of the two geometries match for all times when they

have been adjusted to match at the moment of time symmetry

As the typical particle at the surface of the dust cloud follows a geodesic in the Schwarzschild 4-geometry to ever smaller values of the coordinate r, it finds itself in a geometry that is ever more strongly curved, until at E the Riemann curvature, or in physical terms the tide-producing forces, have grown beyond all limit. In the final stages of this progression conditions grow so extreme that neither the particle nor the geometry in which it moves can be described in classical terms. Prior to that time, however, the classical description of the motion of the particle and of the dynamics of the geometry is straight-forward. Moreover, the salient physical points are all summarized in Figure 21. One only has to note that two separate diagrams are used there for the two parts of a 4-geometry which actually matches smoothly along the entire interface A-A, B-B, . . . , E-E. The connections between corresponding points will be taken as understood in the following discussion. As an elementary example, consider the spacelike hypersurface marked  $r = m^*$  (or  $r = M^*$  in the present terminology) in the right-hand portion of Figure 21. The 3-geometry there is that of a tube. One now sees that this tube is capped and closed at one end by a portion of the Friedmann spherical geometry.

## CONNECTION BETWEEN THE DYNAMICS OF COLLAPSE AND THE ANALYSIS OF MOMENTARILY STATIC CONFIGURATIONS

Before applying Figure 21 to help analyze new questions, like the fate of the energy caught up in the collapse, it is appropriate to ask a question of principle relating to the past analysis of energy, in chapter viii. There we took a specified number of baryons. We disposed them in a spherical configuration of uniform density. We joined the Friedmann geometry inside this configuration onto a Schwarzschild geometry outside, assuming static conditions (time symmetry). We determined in this way the mass-energy, M\*, of the system as sensed externally. We examined how M\* depended upon the degree of compaction of the A-baryon system. In every case we found that  $M^*$  decreased in a family of A-baryon configurations when the density was increased to a finite critical value, the "point of collapse" as it was termed in chapter viii, What possible relevance, it may now be asked, does this analysis of a family of static configurations have to the dynamics of the collapse of a single configuration? The mass-energy as sensed externally stays constant throughout the collapse as envisaged here. Complete absence of radiative transport is assumed from the start. Then how can there be any real connection between gravitational collapse as seen in the light of Figure 21 (fixed  $\dot{M}^*$ ) and gravitational collapse as treated in chapter viii  $(M^*$  going to zero)? How can any connection amount to any more than the trivial agreement between the number A of baryons in the two cases?

A closer look shows that the connection between the dynamic analysis and the static analysis is far deeper and more beautiful.

Theorem 36: Given a cloud of dust of uniform density and of spherical symmetry, which starts from rest in a configuration of time symmetry with an initial mass-energy (as sensed externally) equal to M\*, and which in the course of its subsequent collapse

\*C. G. Callan, Jr. (paper in preparation) has recently constructed Kruskal-like coordinates for the Friedmann region. These coordinates join smoothly to Kruskal's coordinates at the surface of the dust cloud, thereby permitting a single unified diagram for the 4-geometry of the dust cloud. emits no radiation (M\* constant). Then the dynamical history of this configuration—despite its own constant energy—contains all those 3-geometries with mass-energy M<sub>1</sub>\* less than M\* which are found in the analysis of the spherically symmetric and time-symmetric initial-value problem for the same number of baryons!

## A SPACELIKE SLICE CHARACTERIZED BY AN ARBITRARILY SPECIFIED VALUE OF THE MASS-ENERGY

To prove the theorem it is enough to draw through the space-time diagram of Figure 21 (referring to a dynamics in which the mass-energy has the unique and time-independent value  $M^*$ ) a line (the very heavy dashed line in the figure) on which the 3-geometry (1) satisfies the equation

$$^{(3)}R = 16\pi\rho^*$$
 (354)

and (2) has outside the matter the standard Schwarzschild form

$$ds^2 = (1 - 2M_1^4/r)^{-1} dr^2 + r^2(d\theta^2 + \sin^2\theta d\varphi^2)$$
 (355)

with M1\* greater than zero and less than M\* but otherwise arbitrarily specified.

One finds the line in questiion; that is to say, the spacelike hypersurface on which the geometry will take the claimed form, by a prescription which in the Schwarzschild region, and in Schwarzschild coordinates, reads as follows:

$$r$$
 arbitrary,  $\theta$  arbitrary,  $\varphi$  arbitrary,  
 $t = \text{const} + 2(2M^* - 2M_1^*)^{1/2}(r - 2M_1^*)^{1/2}$   
 $-2M^* \ln \frac{(r - 2M_1^*)^{1/2} + (2M^* - 2M_1^*)^{1/2}}{(r - 2M_1^*)^{1/2} - (2M^* - 2M_1^*)^{1/2}}$   
 $\sim \text{const} + 2(2M^* - 2M_1^*)^{1/2}r^{1/2} + \text{terms of order } (1/r^2)$ , (356)

Without entering into details, it is enough to look at the final asymptotic expression to see the main points of the analysis. A motion on the spacelike hypersurface (356) from one point to a neighboring point, r + dr,  $\theta + d\theta$ ,  $\varphi + d\varphi$ , brings about also a change in the Schwarzschild time coordinate,

$$dt_{\rm Sch} \sim [(2M^* - 2M_1^*)^{1/2}/r^{1/2} + \text{terms of order } (1/r^{3/2})]dr$$
. (357)

In consequence the element of proper distance ds discovered in the displacement (found by substitution into eq. [332]) contains a contribution from  $dt_{8:h}^2$  as well as contributions from the changes in the other coordinates; thus,

$$ds^2 \sim [-(2M^* - 2M_1^*)/r + (1 + 2M^*/r)]dr^2 + r^2(d\theta^2 + \sin^2\theta d\varphi^2)$$
. (358)

A more detailed calculation shows that the coefficient of  $dr^2$  is exactly  $(1 - 2M_1^*/r)^{-1}$ . Therefore the geometry on the spacelike hypersurface in question is the Schwarzschild 3-geometry associated with a mass  $M_1^*$  which is less than  $M^*$ !

#### SEGMENT OF OPENING $\chi_1 > \chi_0$ SLICING THROUGH THE FRIEDMANN 4-GEOMETRY!

A similar analysis gives the course of the spacelike hypersurface through the Friedmann portion of the 4-geometry (heavy dashed curve in Fig. 21). The geometry here has two remarkable features: (1) The curvature throughout is constant, despite the gradually varying slope, indicated for the dashed curve. Therefore one is still dealing with the simplest type of section of the Friedmann geometry. (2) However, this dust-occupied

For a brief preliminary discussion of this point, see p. 337 of Wheeler (1964a).

section spans a segment of the hypersurface with an angular opening  $\chi_1$  which is larger than  $\chi_0$ ! One is dealing with the beginning of the eventual pinch-off of a 3-geometry, the feature so decisive for gravitational collapse as it was analyzed for static configurations in chapter viii. One can go further, and find a whole family of spacelike hypersurfaces slicing through the 4-geometry of Figure 21. Successive slices are characterized by (1) the same fixed number of baryons,  $A_i$  (2) successively smaller values of the mass-energy  $M_1$ \* (as one might think of evaluating it from the asymptotic form of the three-geometry); (3) successively higher values of the density in the occupied region; and (4) successively larger values of the hyperspherical angle  $\chi_1$  of the occupied zone, approaching  $\chi_1 = \pi$  as a limit at the point of pinch-off.

#### HOW RECONCILE A CHANGING MASS-ENERGY WITH A CONSTANT MASS-ENERGY?

A double paradox has now presented itself: (1) Spacelike slices through a dynamic configuration reproduce the 3-geometries which had been calculated in chapter viii from the analysis of static configurations. (2) The mass-energy  $M_1^*$  naturally associated with a typical one of these spacelike hypersurfaces nevertheless disagrees with the (conserved) mass-energy  $M^*$  of the dynamic system. Happily each apparent difficulty helps to explain that the other is no difficulty at all! The quantity  $M_1^*$  is the general relativity analog of potential energy. The quantity  $M^*$  measures total energy. The difference measures kinetic energy. In chapters iii—viii the typical configuration was static. Thus a calculation of the potential energy immediately gave the total energy. Here, in contrast, those phases of the motion are being examined which develop after the moment of time symmetry. The configuration is collapsing. Its kinetic energy is positive. In consequence  $M_1^*$  must evidently be less than  $M^*$ .

The calculations of chapters iii-viii, ostensibly so static in character, now reveal themselves as in effect a derivation of the potential-energy-curve for the dynamic analysis of collapse. The concept of such a potential-energy-curve or, more generally, potentialenergy surface, is so widespread throughout the branches of mechanics and hydrodynamics that it requires no elaboration.

#### POTENTIAL AND KINETIC ENERGY RELATED TO INTRINSIC AND EXTRINSIC CURVATURE

An issue remains. It has to do with the asymptotic analysis of the geometry at large distances. The coefficient of the (1/r)-term in the departure from flatness, after division by 2, is taken to give the mass-energy. How can this single coefficient have two different values, M\* and M1\*? The difficulty has to do with the existence of two definitions of asymptotic flatness. Definition 1: The intrinsic 3-geometry is asymptotically flat. All of the spacelike hypersurfaces under discussion have 3-geometries which are asymptotically flat in this sense; yet the approach to flatness within the 3-geometry is different in each case (different values of  $M_1$ \*). Definition 2: The intrinsic 3-geometry of the hypersurface is asymptotically flat. Also the extrinsic curvature of this hypersurface, as it is imbedded in the enveloping 4-geometry, is zero or asymptotically zero. At large r there is only one type of hypersurface which is asymptotically flat in this stronger sense. It is a hypersurface of time symmetry, tseh. = const. The mass defined by its approach to flatness has the well-defined value  $M^*$ , the total mass-energy of the system. From the comparison one concludes that the potential energy, M1\*, has to do with the geometry intrinsic to a spacelike hypersurface, whereas the kinetic energy  $(M^* - M_1^*)$  has to do (cf. eqs. [356]–[358]) with the extrinsic curvature of this hypersurface relative to the geometry of the enveloping space time. Contrast this division of global energy into two parts with the division of local energy into two parts,

$$^{(3)}R + K_2 = 16\pi \rho^* \,, \tag{359}$$

as it appears in the foundation law (eq. [2]) of general relativity!

We generalize this discussion from idealized dust to matter with the equation of state  $\rho = \rho(n)$  by formulating Theorem 37.

Theorem 37: Any spherically symmetric configuration followed from an initial spacelike hypersurface of time symmetry, upon which one determines the total mass-energy to have the value M\*, admits an infinity of spacelike slices, on any one of which the 3-geometry (1) satisfies the initial value equation for the moment of time symmetry problem but (2) shows a Schwarzschild mass-energy M<sub>1</sub>\* which is less than M\* by an amount which represents the kinetic energy of the system.

This principle has the practical consequence that it allows one to give a useful meaning to the concept of potential-energy-curve in general relativity. For example, referring to the collapse barrier depicted in Figure 20, start a system from rest the smallest possible distance to the left of the potential-energy summit. Follow the system in toward collapse by solving the dynamical equations of relativity, without reference to any "potential-energy-curve." Represent the history of this collapse by writing down graphically or numerically or by a formula the resulting 4-geometry. Then by way of spacelike slices through this 4-geometry one can construct the details of the potential-energy-curve to the left of the summit; similarly, with a slightly different starting condition, to the right of the summit.

## GRAVITATIONAL COLLAPSE AS A MODEL FOR THE STUDY OF THE DYNAMICS OF THE UNIVERSE.

Whether successive spacelike slices cut through the 4-geometry of the dust cloud which is illustrated in Figure 21, or through the history of a more compact configuration where the energy of compression plays an important part, in any case the resulting succession of 3-geometries has the qualitative character of the sequence illustrated in Figure 15: an irresistible development of a geometry more and more baglike, until finally there comes a limiting geometry at the verge of complete pinch-off. (Again, these slices provide only one of many possible ways to make a step-by-step analysis of the 4-geometry. There is no principle that compels one to this or any other particular choice of hypersurfaces for his own probing of the entire history of the system.) This circumstance is a reminder of how many points there are in common between the dynamics of collapse and calculations (equally based on Einstein's standard theory) of the expansion and recontraction of a model universe. Insofar as one can hope observationally to trace out the details of gravitational collapse, then to that extent, as Fred Hoyle has emphasized, one has an approach to a working model of the universe itself.

How much difference is there between the model universe and the collapsing collection of matter by reason of the incomplete closure in the second case? No difference in the example of the ideal cloud of dust. There being no radiation and no pressure, there is no way for a particle to feel the altered degree of closure (hyperspherical angle  $\chi_0$  in the one case,  $\pi$  in the other). In any other example, when one starts with matter all initially at uniform density, there will be an important difference between the finite configuration and the closed universe. In the model universe each elementary block of material will keep its  $\chi$ -,  $\theta$ -, and  $\varphi$ -coordinates. Only the proper time dt required to pass from a configuration with one radius a to another radius, a - da, will be altered by reason of the pressure. (The time is not only altered. It is shortened. The time from the momentary condition of rest, with radius  $a_0$ , to collapse is  $\pi a_0$  for the dust-filled universe and  $[\pi/2]a_0$ 

for Tolman's radiation-filled universe, where [pressure] = \(\frac{1}{2}\)[energy density].)

In the finite collection of matter there is a further difference from the Friedmann universe. It arises because uniform density is not and cannot be a solution of the general-relativity equations of hydrostatic equilibrium. The matter senses the sharp drop in pressure between the interior and the exterior. The outer layers start to blow off. A rarefac-

tion front develops and moves backward into the interior with the speed of sound. All the while the unaffected inner part of the configuration is following the law of homogeneous contraction that one expects from identifying it with a segment of a closed and recontracting universe. The collapse will lead to conditions of unlimited density and curvature at the center of the configuration at precisely the same rate and at the same timing as in the closed universe provided only that the rarefaction does not get to the center first. In the time dt it covers the distance  $(dp/d\rho)^{1/2} dt$  on the arc of a great circle which at that time has the radius a(t) (eq. [327]). The ratio of the arc to the radius gives the angle covered. Thus one has two distinct cases:

Case I. 
$$\chi_0 > \int_0^{t_{\text{millapse}}} a^{-1}(t) (dp/d\rho)^{1/2} dt$$
; collapse in central region identical to that in closed universe. (360)

Case II. 
$$\chi_0 < \int_0^t ^{collapse} a^{-1}(l) (dp/d\rho)^{1/2} dl$$
; rarefaction arrives at center before that region has reached extreme conditions; collapse modified in its dynamics but not avoided.

#### COMMUNICATION TO OUTSIDE CUT OFF

Despite the similarity between the collapsing universe and the collapsing cloud of matter there is one significant difference. The bounded configuration can communicate for a time with the outside. The closed system has no outside to communicate with,

From Figure 21 one sees that the particle at the outer boundary of the cloud of dust can send signals to the outside world at A and B but not beyond C. More generally, we formulate Theorem 38:

Theorem 38: As a spherically symmetric configuration undergoes continued gravitational contraction, each region in the interior loses—according to CLASSICAL general relativity—the ability to emit energy by way of its retarded radiation field well BEFORE its energy density—as calculated classically—has risen to infinity.

Oppenheimer and Snyder (1939) have already stressed how this cutoff prevents the system from getting rid of its energy. The distant observer finds the emitted radiation growing redder and redder. In the course of an infinite amount of his own time he manages to pick up only whatever radiation is given off by the surface in the short stretch of its own proper time up to the point C. There is a great deal of energy in the system, but no evident way for it to get out.

Central to the traditional way of disposing of energy by radiation is the mechanism of radiation damping and radiative reaction. That mechanism has been understood in terms of advanced and retarded interactions between the source and the absorber (Wheeler and Feynman 1945, 1949). One might therefore imagine this process to take

<sup>16</sup> For first steps toward numerical or analytical investigation of the dynamics of collapse with all the refinements that one would eventually like to see included—a start from a known solution of unstable equilibrium, realistic equation of state, full hydrodynamics, radiation of photons and neutrinos, production of cosmic radiation, effects of magnetic fields, allowance for all geometrodynamical effects—see Bondi (1947); Colgate and Johnson (1960); Colgate, Grasberger, and White (1962); Colgate and White (1963); Michel (1963); Chiu (1964); Fowler (1964); Hoyle, Fowler, Burbidge, and Burbidge (1964); Hoyle and Fowler (1964); Misner and Sharp (1964); Callan (1964); Ginzburg and Ozernoi (1964); McVittie (1964); May and White (1965); Bardeen (1965). See also the proceedings of the December, 1964, Texas Symposium on Relativistic Astrophysics, edited by I. Robinson, A. Schild, E. L. Schucking, and J. A. Wheeler, to be published by the University of Chicago Press.

some new course under conditions where the retarded radiation cannot get out. In considering the possibilities one notes that the surface of the configuration at points D and E, though not able to communicate to the outside via retarded interactions, nevertheless is coupled to the outer world by advanced potentials. Do these potentials not offer a way to draw out the energy of the system just before its final phase of otherwise infinitely high energy density? Not at all! Just as it is the characteristic feature of retarded waves to take energy out, so advanced waves always bring energy in—the last effect that one is looking for here. Advanced interactions bring no help to the solution of the problem.

The same point can be put in more general terms. There is no difference in principle between (1) the particle following the geodesic ABCDE into a region of infinite curvature (with the retarded radiation which it emits also following into regions of equally violent curvature) and (2) the inhabitant of an expanding and recontracting model universe who emits retarded radiation. The radiation which he gives off, and the individual atoms of which he is made, will also end up in domains of infinite curvature in the late stages of recontraction of the typical model universe. Can one use his own observations in the physical universe to draw conclusions about what will happen in such a model universe? There is not the slightest evidence for any effect on the force of radiative reaction associated with the presumptive ultimate trapping of all particles and all radiation. Yet the calculated mean free time of flight of radiation for the universe in its present state is large compared to the estimated time (a few times 1016 years) for the expansion and recontraction, according to Einstein's theory. On that theory the retarded radiation should therefore for the most part not be absorbed until the terminal conditions of high curvature are approached. That there is nevertheless no observed back action on the law of radiative damping would seem in one sense to be an empirical argument against there being any modification in the law of electromagnetic interaction originating from regions of violent curvature.

The physics in the late stages of the universe and the physics in the final stages of gravitational collapse are evidently not issues to be considered in isolation from each

other. They have the closest possible connection.

Proposition 39: There is no difference of principle between the physics in a body of baryons undergoing gravitational collapse and the physics in the early stages of expansion or the final stages of recontraction of the universe as interpreted by Einstein's theory.

From this follows Proposition 40,

Proposition 40: If matter disappears or appears in the late or early stages of the universe, that is, if the number of baryons is to have the quality of other physical variables, which are dynamic and have their own laws of change with time, then also in gravitational collapse the number of baryons which remain in identifiable form must be subject to change.

#### FOR WHOM THE BELL TOLLS

It is sometimes argued that there is no reason to trouble about the kind of physics which goes on in the collapsing matter during the final stages of the dynamics. The object becomes redder and redder as seen from outside. It keeps its mass-energy—because it cannot radiate it—and therefore preserves also its gravitational attraction. Nothing that goes on inside in the final stages is relevant, it is occasionally said, because there is no way for word of these events to reach the outer observer. Therefore regard questions about these events as meaningless, and forego any attempt to analyze them. However, to an observer located on the falling system the collapse takes only a limited and very modest amount of proper time. Nothing in principle keeps him from observing and measuring as fully as one is accustomed to do in other departments of astrophysics. Of course the question may arise of willingness to undertake this investigation on a collapsing

cloud of matter. In this event one can point to the Einstein-Friedmann picture of the expanding and recontracting universe, according to which we are located on just such a cloud of galaxies, and have no choice but to live with its eventual collapse. Far from being a bystander safely outside of all collapsing systems, one from this point of view is right within the most interesting expanding-and-recollapsing system of all, the universe. To

try to analyze its physics would not seem to be a meaningless occupation.

Another reason is sometimes advanced for not worrying about the physics of the final stages of collapse. Any actual system will depart so much from ideal spherical symmetry, it is suggested, that the dynamics will be completely altered. For example, quadrupole and higher moments of the mass distribution will act as significant sources of gravitational radiation, particularly if these moments change rapidly with time. This radiation will carry away energy. Under suitable conditions the calculated output exceeds one-tenth of the rest mass of the system. Also, large agglomerations of matter which have come together with substantial transverse relative velocities may re-emerge from their encounter much as a comet returns from its near-collision with the Sun. The material may be heated to enormous temperatures by the encounter. In this case it will radiate away large amounts of energy in the form of neutrinos and photons. Moreover, it is conceivable that such periods of strong radiation will recur a number of times as the material periodically falls together and then partially disassembles.

These complications of asymmetry, radiation, and turbulent hydrodynamics are of great interest for the light they may ultimately shed on gravitational collapse as a source of energy. For the understanding of quasi-stellar radio sources these mechanisms would seem more significant than simple spherically symmetric gravitational collapse.

Whatever the importance of asymmetries may be in producing the effects of astrophysical interest, inward fall under the pull of gravitation is the ultimate foundation of these mechanisms for releasing suprathermonuclear energy. The emission of any more than a certain fraction of the rest mass in the form of energy means that the system has dropped to a state of gravitational energy so low that it can never all pull itself out again by its own efforts. The more the subsequent energy emission, the tighter becomes the grip of gravitation on the system. Therefore, any asymmetries in the motion are of no ultimate effect in saving a heavily radiating system from collapse. We conclude that passage of matter to the collapsed state can be made as inescapable in the case of asymmetric infall as in the case of spherically symmetric motion. This point is sufficiently important to be spelled out in terms of an idealized experiment.

(1) Start with a region of empty space. (2) Introduce baryons one by one. (3) Remove all heat at each stage of the addition process, and catalyze the system to the end point of thermonuclear reactions. (4) Slowly approach the LHWW critical point, A<sub>erit</sub> (= 1.4 × 10<sup>57</sup> ± 10 per cent). (5) Add 1 kg of matter in excess of the limit; thus A = A<sub>crit</sub> + ΔA. (6) The system undergoes collapse. Kinetic energy is developed. Nuclear reactions take place. Electromagnetic and gravitational radiation and neutrinos stream off. (7) Some fraction of the matter is ejected. (8) Catch this matter. (9) Extract its kinetic energy. (10) The mass-energy of the system, as determined from measurements of the gravitational attraction exterior to this momentarily static shell, has decreased to the value

$$M_{\rm new}^* = M_{\rm crit}^* + \mu_*^* \Delta A (1 - 2M_{\rm crit}^*/R_{\rm crit})^{1/2}$$
  
-  $M_{\rm e.m.\ rad}^* - M_{\rm grav.\ rad}^* - M_r^* - M_{\rm kin}^*$ .

(11) The ejected shell of matter, now static, is to be lowered back onto the system. Remove the gravitational potential energy of attraction which is set free in the process. (12) The net tally of the baryons which have been brought in from outside remains at the number  $A = A_{\rm crit} + \Delta A$ . (13) If additional explosions occur, again remove the energy, and again have a drop in the mass-energy of the system, but again see to it that no

baryons escape to the outer world. (14) There is no state of stable equilibrium of the system, because  $A > A_{\rm cris}$ . Therefore the material of the system never stops moving. Moreover, all outward motion has been arranged to be stopped, and replaced by inward fall, at a net profit in energy to the stopping agent or agency. (15) Consequently collapse

of the baryons is inescapable.

There is no difference between the spherically symmetric star and the spherically symmetric universe up to this point in the discussion as regards the collapse of the baryons. In both cases the descriptive phrase is inward and inevitable. But what about the energy? It flows outward in the case of the collapsing star, yet has no free space to escape to in the case of the collapsing universe. Or so the two systems seem at first sight to be distinguished from each other. Soon this distinction too fails. The outermost particles of the shrinking star send out the last photons, the last gravitational radiation, the last neutrinos, which will ever reach a faraway observer ("last ray"; event C in Fig. 21). Yet to the star the moment when it sends out the last ray has no special significance. The star sends out further radiation after this event. The important circumstance is this, that the "after-radiation" has no free space to flee to. It gets caught in the infinite curvature that develops outside the star as well as inside. The after-radiation from the star experiences the same fate as all of the radiation caught in the inexorable grip of a deflating universe. According to classical general relativity an "after-photon," like a man running down the slope of the beach from a fire in port, gets caught in disaster. The curvature of space, like the curvature of an incoming ocean wave, comes to a thundering crest (hatched line or rather hatched spacelike hypersurface—through event E in Fig. 21). The geometry develops a singularity. This singularity occurs where there is no matter as well as where baryons are tightly compressed. It marks the end of the line for the predicting power of unquantized general relativity. Here the classical analysis comes to a halt both for the contracting star and for the collapsing universe.

#### NEW QUANTUM ASPECTS OF COLLAPSE

When we turn from classical geometrodynamics to quantum theory, we have to conclude that the prediction of an infinite curvature for space is wrong. The after-radiation may run into many a whither and how on its way out. However, these problems are not

properly described by the words "infinite curvature."

In saying that a quantity as physical as curvature cannot become infinite, we are not saying that the implosion must necessarily be asymmetrical. A symmetric collapse, like the "head-on" collision of an electron with a hydrogenic field of force, may take special conditions to bring about—but these conditions in principle can be satisfied. If a beam of the incoming electron is described by a plane wave of energy E, then collisions with angular momentum  $l=1,2,\ldots$ , are more probable than collisions with l=0. In collisions with finite angular momentum the kinetic energy of the electron, as calculated classically, always remains finite:

(Maximum kinetic energy) = 
$$E + [me^4/l(l+1)\hbar^2]$$
  
  $\times [1 + [1 + 2l(l+1)\hbar^2 E/me^4]^{1/2}]$ .

We understand here by  $A_{\rm crit}$  the largest of the  $A_{\rm crit}$  values associated with the critical points of the star. The calculations of Wakano based on the HW equation of state indicate that the largest  $A_{\rm crit}$  value occurs at the LHWW critical point, in the "white dwarf" regime. This conclusion is accepted as correct in the text. The  $A_{\rm crit}$  value at the LOV critical point, in the neutron star regime, is calculated to be lower in the ratio 0.68/1.19 (Fig. 5). However, the details of the equation of state are uncertain at densities  $\rho_{\rm LOV} \sim 10^{16}\,{\rm g/cm^3}$ . The information available about the equation of state at such compressions is insufficient to exclude completely the possibility that  $A_{\rm crit}$  (LOV) is greater than  $A_{\rm crit}$  (LHWW), as noted, e.g., by Saakyan (1963) and by Hoyle, Narlikar, and Wheeler (1964). In that eventuality the discussion in the text is slightly more complicated: The contained collapse of the white dwarf is the first step in building the core of a neutron star. The mass of the neutron star is then augmented to the point of collapse by adding further baryons. Otherwise the analysis in the text goes through unchanged.

As one considers the softening effect of angular momentum on the collision of the electron, so one can imagine, in the case of the collapsing geometry, departures from ideality which in some cases might keep the curvature from rising to infinite values. However, we are concerned with the most symmetrical type of implosion because it poses most insistently and clearly the "issue of the final state," out of which one hopes ultimately to learn something new about physics. Therefore we note that electron impacts with l=0 frequently occur, and we conclude that symmetrical collapse also has to be accepted as physically possible. We now examine these two dynamical problems. In both cases we look for the new features which have to do with the quantum of action.

What saves the electron from catastrophe in a "head-on" impact upon a Coulomb field is the quantum of action, not any fault in the classical calculation of the kinetic energy within the context of classical theory. That calculation would predict an infinite kinetic energy at closest approach in a collision with l=0. However, the electron will not be localized with the precision assumed in the classical analysis. Moreover, localization demands a wave packet rather than an infinite wave train. A wave packet with a spread of energies from E=0 up to  $E \sim \hbar^2 k_0^2/2m$  will never be localized more closely than

within the distance

$$r \sim k_0^{-1} (1 + k_0^{-1} a^{-1})^{1/3}$$

 $(a = \hbar^2/me^2 = \text{Bohr radius})$  of the singularity at r = 0. The singularity in the potential creates no difficulties for the quantum mechanics of the electron. That particle comes out after the encounter as easily as it went in.

As it was inappropriate to describe the motion of the electron classically, particularly when it came close to the nucleus, so it is out of place to attribute a deterministic dynamic evolution to the geometry in the final stages of collapse. Quantum mechanics provides its own well-known probabilistic description for dynamics. One speaks of the probability amplitude  $\psi(x, t)$  for the electron to be in a unit volume at x at the time t, in the general case (wave packet); and for the electron in its ground state at a given time,

$$\psi = N \exp(-r/a)$$
,

where  $N=(\pi a^{s})^{-1/2}$  is a normalization factor. For the Maxwell field in *its* ground state, the probability amplitude for the divergence-free magnetic field B=B(x) to have any given pattern is

 $\psi\left(\boldsymbol{B}\right) = N\,\exp\left(-\int\!\!\int\!\!\frac{\boldsymbol{B}\left(\boldsymbol{x}\right)\cdot\boldsymbol{B}\left(\boldsymbol{y}\right)d^{z}\boldsymbol{x}d^{z}\boldsymbol{y}}{16\pi^{z}h\,c\,\left|\,\boldsymbol{x}-\boldsymbol{y}\right|^{z}}\right).$ 

A similar functional mathematics describes the probability for the geometry to have any given character at any chosen time. One speaks of the probability amplitude  $\psi(^{(2)}g)$  for the 3-geometry of the spacelike hypersurface under study to have this, that, or the other form. The probability amplitude  $\psi$  does not depend upon this 3-geometry and upon time. Instead, the 3-geometry itself carries all of the relevant information about time. But the geometries that occur with substantial probability amplitude are concluded for the most part to be topologically complex, of a high degree of multiple connectivity, insofar as one can draw any conclusions on this point from simple order of magnitude estimates of quantum fluctuations in the geometry (Wheeler 1964b). By reason of these topological complications the concept of "time" has new features in quantized general relativity to which one is not accustomed in flat space physics. In addition, there occurs the standard quantum-mechanical splitting of "one" history into a number of alternative

<sup>&</sup>lt;sup>12</sup> For the development of singularities in the geometry, and the question of whether these singularities can be avoided, see Lifshitz and Khalatnikov (1963), Wheeler (1964b), and Penrose (1965).

<sup>&</sup>lt;sup>15</sup> On three-dimensional geometry as carrier of information about time, see Baierlein, Sharp, and Wheeler (1962).

histories, with which one is already familiar from other branches of quantum mechanics (Feynman 1948, 1949). This multifoliate character of the history (Fig. 22) comes most pronouncedly into evidence following a time when the geometry has come close to becoming singular. By analogy one recalls how the scattering of an electron occurs primarily in that part of coordinate space where the interaction is strong.

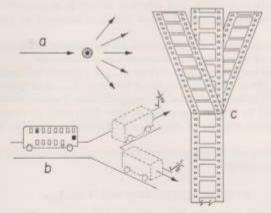


Fig. 22.—Quantum-mechanical split of history into multifoliate histories compared and contrasted for (a) the case when the observer is outside the system and (b,c) the case—today far from being understood—when the observer is part of the system. In (a) an electron experiences scattering in a Coulomb field. The probability distribution of outcomes does not trouble the observer because he stands high above this microscopic physics. In contrast, in the highly idealized case (b), the observer in the bus lives through quite a different history according as he—and the bus—are associated with the branch of the wave function going to the left or the one going to the right. Similarly, in (c) the lower filmstrip shows the geometry of a closed universe collapsing to a condition of near singularity, following which there are many alternative histories of comparable probability amplitude for the development of the geometry. Any observer is necessarily located within the system. He is aware of only one of these histories.

#### OBSTACLES TO DEFINING AND APPLYING THE LAW OF CONSERVATION OF BARYONS

The new character of time in quantum geometrodynamics makes it difficult to define any law of conservation of baryons, and doubtful whether the conservation law has any meaning, in the phenomenon of gravitational collapse. At the center of any application of a conservation law sits a "pillbox." Its top and bottom are spacelike hypersurfaces, One integrates over each hypersurface to get the value of the conserved quantity at two times. The difference between the two values is given by the net outward flow, an integral over the sides of the pillbox. The application of this line of reasoning to the present type of problem is blocked by three obstacles. First, the topology allowable for the spacelike hypersurface is forced to change as time goes on even in certain elementary problems of classical general relativity where one can follow the dynamics of the geometry in all detail (the universe of Taub [Taub (1951); Misner (1963)] and the Reissner-Nordstrøm geometry [Graves and Brill (1960)]). In such instances the construction of a global pillbox cannot be carried through to completion. Second, at the quantum level of analysis of the geometry the typical topology is calculated to be complex down to a scale of dimensions of the order of 10-33 cm. Such a topology makes difficulties for the construction of even a very small pillbox. Therefore the application of the conservation law would seem to be problematical even at the microscopic level. Finally, the multifoliate character of the history of the geometry following collapse (Fig. 22) poses its own difficulties for defining what one means by baryon conservation.

One does not know how to define baryon conservation in gravitational collapse, Still less does one know how to use any such idea under conditions where the collapsing region loses its causal contact with the outside. To be unable to use the idea of conservation nevertheless poses no obstacle to speaking of the disappearance of baryons in the process of collapse, regardless of the formal applicability or inapplicability of conservation to these particles. Furthermore, we can deal with the disappearance of baryons into the final state of collapse whether or not all of their mass is radiated away, whether or not some black center of attraction remains, and whether or not it is possible to put unlimited numbers of baryons into a volume of space which is assessed as finite by Euclidean standards.

What, then, can we say about the process of disappearance of baryons, and about the

time-reversed process of appearance of baryons out of darkness?

When the number of baryons is greater than  $A_{\rm crit}$  the system will collapse without outside assistance. When the number of baryons is less than  $A_{\rm crit}$  (but greater than  $A_{\rm quantum}$ ) and when the system is in one of the stable configurations of equilibrium, then activation energy can be supplied to trigger the collapse (see discussion in chap. viii; illustrative numbers in Table 10; one scheme of initiation illustrated in Fig. 16) or:

THEOREM 41: The system can tunnel quantum mechanically through the collapse barrier and undergo spontaneous collapse.

#### BARRIER PENETRATION FOR $A \sim A_{crit}$

Three methods suggest themselves for analyzing the decay constant for spontaneous collapse. The first two can be seen to lead to gross overestimates of the time required. The third is more reasonable physically but also almost impossible to put numbers to. Figure 23 treats spontaneous collapse as a collective phenomenon. The system is envisaged as undergoing a collective breathing mode. What is the probability per second that the degree of freedom associated with this mode will penetrate the collapse barrier? We follow the Gamow theory of radioactive decay and the theory of spontaneous fission, and write

$$T_{1/2} \sim \begin{pmatrix} \text{Characteristic} \\ \text{time of vibration} \end{pmatrix} \exp (2I)$$
. (362)

Here the Gamow barrier integral I has in the case of a single particle the well-known form

$$2I = (4/\hbar) \int_{\text{barrier}} (m/2)^{1/2} [V(x) - E]^{1/2} dx$$
. (363)

In the case of a system containing a number of particles, such as a fissile nucleus, one introduces a collective deformation parameter  $\alpha$  and replaces  $(m/2)^{1/2}dx$  by

$$\left[\sum_{i} (m_{i}/2) (dx_{i}/d\alpha)^{3}\right]^{1/2} d\alpha.$$
 (364)

In the present instance we take as the parameter  $\alpha$  the radius of the configuration. We idealize it as of uniform density, and preserving uniform density during the breathing mode:

$$dr = (r/R)dR. (365)$$

A simple integration suffices to evaluate expression (363) in terms of the mass of the system. The result of the calculation can be written to a sufficient approximation in the form

$$T_{1/2} \sim 10^{-4} \text{ sec exp } (4/L^{*2}) (3M_{\text{equil}}^*/10)^{1/2} \int (M_R^* - M_{\text{equil}}^*)^{1/2} dR$$
. (366)

Here the rough estimate of the order of magnitude of the breathing period has been taken from the dimensions of a neutron star:

(Period) 
$$\sim 2R/(\text{Velocity of sound}) \sim (10^{6} \text{ cm})/(2 \times 10^{10} \text{ cm/sec}) \sim 10^{-4} \text{ sec}$$
. (367)

Also  $(M_R^* - M_{\text{equil}}^*)$  is the mass-energy required to deform the system to the radius R from the equilibrium dimension.

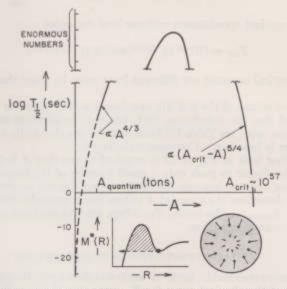


Fig. 23.—Lifetime of an A-baryon system against tunneling through the potential barrier against gravitational collapse by way of the simplest breathing mode of collective deformation (schematic only). The mode of motion envisaged is shown in the inset at the lower right; the barrier to be penetrated appears in the graph of  $M^*(R)$  versus the radius R of the configuration. For  $A < A_{\text{quasiron}}$  the classically calculated size of the configuration at the point of passage over the top of the barrier is too small ( $<10^{-11}$  cm) for classical considerations to be applicable. The classically estimated value of  $\log T_{1/2}$  in this region is marked with a dashed line because it has no relevance whatsoever to a proper quantum calculation of the collapse probability in this regime. The considerations in the text indicate that the lifetime against gravitational collapse—however long it is—is far shorter than indicated in the major portion of this curve. It is fantastically more difficult for an entire system of astronomical size (but with  $A < A_{\rm em}$ ) to tunnel through the barrier all together than for a limited number of baryons together to go through a limited barrier.

The non-vanishing terms of lowest order in the expansion of  $M_R^*$  about the point of inflection at  $A = A_{crit}$ ,  $R = R_{crit}$  are

$$\begin{split} M^*(R,A) &= M_{\rm crit}{}^* + \tfrac{1}{6}(\partial^3 M^*/\partial R^2)_{\rm crit}(R-R_{\rm crit})^3 + (\partial M^*/\partial A)_{\rm crit}(A-A_{\rm crit}) \\ &+ (\partial^2 M^*/\partial A\partial R)_{\rm crit}(A-A_{\rm crit})(R-R_{\rm crit}) \;. \end{split} \tag{368}$$

A simple investigation on the foundation of this expansion gives for the barrier penetration integral of expression (366) near  $A = A_{\text{erit}}$  a result proportional to  $(A_{\text{erit}} - A)^{5/4}$ ; thus,

$$\log_{10} T_{1/2} \sim -4 + \text{const} (A_{\text{crit}} - A)^{5/4}$$
, (369)

#### BARRIER PENETRATION FOR $A <<< A_{\rm crit}$ BUT $A > A_{\rm quantum}$

In the opposite limiting case of small A we make use of the barrier illustrated in Figure 14. Also we note that the system is highly relativistic as it traverses the barrier. Therefore we estimate momentum, not from the square root of the energy, but from the energy itself. The barrier penetration integral is of the order

(Barrier height)(Barrier width) 
$$\sim A^{4/3}$$
, (370)

and the lifetime against spontaneous collapse is of the order

$$T_{1/2} \sim (10^{-20} \text{ or } 10^{-30} \text{ sec}) \exp(-kA^{4/3})$$
, (371)

where k is a numerical constant not different from unity by more than one or two orders of magnitude.

The qualitative course of the half-life as a function of A is shown in Figure 22. It has to be emphasized that the calculation (371) has not the slightest status in the domain  $A < A_{\text{quantum}}$  (some tons; see Table 10) because there the classically calculated size of the

collapsing system is less than a Compton wavelength!

Only the briefest look at Figure 23 is required to see that it is far easier in getting some baryons to collapse to push only a small fraction of the baryons through the potential barrier; not to try to implode the whole system. On this second basis of estimation we take for  $T_{1/2}$  throughout the range of A values the magnitude which  $T_{1/2}$  is calculated to have for  $A = A_{\text{quantum}}$ —the lowest  $T_{1/2}$  where any classical calculation based on the idea of a barrier makes any sense.

#### AN ELEMENTARY-PARTICLE TRANSFORMATION

A third, still more reasonable, basis for analysis offers itself. Recognize from the steep downward slope of the classical curve for  $T_{1/2}$  near  $A = A_{\rm quantum}$  that regardless of details it will be simpler for a small number of elementary particles than for a large number to go over to the collapsed state. On this basis recognize that one has to deal with

what is really a new elementary-particle transformation.

One can compare one's state of ignorance about the details of this process with what one might have been able to say about nuclear physics in 1915 from a liquid-drop model in the absence of any information about the specificities of nuclear interactions. From such a model one would have calculated the energy E required to remove a piece of mass number  $\Delta A$  from a nucleus of mass  $A \sim 70$ . One would have obtained a smooth curve for E as a function of  $\Delta A$ , rising rapidly with  $\Delta A$ . From this curve one would have concluded—wrongly—that it is far easier to remove a neutron or proton from the nucleus than to take out an alpha-particle. The results at higher values of  $\Delta A$  would have been more reasonable. It would be quite wrong to conclude from Figure 22 that spontaneous collapse associated with the disappearance of one baryon necessarily goes much faster than spontaneous collapse associated with the simultaneous disappearance of two or four or some other modest and very specific number of baryons. One will require more guidance from the world of elementary-particle physics before one can reach any conclusions on this point. In the absence of such guidance, denote by N the number of baryons for which the "group disappearance rate" is the fastest of all.

We are led to envisage a process in which N baryons spontaneously disappear with, perhaps, the simultaneous release of energy in the form of radiation. Conversely, granted a region of space of high curvature, one must expect—according to the principle of microscopic reversibility—a process in which N baryons appear as a group out of empty

space.

#### BARYON APPEARANCE AND THE ONE-SIDEDNESS OF MATTER

To fix ideas, adopt 16 as a highly arbitrary figure for the optimum cluster size, N, for appearance or disappearance of baryons in vacuo. Let other baryons be present in the same region of space. They will influence the appearance and disappearance rates, according to standard arguments of statistical mechanics such as come into the comparison of spontaneous emission and induced emission. Therefore a mechanism exists by which the initial presence of baryons in a given neighborhood will influence the probability for additional baryons to appear in that neighborhood. In particular, one can envisage the case where the new baryons preferentially appear with the same sign of baryon number as those already present (matter versus antimatter). In this case one will be confronted with an autocatalytic character of the process in which matter comes into evidence. It will favor the appearance of more particles of the same kind in the same neighborhood. In this connection one calls to mind the character of the spiral molecule of DNA, which sees to it that new DNA molecules are created with the same chirality. The deep puzzle presented by the apparently one-sided character of matter in nature would thus possess a possible solution.

#### OBSERVABLE AT NORMAL DENSITY?

It is quite conceivable that spontaneous collapse occurs in nature and yet that it will never be observed at densities short of say ~1049 g/cm2. One has searched for the spontaneous explosion of protons (Reines and Giamati 1962) or their disappearance (Backenstoss, Frauenfelder, Hyams, Koester, and Marin 1960) with no success. Fraunfelder has set a lower limit of ~1024 years for any process which results in the disappearance of protons. If the lifetime of a baryon against collapse in ordinary matter is 10<sup>40</sup> years, there could be no conflict with the observations. In Rutherford's day it was astonishing that a nucleus like U, containing particles moving back and forth over a distance  $\sim 10^{-12}$  cm at a substantial fraction of the speed of light, should have a half-life as long as ~10° years. Today one knows over what a fantastic range of powers of 10 the Gamow penetration factor can make decay rates vary.

Rutherford (1905, p. 5) describes his search to see if all matter might be radioactive in these words: "It is natural to ask whether ordinary matter possesses this property of radioactivity] to an appreciable extent . . . a definite settlement of the question is experimentally very difficult."

The principles of relativity, applied to the phenomenon of gravitational collapse, leave no evident escape from the following conclusion: All matter must manifest, however weakly, a new form of radioactivity. This radioactivity is associated with a new and previously unrecognized process in elementary-particle physics, the spontaneous collapse of baryons singly or in groups of a characteristic favored size.

#### REFERENCES

- Backenstoss, G., Frauenfelder, H., Hyams, B. D., Koester, L. J., Jr., and Marin, P. C. 1960, Nuovo Cim.,

- Baierlein, R. F., Sharp, D. H., and Wheeler, J. A. 1962, Phys. Rev., 126, 1864.
  Bardeen, J. 1965, unpublished Ph.D. thesis, California Institute of Technology.
  Beckedorii, D. L. 1962, "Terminal Configurations of Stellar Evolution," unpublished A.B. Senior thesis, Princeton University
- Beckedorff, D. L., and Misner, C. W. 1962 (unpublished).
- Birkhoff, G. D. 1923, Relativity and Modern Physics (Cambridge, Mass.: Harvard University Press), p.
- Bendi, H. 1947, M.N., 107, 410.
- Callan, C. G., Jr. 1964, unpublished Ph.D. thesis, Princeton University.
- Chiu, H. Y. 1964, Ann. Phys., 26, 364.

  Colgate, S. A., Grasberger, W. H., and White, R. H. 1962, J. Phys. Soc. Japan, 17, Suppl. A-III, 157.

  Colgate, S. A., and Johnson, M. H. 1960, Phys. Rev. Letters, 5, 235.

  Colgate, S. A., and White, R. H. 1963, Bull. Am. Phys. Soc., 8, 306.

Feynman, R. P. 1948, Rev. Mod. Phys., 20, 367.

\_\_\_\_\_\_. 1949, Phys. Rev., 76, 769. Fowler, W. A. 1964, Rev. Mod. Phys., 36, 549.

Fowler, W. A. 1904, Kev. Mod. Phys., 39, 549.
Fronsdal, C., 1959, Phys. Rev., 116, 778.
Fuller, R. W., and Wheeler, J. A. 1962, Phys. Rev., 128, 919.
Ginzburg, V. L., and Ozernoi, L. M. 1964, Zhur. Eksp. Teor. Fiz., 47, 1030 (English translation in Soviet Phys.—J.E.T.P., in press).
Graves, J. C., and Brill, D. R. 1960, Phys. Rev., 120, 1507.
Hamoui, A. 1964, Acad. Sci. Paris Comptex Rendus, 258, 6085.
Hamber, E. and Ernder, W. A. 1964 in Operiodellas Sources and Gravitational Collapse ed. I. Robinson, A.

Hoyle, F., and Fowler, W. A. 1964, in Quasi-stellar Sources and Gravitational Collapse ed. I. Robinson, A. Schild, and E. L. Schucking (Chicago: University of Chicago Press).

Hoyle, F., Fowler, W. A., Burbidge, G. A., and Burbidge, E. M. 1964, Ap. J., 139, 909. Hoyle, F., Narlikar, J. V., and Wheeler, J. A. 1964, Nature, 203, 914. Klein, O. 1961, in Werner Heisenberg und die Physik unserer Zeit (Braunschweig: Friedrich Vieweg &

Komar, A. 1965, J. Math. Phys., in press.

Kruskal, M. D. 1960, Phys. Rev., 119, 1743.
 Lifshitz, E. M., and Khalatnikov, I. M. 1963, Adv. in Phys., 12, 185.
 Lindquist, R. W., and Wheeler, J. A. 1957, Rev. Mod Phys., 29, 432.

McVittie, G. C. 1964, Ap. J., 140, 401.

Marzke, R. F., and Wheeler, J. A. 1964, Gravitation and Relativity, ed. H. Y. Chiu and W. F. Hoffmann Marzke, K. F., and Wheeler, J. A. 1964, Gravitation and Relativity, ed. (New York: W. A. Benjamin), chap. iii.

May, M. M., and White, R. H. 1965, Bull. Am. Phys. Soc., 10, 15, Michel, F. C. 1963, Ap. J., 138, 1097.

Misner, C. W. 1963, J. Math. Phys., 4, 924.

Misner, C. W., and Sharp, D. H. 1964, Phys. Rev., 136, B571.

Novikov, I. D. 1962, Vestnik, Moscow State University, ser., 3, p. 56.

Oppenheimer, J. R., and Snyder, H. 1939, Phys. Rev., 56, 455. Penrose, R. 1965, Phys. Rev. Letters, 14, 57.

Petrov, A. Z. 1963, Zhur. Eksp. Teor. Fiz., 44, 1525 (English translation in Soviet Phys.-J.E.T.P., 17, 1026)

Reines, F., and Giamati, C. C. 1962, Phys. Rev., 126, 2178.

Rutherford, E. 1905, Pop. Sci., May, 1905. Saakyan, G. S. 1963, Soviet Aste.—A. J., 1, 60. Taub, A. H. 1951, Ann. Math., 53, 472.

1963, Usp. Fiz. Nauk, 80, 357 (English translation in Soviet Phys.—Uspekni, 6, 475).

# NUMERICAL INTEGRATION OF THE GENERAL-RELATIVITY EQUATION OF HYDROSTATIC EQUILIBRIUM:

## appendix A METHODS AND RESULTS

The first numerical integrations were made by one of us (M. W.) in 1957 for forty-four values of the central density. (For the results of these first integrations, see Harrison, Wakano, and Wheeler [1958].) The Schwarzschild radial coordinate r was zoned off into intervals  $\Delta r$  at points  $r_k$ . The density  $\rho(r)$  was taken as the primary quantity. The secondary quantities p and  $dp/d\rho$  needed in the TOV general-relativity equation (11) of hydrostatic equilibrium were evaluated from the analytic expressions for the equation of state, as listed here in chapter ix. From a knowledge of the key quantities  $\rho_k$ ,  $\rho_k$  and  $(dp/d\rho)_k$  at the point k the values of the appropriate quantities at the point  $r_{k+1} = r_k + \Delta r$  were obtained by Milne's centered method of numerical integration. Preliminary values for the increments, labeled with a subscript a, were first calculated for the new zone:

$$\Delta \rho_{h+1/2, q} = (d\rho/dr)_k \Delta r \text{ (from eq. [11])},$$
 (A1)

$$\Delta m_{k+1/2, a} = (dm/dr)_k \Delta r \text{ (from eq. [8])},$$
(A2)

$$\Delta A_{k+1/2, a} = (dA/dr)_k \Delta r \text{ (from eq. [9])}$$
. (A3)

From these increments preliminary values of the quantities themselves (indicated by a superscript †) were obtained at the new point:

$$\rho_{k+1}\dagger = \rho_k + \Delta \rho_{k+1/2, a}$$
,  
 $m_{k+1}\dagger = m_k + \Delta m_{k+1/2, a}$ ,  
 $A_{k+1}\dagger = A_k + \Delta A_{k+1/2, a}$ ,  
 $\rho_{k+1}\dagger = \rho(\rho_{k+1})$ .

From these preliminary values at  $r_{k+1}$  one calculated values (indicated with a subscript b) for the increments in the same zone  $k \to k + 1$ , via equations of the form

$$\Delta \rho_{k+1/2, b} = (d\rho/dr)_{k+1} \dagger \Delta r . \qquad (A5)$$

Final values for the quantities at the point  $r_{k+1}$  were then obtained from equations of the form

$$\rho_{k+1} = \rho_k + \frac{1}{2} (\Delta \rho_{k+1/2, a} + \Delta \rho_{k+1/2, b}). \tag{A6}$$

The calculation proceeded this way, as indicated more fully in Figures 24 and 25. The machine

Described in many texts; see, e.g., Lapidus (1962).

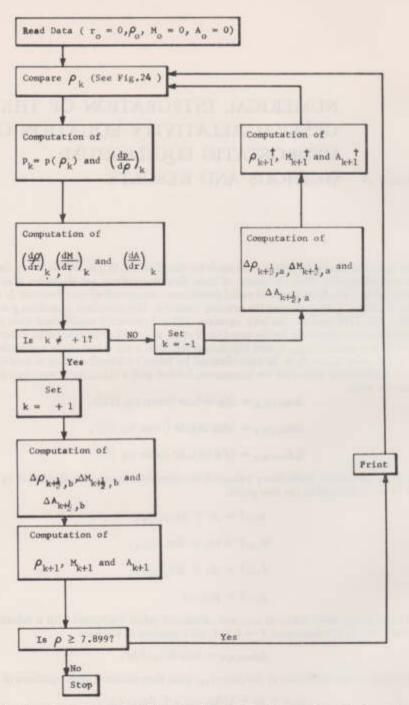


Fig. 24.—Flow diagram for numerical integration of general-relativity equations of hydrostatic equilibrium, in broad outline. The memory cell that contains the symbol k is set at the start of the calculation at k = +1. This is an indication to branch to the right on arrival at the point of division of the calculation, and to set k = -1. On return to this branch point in the calculation, the symbol k = -1 tells the machine to proceed vertically downward in the flow diagram, and to change k back to the value +1. When the density drops below the normal density of iron, the penultimate instruction warns that the point has been passed where the pressure vanishes, and the machine stops the calculation.

was stopped when at the point  $r_{k+1}$  the computed pressure was negative, indicating that the surface of the configuration lay at an appropriately interpolated point r = R between  $r_k$  and  $r_{k+1}$ . The interval  $\Delta r$  was chosen so that this cutoff value of k lay between 100 and 200. No attempt was made to use as a check the alternative expression for the mass-energy given by Tolman (1930).

$$M^* = 4\pi f(\rho^* + 3\rho^*)e^{(\lambda+s)/2}r^2dr$$
, (A7)

Tables A1, A2, and A3 present in number form the equilibrium mass and radius and other relevant parameters as obtained in the 1964 integrations of Harrison. They duplicate within the limits of error of a few per cent the results obtained by Wakano in 1957 by the methods just described. In computing these tables, Harrison fed the equation of state into the computer in the form of a list of 72 values (analogous to the Table 13 of primary values, and obtained from that table by graphical interpolation), while in his 1957 computations Wakano used the equation of state in the form of equations (258)—(261).

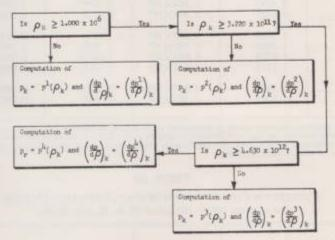


Fig. 25.—Picking the appropriate analytical expression for pressure as a function of density out of the several formulae given in chap, x for various density regimes. The present diagram spells out what is meant by the instruction box "Compare  $\rho_k$ " in Fig. 24.

Table A1 extends from a central density of 10 g/cm<sup>2</sup> up to 10° g/cm<sup>3</sup>, thus encompassing the LHWW critical point.

Table A2 extends from 10° to 3 × 10<sup>14</sup> g/cm³, through the zone where electrons are being crushed onto nuclei and through the HWW critical point where the system is nearly a neutron star and has become stiff. From the last two columns one can read the global packing fraction for the system as a whole and also the effective packing fraction per added particle. Compare with the 1 per cent range of packing fractions in atomic nuclei!

Table A3 includes central densities ranging from 3 × 10<sup>14</sup> to 10<sup>22</sup> g/cm<sup>3</sup>. The star is now well into the neutron-star region; new critical points become evident, as shown pictorially in Figures 5-7. The convergence of the various quantities to constant values is quite apparent in this table. The maximum loss of mass in binding is 2.5 per cent (row 3).

The results listed in Tables A1-A3 are summarized in graphical form in Figures 5-7.

There is no attempt at any coverage of low baryon numbers ( $A < 3 \times 10^{88}$ ; see Table 16) in these tables because it is so much easier to determine the properties of the configurations for

<sup>‡</sup> The equivalence to the  $M^* = 4\pi f \rho^* r^2 dr$  of eq. (5) is shown, e.g., by Landau and Lifshitz (1951), p. 322.

TABLE A1

EQUILIBRIUM CONFIGURATIONS OF COLD, CATALYZED MATTER FOR 
p0 UP TO 10° g/cm² (B. K. H. AND M. W.)\*

ρο(g/cm <sup>3</sup> )	M*(km)	R(km)	$A\mu_0$ *(km)	$M^{\alpha}/\mu_a v_A$	$dM^{+}/\mu_{s}^{+}dA = (1-2M^{+}/R)il$
1.021×10	8.987×10 <sup>-1</sup>	$\begin{array}{c} 3\_196\times10^2 \\ 7.024\times10^2 \\ 1.085\times10^4 \\ 1.410\times10^4 \end{array}$	8.987×10 <sup>-1</sup>	1.0000	1.0000
1.551×10	1.273×10 <sup>-4</sup>		1.273×10 <sup>-4</sup>	1.0000	1.0000
3.153×10	7.066×10 <sup>-4</sup>		7.066×10 <sup>-4</sup>	1.0000	1.0000
9.918×10	3.655×10 <sup>-1</sup>		3.655×10 <sup>-4</sup>	1.0000	1.0000
3.126×10 <sup>a</sup>	1.573×10 <sup>-1</sup>	1.635×10 <sup>4</sup>	1.573×10 <sup>-4</sup>	1,0000	1.0000
1.009×10 <sup>a</sup> .	5.872×10 <sup>-1</sup>	1.770×10 <sup>4</sup>	5.872×10 <sup>-3</sup>	1,0000	1.0000
3.209×10 <sup>a</sup> .	1.672×10 <sup>-1</sup>	1.778×10 <sup>4</sup>	1.672×10 <sup>-2</sup>	1,0000	1.0000
9.983×10 <sup>1</sup> .	4.565×10 <sup>-2</sup>	1.740×10 <sup>4</sup>	4.565×10 <sup>-4</sup>	1,0000	1.0000
3.117×10 <sup>4</sup> .	9.898×10 <sup>-3</sup>	1.626×10 <sup>4</sup>	9.898×10 <sup>-2</sup>	1.0000	1.0000
9.983×10 <sup>4</sup> .	0.1964	1.442×10 <sup>4</sup>	0.1964	1.0000	1.0000
3.228×10 <sup>6</sup> .	0.3795	1.244×10 <sup>4</sup>	0.3795	1.0000	1.0000
9.983×10 <sup>6</sup> .	0.6739	1.076×10 <sup>4</sup>	0.6739	1.0000	0.9999
3.172×10 <sup>6</sup> .	1.0309	9.000×10 <sup>3</sup>	1 0310	0.9999	0.9999
9.983×10 <sup>6</sup> .	1.3855	7.250×10 <sup>3</sup>	1 3858	0.9998	0.9998
3.065×10 <sup>7</sup> .	1.6274	5.943×10 <sup>3</sup>	1 6279	0.9997	0.9997
9.983×10 <sup>7</sup> .	1.7218	4.640×10 <sup>3</sup>	1 7225	0.9996	0.9996
3.209×10 <sup>8</sup>	1.7466	3.525×10 <sup>8</sup>	1,7476	0.9994	0.9995
9.983×10 <sup>8</sup>	1.6895	2.695×10 <sup>8</sup>	1.6908	0.9992	0.9994

<sup>\*</sup> The starred quantities represent masses in geometrized units:  $M^{**}(cm) = (G/\varepsilon^{5}) M(g) = (0.743 \times 10^{-24} \text{ km/g})M$ . With  $M \odot = 1.987 \times 10^{42} \text{g}(Sun)$  one has  $M \odot ^{**} = 1.474 \text{ km}$ . The quantity  $\mu_{t} = 1.659 \times 10^{-28} \text{g}(S_{t})$  of the mass of Fe<sup>30</sup> is taken here as the standard baryon mass;  $\mu_{t}^{**} = 1.231 \times 10^{-28} \text{ km}$ . Thus the baryon number can be obtained directly from column 4 ("mass before assembly"). See chap, v = v if or discussion.

TABLE A2

EQUILIBRIUM CONFIGURATIONS OF COLD, CATALYZED MATTER
FOR \(\rho\_0\) FROM 10° TO 10<sup>14</sup> g/cm<sup>3</sup> (B. K. H. AND M. W.)

μe(g/cm²)	$M^{a}(km)$	E(km)	Aμ <sub>0</sub> * (km)	$M^a/\mu_0^+A$	$dM^*/\mu_s^*dA = (1-2M^*/R)^{ij}$
3 210×10°	1.589	$\begin{array}{c} 1.980\times10^3\\ 1.428\times10^3\\ 1.034\times10^3\\ 7.900\times10^2 \end{array}$	1.5913	0.9989	0.9992
9 983×10°	1.4943		1.4965	.9985	.9990
3 153×10¹0	1.4044		1.4072	.9980	.9986
9 983×10¹0	1.2524		1.2556	.9974	.9984
3 206×10 <sup>11</sup>	1.0858	6 666×10 <sup>p</sup>	1.0890	.9970	.9984
9 983×10 <sup>11</sup>	0.9878	6 872×10 <sup>p</sup>	0.9907	.9971	.9986
3 143×10 <sup>12</sup>	0.9181	8 252×10 <sup>p</sup>	0.9205	.9974	.9989
6 243×10 <sup>12</sup>	0.8761	1 044×10 <sup>q</sup>	0.8781	.9978	.9992
9 983×10 <sup>12</sup>	0.8242	1.413×10 <sup>2</sup>	0.8257	.9982	.9994
1 .314×10 <sup>12</sup>	0.7641	1.916×10 <sup>2</sup>	0.7652	.9986	.9996
1 .775×10 <sup>12</sup>	0.5788	2.897×10 <sup>3</sup>	0.5794	.9989	.9998
2 .176×10 <sup>13</sup>	0.2977	1.246×10 <sup>3</sup>	0.2981	.9987	.9998
2 637×10 <sup>13</sup>	0.2598	3.226×10 <sup>g</sup>	0.2602	.9987	.9992
3 211×10 <sup>13</sup>	0.2648	1.563×10 <sup>g</sup>	0.2652	.9986	.9983
6 446×10 <sup>13</sup>	0.3300	5.172×10	0.3307	.9979	.9936
9 983×10 <sup>14</sup>	0.3909	3.617×10	0.3920	.9970	.9891
1.703×10 <sup>14</sup>	0.4851	2.631×10 2.058×10	0.4875 0.6087	.9952 0.9922	.9814

small A by analytic methods. The pressure is low enough so that the density is practically constant. Under these conditions the equilibrium configuration has the following elementary properties:

$$\rho(r) = \rho_0 = 7.85 \text{ g/cm}^3 \text{ (Fe}^{56});$$

$$M = (4\pi/3)\rho_0 R^3;$$

$$A = (4\pi/3\mu_s)\rho_0 R^3;$$

$$\rho(r) = (2\pi G/3)\rho_0^2 (R^2 - r^2);$$

$$\rho_0 = (2\pi G/3)\rho_0^2 R^2$$

$$= (\rho_0 c^2/2)(M^*/R);$$

$$g(r) = (\text{Acceleration of gravity at } r)$$

$$= (4\pi G/3)\rho_0 R;$$

$$(-g_{00})^{1/2} = e^{r/2} = \frac{(\text{Rate of ticking of clock inside})}{(\text{Rate of ticking of same clock far away})}$$

$$= \frac{(\text{Mass-energy of free uncompressed}}{(\text{Mass-energy, same particle, far away})}$$

$$\approx 1 + c^{-2} \text{ (Newtonian gravitational potential)}$$

$$= 1 + (M^*/R)[-\frac{n}{2} + (r^2/2R^2)].$$

TABLE A3

EQUILIBRIUM CONFIGURATIONS OF COLD, CATALYZED MATTER FOR po FROM 10<sup>14</sup> TO 10<sup>22</sup> g/cm<sup>3</sup> (M. W. AS EXTENDED BY B. K. H.)

ρε (g/cm <sup>2</sup> )	M* (km)	R (km)	Aug* (km)	$M^{*}/\mu_{0}^{*}A$	$\frac{dM^*/\mu_c^*dA = }{(1-2M^*/R)^{1/2}}$
9.983×10 <sup>14</sup>	0.8169	1.414×10	0.8292	0.9852	0.9405
1.75×10 <sup>th</sup>	9798	1.002×10	1.0036	0.9763	.8969
983×10 <sup>18</sup>	. 9844	7.479	1.0094	0.9752	.8584 .8455
3.222×10 <sup>14</sup>		5.893	0.8429	0.9965	.8933
0.983×10 <sup>16</sup>	. 6812	5.149	0.6575	1.0360	8576
. 255×10 <sup>17</sup>		5.208	0.5227	1.0797	.8851
983×10 <sup>17</sup>	.5336	6.002	0.4873	1.0950	-9068
3.183×10 <sup>18</sup>	.5800	6.717	0.5375	1.0789	_9097
9.983×10 <sup>18</sup>	. 6290	6.715	0.5915	1.0635	.9015
.190×10 <sup>18</sup>		6.456	0.6062	1.0592	.8950
.983×1011	6302	6.266	0.5931	1.0624	.8938
1.031×10 <sup>10</sup>	.6216	6.225	0.5837	1.0651	.8946
3.169×10 <sup>m</sup>	.6178	6.218	0.5793	1.0663	.8952
.003×10 <sup>n</sup>		6.288	0.5717	1.0687	.8976
1.162×10 <sup>rt</sup>	.6112	6.327	0.5719	1.0686	.8982
1.00×10 <sup>trs</sup>		6.36			. 8981
Db	46 Gra W	6.4	0.575	1.072	0.898

<sup>.</sup> Data are incomplete at this point.

Extrapolated.

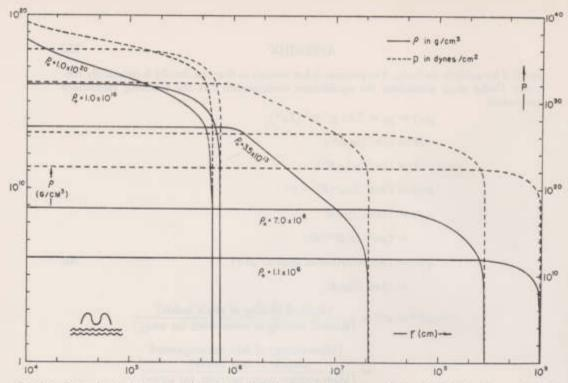


Fig. 26.—Dependence of pressure and density on the Schwarzschild radial coordinate r for 5 of the 44 cases for which electronic machine calculations were made by M. W. Density  $\rho$  in  $g/cm^4$ , pressure  $\rho$  in dynes/cm<sup>3</sup>, r in cm. In the case of the most extreme central density the graph does not reach far enough to show the obvious limiting values at the center.

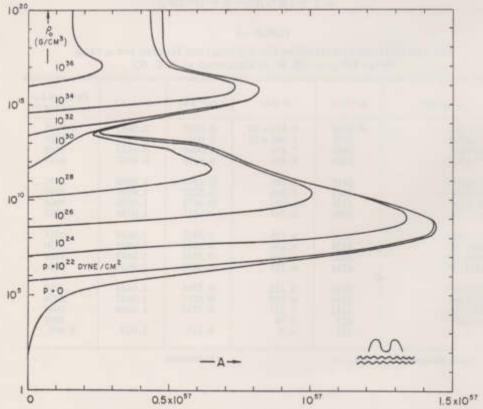


Fig. 27.—The total number of baryons inside the point where the pressure drops to a specified value, p, as a function of central density  $\rho_0$ . The figure is based on the electronic machine calculations of M. W.

No such simple analytic representation of conditions inside is possible in the general case. Instead, graphs are given for a few selected configurations in Figures 26 and 27. All these results refer of course to the ideal case of cold matter catalyzed to the end point of thermonuclear evolution. Actually, the existence of a central temperature as high as 107° K or 108° K would produce very little change in the calculated conditions in the interior. Only near the surface would conditions be changed. To analyze such a case one can take over the results of the appropriate one of the present integrations. One can use these results out to a point where the density is low enough for the pressure to begin to make a difference. From there out a new, hot, atmosphere can be fitted on by the appropriate subsidiary numerical integration,3

#### REFERENCES

- Harrison, B. K., Wakano, M., and Wheeler, J. A. 1958, in Onzieme Concell de Physique Solvay, La
- Structure et Pevolution de l'universe (Brusseis: Stoops).

  Landau, L. D., and Lifshitz, E. M. 1951, The Classical Theory of Fields (Reading, Mass.: Addison-Wesley
- Publishing Co.).

  Lapidus, L. 1962, Digital Computation for Chemical Engineers (New York: McGraw-Hill Book Co.).

  Tolman, R. C. 1930, Phys. Rev., 35, 875.

  Tsuruta, S. 1964, "Neutron Star Models," unpublished Ph.D. thesis, Columbia University.
- - Tsuruta (1964) has calculated hot neutron star models in this manner.

# THEORY OF THE STABILITY OF EQUILIBRIUM CONFIGURATIONS: DERIVATION FROM ENERGY

## appendix B CONSIDERATIONS

#### MOTIVATION

In chapter iii we found that the time-symmetric initial-value equation of general relativity is a sufficient basis from which to derive all hydrostatic properties, and the spacetime geometry, of any spherically symmetric, equilibrium configuration of cold, catalyzed matter: From the initial-value equation one obtains an expression for the total mass-energy,  $M^*$ , of such a configuration (Theorem 2), and by extremizing that mass-energy while holding the total number of baryons, A, fixed, one derives the equation of hydrostatic equilibrium (Theorem 3) and the theorem of constant injection energy (Theorem 4). Once the central pressure and equation of state for a given configuration are specified, the equation of hydrostatic equilibrium uniquely determines the pressure, the proper mass density, and the baryon density at all points in the star. The initial-value equation then yields the space part of the spacetime metric, and the theorem of constant injection energy gives the time part.

It is of interest to ask whether one can go even further than this without reference to the full Einstein field equations of general relativity. On the sole basis of the Fourès initial-value equation and mass-energy considerations stemming from it, can one determine whether an equilibrium configuration is stable or unstable against small radial perturbations? And can one even go so far as to predict the dynamical behavior of an equilibrium configuration and of the geometry of spacetime when the fluid is subjected to a small radial perturbation? Yes, one can—with one exception: No way has been found to obtain  $g_{00} = -e^{\nu}$  of the Schwarzschild metric for non-equilibrium configurations from mass-energy considerations alone.

The purpose of this Appendix is to discuss these dynamical issues from the mass-energy point of view, and to relate this viewpoint to the full field equation approach of Chandrasekhar (1964) and Misner and Zapolsky (1964).

#### OUTLINE OF THE ANALYSIS

Before we enter into the details of the analysis, let us give a general outline of what is to be proved.

We consider a sphere of perfect fluid performing radial motion near its equilibrium configuration. Working in the Lagrangian coordinates used in the proof of Theorem 3, we calculate the mass-energy of the configuration,  $M^*$ , to second order in the displacement from equilibrium,  $\xi(a, t) = \delta r(a, t)$ . The first-order correction to the mass vanishes because the equilibrium configuration about which the expansion is made extremizes the mass (Theorem 3); so we are left with only a second-order correction:

$$M^* = M_0^* + P^* + K^*$$
. (B1)

Here  $M_0$ \* is the mass-energy of the equilibrium configuration; P\*—the "potential" energy associated with the perturbation—is of the form

$$P^* = \int_a^A [g(a)\xi^2 + 2h(a)\xi(\partial\xi/\partial a) + j(a)(\partial\xi/\partial a)^2]da$$
, (B2)

and K\*-the "kinetic" energy-takes the positive-definite form

$$K^* = \int_0^A f(a)(\partial \xi/\partial t)^2 da$$
 (B3)

(see Theorem B1 below).

Regardless of the nature of any initial small perturbation imposed on the configuration, the evolution of  $\xi(a,t)$  with time must be such as to keep the total mass  $M^*$  fixed— $K^*+P^*$  is a constant of the motion. Since  $K^*$  is positive-definite, the equilibrium configuration will be stable if and only if  $P^*$  is also positive-definite (Theorem B2). Furthermore, if a time dependence of the form  $\xi = e^{i\omega t} \xi(r)$  is assumed ( $\omega$  possibly imaginary), the condition  $K^*+P^*=$  constant takes the form

$$\omega^2 = P^* / \int_0^A f(a)\xi^2 da \qquad (B4)$$

(see Theorem B3). Not only do we have a method for distinguishing between stable and unstable configurations, but we also have in equation (B4) a method for calculating the angular frequencies  $\omega$  (or exponential growth rates  $\alpha = i\omega$ ) of the normal modes once the space dependence of the amplitudes of those modes is known.

But how can the space dependence,  $\xi(a)$ , of the normal modes be determined? It is determined as follows: Take the kinetic energy minus the potential energy as a Lagrangian for calculating the wave equation that governs the evolution of arbitrary perturbations  $\xi(a,t)$ . In that wave equation specialize to sinusoidal time dependence and then notice that equation (B4) is a variational principle from which the space parts of the normal modes as well as their frequencies can be calculated—the normal modes are those displacements  $\xi(a)$  which extremize  $P^*$  for fixed  $ff(a)\xi^2da$  (Theorem B3).

This variational principle for studying the acoustical modes of a spherically symmetric configuration of cold, catalyzed matter is identical to the one derived from the full Einstein equations by Chandrasekhar (1964) and discussed in chapter vii.

#### DETAILS OF THE ANALYSIS-CALCULATION OF THE MASS TO SECOND ORDER

So much for the outline; now for the details: Consider a spherically symmetric configuration of cold, catalyzed matter containing A baryons and executing spherically symmetric motion near an equilibrium configuration. Introduce Schwarzschild coordinates<sup>t</sup>

$$ds^2 = -e^{\mu}dt^2 + e^{\lambda}dr^2 + r^2d\theta^2 + r^2\sin^2\theta d\varphi^2$$
,

as well as the baryon number coordinate a(r) = (number of baryons inside a given shell of matter). Take a and t as independent variables, and describe the motion of the fluid by giving

<sup>1</sup> For a proof that Schwarzschild coordinates can be introduced despite the non-static character of the problem see, e.g., Tolman (1934), p. 239. The Schwarzschild radial coordinate, τ, is uniquely defined by requiring the Schwarzschild line element to exhibit spherical symmetry and by demanding that the circumference of a circle about the origin be 2πr for all times t. For static configurations the time coordinate was uniquely defined by the demand for a static metric which approaches Minkowski form at radial infinity; but for non-static configurations, t is defined only up to a function of itself, t→f(t). In this analysis we shall require that go = e<sup>\*</sup> depart from its equilibrium value by an amount only of order δr(a); this requirement "ties" the time coordinate to that of the equilibrium configuration, thereby determining it up to order δr(a). The considerations which follow are valid for all Schwarzschild time coordinates so defined.

the radial coordinate displacement of the fluid at a as a function of coordinate time t (Lagrangian formulation):

$$\xi(a, t) \equiv \delta r(a, t) \equiv r(a, t) - r_0(a, t)$$
, (B5)

Label the equilibrium values of all quantities by a subscript 0, the first-order corrections due to the fluid's motion by a subscript 1, and the second-order corrections by a subscript  $2-\rho^*(a)=\rho_0^*(a)+\rho_1^*(a)+\rho_2^*(a)$ , etc.; and work toward the goal of expressing all first-order quantities as linear functions of  $\xi$  and  $\partial \xi/\partial a$  with coefficients constructed from equilibrium parameters, and all second-order quantities as quadratic functions of  $\xi$ ,  $\partial \xi/\partial a$ , and  $\partial \xi/\partial t$  with equilibrium coefficients. Denote derivatives with respect to a by primes and derivatives with respect to b by dots:  $\xi' = \partial \xi/\partial a$ ,  $\xi = \partial \xi/\partial t$ .

The quantity of greatest interest is the mass-energy of the configuration, as defined for instance by particles orbiting it at great distances. The mass is given in terms of the "Schwarzschild correction factor" \( \lambda \) by

$$c^{\lambda} = [1 - 2m^{*}(r)/r]^{-1}, \quad M^{*} = m^{*}|_{\text{surface of configuration}}$$
 (B6)

The Schwarzschild correction factor can be calculated from the initial value equation (Theorem 1). The intrinsic scalar curvature of the hypersurface of constant  $t_i$  (3)  $R_i$  is

$$^{(3)}R = 4r^{-2}dm^*(r)/dr$$
 (7)

(see Theorem 2), while the extrinsic curvature

$$K_{ij} = \begin{cases} -\frac{1}{2} \dot{\lambda} e^{\lambda \rightarrow j/2} & \text{if } i = j = 1 \\ 0 & \text{otherwise} \end{cases}$$
 (B7)

has a vanishing second invariant:  $K_2 = 0.2$  Consequently, as in the static case, the initial-value equation reads<sup>2</sup>

$$dm^*/dr = 4\pi r^2 T_0^{0*}$$
 (B8)

For a perfect fluid in Schwarzschild coordinates,  $T_0^{0*}$  takes the form (to second order in  $\xi$ )

$$T_0^{0+} = \rho^* + (\rho^* + \dot{p}^*)e^{\lambda - \epsilon}\dot{\xi}^2$$
, (B9)

where  $\rho^*$  and  $\rho^*$  are the proper density and pressure of the fluid (density and pressure measured in a Lorentz frame moving with the fluid). Consequently, when a is taken as the independent variable in equation (B8), and both sides are expanded in powers of  $\xi$ , there results

$$m_0^{*'} = 4\pi r_0^2 \rho_0^* r_0^{'},$$
 (B10)

$$m_1^{*'} = 4\pi r_0^2 r_0' [(2 \xi/r_0 + \xi'/r_0') \rho_0^* + \rho_1^*],$$
 (B11)

$$m_2^{*'} = 4\pi r_0^2 r_0' [(\xi^2/r_0^2 + 2 \xi \xi'/r_0 r_0')\rho_0^* + (2 \xi/r_0 + \xi'/r_0')\rho_1^* + \rho_2^* + (\rho_0^* + \rho_0^*)\epsilon^{\lambda_0 - \nu_2} \xi^2],$$
  
(B12)

The zero-order equation was presented in Theorem 2, and the first-order equation was derived (in slightly different form) and solved in the proof of Theorem 3:

$$m_1^* = -4\pi r_0^2 \dot{p}_0^* \xi$$
, (B13)

<sup>&</sup>lt;sup>2</sup> This result demonstrates the very special nature of the Schwarzschild time coordinate—the t coordinate lines are orthogonal to a space-filling family of hypersurfaces with vanishing second extrinsic-curvature invariant.

<sup>&</sup>lt;sup>3</sup> In Theorem 1 we used  $\rho^*$  to denote the total mass-energy density in the synchronous local Lorentz reference frame. However, in this Appendix we shall denote that quantity by  $T_0^{a*}$  and reserve the symbol  $\rho^*$  for the *proper* mass-energy density of the fluid.

Returning to equation (B11) with this first-order solution, we find

$$\rho_1^* = -(\rho_0^* + p_0^*)(2 \xi/r_0 + \xi'/r_0') - p_0^{*'}\xi/r_0'$$
. (B14)

If we only knew  $\rho_2^*$  in terms of  $\xi$ , we could insert it and  $\rho_1^*$  into equation (B12) and integrate to obtain the mass-energy of the configuration to second order.

The easiest way to obtain  $\rho_2^*$  is to first calculate the proper baryon density, n(a), and to then find  $\rho^*$  from n via equation (13). The proper baryon density is

$$n(a) = \frac{d(\text{Number of baryons})}{d(Proper \text{ volume})}$$

$$= \frac{d(\text{Number of baryons})}{d(\text{Volume in Schwarzschild coordinates}) \times (\text{Lorentz contraction factor})}$$
(B15)

$$= \frac{1}{4\pi r^2 r' [1 - 2m^*/r]^{-1/2} [1 - e^{\lambda - \nu} \xi^2]^{1/2}}.$$

When expanded in powers of  $\xi$  this equation takes the form

$$n_1/n_0 = -2\xi/r_0 - \xi'/r_0' - e^{\lambda_0}[m_1^*/r_0 - m_0^*\xi/r_0^2],$$

$$n_2/n_0 = 3\xi^2/r_0^2 + 2\xi\xi'/r_0r_0' + \xi'^2/r_0'^2 + e^{\lambda_0}[m_1^*/r_0 - m_0^*\xi/r_0^2][3\xi/r_0 + \xi'/r_0']$$
  
 $-\frac{1}{2}e^{2\lambda_0}[m_1^*/r_0 - m_0^*\xi/r_0^2]^2 - e^{\lambda_0}m_2^*/r_0 - \frac{1}{2}e^{\lambda_0-r_0}\dot{\xi}^2.$ 

By inserting expression (B13) for  $m_1^*$ , and employing the equation of hydrostatic equilibrium (eq. [11]) and the relation<sup>4</sup>

$$\nu_0' = -2p_0^{*'}/(\rho_0^* + p_0^*),$$
 (B16)

we make these baryon density corrections read

$$n_1/n_0 = -e^{\nu_0/2} [e^{-\nu_0/2} r_0^2 \xi]'/(r_0^2 r_0'),$$
 (B17)

$$\begin{split} \frac{n_2}{n_0} &= 3 \cdot \frac{\xi^2}{r_0^2} + 2 \cdot \frac{\xi \, \xi'}{r_0 r_0'} + \frac{\xi'^2}{r_0'^2} + \frac{p_0^{*'} \, \xi}{\left( \, \rho_0^{\,*} + p_0^{\,*} \, \right) \, r_0'} \left[ \, \frac{3 \, \xi}{r_0} + \frac{\xi'}{r_0'} \right] \\ &- \frac{p_0^{*'2} \, \xi^2}{\left( \, \rho_0^{\,*} + p_0^{\,*} \, \right)^2 r_0'^2} - e^{\lambda_0} \, \frac{m_2^{\,*}}{r_0} - \frac{1}{2} \, e^{\lambda_0 - r_0} \, \xi^2 \,. \end{split} \tag{B18}$$

In the second-order expression all terms except the next to the last one are quadratic in  $\xi$  and its derivatives. Note in passing that in terms of the physical variables  $\rho_0^*$ , and  $n_0$ , equation (B17) takes the form

$$n_1/n_0 = (dn_0/d\rho_0^*)r_0^{-2}[(d/dr_0)(r_0^2\xi d\rho_0^*/dn_0)].$$
 (B17')

The proper baryon density and the proper mass density are related by

$$n = (\rho^*/\mu_s^*) \exp \left[ - \int_0^{\rho^*} (p^*/\rho^*) (\rho^* + p^*)^{-1} d\rho^* \right],$$
 (B19)

as is seen by integrating equation (13). Expanding this about the equilibrium configuration, we obtain

$$\rho_1^*/(\rho_0^* + p_0^*) = n_1/n_0$$
 (B20)

<sup>\*</sup>This relation follows from  $\nu_0(r) = -2 \ln \mu(r) + \text{constant (eq. [28])}$ , and from eqs. (13) and (14) for the chemical potential.

and

$$\rho_2^*/(\rho_0^* + p_0^*) = n_2/n_0 + \frac{1}{2}\gamma_0p_0^*/(\rho_0^* + p_0^*)n_1^2/n_0^2$$
,

where

$$\gamma_0 = [(\rho_0^* + p_0^*)/p_0^*]dp_0^*/d\rho_0^*.$$
(B21)

Insertion of expressions (B17) and (B18) for the baryon density corrections into equation (B21) gives

$$\begin{split} \rho_2^* &= \frac{1}{2} p_0^* \gamma_0 e^{i_0} [(e^{-r_0} r_0^2 \xi)' / (r_0^2 r_0')]^2 + p_0^{*'} [3\xi^2 / r_0 r_0' + \xi \xi' / r_0'^2] \\ - \frac{1}{2} p_0^{*'2} (\rho_0^* + p_0^*)^{-1} \xi^2 / r_0^2 + (\rho_0^* + p_0^*) [3\xi^2 / r_0^2 + 2\xi \xi' / r_0 r_0' + \xi'^2 / r_0'^2] \\ - (\rho_0^* + p_0^*) e^{\lambda_0} m_2^* / r_0 - \frac{1}{2} (\rho_0^* + p_0^*) e^{\lambda_0 - r_0} \xi^2 \,, \end{split}$$
 (B22)

By combining equations (B12), (B14), and (B22), we finally obtain a very simple differential for  $m_2$ \*, the second-order correction to the mass:

$$\begin{split} dm_2^*/dr_0 + \frac{1}{2}m_2^*d(\lambda_0 + \nu_0)/dr_0 &= 2\pi \{p_0^*\gamma_0 e^{i\phi}r_0^{-2}[(d/dr_0)(r_0^2e^{-i\phi}\xi)]^2 \\ - (\rho_0^* + p_0^*)^{-1}(dp_0^*/dr_0)^2r_0^3\xi^2 + 4(dp_0^*/dr_0)r_0\xi^2 + 8\pi r_0p_0^*(\rho_0^* + p_0^*)e^{\lambda_0}\xi^2 \text{ (B23)} \\ + (\rho_0^* + p_0^*)r_0^2e^{\lambda_0-i\phi}\xi^2 - 2e^{-(\lambda_0+i\phi)/2}(d/dr_0)[e^{(\lambda_0+i\phi)/2}p_0^*r_0\xi^2]\} \end{split}$$

To put the equation in this form we have performed the partial integration which leaves the last term; we have used the relation<sup>5</sup>

$$\lambda_0' + \nu_0' = 8\pi r_0 r_0' (\rho_0^+ + \rho_0^+) e^{\lambda_0};$$
 (B24)

and we have converted to  $r_0$ , the equilibrium Schwarzschild coordinate, as the independent variable— $dr_0 = r_0' da$ .

Equation (B23), like its first-order counterpart, equation (19), is easily integrated to obtain the mass-energy of the configuration to second order:

Theorem B1: The total mass-energy of a spherically symmetric configuration of cold, catalyzed matter, performing radial motion near an equilibrium configuration is

$$M^* = M_0^* + P^* + K^*$$
. (B25)

Here M<sub>0</sub>\* is the mass of the equilibrium configuration, while P\* and K\*, the potential and kinetic energies originating in departures from equilibrium, are (to second order)

$$\begin{split} P^* &= 2\pi \, e^{r_0(0)/2} \, \Big\{ 4 \int_0^{R_0} e^{(\lambda_0 + r_0)/2} r_0 (\, d\, p_0^* / d\, r_0) \, \xi^2 d\, r_0 \\ &+ \int_0^{R_0} e^{(\lambda_0 + 3r_0)/2} \gamma_0 p_0^* \, [\, (d / d\, r_0) \, (\, r_0^2 \xi \, e^{-r_0/2}) \, ]^2 r_0^{-2} d\, r_0 \\ &+ 8\pi \int_0^{R_0} e^{(3\lambda_0 + \nu_0)/2} p_0^* \, (\, \rho_0^* + p_0^*) \, r_0^2 \xi^2 d\, r_0 \\ &- \int_0^{R_0} e^{(3\lambda_0 + \nu_0)/2} (\, \rho_0^* + p_0^*)^{-1} (\, d\, p_0^* / d\, r_0)^2 r_0^2 \xi^2 d\, r_0 \\ &= 2\pi \, e^{r_0(0)/2} \mu_s^* (\, 1 - 2M_0^* / R_0)^{1/2} \{ \Pi - (\Pi\Pi + 1) - \PiV \} \,, \end{split}$$

<sup>5</sup> This follows from eqs. (6), (8), (11), and (B14).

where II, (III + I), and IV are given in equation (117); and

$$K^{+} = 2\pi e^{\tau_{0}(0)/2} \int_{0}^{R_{0}} e^{(3\lambda_{0} - r_{0})/2} (\rho_{0}^{*} + p_{0}^{*}) r_{0}^{2} \dot{\xi}^{2} dr_{0}$$

$$= 2\pi \int_{0}^{R_{0}} (1 - 2m_{0}^{*}/r_{0})^{-2/2} (\rho_{0}^{*} + \dot{p}_{0}^{*}) [d\rho_{0}^{*}/dn_{0}]$$

$$\times [dn_{0}(0)/d\rho_{0}^{*}(0)] \dot{\xi}^{2} r_{0}^{2} dr_{0}.$$
(B27)

Comments: Aside from the trivial multiplicative constant  $2\pi e^{v_0(0)/2}$ ,  $P^*$  is precisely the right-hand side of Chandrasekhar's variational principle\* for the acoustical modes of the configuration; and  $K^*$  differs from Chandrasekhar's left-hand side by the same factor  $2\pi e^{v_0(0)/2}$  and by the replacement  $\sigma^2 \xi^2 \rightarrow \dot{\xi}^2$ . Thus, we are well on our way toward a derivation of his variational principle from energy considerations alone.

#### NECESSARY AND SUFFICIENT CONDITION FOR STABILITY

Because the mass-energy of the configuration is a constant of its motion (there cannot exist gravitational monopole radiation),  $K^* + P^*$  is independent of time. But  $K^*$  is positive-definite, increasing as the square of the velocity of the fluid; and  $P^*$  increases in absolute magnitude with the square of the displacement of the fluid from equilibrium. Consequently, the equilibrium configuration is stable if and only if it corresponds to a (local) minimum of the potential energy:

Theorem B2: An equilibrium configuration for a sphere of cold, catalyzed matter is stable against radial deformations if and only if the expression (B26) for the potential energy is a positivedefinite functional of E.

#### EQUATIONS OF MOTION AND NORMAL MODES

If we assume a sinusoidal (or exponential) time dependence,  $\xi(a, t) = \xi(a)e^{i\omega t}$ , then the constancy of  $K^* + P^*$  tells us

$$ω^2 = P^*/(\text{Expression [B27] for } K^* \text{ with } \xi \text{ replaced by } \xi)$$
. (B28)

This gives us a method for calculating the frequencies of stable radial modes, and the rates of growth of unstable modes from a knowledge of the radial dependence of their amplitudes,  $\xi(a)$ . But how does one determine that radial dependence? The answer is provided by Theorem B3:

Theorem B3: The normal radial modes of collective vibration of a sphere of cold, catalyzed matter are given by  $\xi(a, t) = \xi(a) e^{i\omega t}$ , where  $\xi(a)$  is any function which makes

$$\omega^2 = \frac{P^*}{(\text{expression [B27] for } K^* \text{ with } \xi \text{ replaced by } \xi)},$$
 (B29)

stationary, and where the corresponding normal frequency,  $\omega$ , is the square root of the stationary value of expression (B29).

Comment: This is precisely the variational principle of Chandrasekhar (1964) and Misner and Zapolsky (1964) which was discussed in chapter vii (eq. [116]).

Proof: To obtain this variational principle from equations (B25), (B26), and (B27) for the mass-energy, we must first use the mass-energy to derive the dynamical equation governing arbitrary radial motion. All of our experience with small-oscillation problems in classical mechanics urges us to take the kinetic energy minus the potential energy,  $K^* - P^*$ , as a Lagrangian

<sup>6</sup> Chandrasekhar (1964), eq. (15'); see also chap. vii of this paper, especially eqs. (116) and (117).

<sup>7</sup> Cocke (1964) has independently derived this result.

for the equation of motion. However, our problem arose within the framework of general relativity, not classical mechanics, so to be absolutely certain of the validity of  $K^* - P^*$  as a Lagrangian, we should go back to the first principles of relativity. Rather than doing so here. we shall simply note that the Euler-Lagrange equation arising from

$$\delta \int_{0}^{t_{*}} (K^{*} - P^{*}) dt = 0$$

is, indeed, identical to the equation of motion derived from the full Einstein field equations by Chandrasekhar (1964, eqs. [9], [10], [11], [13]).

The equation governing arbitrary radial motion near equilibrium is thus

$$\frac{\delta P^*}{\delta \, \xi} = \, - \, 4 \pi \, e^{\, r_0(0)/2} \, e^{(3 \lambda_1 - r_0)/2} (\, \, \rho_0^{\, \, *} + \, p_0^{\, \, *} \,) \, r_0^{\, \, 2} \, \xi \, . \tag{B30}$$

If a sinusoidal time dependence is assumed, the eigenvalue equation for the amplitude  $\xi(a)$  then becomes

$$\frac{\delta P^*}{\delta \, \xi} = \, + \, \omega^2 \cdot 4 \pi \, e^{\nu_{\delta}(0)/2} e^{(3\lambda_0 - \nu_0)/2} \big( \, {\rho_0}^* + \, {p_0}^* \, \big) \, r_0{}^2 \xi \; , \tag{B31} \label{eq:B31}$$

and equation (B29) is the basis of a variational principle for this eigenvalue equation. O.E.D. This completes our discussion of the dynamics of spherically symmetric configurations of cold, catalyzed matter near equilibrium.

#### REFERENCES

Chandrasekhar, S. 1964, Phys. Rev. Letters, 12, 114, 437.

Cocke, W. J. 1964, private communication.

Misner, C. W., and Zapolsky, H. S. 1964, Phys. Rev. Letters, 12, 635.

Tolman, R. C. 1934, Relativity, Thermodynamics and Cosmology (Oxford: Clarendon Press).

# VARIATIONAL TECHNIQUE TESTED IN NON-RELATIVISTIC DOMAIN ON

### appendix C POLYTROPES

The general-relativity equation of hydrostatic equilibrium was derived in chapter iii by extremizing the energy subject to the number of baryons being kept constant. The corresponding procedure in non-relativistic physics is well known; extremize the energy (apart from restmass energy) keeping constant the mass (looking apart from the mass associated with the gravitational and elastic energy of the system). This approach is described here for four reasons. First, it provides a unified foundation for deriving the non-relativistic equation of hydrostatic equilibrium as has long been known. Second, it offers a good way to get reasonable approximate solutions of the equations of hydrostatic equilibrium without actually doing any numerical integration (analytical Rayleigh-Ritz procedure). Third (the immediate application mentioned in Table 11 of the text), it supplies a means to determine the gravitational energy of a system containing N neutrons when N is very small compared to 10<sup>N</sup>. Fourth, it suggests the possibility of a similar analytic Rayleigh-Ritz treatment in the relativistic domain (not investigated here).

Let  $e(\rho)$  represent the compressional energy per unit mass, so that

$$d\epsilon = -pd$$
 (Volume per unit mass) =  $-pd(1/\rho)$ . (C1)

Then the sum of the gravitational and compressional energies of the system is

$$E = -(G/2) \int r_{12}^{-1} \rho_1 \rho_2 d(\text{vol}_1) d(\text{vol}_2) + \int \rho \epsilon(\rho) d(\text{vol})$$
. (C2)

Vary the energy with respect to the density function,  $\rho(r)$ , subject to the condition that the mass remain fixed:

$$M = \int \rho d \text{ (vol)} = \text{Const.}$$
 (C3)

Introduce a Lagrange multiplier  $\lambda$  (chemical potential per unit mass, as contrasted with the chemical energy per baryon of chaps, iii and ix). Vary  $E - \lambda M$  without any supplementary condition. In order that the coefficient of  $\delta \rho(r)$  shall vanish it is necessary and sufficient that the energy for the injection of a unit mass should have everywhere the constant value  $\lambda$ :

$$\varphi(r) + \int_{n=0}^{n=p(r)} \rho^{-1} dp = \lambda = \text{Constant},$$
 (C4)

Here

$$\varphi(r_1) = -G \int r_{12}^{-1} \rho_2 d(\text{vol}_2) \qquad (C5)$$

is an abbreviation for the gravitational potential at the point  $r_1$ . The equation of hydrostatic equilibrium,

$$d\varphi/dr + \rho^{-1} d\phi/dr = 0$$

or

$$dp/dr = -\rho d\varphi/dr = -G \rho m(r)/r^2, \qquad (C6)$$

follows from differentiation of equation (C4). So much for the foundation of the variational approach,

Now take the case where the equation of state has the Emden form,

$$\phi = K \rho^{\gamma}$$
. (C7)

Integrate equation (C1) and find for the amount of compressional energy per unit of volume

$$\epsilon \rho = K(\gamma - 1)^{-1} \rho^{\gamma}. \tag{C8}$$

Take three types of trial functions for the distribution of matter in the system, all three normalized to have the specified mass M, and all three having an adjustable constant b which has to do with the *size* of the object; thus,

$$\rho_1(r) = (3M/4\pi b^3) \text{ for } r < b;$$
 0 for  $r > b$  ("Uniform model");

$$\rho_{\rm H}(r) = (M/\pi^{3/2}b^3) \exp{-(r/b)^2}$$
 ("Gaussian model");

and

$$\rho_{III}(r) = [M/4\pi(2-s)! b^s][(b/r)^s \exp - (r/b)],$$
 (C9)

Here the third function contains two adjustable constants, not only the size factor h, but also the exponent s. From these expressions one calculates the contributions to the energy listed in Table C1.

#### TABLE CI

CONTRIBUTIONS TO THE ENERGY OF EQUILIBRIUM CONFIGURATIONS AS CALCU-LATED FROM THE TRIAL FUNCTIONS OF EQUATION (C9)

Trial	Gravitational Energy	Compressional Energy	
Function	in Units (GM*/5)	in Units KM7hs av	
II $-(2\pi)^{-1/2}$ $(\gamma -$		$\begin{array}{l} -1)^{-1}(3/4\pi)^{\gamma-1} \\ -1)^{-1}\gamma^{-s/t}\pi^{(2-s\gamma)/t} \\ -1)^{-1}(4\pi)^{1-\gamma}\gamma^{s\gamma-s}(2-s\gamma)!/[(2-s)!]^{\gamma} \end{array}$	

The total energy has the form

$$E = -c_1(GM^2/b) + c_2(KM^{\gamma}b^{1-3\gamma})$$
, (C10)

where the purely numerical constants  $c_1$  and  $c_2$  are listed in the table. Extremize with respect to the size factor b. Thus find that the extremum comes, as expected (virial theorem!) when

(Gravitational energy) = 
$$(3 - 3\gamma)$$
(Compression energy) (C11)

and

(Total energy, 
$$E$$
) =  $(4 - 3\gamma)$ (Compression energy). (C12)

The equilibrium is stable when  $\gamma > \frac{4}{3}$  and unstable when  $\gamma < \frac{4}{3}$ . When  $\gamma = \frac{4}{3}$  there is, as is well known, no equilibrium, unless the coefficient of (1/b) in equation (C10) exactly cancels, in which case the equilibrium is neutral.

The total energy at the extremum has the value

$$E = -Q(G^{3\gamma-3}M^{5\gamma-6}/K)^{1/(5\gamma-6)}$$
, (C13)

Here the dimensionless coefficient O has the value

$$Q = (3\gamma - 4) \left[ c_1^{3\gamma - 3} (3\gamma - 3)^{-(3\gamma - 3)} / c_2 \right]^{1/(3\gamma - 4)}$$
(C14)

$$= \frac{(3\gamma - 4)}{(\gamma - 1)} \begin{cases} (4\pi/375)^{(\gamma - 1)(3\gamma - 4)} & \text{for I} \\ \gamma^{3/(6\gamma - 8)}(\frac{1}{18})^{3(\gamma - 1)/(6\gamma - 8)} & \text{for II} \\ \gamma^{(3-6\gamma)/(6\gamma - 4)} [\pi/54(2-s)^3]^{(\gamma - 1)/(8\gamma - 4)} & \times \frac{[(2-s)1]^{\gamma/(6\gamma - 4)}}{[(2-s\gamma)1]^{3/(6\gamma - 4)}} [1 - \frac{(3/2-s)1}{\pi^{1/2}(2-s)1}]^{(3\gamma - 3)/(3\gamma - 4)} & \text{for III}. \end{cases}$$

To go further with Trial Function III it seems necessary to be given a particular value of  $\gamma$ . Then one can evaluate the binding constant  $Q_{\rm III}$  for a variety of choices of the trial exponent s and select that value of s which comes closest to maximizing  $Q_{\rm III}$ . We have not carried through this numerical work. The situation is much simpler for the Trial Functions I and II: there is no constant to adjust. In these two cases values of the binding constant as given by equation (C15), I and II, are listed in Table C2, where they are compared with the values obtained by Emden by detailed integration of the elementary equation of hydrostatic equilibrium. Also

TABLE C2
EQUILIBRIUM CONFIGURATIONS: VARIATIONAL TREATMENT COMPARED
WITH EMDEN'S EXACT ANALYSIS\*

7	I (Uniform)	II (Gaussian)	Emden
Binding factor Q: 2 1.6666 1.50 1.40 1.3333	0.366 .156 .0335 .00056	0.386 .181 .0442 .00107	0.398 .182 .0442 .00107†
Central density factor R: 2 1.6666 1.50 1.40 1.3333	0.183 0.0335 0.00112 4.20×10 <sup>-8</sup>	0.543 0.132 0.00664 7.54×10 <sup>-4</sup> 0	0.398 0.109 0.00622 8.32×10 <sup>-6</sup>

<sup>\*</sup> Comparison of the dimensionless binding factor Q (eq. [C13]) and the dimensionless density factor R (eq. [C16]) as obtained from the two trial density distributions I (uniform density inside, zero outside) and II (Gauss function) after the size factor b has been adjusted to give maximum binding. The last column lists the values that come out of Emden's detailed numerical integration of the (non-relativistic) equation of hydrostatic equilibrium.

† Emden's value, corrected in the light of more recent calculations (cf. Chandrasekhar [1939]).

listed are the values of the numerical constant R in this expression for the central density:

$$\rho_0 = R(G^3M^2/K^3)^{1/(3\gamma-4)}$$
, (C16)

We calculate

$$R = \left\{ \begin{array}{ll} (4\pi/375)^{1/(3\gamma-4)} & \text{for I} \\ (\gamma^2/18)^{3/(6\gamma-5)} & \text{for II} \end{array} \right\}. \tag{C17}$$

It is remarkable how small the error in energy is for the uniform model considering how very far off this model is on its prediction of the central density. The error is least where  $\gamma$  is largest, as is to be expected. Very large  $\gamma$  signifies an almost incompressible fluid, a limit where the uniform model obviously makes sense. On the other hand, in the other limit,  $\gamma = \frac{4}{3}$ , the exact density distribution departs from uniformity to the maximum extent;  $\rho$  becomes singular at

<sup>1</sup> Emden (1907), chaps. v and viii, Chandrasekhar (1939). For more on polytropes see, e.g., Bucerius (1938a, b, c) and Bonnor (1958).

the origin. Therefore it is not surprising that the uniform model gives a poorer binding as this limit is approached.

The application of these considerations required in the text (Table 11) is the binding energy of a system containing N neutrons, held together by gravitational forces. We treat this system as an ideal non-relativistic Fermi gas at the absolute zero temperature. In the equation of state  $p = K \rho^{\gamma}$  the exponent has the value 4 and the constant is

$$K = (8\pi/15 \mu h^3)(3h^3/8\pi\mu)^{5/3}.$$
 (C18)

Here \( \mu\) represents the mass of a neutron. The mass of the system as it appears in equation (C13) is  $M = N\mu$ . Also we insert into that equation the K of equation (C18) and the Q = 0.182 of Table C2. Thus we find for the sum of the negative gravitational energy and the positive zeropoint kinetic energy the total

$$E = -0.182 G^2(N\mu)^{7/8}/K = -0.0952 N^{7/8} G^2\mu^5/\hbar^2$$
, (C19)

This is to be compared with the expression for the gravitational binding of two neutrons,

$$E = -0.25 G^2 \mu^5 / \hbar^2 \qquad (C20)$$

derived from the Bohr formula for hydrogen as outlined in the discussion of equations (185)-(187). To obtain the result (C20) from equation (C19) we must insert for N the "reduced neutron number"  $N = (0.25/0.0952)^{3/7} = 1.514 = 2 - 0.486$ . Therefore as an empirical procedure for calculating the binding of systems with small N values the modified formula

$$E = -0.0952 (N - 0.486)^{7/3} G^2 \mu^5 / \hbar^2$$
(C21)

suggests itself. The corresponding expression for the gravitational packing fraction is

$$f_{grav} = E/N\mu c^2 = -0.0952 (N - 0.486)^{7/8} N^{-1} (G\mu^2/\hbar c)^2 = -3.33 \times 10^{-78} \times (N - 0.486)^{7/8} / N = -1.2 \times 10^{-76} \text{ for } N = 16 \text{ (used in Table 11)},$$

We calculate from equation (C22), inappropriate though it is in the relativistic domain, a critical baryon number of the order of  $A_{\rm crit} \sim (\hbar c/G\mu^2)^{3/2} \sim (1.691 \times 10^{10})^{3/2} \sim 10^{17}$ , as expected.

The good results given by the Gaussian trial function for the density, as evidenced from the comparison of the last two columns in Table C2, suggest a corresponding variational calculation in the relativistic domain to determine the properties of equilibrium configurations. For this end we may use equation (9) to normalize the baryon number to the specified value A and equation (8) to evaluate the mass-energy of the system. To simplify the problem to the point where it can be treated by analytical methods it is appropriate to look apart from the less important LHWW critical point (connected with the crushing of electrons into union with protons) and to concentrate on a treatment of the LOV critical point (point of instability of neutron star). For this purpose it is enough to employ an equation of state (see eq. [318] and the discussion at the end of chap, x) which describes to good accuracy the transition of a neutron gas from the non-relativistic domain to the relativistic domain,

$$\rho_{ZW} = n\mu^* [1 + (3^{8/2}\pi^{4/3}L^{*4}/16\mu^{*2})n^{2/3}]^{1/2}. \tag{C23}$$

#### REFERENCES

Bonnor, W. B. 1958, M.N., 118, 523. Bucerius, H. 1938a, Astr. Nach., 265, 145.

-. 1938b, ibid., 266, 49. -. 1938c, ibid., 267, 253.

Chandrasekhar, S. 1939, Introduction to the Study of Stellar Structure (Chicago: University of Chicago

Emden, R. 1907, Gaskugeln (Leipzig: Teubner).

### AUTHOR INDEX

Albada, G. B. van, 45, 49, 112–113, 123 Ambartsumyan, V. A., 1 n., 9, 118, 123 Auluck, F. C., 112, 123

Backenstoss, G., 147 Baierlein, R. F., 142 n., 147 Bardeen, J. M., vii, 138 n., 147 Bassett, W. A., 110 n., 123 Beckedorff, D. L., 126, 128, 147 Birch, F., 110 n., 123 Birkhoff, G. D., 128 n., 147 Bondi, H., vii, viii, 28-32, 36-37, 41, 101, 107, 138 n., Bonnor, W. B., 165-166 Boyd, F. R., 110 n., 123 Brandt, W., 112 n., 123 Brill, D. R., viii, 14-15, 56-57, 68, 143, 147 Brueckner, K., viii Bucerius, H., 165-166 Burbidge, E. M., 1, 9, 45, 49, 83 n., 107, 138 n., 147 Burbidge, G. R., 1, 9, 45, 49, 83 n., 107, 138 n., 147

Callan, C. G., 134 n., 138 n., 147
Cameron, A. G. W., vii, viii, 118, 123
Carter, R. E., 84, 107
Casimir, H. B. G., 87 n., 107
Chandrasekhar, S., vii, 2, 5, 6, 9–10, 18 n., 24–25, 31, 41, 43–46, 49–50, 52, 67–68, 105 n., 107, 111–112, 121, 123, 156, 157, 161–162, 165–166
Chiu, H. Y., vii, viii, 86 n., 107, 138 n., 147
Cocke, W. J., viii, 6, 16 n., 18 n., 25, 161–162
Colgate, S. A., vii, viii, 138 n., 147
Cowan, C. L., 84, 107
Curtis, A. R., 104, 105 n., 107

Derjaguin, B. V., 87 n., 107 De Witt, B., viii Dicke, R. H., viii, 11, 15 Dirac, P. A. M., viii Dyson, F., viii

Eddington, A. S., 105 n. Eden, R., viii, 80 Einstein, A., 6, 9, 11, 54, 68 Emden, R., 1, 10, 165–166 England, J. L., 110 n., 123 Eötvös, B. R. von, 11

Feynman, R. P., 110, 123, 138, 143, 148
Field, G., 1, 10
Fourès-Bruhat, Y., 3, 5, 13, 15
Fowler, W. A., vii, viii, 1, 10, 45, 49, 77, 83 n., 107, 138 n., 148
Frauenfelder, H., 147
Fronsdal, C., 128, 148
Fuller, R. W., 112 n., 123, 129, 148

Gamow, G., 83 n., 86 n., 107 Geronimus, J. L., 52, 68 Giamati, C. C., 147-148 Ginzburg, V. L., 138 n., 148 Goeppert-Mayer, M., 112 n., 123 Gold, T., 1 n. Gombas, P., 21, 25 Grasberger, W. H., 138 n., 147 Gratton, L., vii, 58, 106 n. Graves, J. C., 143, 147 Gray, D. E., 88-89, 107 Green, A. E. S., 113, 123 Greenstein, J. L., 1 n., 10 Grommer, L., 12 n.

Hamoui, A., 128 n., 148

Harrison, B. K., viii, 2 n., 6-7, 18, 19 n., 25, 31, 41, 45, 46-50, 75, 108-109, 121, 123, 149, 151-153, 155

Harrison, F. B., 84, 107

Hartle, J. B., 56-57, 68

Hayashi, C., 83 n., 107

Hoffieit, D., 1 n., 10

Hoffmann, B., 12 n.

Hoshi, R., 83 n., 107

Hoyle, F., vii, viii, 1, 10, 45, 49, 118, 123, 137, 138 n., 141 n., 148

Hyams, B. D., 147

Iben, I., 1 n., 10 Infeld, L., 12 n. Johnson, M. H., 138 n., 147

Kaplan, S. A., 45 n., 49 Khalatnikov, I. M., 142 n., 148 Kihara, T., 87 n., 107 Klein, O., vi, vii, 126, 148 Knopoff, L., 110 n., 123 Koester, L. J., Jr., 147 Komar, A., 128 n., 148 Kruse, H. W., 84, 107 Kruskal, M. D., 127–129, 132 n., 148

Landau, L. D., vi, 2, 5–6, 10, 12, 15, 18, 25, 42–44, 46, 49, 112, 123, 151, 155

Langer, L., 84 n.
Lapidus, L., 148, 155

Ledoux, P., 52, 68

Liapounoff, A. M., 52

Lifshitz, E. M., 2 n., 10, 12, 15, 18, 25, 87 n., 107, 142 n., 148, 151, 155

Lindquist, R. W., viii, 128, 147 Lynds, C. R., 1 n., 10 Lyttleton, R. A., 52, 68

McGuire, A. D., 84, 107 McQueen, R. C., 110 n., 123 McVittie, G. C., 138 n., 148 Machly, H. T., 47 n. Marin, P. C., 147 Marsh, S. P., 110 n., 123 Marshak, R., viii, ix

Marzke, R. F., 11 n., 15, 126 n., 148 Mathur, C. S., 112, 123 May, M. M., viji, ix, 138 n., 148

Melvin, M. A., ix

Metropolis, N., 110, 112 n., 123 Michel, F. C., 1 n., 10, 138 n., 148

Misner, C. W., vii, ix, 18 n., 25, 29, 46, 48-50, 52, 68, 126, 128, 132 n., 138 n., 143, 147-148, 156, 162

Morse, M., 23, 25, 52

Narlikar, J. V., 141 n., 148 Novikov, I. D., 132 n., 148

Oppenheimer, J. R., vii, 2, 5, 10, 16, 18, 23, 25, 28–29, 44–46, 49–50, 110 n., 112, 123, 126, 138 n., 148 Ozernoi, L. M., 138 n., 148

Peierls, R. E., ix Penrose, R., 141 n., 148 Petrov, A. Z., 128 n., 132 n., 148 Poincaré, H., 52, 65 Polder, D., 87 n., 107 Power, E. A., 56, 68 Raychaudhuri, A. K., 54, 68 Reines, F., 84–85, 107, 147–148 Robinson, L., 1 n., 10, 138 n. Rudkjøbing, M., 84, 107 Rutherford, E., 147–148

Sankyan, G. S., 118, 123, 141 n., 148 Salpeter, E. E., vii, ix, 83 n., 107, 112, 118, 123 Sandage, A. R., 1 n., 9-10 Schatzman, E., vii, ix, 5, 45-46, 49, 112, 123 Schild, A., 1 n., 10, 138 n. Schmidt, M., 1 n., 10 Schonberg, E., 83 n., 86 n., 107 Schucking, E. L., ix, 1 n., 10, 138 n. Schwarzschild, K., 27 n., 54 Schwarzschild, M., ix. 83 n., 107 Sciama, D., ix Sedov. L. I., 31, 41 Serber, R., ix, 2 n., 10, 44, 49, 112, 123 Sharp, D. H., vii, ix, 138 n., 142 n., 147-148 Shepley, L., ix Skyrme, T. H. R., 118, 123 Smith, H., 1 n., 10 Snyder, H., 126, 138 p., 148 Som, M. M., 54, 68 Sommerfeld, A., 31, 41 Sparney, M. L. 87 n., 107 Stoner, E. C., 2 n., 10 Strømgren, B., ix

Takehashi, T., 110 n., 123
Taub, A. H., 18 n., 25, 143, 148
Teller, E., 110, 112 n., 123
Thorne, K. S., viii, 6, 76, 117 n.
Tolman, R. C., 2, 10, 16, 18, 23, 25, 27 n., 29, 126, 137, 147, 151, 155, 157 n., 162
Tooper, R. F., 30, 41
Treiman, S., ix
Tsuruta, S., 48–49, 155

Ulam, S. M., 1 n., 10

Sugimoto, D., 83 n., 107

Van Hove, L., ix Volkoff, G., vi, 2, 5, 16, 18, 23, 25, 28–29, 44–46, 49–50, 110 n., 123 Von Neumann, J., 16

Wakano, M., viii, 2 n., 6, 10, 18, 19 n., 25, 45-50, 108, 112 n., 121, 123, 149, 151-155 Walden, W. E., 1 n., 10 Wagner, J. J., 85, 107 Weinberg, J., ix Weinberg, S., 84-85, 107 Werner, F. G., 112 n., 123 Weymann, B., 47 n., 49

Wheeler, J. A., vii, ix, 2 n., 6-7, 10, 11 n., 13 n., 15, 18, 19 n., 25, 45-50, 52, 56-57, 68, 75, 85, 87 n., 88, 107-108, 112 n., 121, 123, 126 n., 128-129, 135 n., 138, 141-142, 147-148, 155

White, R. H., vii, 138 n., 147

Witten, L., 13 n., 15 Wyman, M. E., 85, 107

Young, H., 110

Zapolsky, H. S., 18 n., 25, 29, 46, 48–50, 52, 68, 156, 162

Zel'dovich, Ya. B., vii, 2, 5–6, 8, 10, 18, 19 n., 24–25, 53–54, 59, 61, 68, 84, 105 n., 107, 120–121, 126 n., 148

## SUBJECT INDEX

A-baryon system definition of, 83–84 equilibrium configurations of (see Equilibrium

configurations)  $A_{\text{star}}$  critical baryon number beyond which collapse

is inevitable, 2, 3, 7, 122 calculated from non-relativistic consideration, 166 determined by studying uniform density configurations, 82

Landau's pioneering calculation of, 42-43 relative sizes of, at LOV and LHWW critical points, 141 n.

see also Critical mass; Gravitational collapse

A<sub>monton</sub>, smallest number of baryons whose collapse can be treated classically, 7, 82; see also Quantum gravitational effects

Acceleration of electron so curvature of universe appears to be Compton wavelength, 98-99

Acceleration of gravity in neutron star and in atoms and nuclei, compared, 97–98

Achilles and the hare, and the dynamics of the Schwarzschild solution, 132

Acoustical modes of equilibrium configuration; see Oscillations, normal acoustical modes

Action at a distance, 118

Adiabatic decompression to determine baryon number density, 100

Adjusted mass perturbation factor, v, 35-36

Advanced and retarded potentials, related to gravitational collapse, 138-139

After-radiation, 141-142

Antiparticles and particles and one-sidedness of matter, 147 symmetry between, 83–84

Appearance of baryons out of empty space; see Baryons, spontaneous disappearance and appearance of

Area in phase space, normalized definition of, 37 conservation of, 5, 37–39 normalization of, 38–39

Barrier against gravitational collapse, 3, 7, 24, 78–82 compared with nuclear fission barrier, 4 dependence upon A, 82 for  $A < A_{quantum}$ , not well-defined, 82 for  $A_{quantum} < A \ll A_{eris}$ , 78–80 for  $A \sim A_{tris}$ , 76 for γ-law equation of state, 80–82 for Harrison-Wheeler equation of state, 76 for relativistically degenerate Fermi gas, 78–80 for Zel'dovich sequence, 24–25 collapse over barrier from infinity, 125–126 not technologically feasible to push substellar mass over barrier, 80–82

tunneling of (see Tunneling of barrier)

Baryon, precise definition of, 84

Baryon number density; see Number density of baryons: Thermodynamic potentials

Baryon number parameter, a, 16, 95-96, 157-158

Baryons, law of conservation of may break down at high densities, 85

may break down at mgn densities, 85 may break down in gravitational collapse, 9, 143– 144

may not be well-defined in regions of high curvature, 143-144

see also Baryons, spontaneous disappearance and appearance of

Baryons, spontaneous disappearance and appearance of, 9, 124, 139, 146-147 experimental search for, 147

experimental search for, 147 and the one-sidedness of matter, 147 see also Baryons, law of conservation of

Baryons as markers in fluid, 16, 95-96, 157-158

Beta-decay and hysterisis in equation of state, 86

assumed gone to completion in cold, catalyzed matter, 84

consequences for, if Fermi energy of neutrino sea is non-zero, 84-85

rate of, connected to energy excess, 86 see also Inverse beta-decay

Beta-equilibrium for cold, catalyzed matter at high densities, 112-114, 118-121

Birkhoff's theorem, 128

Bohr radius of a gravitationally bound HHe molecule, 87

Causality, demands  $\gamma \leq 2$ , 75, 105

Central crush, 29, 30–34, 44–45; see also Incompressible fluid; Static oscillations

Chandrasekhar equation of state; see Fermi gas, equation of state for

Chandrasekhar limit for mass of white dwarf, 43–46 comparison with neutron star limit, 141 n., 152–153

Chandrasekhar variational principle for acoustical modes, 50-52, 156-157 INDEX 171

Chemical potential definition of, 17, 20, 99 equivalence to Fermi energy, 20–21, 99 see also Thermodynamic potentials

Cold, catalyzed matter, 83–107
beta-decay gone to completion in, 86
beta-equilibrium in, 112–114
electrical neutrality of, 84
neutrino neutrality of, 84–86
shear stresses absent in, 95
zero excitation of, 86
dominant nucleus in at various pressures, 117
hyperons stable in at high pressures, 118
completely described by  $\rho = \rho$  (n), 94

equation of state for (see Equation of state; Harrison-Wheeler equation of state; Schatzman equation of state; Skyrme equation of state) equilibrium configurations for (see Equilibrium configurations)

Comoving local Lorentz frame

definition, 93-94

velocities at which Lorentz covariance breaks down, 99

Configuration of lowest energy; see Equilibrium configurations

Configuration space; see Morse theory

Conservation of baryons; see Baryons, law of conservation of

Conservation of normalized area in phase space, 5, 37-39

Creation and annihilation of matter in gravitational collapse; see Baryons, spontaneous disappearance and appearance of

Critical mass, denumerable infinity of, 30-41; see also A<sub>suk</sub>; Equilibrium configurations

Critical point in equilibrium configurations; see Equilibrium configurations; HWW configurations; Oscillations, normal acoustical modes; Static oscillations

Curtis' equation of state, 105 n., 120

Curvature of space
infinite, arising in gravitational collapse, 141–143
(see also Quantum gravitational effects)
in collapsing dust cloud, 133–134
key to gravitational collapse, 124
related to mass-energy density, 14

related to mass-energy density, 14 seen by high-velocity electron, 98-99 see also Tide-producing forces

Dallas Conference on Gravitational Collapse ("CGC"), vii, 1 n.

Degenerate Fermi gas; see Fermi gas, degenerate

Density of baryons or mass-energy; see Mass-energy density; Number density of baryons; Thermodynamic potentials

Dicke-Eötvös experiment, 11

Disappearance of baryons; see Baryons, spontaneous disappearance and appearance of

DNA, and one-sidedness of matter, 147

Dust cloud, gravitationally collapsing, 8, 126-128 event horizon in, 127, 138-139 geometry of, 127, 134 (see also Friedmann universe; Schwarzschild solution)
mass-energy constant in, 128
motion of photons in, 126, 127, 138-139
motion of surface of, 133-134
relation to momentarily static, uniform density
configurations, 134-137

configurations, 134-137
relations among density, mass, radius, and space
curvature, 133-134

Einstein's assemblage of particles; see Energy excess, configurations of

Einstein's theory of relativity; see General relativity Electric field, transmits to protons sustaining electron pressure in massive stars, 84, 96

Electrical neutrality, in cold equilibrium configurations, 84

Electron gas, equation of state for, 111-112, 120 in beta-equilibrium with nuclei, 112-114 in beta-equilibrium with nuclei and neutron gas, 114-116 in beta-equilibrium with proton and neutron

in beta-equilibrium with proton and neutron gases, 116-121

see also Fermi gas; Beta-decay; Inverse beta decay; Beta-equilibrium

Elementary particles spontaneous disappearance of, 9, 124, 146–147 spontaneous appearance of, 139, 146

Energy excess, configurations of Einstein's assemblage of particles, 6, 54–56, 58 geon, 6, 56–58 (see also Geon)

HWW equilibrium configurations, 6, 53, 54, 58–60 (see also HWW configurations)

comparison of types of, 58 similarities to Fermi-Thomas atom model, 54 stability against one-at-a-time removal of particles, 54, 56 Zel'dovich on, 53-54

Energy generation in astrophysical bodies, 1, 2 Ectvos-Dicke experiment, 11

Equation of state concept of, 7, 8, 83-107 quantum limits on concept of, 7, 79-81

non-relativistic and relativistic formulations compared, 101–102

relations among thermodynamic quantities (see Thermodynamic potentials)

hysterisis in, 86 phase transitions in, 34, 103-104

none can prevent collapse of massive body, 7, 28-29, 69, 75, 105

collapse hastened by stiff equation of state, 26–28, 105

analytic expressions in special cases, 120 of cold, catalyzed matter, 6, 7, 8, 45-47, 83-123 (see also Harrison-Wheeler; Schatzman; Skyrme)

specific (see under name: Curtis, Electron gas; Fermi gas; Gamma-law; Gratton; Harrison-Wheeler; Iron; Neutron gas; Polytropic; Schatzman; Skyrme; Zel'dovich; Zel'dovich-Wheeler)

Equilibrium configurations of cold, catalyzed matter, for A < 10<sup>10</sup>, 86–92, 122 Equilibrium configurations of cold, catalyzed matter, for  $A > 10^{40}$ 

approximated by uniform density configurations,

configuration of tightest binding, 59 constancy of injection energy in, 5, 20 for Curtis equation of state, 105 n.

electric field in, 84, 96 energy excess in, 6, 53-54, 58-60 (see also Energy excess)

for γ-law equation of state, 30 n., 31-33, 163-166 history of knowledge of, 5, 42-49 HWW configurations (see HWW configurations)

of infinite central density, 29, 30-34, 44-45 monotonic fall of pressure and density in, 26

polytropes (see Polytropes)
"pumping up" of, 53, 58-60
radial oscillations of (see Oscillations; Stability) separation of long- and short-range forces in, 69-70, 92-93, 97

for small sphere of iron, 151-153 stability of (see Oscillations; Stability)

static oscillations in, as central density rises, 5-7, 28, 30-41, 42

summary of features of, for selected A-values, 122 unique configuration for each central density, 26 variation of mass-energy near critical points, 7, 63-64

also HWW configurations; Neutron star; Polytropes; White dwarf

Equivalence principle experimental test of, 11

as hypothesis in general relativity, 11 permits arbitrarily large gravitational field in nonquantized relativity, 96-97

Event horizon in collapsing dust cloud, 127, 138-139 in general gravitational collapse, 141

Extrinsic geometry of a hypersurface, 13-14 of hypersurface of constant Schwarzschild time,

related to kinetic energy, 136

Fermi gas, degenerate barrier against gravitational collapse for, 78-80 Fermi energy equivalent to chemical potential, 20-21, 99

Fermi gas, degenerate, equation of state for Chandrasekhar's exact analysis, 43, 79, 105 n., 111-112

corrections to, for clustering of electrons about nuclei, 110-111

non-relativistic limit, 120 relativistic limit, 42-43, 121

Zel'dovich-Wheeler approximate form for, 121, 165

see also Electron gas; Equation of state; Neutron

Fermi-Thomas statistical model of atom analogy to configurations of energy excess, 54 Dirac exchange corrections, 110 injection energy for, 21 scaling law in, 31 n. used to calculate equation of state of iron, 110-111 Feynman, Metropolis, Teller, their equation of state for iron at high temperatures, 110-111

Field equations of general relativity, 12 derivation from action principle, 18 n.

for equilibrium configurations, satisfied by extremizing mass-energy, 23 initial value equations, 3, 5, 13-14, 23, 156, 158

Final energy state of A-baryon system, concept of, 83; see Equilibrium configurations

Final state of gravitational collapse, 2, 3, 141

Fission, nuclear

compared with gravitational collapse, 4 as generator of energy in astrophysical bodies, 1

Fluctuations in geometry, quantum; see Quantum fluctuations

Fourès initial value equations, 3, 5, 13-14, 23, 156,

Frequencies of oscillation of equilibrium configurations, see Oscillation, normal acoustical modes

Friedmann universe geometry of, 71, 126-128 motion of photons in, 127

and interior of momentarily static, uniform density configuration, 71-72, 79 and interior of collapsing dust cloud, 8, 126-128,

133-134

Fusion, as generator of energy in astrophysical bodies, 1

Galaxies, violent energy generation in the nuclei of, 1 n.

Gamma-law equation of state definition of, 101

relations among thermodynamic quantities for,

non-relativistic and relativistic, compared, 101-102

as approximation to other equations of state, 101 75, 102-104

 $\gamma \le 2$  for causality, 8, 75, 105  $\gamma = 2$  attainable in principle, 105–107

barrier against gravitational collapse for, 80-82 equilibrium configurations for (see Polytropes) uniform density configurations with, 73, 75, 78-81

General relativity hypotheses of, 11–12

field equations of (see Field equations)

justification for using instead of other gravitation theories, 11 nature of time in, 130

quantization of (see Quantum fluctuations; Quan-

tum gravitational effects) see also Equivalence principle

Geodesic hypothesis in general relativity, 12

Geodesics null (see photons, motion of) timelike (see particles, motion of)

Geometrized units, relation to conventional units, 12

Geometrodynamics, 12-13, 56-58; see also General relativity; Quantum gravitational effects

Geometry, fluctuations in, see Quantum fluctuations

173 INDEX

Geon. 6 definition of, 56 method for constructing from Einstein's cluster of particles, 58 as configuration of energy excess, 56-58 simple spherical, 57 Gratton's equation of state for nucleons with hard core, 106 n. Gravitational collapse advanced potentials cannot carry away energy during, 138-139 application of Morse theory to, 23-24 asymmetries cannot prevent, 140-141 barrier against (see Barrier) compared with scattering electrons off a proton, 141-142 critical mass for (see A .....) cutoff from outside world in, 127, 138-139, 141 disappearance and appearance of matter in (see Baryons, law of conservation of; Baryons, spontaneous disappearance and appearance no) effect of rotation on, 1 n., 138, 140 event horizons in, 127, 138-139, 141 Fermi energy of neutrino sea elevated locally during, 85 of a finite body and of universe compared, 137-139, 141 gravitational radiation from, 140 inevitability of for massive systems, 5, 7, 28-29, 42-43, 69, 75, 82, 105, 140-141 from infinity, over a barrier, 125-126 infinite curvature arising from, 141-142 as mechanism for energy generation in astrophys-ics, 1, 2, 138, 140 no equation of state can prevent, 7, 28-29, 69, 75, 105 quantum aspects of (see Quantum gravitational effects) realistic models for, 1, 138, 140 spontaneous collapse of elementary particles, 9, 124, 147 by tunneling the barrier against (see Tunneling of the barrier) of uniform-density dust cloud (see Dust cloud) Gravitational interaction between atoms, 87-88 compared to short-range interactions (see Longrange and short-range forces) Gravitational radiation from collapsing body, 140 "Gravitationally collapsed configuration" of uni-

form density, 75, 77, 134-137; see also Dust cloud; Uniform density configurations Gravity, acceleration of; see Acceleration of gravity Hard core of nucleons, and the equation of state at high densities, 106, 118-119 Harrison-Wheeler equation of state, 108-123 table of, 109 interpolation in, 108 analytical fits to, 108, 110 simple analytic forms in limiting cases, 120 derivation of, 110-121

uncertainties in at high densities, 118

barrier against gravitational collapse for, 76 uniform density configurations for, 75-77 see also Cold, catalyzed matter; Equation of state; HWW configurations HHe molecule, bound by gravitational forces, 87-88 HWW configurations for cold, catalyzed matter, 45-49, 53, 149-155  $M(\rho_0)$ , 46, 151–153  $R(\rho_0)$ , 47, 151–153 M(R), 48, 151–153 M(A), 53, 63, 151–152 coupled rates of change of  $M(\rho_0)$  and  $A(\rho_0)$ , 60-61 pressure and density distributions in, 154 computation of, 149-155 stability of (see Stability; Oscillations, normal acoustical modes; Oscillations about equilibrium configurations) approximated by uniform density configurations, see also Equilibrium configurations; Harrison-Wheeler equation of state Hydrostatic equilibrium, configurations of, see Equilibrium configurations; HWW configurations; Polytropes Hydrostatic equilibrium, general relativity equation of, 4, 13, 16-19, 22 derivation by extremizing mass-energy, 4, 13, 16-19 Newtonian limit of, 26, 163 regenerative multiplication of pressure in, 26-28 special form for \gamma-law equation of state, 31 for perturbations from configuration of infinite central density, 34-35 numerical integration of, 149-155 solution by Rayleigh-Ritz procedure, 163, 166 Hyperons, stable in cold, catalyzed matter at very high density, 118 Hypersphere geometry of, 71, 126 as geometry of Friedmann universe, 71, 126 as interior geometry of uniform density configuration, 71, 74 Incompressible fluid equilibrium configurations for, 22, 27-28

Hysterisis in equation of state, 86

Einstein disturbed by, 54 not described by Curtis' equation of state, 105 n. not described by  $T_{\mu}{}^{\mu}=$  constant, 105 n. Inevitability of gravitational collapse for massive

bodies; see A.m.; Gravitational collapse Initial value equations of general relativity, 3, 5, 13,

14, 23, 156, 158 Injection energy

related to potential energy, 136-137

definition of, 20 constancy of, throughout equilibrium configura-tion, 5, 20 for Fermi-Thomas model of atom, 21 Intrinsic geometry of a hypersurface, 13 probability amplitude for, in quantized geometrodynamics, 124

Inverse beta-decay

in equation of state for cold, catalyzed matter, 45,

in a collapsing star, 85 see also Beta-decay

fron, equation of state for, 110-111

Iron, small sphere of

equilibrium configurations, 151, 153 normal acoustical modes for, 51, 65

Issue of the final state of gravitational collapse, 2–3, 141

Kinetic energy, related to extrinsic curvature of a spacelike hypersurface, 136

Kruskal diagram, 127 discussion of, 130

invariance under "Lorentz transformations," 131-132

see also Schwarzschild solution

Landau's pioneering analysis of inevitability of collapse, 5, 42–43

Lane-Emden equation, 44 n.; see also Polytropes

Local Lorentz frame, comoving; see Comoving local Lorentz frame

Long-range and short-range forces

relative importance of, in A-baryon system for various A's, 92-93

separated in analysis of uniform density configurations, 69–70

limits on density at which they are separated, 97

Lorentz covariance, breakdown of, at high velocities,

Lorentz frame, comoving; see Comoving local Lorentz frame

Lowest energy configurations for A baryons; see Equilibrium configurations; Final energy state

Mass-energy density, measurement of, 95-96; see also Thermodynamic potentials

Mass-energy measured by external observer calculation of, on a spacelike hypersurface, ii, 3-4, 14-15

measurement of, 4, 14

proper mass-energy not useful concept, 14-15 related to zero frequency modes of oscillation, 61-62

extremization of, to give relativity equation of hydrostatic equilibrium, 4, 13, 16-19

drostatic equilibrium, 4, 13, 16-19 extremization of, to give Newtonian equation of hydrostatic equilibrium, 163

second variation of, related to stability of star, 6, 156-162

of equilibrium configurations (see Equilibrium configurations; HWW configurations)

of configurations perturbed from equilibrium, 156-161

of arbitrary spherical configurations, 158 of non-relativistic polytropes, 164-165

of uniform density configurations (see Uniform density configurations)

Mass perturbation factor, adjusted

definition of, 35 form of, for  $\gamma = 4/3$ , 36

Massive configurations

inevitability of collapse for (see A<sub>era</sub>; Gravitational collapse)

hot, in equilibrium (see Superstar)

Maxwell equations and initial value formalism, 13

Microscopic collapse of matter, occurs if  $\gamma < 1$ , 8, 75, 102–104

Morse theory (calculus of variations in the large) applied to study of gravitational collapse, 23–24 applied to study of equilibrium configurations and their stability, 61 see also Variational principle

Neutrino field pervading space, 84-85

consequences for beta-decay if Fermi energy is non-zero, 84-85

measurements of Fermi energy of, 84

Fermi energy of, elevated locally in a collapsing star, 85

Neutrino-neutrality definition of, 84-86

possibility of error concealed in concept of, 85

Neutrinos

detection of, 84-83

do elementary particles have hidden, internal store of? 85

Neutron agglomeration into drops, probably does not occur, 112 n.

Neutron drip

definition of, 112

stabilized in cold, catalyzed matter, 112-116

Neutron gas

density at which cold, catalyzed matter becomes, 113, 116, 118

in beta-equilibrium with nuclei and electron gas, 114-116

in beta-equilibrium with electron and proton gases, 118–121

Neutron gas, equation of state for, 24, 28, 115

approximate, 120-121 relativistic limit, 120-121

non-relativistic limit, 120-121, 166

in beta-equilibrium with nuclei and electron gas, 114-116

in beta-equilibrium with electron gas and proton gas, 116-121

see also Fermi gas, equation of state of

Neutron star

Oppenheimer-Volkoff calculations, 44–45, 50 HWW calculations, 45–48

acceleration of gravity in, 97-98 configuration of tightest binding, 59

maximum mass of, compared to maximum mass of white dwarf, 140, 152-153

with hot atmospheres, 165

see also Equilibrium configurations; HWW configurations

Normalized area in phase space; see Area in phase space

Nuclear fission; see Fission

INDEX 175

Nuclear fusion: see Fusion Nuclear interactions hard core, 106, 118-119 repulsive, must not be analyzed by instantaneous action at a distance, 118 see also Long-range and short-range forces Ninelei acceleration of gravity in, 97-98 dominant species of, in cold, catalyzed matter at various pressures, 117 electron distribution about at high density, 110neutron-rich, stable at high densities, 112-116 radii of, 116 semi-empirical mass formula, 112-113 Number density of baryons definition of, 94, 96 determination of, by adiabatic decompression, 100 not measured by trace of stress-energy tensor, 105 n. see also Thermodynamic potentials One-sidedness of matter, 147 Operator rings, theory of compared with geometry of geometrodynamical systems, 72 Oppenheimer-Volkoff cold neutron star, 44-45, 50; see also Equilibrium configurations; Neutron stars Oscillations, normal acoustical modes Chandrasekhar variational principle for statement of, 50-52 derivation from energy considerations, 156-162 application to HWW configurations, 52 of zero frequency, 61-62 change of stability of, 62-67 frequencies versus central density for HWW configurations, 65-66 analytic expression for frequency of critical mode near a critical point, 66-67 why more modes become unstable as central density rises, 67-68 of a small sphere of iron, 51-65

equations of motion for, 161–162
Lagrangian for, 161–162

\*\*\*\*\*\*ref also Oscillations, normal acoustical modes;
Stability of equilibrium configurations

Packing fraction
definition of, 88, 90
gravitational, 93, 165
for nuclei, reasons for its behavior, 112
variation-effective, defined, 114
scallops in packing fraction curve, 90–91
used to determine lowest energy state of A-baryon
system, 88–92
used to study equilibrium between electrons, neutrons, protons, and nuclei, 113–115

see also Oscillations about equilibrium configura-

Oscillations, static; see Static oscillations; Zones

Oscillations about equilibrium configurations

tions; Stability of equilibrium configurations

Particles, motion of in Schwarzschild solution, 133-134

Pencils or ladders, standing tip-to-top as model for

instability of equilibrium configurations, 52–53, 60

Phase space, normalized area in; see Area in phase space

Phase transitions, 34, 103-104

Photons, motion of

in collapsing dust cloud, 127, 138-139, 141 in Friedmann universe, 127 see also Redshift

Polytropes

non-relativistic, 163-166 relativistic, 29-33

see also Gamma-law equation of state

Polytropic equation of state; see Gamma-law equation of state

Potential energy curve in general relativity, 136-137 Pressure, regenerative multiplication of, 26-28

Pressure; see Thermodynamic potentials

Pressure perturbation factor, ξ definition of, 35

form of, for  $\gamma = 4/3$ , 35–36

Principle of equivalence; see Equivalence principle Pumping up energy of equilibrium configuration, 53, 58-60 stabilizer for, 60

see also Energy excess, configurations of

Q factor, measuring strength of perturbation from configuration of infinite central density, 34-37 definition of, 34 evaluation of, 36-37 value of, for γ = 4/3, 36-37

Quantum fluctuations in geometry characteristic energy density associated with, 12, 88

compared with gravitational binding of HHe molecule, 88 as limit on validity of general relativity, 11

Quantum gravitational effects, 9, 124, 141-147

changes of topology due to, 142 effects on law of conservation of baryons (see Baryons, law of conservation of)

limits on concept of equation of state due to, 7, 79-81

probability distribution for outcomes of gravitational collapse, 124, 141-143 advanced potentials cannot carry away energy in,

139

see also Quantum fluctuations; Tunneling of barrier Quasi-stellar radio sources, 1, 140

Radio sources, extragalactic, 1

Rayleigh-Ritz technique, used to study non-relativistic polytropes, 163-166

Redshift

case of compensating redshift and blueshift, 19 of light from a collapsing body, 139 upper limit on redshift from surface of equilibrium configuration, 28 n., 60 n. see also Event horizon

Regenerative multiplication of pressure, 26-28

Relativity, general; see General relativity

Riemannian geometry as a hypothesis in general relativity, 11

Rotation, effect on gravitational collapse, 1 n.

Scallops in packing fraction curve, 90-91

Schatzman equation of state for cold, catalyzed matter, 45

Schwarzschild coordinates

definition of r-coordinate, 14, 157 n. definition of t-coordinate, 18, 21, 157 n. difficulties with r-coordinate, 72 for dynamical systems, 157 n.

Schwarzschild correction factor eh, 14, 18

Schwarzschild correction factor e\*

definition, 18, 19

uniquely defined only for equilibrium configurations, 21, 156 n.

as relativistic generalization of gravitational potential, 19, 22

expressed in terms of pressure and density, 22, 159
sense in which it does and does not appear in variational derivation of TOV equation, 21-23

Schwarzschild singularity

impossible to build up with Einstein's orbiting particles, 54

will not occur in quantized relativity, 141-142

Schwarzschild solution

Schwarzschild line element for, 128 conformal coordinates for, 128-129 Kruskal coordinates for, 128-131 Kruskal diagram for, 127, 130-132 Birkhoff's theorem for, 128 dynamics of, 130-133

extrinsic geometry of hypersurface of constant to the state of the sta

geometry of hypersurface of time-symmetry, 71, 79, 128-130

geometry of other hypersurfaces, 121-133 motion of a particle in, 133-134

and exterior of collapsing dust cloud, 127-128, 133-134

and exterior of momentarily static configuration, 8, 69-74, 79

Semi-empirical mass formula, 113

Shear stresses, absent from cold, catalyzed matter, 95

Singularity resulting from classical gravitational collapse, 141–142; see also Gravitational collapse; Quantum gravitational effects; Schwarzschild singularity

Skyrme equation of state for cold, catalyzed matter, 118

Slide rule for computing uniform density configurations

description of, 7, 69-70 construction of long-range-forces part, 70-73

construction of short-range-forces part, 73-75 operation of, 69-70, 75

configurations calculated with, 75-76

Sound, speed of, 105 limits on, due to causality, 75, 105 equality to speed of light attainable in principle, 107

Spacelike hypersurfaces

and nature of time in general relativity, 130 calculation of mass-energy on, 3-4, 11-15 see also Dust cloud; Extrinsic geometry; Intrinsic geometry; Schwarzschild solution

Stability of equilibrium configurations, 6, 7, 50-68, 156-162

Chandrasekhar variational principle for

statement of, 50-52 derivation from mass-energy considerations.

derivation from mass-energy considerations, 156-162

application to HWW configurations, 52 comparison with  $M(\rho_0)$ ,  $R(\rho_0)$  analysis, 67

changes in, diagnosed from  $M(\rho_0)$  and  $R(\rho_0)$ one acoustical mode changes stability at each critical point, 62

diagnosis of direction of change, 64-65

analytic expression for critical frequency near critical point, 66-67

this analysis compared with Chandrasekhar variational principle, 67

result of analysis for HWW configurations, 65-66

diagnosed from second variation of mass-energy, 6, 160-161

for neutron stars, Oppenheimer-Volkoff analysis, 45, 50

for non-relativistic polytropes, 163

for configurations of energy excess, 54, 56

why more modes become unstable as central density rises, 67-68

pencils or ladders standing tip-to-top, as model for instability, 52–53, 60

see also Oscillations, normal acoustical modes

Stability parameter, 65

Static oscillations with increasing density of equilibrium configurations, 5, 28, 30-41, 42; see also Zones

Stress-energy tensor

trace of, can be negative, 105 does not measure particle density, 105 n.

Superdense stars; see Equilibrium configurations; HWW configurations; Neutron stars; Polytropes; White dwarf stars

Supernova explosions, many occurring at once in dense region of a galaxy, 2 n.

Superstar, of  $M \ge 10^8 M_{\odot}$ , 2 n., 77

Synchroton radiation, from extragalactic radio sources, 1 n.

Thermodynamic potentials for cold, catalyzed mat-

 $\rho(n)$  as potential, 94, 99  $p(\mu)$  as potential, 99–100

 $p(\rho)$  as potential, 100

at a phase transition, 103-104 relations among, 17, 95, 99-100, 159

relations among, for gamma-law equation of state,

non-relativistic, compared with relativistic, 101-102, 163

177 INDEX

see also Chemical potential; Equation of state; Mass-energy density; Number density of bar-

Thermonuclear reactions in stars, 1, 83

Tide-producing forces

infinite, arising in classical gravitational collapse, 141-142

order of magnitude of, in gravitating body, 97 see also Curvature

Time, nature of

in classical general relativity, 130 in quantized general relativity, 142

Time-symmetric gravitational collapse; see Gravitational collapse

Time symmetry

definition of, 13-14

hypersurface of, mass-energy on, 14

as initial condition for studying collapse dynamics, 8, 125-126

initial value equation for hypersurface of, 3, 13 used in studying uniform density configurations,

Tolman's radiation-filled universe, 137

TOV equation of hydrostatic equilibrium, see Hydrostatic equilibrium, general relativity equation of

Tunneling of the barrier against collapse, quantum mechanical, 3, 9, 143-147

half-life for, 144-146

spontaneous collapse of elementary particles, 9, 124, 146-147

experimental search for spontaneous collapse of protons, 146-147

see also Barrier against gravitational collapse; Baryons, spontaneous disappearance and appearance of

Uniform density configurations, momentarily static as approximation to equilibrium configurations, 69 and the dynamics of gravitational collapse, 8, 134-137

for y-law equation of state, 78-81 geometry of, 69-72, 79 for Harrison-Wheeler equation of state, 76-77 and the inevitability of collapse, 7, 69 limiting cases of, 72-73

potential energy-curves for, 7-8, 76, 134-136 for pressureless dust, 76-77 (see also Dust cloud) properties of, 72-74

slide rule for computing, 7, 69-75

see also Friedmann universe: Schwarzschild solution: Dust cloud

Universe, gravitational collapse as a model for the dynamics of, 137-141; see also Friedmann uni-

Urca process, 83 n.

van der Waals equation of state, and phase changes,

van der Waals force, 87

Variational principle

for general relativistic configurations of hydrostatic equilibrium, 4, 13, 16-19

for non-relativistic configurations of hydrostatic equilibrium, 163-166

for normal acoustical modes of an equilibrium configuration, 156-162

see also Morse theory

Vector boson, as intermediary in Zel'dovich's model for nucleon-nucleon repulsion, 106

Vibrations of equilibrium configurations; see Oscilla-

Volume-occupation factor, 115-117

White dwarf star

Landau's pioneering analysis, 42-43

Chandrasekhar's calculations, 43-44

Kaplan's analysis, 45 n. Schatzman's analysis, 45

HWW analysis, 45-48

Chandrasekhar limit for, 43-46

comparison of Chandrasekhar limit with maxi-mum mass of neutron star, 140, 152-153

see also Equilibrium configurations; HWW configurations

Zel'dovich's model for material with  $\gamma = 2, 105-107$ ,

Zel'dovich sequence of configurations leading to collapse, 24-25

Zel'dovich-Wheeler equation of state, 121, 166

Zones used in proof of existence of infinity of critical masses

definitions of, 31-33

discussion in Zone I, 31-33 discussion in Zone II, 33-35, 37-39

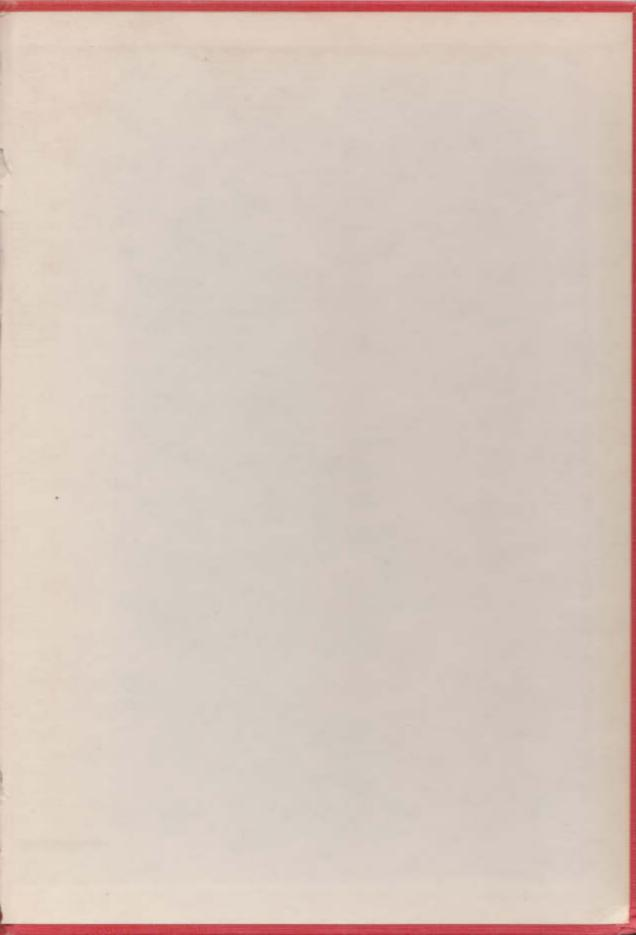
discussion in Zone III, 33, 34, 37-41

fitting Zone I to Zone II, 33-37

fitting Zone II to Zone III, 37-39







GRAVITATION THEORY
and GRAVITATIONAL COLLAPSE

WAKANO - WHEELER

CHICAGO

### (Continued from front flap)

rems on the conditions where collapse sets in. In addition to expounding their theory of the disappearance of baryons, they present the first concise study of the strange behavior of matter at ultra-high densities.

John Archibald Wheeler is Professor of Physics and Kip S. Thorne is an N.S.F. Predoctoral Fellow, Palmer Physical Laboratory, Princeton University. B. Kent Harrison is on the staff of the Physics Department at Brigham Young University. Masami Wakano is on the physics faculty of Kyoto University, Japan.

Two important new works in astrophysics . . .

## QUASI-STELLAR SOURCES AND GRAVITATIONAL COLLAPSE

Including the Proceedings of the First Texas Symposium on Relativistic Astrophysics

Edited by IVOR ROBINSON, ALFRED SCHILD, and E. L. SCHUCKING

The papers given at the conference held in Dallas, December, 1963, are published here, together with considerable reprinted supplementary material.

### NUCLEOSYNTHESIS IN MASSIVE STARS AND SUPERNOVAE

By WILLIAM A. FOWLER and FRED HOYLE

The authors trace the physical properties of matter inside highly evolved massive stars where the electronpositron pair-formation occurs and neutrino processes lead to large energy losses.

(Also published as Supplement No. 91 in the Astrophysical Journal Supplement Series).

HARRISON THORNE WAKANO WHEELER

THE UNIVERSITY OF CHICAGO PRESS

